Development and Use of Avian *In Vitro* and *In Vivo* Models for Toxicological Screening and Prioritization of Five Bisphenol A Replacement Compounds: Bisphenol F, TGSH, DD-70, Bisphenol AF, and BPSIP

Tasnia Sharin

Thesis submitted to the University of Ottawa
in partial fulfillment of the requirements for the
Doctor of Philosophy in Biology
Specialization in Chemical and Environmental Toxicology

Department of Biology

Faculty of Science

University of Ottawa

Abstract

Toxicity testing is moving from animal-based studies to faster, more ethical *in vitro* approaches that focus on mechanistic toxicology. The use of bisphenol A (BPA) replacement compounds is increasing and there is limited toxicity data available for these compounds in avian species. The overall goals of this thesis were to: a) determine if avian cell lines are suitable alternatives to primary hepatocytes for chemical screening; b) generate toxicity data for five BPA replacement compounds: bis(4-hydroxyphenyl)methane (BPF), bis(3-allyl-4-hydroxyphenyl)sulfone (TGSH), 7-bis(4-hydroxyphenylthio)-3,5-dioxaheptane (DD-70), 2,2-bis(4-hydroxyphenyl)hexafluoropropane (BPAF) and 4-hydroxyphenyl 4-isoprooxyphenylsulfone (BPSIP) in three *in vitro* models: primary chicken embryonic hepatocytes (CEH), double-crested cormorant (DCCO) embryonic hepatocytes (DCEH) and chicken LMH cell line; and 3) prioritize two replacements for early-life stage testing (ELS). LMH cells cultured as 3D spheroids, as opposed to 2D monolayer, had enhanced mRNA expression and CYP1A activity and were therefore used for screening. Additionally, an immortalized DCCO hepatic cell line, DCH22, was established, which may be useful for future avian toxicity testing. DD-70 and BPAF were the most cytotoxic across the three *in vitro* models. TGSH and DD-70 altered expression of genes associated with multiple toxicity pathways, but not estrogen response, and are potential non-estrogenic replacements. BPAF, BPF and BPSIP are potential estrogenic replacements. In general, the replacements were more cytotoxic and/or transcriptionally active than BPA. There was species-specific variability in toxicity; the replacements were more transcriptionally active in CEH compared to DCEH. LMH spheroids were more sensitive to estrogenic endpoints than CEH. DD-70 and BPAF were prioritized for ELS studies based on *in vitro* results. All of the replacements modulated the expression of genes

related to bile acid regulation *in vitro* and an increase in gallbladder mass was observed in chicken embryos after exposure to DD-70 or BPAF. Overall, this thesis evaluated the utility of LMH cells cultured as spheroids as an animal free alternative for chemical screening, established a DCCO cell line, and generated novel cytotoxicity and gene expression data for five BPA replacement compounds in three *in vitro* avian models and determined ELS toxicity of two replacement compounds.

Résumé

Les tests de toxicité passent de plus en plus des études sur les animaux à des approches *in vitro* plus rapides et plus éthiques, axées sur la toxicologie mécanistique. L'utilisation de composés de remplacement du bisphénol A (BPA) est en augmentation et il existe peu de données sur la toxicité de ces composés chez les espèces aviaires. Les objectifs généraux de cette thèse étaient de : a) déterminer si les lignées cellulaires aviaires sont des alternatives appropriées aux hépatocytes primaires pour la sélection de substances chimiques; b) générer des données de toxicité pour cinq composés de remplacement du BPA: bis(4-hydroxyphényl)méthane (BPF), bis(3-allyl-4-hydroxyphényl)sulfone (TGSH), 7-bis(4-hydroxyphénylthio)-3,5-dioxaheptane (DD-70), 2,2-bis(4-hydroxyphényl)hexafluoropropane (BPAF) et 4-hydroxyphényl 4-isoprooxyphénylsulfone (BPSIP) dans trois modèles *in vitro*: hépatocytes embryonnaires primaires de poulet (CEH), hépatocytes embryonnaires de cormoran à aigrettes (DCEH) et lignée cellulaire LMH de poulet; et 3) classer par ordre de priorité deux remplaçants pour les essais aux stades de vie précoces (SVP). Les cellules LMH cultivées sous forme de sphéroïdes 3D, par opposition aux monocouches 2D, présentaient une expression de l'ARNm et une activité CYP1A accrues et ont donc été utilisées pour la sélection. De plus, une lignée de cellules hépatiques immortalisées de cormoran à aigrettes, DCH22, a été établie, ce qui pourrait être utile pour de futurs tests de toxicité aviaire. Le DD-70 et le BPAF ont été les plus cytotoxiques dans les trois modèles in *vitro*. Le TGSH et le DD-70 ont modifié l'expression des gènes associés à de multiples voies de toxicité, mais pas la réponse aux œstrogènes, et sont donc des substituts non œstrogéniques potentiels. Le BPAF, le BPF et le BPSIP sont des substituts œstrogéniques potentiels. En général, les substituts étaient plus cytotoxiques et/ou transcriptionnellement actifs que le BPA. Il y avait une variabilité de la toxicité selon les espèces; les substituts étaient plus

actifs sur le plan transcriptionnel chez les CEH que chez les DCEH. Les sphéroïdes LMH étaient plus sensibles aux paramètres œstrogéniques que les CEH. Le DD-70 et le BPAF ont été priorisés pour les études SVP sur la base des résultats *in vitro*. Tous les substituts ont modulé l'expression des gènes liés à la régulation des acides biliaires in vitro et une augmentation de la masse de la vésicule biliaire a été observée chez les embryons de poulet après exposition au DD-70 ou au BPAF. Dans l'ensemble, cette thèse a évalué l'utilité des cellules LMH cultivées sous forme de sphéroïdes comme alternative sans animaux pour la sélection de substances chimiques, a établi une lignée cellulaire de cormoran à aigrettes, a généré de nouvelles données de cytotoxicité et d'expression génique pour cinq composés de remplacement du BPA dans trois modèles aviaires *in vitro* et a déterminé la toxicité de deux composés de remplacement aux SVP.

Acknowledgement

First and foremost, I would like to thank my supervisors (extraordinaire), Jason O'Brien and Doug Crump, for their endless encouragement, guidance and patience. Both of you always made time to discuss my research with me and never hesitated to let me explore new ideas, which has kept me motivated and made this experience enjoyable. Thank you for giving me the opportunity to be a part of the MolTox family. I would also like to thank my uOttawa supervisor, Laurie Chan, for suggesting the MolTox lab when I decided to pursue a PhD and the opportunity to continue my research at CAREG. I would like to extend my sincerest gratitude to my thesis advisory committee members, Iain Lambert and Paul White, for their thoughtful comments and suggestions throughout the course of this thesis.

I would like to thank MolTox lab members, past and present, for making my experience fun and memorable. Thank you to Suzanne Chiu, Stephanie Jones and Kim Williams for their technical expertise and troubleshooting ideas. To Florence Pagé-Larivière and Amani Farhat thank you for the encouragement and numerous brainstorming sessions. Special thanks go out to Jared Browning, Jory Curry, Helina Gyasi, Tyler Nguyen and Yasmeen Zahaby for the laughs, the random conversations during our "lab meetings", all the outings, and the hours spent searching for (non-existent) cormorant and chicken antibodies. It was a pleasure to work alongside with you all.

I was fortunate enough to work at the Chan lab in the past year. I am grateful to Kayla Greydanus for taking care of the paperwork required for me to work at the lab. Special thanks to Dr. Emmanuel Yumvihoze for clearing out a lab bench and cabinet for me, and taking the time to help with my experiments. To Florence Pagé-Larivière and Galen Guo thank you for proofreading the French abstract.

To my family and friends, I cannot thank you enough for the support you have shown the last four years. A special thank you goes to the BEST crew for their friendship and for keeping me sane during this journey. To my parents, thank you for the constant encouragement, help and unwavering belief in me.

Table of Contents

Abstract ..... **II**
Résumé ..... **IV**
Acknowledgement ..... **VI**
Table of Contents ..... **VII**
List of Abbreviations ..... **X**
List of Tables ..... **XV**
List of Figures ..... **XVII**
Statement of Contributions ..... **XIX**
Chapter 1. Introduction **1**
1.1Toxicity Testing 1
1.1.1Traditional Toxicity Testing 1
1.1.2 Avian Toxicity Testing 2
1.1.3 Alternative Toxicity Testing 4
1.1.4 Importance of Liver for Toxicity Testing 6
1.1.5 In Vitro Liver Models 8
1.1.6 Toxicogenomics and PCR arrays in HTS 11
1.2 Endocrine Disrupting Chemicals 12
1.2.1 Bisphenol A 13
1.2.2 Bisphenol A Replacement Compounds 14
1.2.3 Environmental Occurrence and Fate of BPA Replacement Compounds 16
1.2.4 Toxicokinetics of Bisphenol A and Replacement Compounds 17
1.2.5 Toxicological Targets of Bisphenols 19
1.2.6 Toxicity of Bipshenols in Birds 27
1.3 Thesis Overview 28
1.3.1 Rationale for Thesis 28
1.3.2 Thesis Objectives and Chapter Objectives 29
1.4 References 32
Chapter 2: Evaluating Aryl Hydrocarbon Receptor Response in LMH 3D Spheroids **47**
2.1 Abstract 47
2.2 Introduction 48
2.3 Materials and Methods 50
2.4 Results 55
2.5 Discussion 61

2.6 References 67
Chapter 3. Concentration- and Time-Dependent Induction of CYP1A and DNA Damage Response by Benzo(a)pyrene in LMH 3D Spheroids 74
3.1 Abstract 74
3.2 Introduction 75
3.3 Materials and Methods 77
3.4 Results 81
3.5 Discussion 88
3.6 References 93
Chapter 4. Development and Characterization of a Double-Crested Cormorant Hepatic Cell Line for Chemical Screening 97
4.1 Abstract 97
4.2 Introduction 97
4.3 Materials and Methods 99
4.4 Results and Discussion 102
4.5 References 107
Chapter 5. Toxicity Screening of Bisphenol A Replacement Compounds: Cytotoxicity and mRNA Expression in Primary Hepatocytes of Chicken and Double-Crested Cormorant 110
5.1 Abstract 110
5.2 Introduction 111
5.3 Materials and Methods 114
5.4 Results and Discussion 118
5.5 References 132
Chapter 6. Toxicity Screening of Bisphenol A Replacement Compounds: Cytotoxicity and mRNA Expression in LMH 3D Spheroids 137
6.1 Abstract 137
6.2 Introduction 138
6.3 Materials and Methods 140
6.4 Results and Discussion 143
6.5 References 154
Chapter 7: Effects of DD-70 and BPAF on mRNA Expression and Developmental Toxicity in Chicken Embryos 160
7.1 Abstract 160
7.2 Introduction 161
7.3 Materials and Methods 164

7.4 Results 168
7.6 References 179
8.0 General Conclusions 184
8.1 Chapter Summaries Based on Objectives 185
8.2 Future Directions 193
8.3 Concluding Remarks 198
8.4 References 199
Appendix 202
Supplemental Information 202
A1. Chapter 2: Evaluating Aryl Hydrocarbon Receptor Response in LMH 3D Spheroids 202
A2. Chapter 3: Concentration- and Time-Dependent Induction of CYP1A and DNA Damage Response by Benzo(a)pyrene in LMH 3D Spheroids 208
A3. Chapter 5: Toxicity Screening of Bisphenol A Replacement Compounds: Cytotoxicity and mRNA Expression in Primary Hepatocytes of Chicken and Double-Crested Cormorant 213
A4. Chapter 6: Toxicity Screening of Bisphenol A Replacement Compounds: Cytotoxicity and mRNA Expression in LMH 3D Spheroids 227
A5. Chapter 7: Effects of DD-70 and BPAF on mRNA Expression and Developmental Toxicity in Chicken Embryos 234

List of Abbreviations

2D	Two-dimensional
3D	Three-dimensional
γH2AX	Phosphorylated H2A histone family member X
ACSL5	Acyl-CoA synthetase long-chain family member 5
AhR	Aryl hydrocarbon receptor
ALAS1	Aminolevulinate, delta-, synthase 1
ALDH1A1	Aldehyde dehydrogenase 1 family, member A1
ANOVA	Analysis of variance
AOC1	Amine oxidase, copper containing 1
AOP	Adverse outcome pathway
AMR	ATP monitoring reagent
APC	Allophycocyanin
APOB	Apolipoprotein B (including Ag(x) antigen)
APOV1	Apovitellenin-1
AREGB	Amphiregulin B
ATP	Adenosine triphosphate
ATP12A	ATPase, H+/K+ transporting, nongastric, alpha polypeptide
AVD	Avidin
B3GNT7	UDP-GlcNAc:betaGal beta-1,3-N-acetylglucosaminyltransferase 7
BaP	Benzo(a)pyrene
BATF3	Basic leucine zipper transcription factor, ATF-like 3
BCF	Biocentration factor
BER	Base excision repair
BMD	Benchmark dose
BMDL	Lower bound of the BMD confidence interval
BMDU	Upper bound of the BMD confidence interval
BMR	Benchmark response
BPA	4,4'-(propane-2,2-diyl) diphenol; Bisphenol A
BPAF	2,2-Bis(4- hydroxyphenyl) hexafluoropropane; Bisphenol AF
BPAF-G	BPAF glucuronide
BPA-G	BPA glucuronide
BPDE	Benzo[a]pyrene diol epoxide
BPF	Bis(4-hydroxyphenyl)methane; Bisphenol F
BPS	4,4'-Sulfonyldiphenol
BPSIP	4-hydroxyphenyl 4-isopropoxyphenyl sulfone
CA3B	Carbonic anhydrase III-like
CAR	Constitutive androstane receptor

CDKN1A	Cyclin-dependent kinase inhibitor 1A
cDNA	Complementary deoxyribonucleic acid
CED	Critical effect dose
CEH	Primary chicken embryonic hepatocytes
CES	Critical effect size
COL7A1	Collagen Type VII Alpha 1 Chain
CPT1A	Carnitine O-palmitoyltransferase 1
CRYAB	Crystallin, alpha B
Ct	Cycle threshold
CTSD	Cathepsin D-like
CWH43	Cell wall biogenesis 43 C-terminal homolog (S. cerevisiae)
CXR	Chicken xenobiotic receptor
CYP	Cytochrome P450 enzyme
CYP1A4	Cytochrome P450 1A4
CYP1A5	Cytochrome P450, family 1, subfamily A, polypeptide 5
CYP1B1	Cytochrome P450, family 1, subfamily B, polypeptide 1
CYP24A1	Cytochrome P450, family 24, subfamily A, polypeptide 1
CYP3A7	Cytochrome P450 A 37
CYP7A1	Cholesterol 7-alpha-monooxygenase
CYP7B1	Cytochrome P450, family 7, subfamily B, polypeptide 1
DACT2	Dapper, antagonist of beta-catenin, homolog 2 (Xenopus laevis)
DCCO	Double-crested cormorant
DCEH	Primaty double-crested embryonic hepatocytes
DCH22	Double-crested cormorant hepatocytes, embryonic day 22
DD-70	1,7-bis(4-hydroxyphenylthio)-3,5-dioxaheptane
DDB2	Damage Specific DNA Binding Protein 2
DMEM/F12	Dulbecco's Modified Eagle Medium: Nutrient Mixture F-12
DMSO	Dimethyl sulfoxide
DSB	DNA double strand break
E2	17β-estradiol
EC50	Half maximal effective concentration
ECHA	European Chemicals Agency
EDC	Endocrine disrupting compound
EEF1A1	Eukaryotic Translation Elongation Factor 1 Alpha 1
ELS	Early-life stage
EFCAB4B	EF-hand calcium binding domain 4B
ELVOL2	ELOVL fatty acid elongase 2
ER	Estrogen receptor
EPA	U.S. Environmental Protection Agency
ERE	Estrogen responsive element
EROD	7-ethoxy-resorufin-*O*-deethylase

ERR	Estrogen related receptor
EU	European Union
FABP3	Fatty acid binding protein 3, muscle and heart (mammary-derived growth inhibitor)
FDA	U.S. Food and Drug Administration
FDR	False discovery rate
FGA	Fibrinogen alpha chain
FGF19	Fibroblast growth factor 19
FGFBP1	Fibroblast growth factor binding protein 1
FOXA1	Forkhead box A1
FRZB	Frizzled-related protein
FXR	Farnesoid X receptor
G6PC	Glucose-6-phosphatase-like
GADD45	Growth arrest and DNA-damage-inducible, alpha
GAPDH	Glyceraldehyde-3-phosphate dehydrogenase
GGDC	Chicken Genomic DNA Contamination
GPER1	G protein-coupled estrogen receptor 1
GPR30	G-protein coupled receptor 30
GPX3	Glutathione peroxidase 3
GST	Glutathione s-transferase
GSTM3	Glutathione s-transferase M3
ITS	Insulin transferrin selenium solution
HI-FBS	Heat-Inactivated Fetal Bovine Serum
HK1	Hexokinase 1
HMGCR	3-hydroxy-3-methylglutaryl-Coenzyme A reductase
HMOX1	Heme oxygenase 1
HTS	High throughput screening
IAPP	Islet amyloid polypeptide
IC50	Half maximal inhibitory concentration
IGF1	Insulin-like growth factor 1 (somatomedin C)
IGFBP4	Insulin-like growth factor binding protein 4
IL16	Interleukin 16 (lymphocyte chemoattractant factor)
IL1B	Interleukin 1, beta
KLHDC8B	Kelch domain containing 8B
KOW	Octanol/water partition coefficient
KRT20	Keratin 20
LBD	Ligand binding domain
LBFABP	Liver basic fatty acid binding protein
LC50	Lethal median concentration
LD50	Lethal median dose
LEAP2	Liver expressed antimicrobial peptide 2

LIPC	Lipase, hepatic
LMH	Leghorn male hepatoma
LOAEL	Lowest-observed-adverse-effect level
LSECs	Liver sinusoidal endothelial cells
LSS	Lanosterol synthase (2,3-oxidosqualene-lanosterol cyclase)
LXR	Liver X receptor
M2B	Beta-2-microglobulin
MAT1A	Methionine adenosyltransferase I, alpha
MDM2	E3 ubiquitin-protein ligase
MGMT	O-6-methylguanine-DNA methyltransferase
MGP	Matrix Gla protein
MGST3	Microsomal glutathione S-transferase 3
MMP7	Matrix metallopeptidase 7 (matrilysin, uterine)
mRNA	Messenger ribonucleuc acid
MSH2	MutS homolog 2, colon cancer, nonpolyposis type 1 (E. coli)
MT4	Metallothionein 4
NADPH	Nicotinamide adenine dinucleotide phosphate
NAT2	N-acetyltransferase 2 (arylamine N-acetyltransferase)
NCGC	NIH Chemical Genomics Center
NCOA3	Nuclear receptor coactivator 3
NER	Nucleotide excision repair
NOAEL	No observed adverse effect level
NOS2	Nitric oxide synthase 2, inducible
NRC	National Research Council
NTP	National Toxicology Program
NTC	No template control
OECD	Organisation for Economic Co-operation and Development
ORM1	Orosomucoid 1
PAH	Phenylalanine hydroxylase
PCB-126	3,3',4,4',5-Pentachlorobiphenyl
PC	Principal component
PCA	Principal component analysis
PCB	Polychlorinated biphenyls
PDK4	Pyruvate dehydrogenase kinase, isozyme 4
PerCP	peridinin-chlorophyll-protein
POD	Point of departure
PODXL	Podocalyxin-like
POLB	DNA Polymerase Beta
POLK	Polymerase (DNA) kappa
PPC	Positive PCR Control
PXR	Pregnane X receptor

REACH	Registration, Evaluation, Authorisation and Restriction of Chemicals
RGN	Regucalcin
RIVM	Dutch National Institute for Public Health and the Environment
RLU	Relative luminescene unit
RPL4	Ribosomal protein L4
RTC	Reverse Transcription Control
RT-PCR	Real time polymerase chain reaction
SCD	Stearoyl-CoA desaturase (delta-9-desaturase)
SEM	Standard error of the mean
SEURAT-1	Safety Evaluation Ultimately Replacing Animal Testing
SLCO1A2	Solute carrier organic anion transporter family, member 1A2
SREBP	Sterol regulator element binding protein
SULT	Sulfontransferases
SULT1B1	Sulfotransferase family, cytosolic, 1B, member 1
SULT1E1	Sulfotransferase family 1E, estrogen-preferring, member 1
SVHC	Substance of very high concern
T3	Triiodothyronine
TGM2	Transglutaminase 2 (C polypeptide, protein-glutamine-gamma-glutamyltransferase)
TGSH	4 Bis (3-allyl-4- hydroxyphenyl)sulfone
THRSP	Thyroid hormone responsive (SPOT14 homolog, rat)
TIPARP	TCDD-inducible poly(ADP-ribose) polymerase
TMM	Trimmed mean of M values
TP63	Tumor protein p63
TR	Thyroid receptor
TTR	Transthyretin
TXN	Thioredoxin
UGT	Uridine 5'-diphospho-glucuronosyltransferase
UGT1A1	UDP glucuronosyltransferase 1 family, polypeptide A1
ULA	Ultra low attachment microplate
VCAM1	Vascular cell adhesion molecule 1, transcript variant X2
VTG1	Vitellogenin-1
VTG2	Vitellogenin-2
XPC	Xeroderma Pigmentosum Group C-Complementing Protein

List of Tables

Table 1.1. Half maximal inhibitory concentration (IC50) and half maximal effective concentration (EC50) of BPA and the five replacement compounds for estrogen receptors in human and zebrafish cell lines.

Table 1.2. Effects of BPA, BPF and BPAF on plasma cholesterol, lipid accumulation and triglyceride levels in *in vivo* and *in vitro* studies.

Table 2.1. EC50 ± SEM values for LMH cells grown in two culture conditions exposed to PCB-126 for 24h.

Table 2.2. Mean fold changes of significantly dysregulated target genes on the AhR pathway array following exposure to 0.1 nM PCB-126 in confluent and spheroid LMH cells, and CEH.

Table 3.1. Concentration- and time-dependent effects of Benzo(a)pyrene (BaP) exposure on gene expression in 2D monolayer cells.

Table 3.2. Concentration- and time-dependent effects of Benzo(a)pyrene (BaP) exposure on gene expression in 3D spheroids.

Table 5.1. Common name, CASRN, molecular weight and structure of Bisphenol A and the five Bisphenol A replacement compounds.

Table 5.2. LC50 ± SEM values of BPA and the five replacement compounds in chicken embryonic hepatocytes (CEH) and double-crested cormorant embryonic hepatocytes (DCEH).

Table 5.3. Mean log2 fold change of significantly altered genes on the ToxChip array in chicken embryonic hepatocytes following exposure to 30 μM of BPF, TGSH, BPSIP and BPA, and 10 μM of DD-70, BPAF and E2.

Table 5.4. Mean log2 fold change of significantly altered genes on the AestroChip array in chicken embryonic hepatocytes following exposure to 30 μM of BPF, TGSH, BPSIP, BPA, and 10 μM of DD-70, BPAF and E2.

Table 5.5. Mean log2 fold change of significantly altered genes on the ToxChip array in double-crested cormorant embryonic hepatocytes following exposure to 10 μM TGSH, DD-70, BPAF, and E2, and 30 μM BPSIP.

Table 6.1. Common name, CASRN, LC50 (μM) ± SEM and structure of Bisphenol A and five replacement compounds.

Table 7.1. Chemical Structures of Bisphenol A (BPA), 1,7-bis (4-Hydroxyphenylthio)-3,5-dioxaheptane (DD-70), and Bisphenol AF (BPAF).

Table 7.2. Injected and embryo homogenate concentrations of 1,7-bis (4-Hydroxyphenylthio)-3,5-dioxaheptane (DD-70) and Bisphenol AF (BPAF) and effects on embryonic viability.

Table 7.3. Hepatic mRNA expression results from chicken embryos exposed to 88.2 μg/g 1,7-bis (4-Hydroxyphenylthio)-3,5-dioxaheptane (DD-70) and 114 μg/g Bisphenol AF determined using two custom PCR arrays.

Table 8.1. Ranking of the relative cytotoxicity, ToxChip and AestroChip gene expression of BPA and the replacement compounds in CEH, LMH spheroids and DCEH.

List of Figures

Figure 1.1 Chemical structures of BPA and the five BPA replacement compounds, BPF, TGSH, DD-70, BPAF and BPSIP.

Figure 2.1. LMH cells in two culture conditions grown in 96-well plates: A) 2D confluent cells, B) 3D spheroid, and C) primary chicken embryonic hepatocytes (CEH).

Figure 2.2. Concentration-dependent effects of PCB-126 on EROD activity in LMH 2D confluent cells and 3D spheroids, and CEH after 24 h exposure.

Figure 2.3. Concentration-dependent effects of PCB-126 exposure on A) CYP1A4 and B) CYP1A5 mRNA expression in LMH 2D confluent cells and 3D spheroids, and CEH after 24h.

Figure 2.4. Heatmap of significant gene changes on the chicken AhR pathway PCR array for LMH 2D confluent cells and 3D spheroids, and CEH exposed to 0.1 nM PCB-126 for 24h, hierarchically clustered by gene expression and cell culture condition.

Figure 3.1. Concentration- and time-dependent effects of benzo(a)pyrene (BaP) on CYP1A activity (measured by EROD) in LMH cells cultured as A) 2D monolayer cells and B) 3D spheroids following 8, 24 and 48h exposure.

Figure 3.2. Concentration- and time-dependent effects of benzo(a)pyrene exposure (BaP) on H2AX phosphorylation (γH2AX) in 3D spheroids after 8, 24 and 35h.

Figure 4.1. DCH22 cells in two culture conditions grown in 96-well plates: A) 2D monolayer cells, and B) 3D spheroid.

Figure 4.2. Concentration-dependent effects of PCB-126 exposure on EROD activity in DCH22 2D monolayer cells and 3D spheroids after 24h exposure.

Figure 4.3. Concentration-dependent effects of metyrapone on CYP3A activity (measured as relative luminescence units [RLU]) in DCH22 2D monolayer cells after 24h exposure.

Figure 5.1. Principal component analysis of significant genes on the ToxChip array in CEH following exposure to BPA, BPA replacement compounds (BPF, TGSH, DD-70, BPAF and BPSIP), and 17β estradiol (E2).

Figure 5.2. Principal component analysis of significant genes on the AestroChip array in CEH following exposure to BPA, BPA replacement compounds (BPF, TGSH, DD-70, BPAF and BPSIP), and 17β estradiol (E2).

Figure 5.3. Principal component analysis of significant genes on the double-crested cormorant ToxChip array in DCEH following exposure to the BPA replacement compounds, TGSH, DD-70, BPAF and BPSIP, and 17β estradiol (E2).

Figure 5.4. Principal component analysis of significant genes from the ToxChip array in CEH and DCEH following exposure to the BPA replacement compounds, TGSH, DD-70, BPAF and BPSIP, and 17β estradiol (E2).

Figure 6.1. Principal component analysis of significant genes on the ToxChip and AestroChip arrays in A) LMH 3D spheroids and B) CEH following exposure to BPA, BPA replacement compounds (BPF, TGSH, DD-70, BPAF and BPSIP), and 17β estradiol (E2).

Figure 7.1. Effect of (A) 1,7-bis (4-Hydroxyphenylthio)-3,5-dioxaheptane **(**DD-70), and (B) Bisphenol AF (BPAF) on embryonic viability at mid-incubation (embryonic day 11; n= 14-19).

Figure 7.2. Effect of *in ovo* DD-70 exposure on (A) embryo mass, and (B) gallbladder mass for all embryos at term (embryonic day 20; n= 4-19/dose group).

Figure 7.3. Effect of *in ovo* Bisphenol AF (BPAF) exposure on gallbladder mass for all embryos at term (embryonic day 20; n= 5-12/dose group).

Statement of Contributions

Chapter 2. Evaluating Aryl Hydrocarbon Receptor Response in LMH 3D Spheroids

Authors: Tasnia Sharin, Doug Crump, Jason M. O'Brien

Published in: *Environmental Toxicology and Chemistry* 2020, 39(9): 1693-1701, DOI: 10.1002/etc.4783

Study design	Tasnia Sharin, Doug Crump, Jason M. O'Brien
Cell culture	Tasnia Sharin
Cell viability	Tasnia Sharin
EROD assay	Tasnia Sharin
RNA isolation & cDNA synthesis	Tasnia Sharin
Gene expression	Tasnia Sharin
Data analysis	Tasnia Sharin, Jason M. O'Brien
Manuscript Preparation	Tasnia Sharin, Doug Crump, Jason M. O'Brien

Chapter 3. Concentration- and Time-Dependent Induction of CYP1A and DNA Damage Response by Benzo[a]pyrene in LMH 3D Spheroids

Authors: Tasnia Sharin, Helina Gyasi, Stephanie P. Jones, Doug Crump, Jason M. O'Brien

Published in: *Environmental and Molecular Mutagenesis* 2021, 62(5): 319-327, DOI: 10.1002/em.22433

Study design	Tasnia Sharin, Doug Crump, Jason M. O'Brien
Cell culture	Tasnia Sharin
Cell viability	Tasnia Sharin
EROD assay	Tasnia Sharin, Helina Gyasi
RNA isolation & cDNA synthesis	Tasnia Sharin
PCR array	Tasnia Sharin
Flow cytometry	Tasnia Sharin, Helina Gyasi
Data analysis	Tasnia Sharin, Stephanie P. Jones, Jason M. O'Brien
Manuscript Preparation	Tasnia Sharin, Doug Crump, Jason M. O'Brien

Chapter 4. Development and Characterization of a Double-Crested Cormorant Hepatic Cell Line for Chemical Screening

Project Status: In progress (on hold due to COVID-19 related lab restrictions at National Wildlife Research Centre)

Study design	Tasnia Sharin, Doug Crump, Jason M. O'Brien
Cell culture	Tasnia Sharin
EROD assay	Tasnia Sharin
CYP3A assay	Tasnia Sharin

Chapter 5. Toxicity Screening of Bisphenol A Replacement Compounds: Cytotoxicity and mRNA Expression in Primary Hepatocytes of Chicken and Double-Crested Cormorant

Authors: Tasnia Sharin, Kim L. Williams, Suzanne Chiu, Doug Crump, Jason M. O'Brien

Published in: *Environmental Toxicology and Chemistry* 2021, 40(5):1368-1378, DOI: 10.1002/etc.4985

Study design	Tasnia Sharin, Doug Crump, Jason M. O'Brien
DCCO egg collection	Doug Crump, Kim L. Williams
Primary hepatocyte culture	Kim L. Williams
Cell Viability	Suzanne Chiu
RNA extraction & cDNA synthesis	Tasnia Sharin
PCR arrays	Tasnia Sharin
Data analysis	Tasnia Sharin, Jason M. O'Brien
Manuscript preparation	Tasnia Sharin, Doug Crump, Jason M. O'Brien

Chapter 6. Toxicity Screening of Bisphenol A Replacement Compounds: Cytotoxicity and mRNA Expression in LMH 3D Spheroids.

Project Status: Submitted to *Ecotoxicology and Environmental Safety*

Study design	Tasnia Sharin, Doug Crump, Jason M. O'Brien
Cell culture	Tasnia Sharin
Cell viability	Tasnia Sharin
EROD assay	Tasnia Sharin
RNA isolation & cDNA synthesis	Tasnia Sharin
Gene expression	Tasnia Sharin
Data analysis	Tasnia Sharin, Jason M. O'Brien
Manuscript Preparation	Tasnia Sharin, Doug Crump, Jason M. O'Brien

Chapter 7. Effects of DD-70 and BPAF on mRNA Expression and Developmental Toxicity in Chicken Embryos.

Authors: Tasnia Sharin[a], Helina Gyasi[a], Kim L. Williams, Doug Crump, Jason M. O'Brien
[a]Co-first authors

Published in: *Ecotoxicology and Environmental Safety* 2021, 215(Suppl 1):112140, DOI:10.1016/j.ecoenv.2021.112140

Study design	Tasnia Sharin, Helina Gyasi, Doug Crump, Jason M. O'Brien
Egg injection and dissection	Tasnia Sharin, Doug Crump, Kim Williams
Chemical analysis	Applied Technical Services
RNA isolation &cDNA synthesis	Helina Gyasi
PCR arrays	Tasnia Sharin, Helina Gyasi
Data analysis	Tasnia Sharin, Jason M. O'Brien
Manuscript Preparation	Tasnia Sharin, Helina Gyasi, Doug Crump, Jason M. O'Brien

Chapter 1. Introduction

1.1Toxicity Testing

1.1.1Traditional Toxicity Testing

Traditional toxicity testing involves *in vivo*, whole animal studies, in which animal models are treated with concentrations up to the maximum tolerated dose of a chemical of interest to determine apical adverse effects. The endpoints determined in traditional toxicity tests include lethality, organ abnormality, carcinogenesis, reproductive and development toxicities (Shukla et al. 2010). Traditional toxicity tests cover a wide range of exposure scenarios; acute (1-4 days), sub-chronic (7 to 90 days) and chronic (2 years) (Chhabra et al. 2003). *In vivo* studies offer the advantage of determining toxicity in a living organism with intact cellular structure, metabolism, and biological signalling and feedback mechanisms. Since animal toxicity testing has been used for decades, there are standardized guidelines and international acceptance of the resulting data (Hartung and Daston 2009). Despite these advantages, traditional toxicity testing provides very little or no information on the mechanism(s) of toxicity of chemicals (Shukla et al. 2010). Furthermore, *in vivo* tests in model species are time-consuming, expensive, require large numbers of animals and are not necessarily predictive of toxicity in humans or wildlife (Hartung 2009). Due to the nature of *in vivo* testing, these tests are inadequate to evaluate the toxicity of the large number of chemicals in the environment and there are ethical concerns regarding animal use.

1.1.2 Avian Toxicity Testing

Birds are widely used as indicator species of terrestrial and aquatic ecosystem health. High trophic level birds such as raptors and seabirds accumulate high levels of contaminants through diet and are used for assessing bioaccumulation and biomagnification of environmental chemicals (Guigueno and Fernie 2017). Exposure to chemicals like dichloro-diphenyl-trichloroethane (DDT) induced eggshell thinning in many avian species such as peregrines (*Falco peregrinus*) and bald eagles (*Haliaeetus leucocephalus*) resulting in embryo lethality (Lundholm 1997). Similarly, perfluorooctanesulfonic acid (PFOS) has been implicated in decreased hatching success in tree swallows (*Tachycineta bicolor*) and laboratory-based studies in chickens (*Gallus gallus domesticus*) (Custer et al. 2012). Many other chemicals have been found to alter behaviour, decrease reproductive success and increase mortality in birds (Carere et al. 2010).

Birds have been used to monitor toxicity and changes in concentration of pesticides in the environment and are used as model organisms in the National Pesticides Monitoring Program in the United States (Hill and Hoffman 1984). In many avian species, changes in behaviour, development, physiological abnormalities and reproduction can be observed over a relatively short span of time following exposure to chemicals (Smits and Fernie 2013). The Organization for Economic Cooperation and Development (OECD) regulates international guidelines for toxicity test methods and there are three tests (Test numbers 223, 205 and 206) that determine the effects of chemicals in avian species as part of ecological risk assessment. The acute avian oral toxicity test (Test No. 223) determines the lethal median dose (LD50) of chemicals by administering a single dose of a chemical by gavage in adult birds such as bobwhite quail (*Colinus virginianus*) (n=10 birds/concentration) and observing effects and lethality for a period

of 14 days (OECD 2016). In the avian dietary toxicity test (Test No. 205), various concentrations of a chemical are administered to birds via diet for 5 days, followed by a normal diet for three days. After 8 days, changes in weight, behaviour, food consumption, and signs of intoxications are measured (OECD 1984a). In the avian reproduction test (Test No. 206), breeding birds are exposed to test substances at various concentrations (at least three concentrations, n=20 birds/concentration) via diet for a minimum of 20 weeks. Eggs are collected over a 10 week period and artificially incubated and hatched. Reproductive endpoints measured include the number of eggs laid, eggshell thickness, hatchability, embryo viability, developmental abnormalities, and body weight in 14 day old chicks. Species included in this test are bobwhite quail, Japanese quail (*Cortunix japonica*) or mallard duck (*Anas platyrhynchros*) as these species are widely available and easy to rear (OECD 1984b). All three tests are expensive, resource intensive and require large numbers of adult birds. In order to minimize animal use, the acute avian oral toxicity test was modified to integrate prior knowledge of LD50 values of selected chemicals in other species; however, the modified test still requires 5 to 20 animals to determine the LD50 of a single chemical (Edwards et al. 2016). Acute avian oral and dietary tests have been used for pesticide registration and regulation. In a recent study of 119 pesticides, it was found that the dietary toxicity test did not generate novel data compared to the oral toxicity test (Hilton et al. 2019).

An alternative testing strategy to reduce animal use in avian toxicity testing involves the use of early-life stage (ELS) exposures. The avian embryo is an isolated system that can used to determine the adverse effects of chemicals of interest without the use of adult birds. Embryonic development of laboratory model avian species such as chicken (*Gallus domesticus*) and quail are well-described (Farhat et al. 2019). Advantages of ELS include the accessibility of eggs of

laboratory species year-round, the limited resources/equipment required (i.e. an incubator, dremel tool, repeater pipet), and the relatively inexpensive cost (Huss et al. 2019). The cost of an egg injection study ranges from $2000 to 3000 (Doug Crump, personal communication) per chemical, the majority comprising technician labour costs, compared to ~$8300 for the avian dietary test (Hilton et al. 2019). Numerous studies have employed avian ELS testing to investigate the adverse effects of chemicals such as dioxins, flame-retardants, and heavy metals on the developing embryo (Farhat et al. 2014; Augspurger et al. 2008; Gilani and Alibhai 1990).

1.1.3 Alternative Toxicity Testing

In 2007, the National Research Council (NRC) released a pivotal report entitled "Toxicity Testing in the 21st century: A Vision and a Strategy", which outlined a long-term vision for toxicity testing. The report stressed the limitations of traditional toxicity testing to determine the toxicity of new and existing chemicals in the environment (Krewski et al. 2010). There are a large number of chemicals (~82 000) that are data poor or require testing with an additional 600 new chemicals being introduced each year (Government of Canada 2019). The NRC report and subsequent publications emphasized the need to change toxicity testing from *in vivo* approaches to tiered-based, *in vitro* high-throughput approaches, which harness advancements in molecular biology and information technology to screen and prioritize chemicals for further testing (Thomas et al. 2013; Krewski et al. 2010). In addition, the report highlighted that *in vitro* cell-based approaches would permit determination of dose-response and mechanistic data of chemicals relevant to toxicity pathways, and reduce the number of animals required (Kavlock et al. 2011). *In vitro* approaches are amenable for high-throughput screening (HTS), allow for high numbers of replicates and are cheaper than animal studies (Hartung and Daston 2009). Overall, the report suggests a shift in toxicity testing towards a "bottom up"

approach, where molecular interactions and perturbations in cellular pathways are used to predict adverse effects (Parfett and Desaulniers 2017).

Around the same time as the NRC report was published, the European Union's Registration, Evaluation, Authorisation and Restriction of Chemicals (REACH) regulation framework for chemicals manufactured or imported at more than 1 ton per year came into effect. The framework also acknowledged the need to accelerate toxicity testing by implementing and standardizing *in silico* and *in vitro* methodologies, minimizing animal use, and incorporating previously validated *in vitro* tests such as skin irritation into the toxicity testing framework. It was estimated that without the use of alternative methods, 4 150 test animals would be required to determine the toxicity of a single chemical. Under the REACH regulation, animal tests are to be used only when there are no alternative options available (Schoeters 2009).

In order to meet the challenges outlined in the NRC report, there has been an international effort to develop and validate alternative methods. The Tox21 program, a collaboration between four US federal agencies (EPA, FDA, NTP and NCGC), was launched in 2008 to develop and identify *in vitro* HTS assays that can be used to predict changes in toxicity pathways of relevance to *in vivo* toxicity (NIH 2019). Similarly in Europe, EU-ToxRisk and Safety Evaluation Ultimately Replacing Animal Testing (SEURAT-1) were launched to develop animal free mechanistic based approaches, biological and chemical read-across, and adverse outcome pathways (AOP) for chemical safety assessment (Daneshian et al. 2016).

In vitro HTS assays are generally performed on either 96, 384 or 1536 well microplates, and can be either biochemical (cell-free) or phenotypic (cell-based) in nature. Biochemical assays usually measure the binding of ligands to receptors in competition with the natural ligand in purified target proteins (Blay et al. 2020; Mayr and Bozanic 2009). Phenotypic assays utilize

cell lines specific to organs of interest to determine cytotoxicity, gene expression and cell signalling (Dorval et al. 2018). These assays require small quantities of reagents and test chemicals and are suitable for automation, cost and time effective for analyzing large numbers of chemicals, and animal free (Blay et al. 2020).

1.1.4 Importance of Liver for Toxicity Testing

The liver is a complex organ associated with a multitude of physiological processes such as lipid and cholesterol homeostasis, xenobiotic and macromolecule metabolism, bile acid synthesis, immune system support and glycogenesis. Due to these important activities, the liver is an important target organ for toxicity testing (Malarkey et al. 2005). The liver primarily consists of five cell types: hepatocytes, cholangiocytes, stellate cells, Kupffer cells, and liver sinusoidal endothelial cells (LSECs). Hepatocytes are the most abundant cell type (70-80% of liver volume) and perform most of the functions of the liver. Hepatocytes are polarized with the apical end facing the lumen and the lateral side consists of hepatocytes connected by tight junctions and desmosomes, and organized in cords. Cholangiocytes are the second most common type of cells and line the lumen of the biliary duct. Stellate cells are fat reservoirs and form scar tissue in response to hepatic injury, and Kupffer cells function as hepatic macrophages and produce cytokines (Trefts et al. 2017). LSECs are fenestrated cells that filter solutes and particles between sinusoids and the blood (Malarkey et al. 2005).

One of the key toxicological functions of the liver is to metabolize xenobiotic chemicals using phase I and II metabolic pathways. Phase I metabolizing enzymes participate in oxidation, reduction and hydrolysis of compounds in order to create a hydrophilic metabolite by adding –OH, –SH or $–NH_2$ groups. In some cases, the addition of hydrophilic groups can lead to the activation of a prodrug or procarcinogen. Cytochrome P450 (CYP) enzymes are hemeproteins

that are present in a variety of species and are the most important enzymes in phase I metabolism. There are many CYP450s (~57 in humans) but 90% of phase I metabolism is performed by CYP1A, CYP2C/D/E, and CYP3A (Guengerich 2006). CYP1A substrates are usually planar compounds like polyaromatic hydrocarbons and biphenyls (Brown et al. 2008). The activity of CYP1A is regulated by the receptor, aryl hydrocarbon receptor (AhR), which is present in diverse species including birds (Hahn 2002). CYP2C/D/E metabolize low to medium molecular weight compounds with a broad range of polarities and CYP3A has a broad range of substrates, although most are weakly hydrophilic with aromatic rings (Brown et al. 2008). Expression of CYP2C/D/E and CYP3A are regulated by pregnane X receptor (PXR) and constitutive androstane receptor (CAR) in mammals (Honkakoski and Negishi 2000). However in birds, CYP2C/D/E and CYP3A expression is mediated by the chicken xenobiotic receptor (CXR) (Handschin et al. 2000).

Phase II enzymes further prepare xenobiotic compounds for biliary or renal clearance or inactivate reactive metabolites by making them water-soluble. This is done by adding a glucuronide, sulfate, glutathione or amino acids to compounds by UDP-glucuronosyltransferases (UGTs), sulfotransferases (SULTs), glutathione S-transferases (GSTs) and methyltransferases. The most active phase II enzymes are UGTs and SULTs; UGTs metabolize diverse groups of compounds, whereas SULTs prefer low molecular weight compounds. In addition, SULTs are the primary phase II enzymes in the developing fetus since UGTs are not expressed until 20 weeks of gestation (Jancova et al. 2010).

1.1.5 In Vitro Liver Models

Hepatocytes are the most common hepatic cells used for toxicity testing due to their critical role in hepatic processes. There are three types of *in vitro* liver models that are commonly used: liver slices, primary hepatocytes and immortalized hepatic cell lines. Liver slices contain all types of hepatic cells, retain cellular morphology and architecture of the hepatic environment, and can be cultured for up to 5 days (Palma et al. 2018). The sectioning procedure is fairly simple, avoids the use of proteases that breakdown cellular connections and the preparation does not vary among species (Lerche-Langrand and Toutain 2000). Rat liver slices have the closest gene expression profiles to *in vivo* conditions compared to other *in vitro* models (Elferink et al. 2008). However, gene expression in liver slices becomes more similar to primary hepatocytes than whole liver after 24h. Liver slices also have increased expression of inflammatory genes post slicing (~6h) compared to other *in vitro* models and show signs of necrosis between 48 to 72h; thus, liver slices are more suitable for acute short-term studies (Boess et al. 2003).

Primary hepatocytes, that is, hepatocytes that are directly isolated from livers, have become one of the most common *in vitro* models to determine the metabolism and toxicity of chemicals. Primary hepatocytes retain expression and activity of metabolizing enzymes, transport proteins, and nuclear receptors such as AhR, CAR and PXR, similar to *in vivo*. However, primary hepatocyte cultures show significantly diminished CYP and phase II enzyme expression within 72h of isolation (Hewitt et al 2007). Primary hepatocytes are typically cultured under conventional 2D monolayer conditions, and freshly isolated hepatocytes attach to the surface of the cell culture dish within 4h. In order to re-establish intercellular connections and polarity, hepatocytes form aggregates of 2-10 cells and bile canaliculi are established 24h post-isolation (Wanson et al. 1997). After 48h, hepatocytes lose polarity, proper intercellular

connections and adopt a fibroblast-like flattened morphology. The change in morphology is known as dedifferentiation, which causes loss of metabolic activity in primary hepatocytes (Fraczek et al. 2013). In order to prevent dedifferentiation, primary hepatocytes can be cultured between two layers of collagen or matrigel known as sandwich culture (Soldatow et al. 2013). In this technique, cellular interaction, extracellular matrix, tight junctions and bile canaliculi are re-established for longer durations. Sandwich cultured hepatocytes have improved metabolic competence in terms of gene expression and activity of Phase I and II metabolizing enzymes and are more similar to *in vivo* expression and activity than monolayer culture (Kienhuis et al. 2007). However, a significant decrease in mRNA expression (~50%) and activity (~65%) of phase I metabolizing enzymes between 42 to 72h was observed in sandwich cultures, whereas phase II enzyme expression remained relatively unchanged up to 90h (Mattjis et al. 2009). Primary hepatocytes are excellent options for short-term studies; however, both primary hepatocytes and liver slices rely on animal use.

Immortalized hepatic cell lines are frequently used as an *in vitro* model for toxicity testing due to ease of use. In addition, many cell lines are readily available, can be stored cryogenically for long periods, can be cultured for long durations and do not require animal use. Cells lines are usually derived from cancer or stem cells, or transformed by viruses (Roggen 2011). Some cell lines are poorly characterized, especially for toxicity testing, and hepatic cell lines that are characterized tend to have poor expression of metabolizing enzymes. For example, expression of CYP2D6, CYP2E1 and CYP3A4 was 60, 50 and 100 times lower in the human HepG2 cell line compared to primary hepatocytes (Gerets et al. 2012). In contrast, the human HepaRG cell line had stable expression of CYP1A2, CYP2B6, and CYP3A4 genes and responded to CYP inducers in a similar manner as *in vivo* (Anthérieu et al. 2011; Aninat et al.

2006). The expression and activity of metabolizing enzymes are likely influenced by the methods used to establish the cell line and conventional 2D monolayer cell culture techniques. In normal 2D monolayer cell culture, hepatocytes are forced to adopt a flattened morphology to adhere to cell culture vessels. This physical change in cellular shape is accompanied by diminished cellular interactions and changes in structural components of the hepatocytes. In addition, hepatocytes cultured under 2D conditions are more prone to apoptosis due to loss of the extracellular matrix, which provides cells with environmental stimuli (Vinken and Hengstler 2018). These changes are part of the reason for decreased expression of metabolizing enzymes.

Three-dimensional (3D) cell culture is a rapidly evolving field, which attempts to recreate the complex *in vivo* microenvironment of the cell in order to improve *in vitro* testing. Even though 3D culture is more time intensive and costly compared to 2D culture, the prevalence of 3D cell culture is increasing due to improved intercellular and cell to extracellular matrix interactions, and the spatial arrangement of the cells, which resemble that of *in vivo* conditions (Edmondson et al. 2014). Spheroid culturing is one of the most common 3D culture techniques used for hepatocytes. Hepatic spheroid cultures have re-established polarity and bile canaliculi, (Abu-Absi et al. 2002) and have improved viability, hepatic functions and metabolic competence (Lauschke et al. 2019). Primary hepatocytes cultured as spheroids can be maintained for 35 days with CYP1A2, CYP2D6 and CYP3A4 activities, functional bile canaliculi and low levels of apoptotic markers (Bell et al. 2016). Similarly HepG2 and HepaRG spheroids can be cultured for more than 20 days with functional hepatic biomarkers and CYP activities (Ramaihgari et al. 2017; 2014). Spheroids can be used for repeated dosing experiments or co-culture with other hepatic cells such as Kupffer cells to attain a more similar in vivo microenvironment and are compatible for HTS (Bell et al. 2016, Ramaihgari et al. 2014).

1.1.6 Toxicogenomics and PCR arrays in HTS

Toxicogenomics is a promising approach, with relevant applications to HTS, to measure changes in gene, protein and metabolite expression in order to determine the mechanism of action of a toxicant (Waters and Fostel 2004). It can aid in understanding the mechanisms of action and the adverse effects of chemicals considering modulation in gene expression is one of the first cellular events in response to chemical exposure. Changes in gene expression occur rapidly and at concentrations below those required for apical changes. Gene expression analysis can be incorporated into dose-response studies to determine a point of departure (POD), which is the dose that is likely to cause an adverse effect. POD can be the no-observed-adverse-effect level (NOAEL) or lowest observable adverse effect level (LOAEL) or the benchmark dose (BMD), the dose that will lead to a predetermined change resulting in an adverse effect compared to control (Johnson et al. 2014; Filipsson et al. 2003). Furthermore, changes in cellular pathways induce characteristic gene expression profiles, which can be used to classify chemicals with similar mechanism of actions (Hamadeh et al. 2002).

Gene expression profiling, which examines changes in mRNA expression following chemical exposure is commonly measured using quantitative real-time PCR (RT-qPCR) or RNA sequencing (Bourdon-Lacombe et al. 2015). RT-qPCR is used to measure mRNA expression of a select set of gene markers associated with target pathways and is one of the most sensitive methods (Alexander-Dann et al. 2018). RT-qPCR is frequently used to detect changes in gene expression using customized PCR arrays in avian toxicity testing. This technology permits the assessment of numerous chemicals that can be performed simultaneously and/or in parallel to generate a large amount of data in a short time allowing prediction of toxicity based on molecular signature (Gatzidou et al. 2007). The number of genes and pathways covered by a

PCR array can be customized. For example, the customized species-specific PCR array, ToxChip, has been used in our lab to measure changes in gene expression associated with several biological pathways. The ToxChip is focused on hepatic genes, which are markers of important pathways in the liver (Crump et al. 2016).

1.2 Endocrine Disrupting Chemicals

The endocrine system is responsible for mediating many biological processes including growth and development, metabolism, homeostasis, and reproduction. There are eight major endocrine glands dispersed throughout the body such as pituitary and adrenal glands, and each of these glands secrete hormones that are transported via the bloodstream to target tissues. Hormones are tightly regulated via feedback mechanisms due to their high potencies and short half-lives (Gore et al. 2015). Even though the liver is not an endocrine gland, it is a target of several hormones and plays an essential role in metabolism and regulation of hormones (Burra 2013). In oviparous species, such as birds, the liver is an important organ involved in hormonal control of reproduction and produces many important precursor proteins such as vitellogenin (Kime et al. 1999). Chemicals that can interfere with the endocrine system are known as endocrine disrupting chemicals (EDCs). An EDC is defined as, "an exogenous agent that interferes with synthesis, secretion, transport, metabolism, binding action, or elimination of natural blood-borne hormones that are present in the body and are responsible for homeostasis, reproduction, and developmental process" by the Environmental Protection Agency (EPA) (Diamanti-Kandarakis et al. 2009). EDCs represent a diverse group of chemicals that are widespread in the environment and have been detected in both humans and wildlife. The primary exposure route is believed to be via the diverse commercial and industrial products in which

EDCs can be found, including pesticides, building materials, and plastics (Casals-Casas and Desvergne 2011).

1.2.1 Bisphenol A

Bisphenol A (BPA) was first synthesized in the 1890s and has been used as a plasticiser since the 1950s. BPA is used as a monomer in the synthesis of polycarbonate plastics and epoxy resins. It is one of the highest volume chemicals produced worldwide with 7.7 million metric tons used in 2015 (Almeida et al. 2018). As a component of polycarbonate plastics, BPA is found in a wide range of products such as electronic equipment, optical devices, and household plastic products. Epoxy resins are used for a variety of applications such as protective coatings (e.g. metal containers and thermal paper), adhesives (e.g. in sports equipment), or as structural reinforcement in composite materials (e.g. in polyvinyl chloride plastics). Due to the extensive use of BPA, it is widespread in the environment and has been detected in diverse environmental samples, including humans, wildlife and abiotic compartments. Concentrations of BPA ranging from 1.96 to 56 µg/L and 12 to 3 300 ng/g were detected in surface water and indoor dust, respectively (Chen et al. 2016; Corrales et al. 2015). In addition, BPA was detected in the liver (~0.001 µg/g wet weight) of the great cormorant (*Phalacrocorax carbo*) (Nakayama et al. 2006).

The endocrine disrupting properties of BPA came into focus in the 1990s when a research group reported estrogenic activity in yeast that was associated with BPA that leached from autoclaved polycarbonate flasks (Krishnan et al. 1993). The estrogenic effects of BPA along with perturbations in androgen and thyroid systems have been reported in *in vivo* and *in vitro* studies (Siracusa et al. 2018; Rochester and Bolden 2015; Rubin 2011). BPA was assessed under Canada's Chemical Management plan in 2008-2009 and met the criteria for having immediate or long-term harmful effects on humans and the environment, and as a result was added to the

Toxic Substances List. In 2010, Canada banned the importation and sale of baby bottles containing BPA (Government of Canada, 2010). BPA is classified as a substance of very high concern (SVHC) by the European Chemical Agency (ECHA) due to its endocrine disrupting potential and effects on reproductive toxicity. In the European Union, the use of BPA in baby bottles was banned in 2011 and restrictions on other infant products and thermal paper came into effect in 2018 and 2020 (ECHA 2020). Due to the toxic properties and restrictions on BPA, manufacturers have shifted to the production of "BPA-free" products, which contain structural analogs of BPA with similar chemical properties.

1.2.2 Bisphenol A Replacement Compounds

The production and use of BPA replacement compounds in consumer products are on the rise and some have been detected in environmental samples. To date, a large number of alternatives (~30-40) have been identified as having properties similar to those of BPA. Unfortunately, with the exception of bisphenol S, the majority of replacement compounds are relatively data poor in terms of toxicity endpoints. Studies have found that certain replacement compounds have similar toxicity as BPA and can target diverse biological pathways (Pelch et al. 2019). Five BPA replacement compounds identified as priorities for data generation by Canada's Chemicals Management Plan were chosen for this thesis: 1) bis(4-hydroxyphenyl)methane (Bisphenol F; BPF), 2) bis-(3-allyl-4- hydroxyphenyl)sulfone (TGSH/TGSA), 3) 1,7-bis(4-hydroxyphenylthio)-3,5-dioxaheptane (DD-70), 4) 2,2-bis(4- hydroxyphenyl) hexafluoropropane (Bisphenol AF; BPAF), and 5) 4-hydroxyphenyl 4-isopropoxyphenyl sulfone (BPSIP).

The five BPA replacement compounds included in this thesis have one or two phenol groups connected by a carbon or other scaffold and side chains. The structures of the replacements compounds are shown in Figure 1.1. BPF is structurally similar to BPA but is

missing the two methyl groups on the central carbon. BPF is used in the synthesis of epoxy resins and is found in industrial and consumer products such as tank and pipe linings, electrical varnishes, adhesives, lacquers and the inner coating of metal food containers. TGSH is a sulfone (RSO_2R) derivative of BPA with 2 phenol groups connected by a central sulfone group and each phenol group contains an allyl ($-CH=CHCH_2$) side chain (Figure 1.1). TGSH is used as a developer in thermal paper and is found in cash receipts (Bjornsdotter et al. 2017). There was a significant increase in the production of TGSH from 4.5 to 225 tonnes in 2002 to 452 to 4535 tons in 2006 in the United States (EPA 2002). Among the replacement compounds included in this thesis, DD-70 is structurally the most different from BPA. Similar to BPA, DD-70 has two phenol groups but these groups are connected by a chain consisting of sulfur, oxygen and carbon atoms. DD-70 is another replacement used as a developer in thermal paper (EPA 2015) and is found in cash receipts (Keminer et al. 2009). In terms of toxicity, there are limited data available. BPAF is structurally very similar to BPA except that the two methyl (CH_3) groups on the central carbon are replaced with two trifluoromethyl (CF_3) groups (Figure 1.1). BPAF is used as a monomer in polycarbonate and polymers and as a cross linker for certain fluoroelastomers, which are fluorinated synthetic polymers that can withstand harsh temperature and/or chemicals; as such, it has diverse industrial applications. BPAF-containing fluoroelastomers were approved by the U.S. Food and Drug Administration and these can contain up to 2% BPAF by weight (NTP 2008). The estimated use of BPAF is between 100 to 1000 tons/ year in the EU (ECHA 2018). BPSIP is structurally more similar to TGSH than BPA; a central sulfone group joins the two benzene rings and one of the phenol hydroxyl groups is substituted with an isoproxy group (C_3H_7O) (Figure 1). BPSIP has been detected in thermal paper from the Netherlands

(Bjornsdotter et al. 2017) and Switzerland (Goldinger et al. 2015). The highest concentration was found in thermal paper, 3.4–13.2 mg/g, in Switzerland (Goldinger et al. 2015).

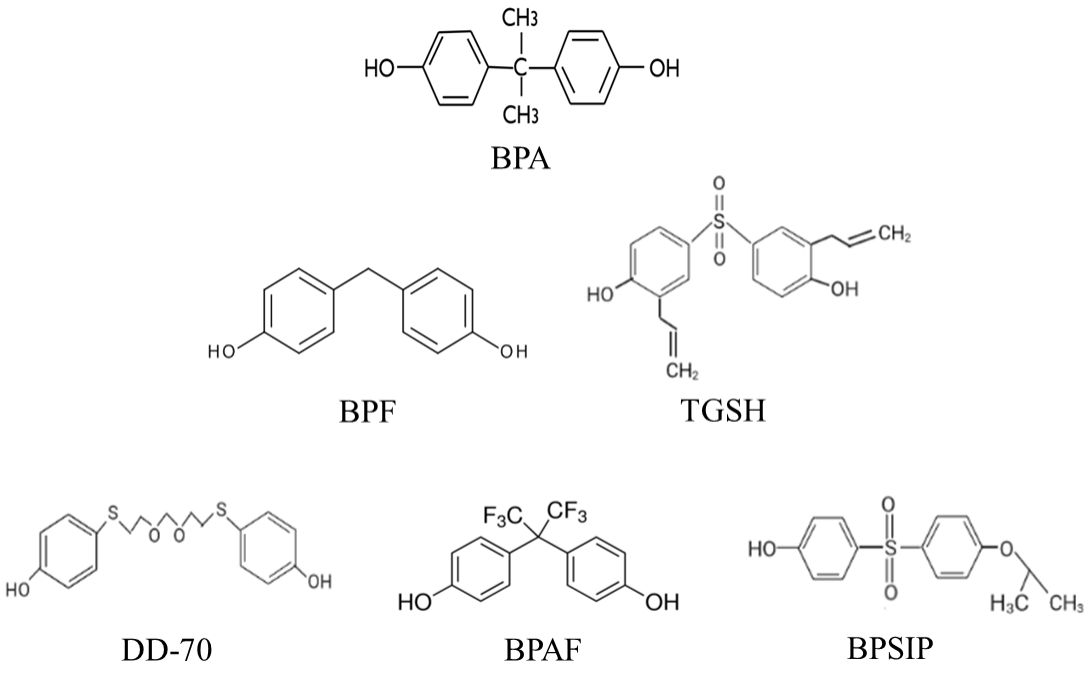

Figure 1.1. Chemical structures of BPA and the five BPA replacement compounds, BPF, TGSH, DD-70, BPAF and BPSIP.

1.2.3 Environmental Occurrence and Fate of BPA Replacement Compounds

Compared to BPA, BPF and BPAF have been detected in environmental samples at similar concentrations. In sediment samples from Japan, South Korea and the United States, BPF concentrations ranged from 3.24-338 ng/g d.w. (Liao et al. 2012). BPF concentrations were greater in surface water (~1000 ng/L) than sediment samples in China, Japan and South Korea (Yamazaki et al. 2015). In the Tamagawa River of Tokyo, concentrations of BPF as high as 2850 ng/L were detected, which is greater than the 1500 ng/L predicted no-effect concentration for

BPA set by the EU (Chen et al. 2016). BPAF (0.9-246 ng/L) has been detected at similar concentrations as BPA (6.6–74.6 ng/L) in river water, but at lower concentrations (1.4-43 ng/L) than BPA (0.18-2010 ng/L) in sediment samples in China (Yang et al. 2014). There is no information available on the environment occurrence of TGSH, DD-70 or BPSIP.

The bioconcentration factor (BCF) is often used to assess the tendency for a particular compound to accumulate in an organism from the environment. BPF, TGSH, DD-70 and BPSIP have BCF values less than 100, indicating low potential for accumulation. *In silico* aerobic and anaerobic biodegradation models show that TGSH and DD-70 have a high potential to be persistent in the environment with a half-life of 75 days in soil (EPA 2015). BPAF has been detected in phytoplankton and fish (anchovy, whitebait) in China and based on the lipophilic nature of the compound it is likely to accumulate in organisms at higher concentrations than BPA (Wang et al. 2017).

1.2.4 Toxicokinetics of Bisphenol A and Replacement Compounds

BPA was rapidly metabolized to an inactive metabolite BPA- glucuronide (BPA-G) via glucuronidation by UGT2B1 following oral exposure in rats and humans (Nachmann et al. 2015; Volkel et al. 2008). Plasma concentrations of BPA were below the detection limit after 18h in rats exposed to 10 or 100 mg/kg of BPA (Pottenger et al. 2000) and it could pass the placental barrier in pregnant rats (Kurebayashi et al. 2005). In embryos, unconjugated BPA was detected instead of BPA-G, suggesting that babies might not be able to metabolize BPA properly (Vandenberg et al. 2007). BPA was biotransformed into an active metabolite, 4-methyl-2,4-bis(4-hydroxyphenyl) pent-1-ene via CYP450 oxidation in MCF-7 cells incubated with rat S9 fraction for 1h and may account for differences in metabolism observed between species (Yoshihara et al. 2001).

In pregnant and non-pregnant rats given a single oral dose of 7 mg/kg of tritium-labeled BPF ([3H] BPF), the compound was rapidly absorbed and distributed throughout the body. The major metabolite was BPF-sulfate generated by phase II sulfonation, which was mainly excreted in the urine within 6h of exposure. The highest deposition of [3H] BPF was found in the liver and BPF was able to pass the placental barrier in pregnant rats (Cabaton et al. 2006).

There are no toxicokinetics studies available for TGSH or DD-70 in any species. Exposure to TGSH in chicken embryos resulted in increased hepatic expression of CYP3A7, UGT1A9 and SULT1E1 (Crump et al. 2018), indicating phase I and II metabolism in a similar manner as BPA.

BPAF is rapidly metabolized to the major metabolite BPAF glucuronide (BPAF-G), via glucoronidation in rats (Li et al. 2013) and in rodent hepatocytes (Waidyanatha et al. 2015). BPAF-G was found to be a biologically active metabolite *in vitro* (Skledar et al. 2019). The main enzyme responsible for BPAF-G production was UGT2B7 in human liver microsomes (Li et al. 2013). The highest concentrations of BPAF were detected in the liver following oral or intravenous exposure routes and clearance of BPAF was slower than BPA in human and rodent hepatocytes (Waidyanatha et al. 2015). BPAF was found in maternal plasma, cord plasma, and placenta samples ranging from 9 to 20, 26 to 168, and 16 to 60 pg/g, respectively (Pan et al. 2020).

BPSIP was detected in maternal plasma, cord plasma, and placenta samples ranging from 230 to 2 400, 129 to 686, and 78.5 to 1 310 pg/g, respectively. BPSIP was the most common replacement compound detected in these samples after BPA (Pan et al. 2020). BPSIP was more commonly detected than BPA in plasma of cashiers, suggesting that clearance of BPSIP from the body may be slower than BPA (Thayer et al. 2016).

1.2.5 Toxicological Targets of Bisphenols

1.2.5.1 Estrogen pathway

Estrogen is a steroid hormone derived from cholesterol and plays a critical role in development and maintenance of physiological systems including reproductive, cardiovascular, immune, neuroendocrine, adipose and skeletal. Estrogen primarily acts via two mechanisms, genomic and non-genomic. Genomic signalling is carried out by the nuclear receptors, estrogen receptors (ER) α and β, which control complex processes such as carcinogenesis, growth and proliferation (Fuentes and Silveyra 2019). In genomic signalling, estrogen binds to either ERα or ERβ in the cytoplasm of target cells resulting in receptor dimerization followed by the translocation of the receptor-ligand complex to the nucleus, where it binds to the estrogen response element (ERE) to modulate the transcription of target genes (Fuentes and Silveyra 2019). In non-genomic signalling, estrogen binds to G-coupled estrogen receptor (GPER1; formerly called GPR30) in the cell membrane resulting in activation of secondary messengers and signalling pathways. Non-genomic signalling carries out rapid estrogen actions that occur much faster than genomic signalling and play critical roles in the nervous system and liver (Bjornstorn and Sjoberg 2005). Furthermore, there are a group of orphan nuclear receptors known as estrogen related receptors, ERRα, ERRβ and ERRγ, which are closely related to ERα and ERβ, and can modulate estrogen response (Giguere 2002). Interestingly, estrogen is not a natural ligand of these receptors, but synthetic estrogens like diethylstilbesterol can bind to ERRs (Tremblay and Giguere 2007).

BPA can bind to both ERα and ERβ, with a higher affinity for ERβ. However, BPA has a much lower affinity than 17β estradiol (E2) (1000 and 100 000-fold less, for ERα and ERβ

respectively) (Kurosawa et al. 2002; Matthews et al. 2001). The half maximal inhibitory concentration (IC50) values of BPA for ERα and ERβ binding were 1.04 μM and 1.32 μM, respectively (Matsushima et al. 2010) (Table 1.1). BPA has a stronger binding affinity for GPER1 than ERα and ERβ and the IC50 value was 0.693 μM in HEK293 cells (Thomas & Dong 2006). For example, low concentrations of BPA (1-200 nM) induced GPER1-dependent pathways (Thomas & Dong, 2006; Nadal et al. 2000). BPA binds very strongly to ERRγ with an IC50 value of 0.0131 μM and prefers ERRγ 105x more than ERα (Takayanagi et al. 2006; Okada et al. 2008; Tohme et al. 2014). In zebrafish cell lines, BPA has freater affinity for ERα (EC50 = 0.47 to 0.81 μM) than ERβ1 and ERβ2 (EC50 = 3.3 to 5.5 and 2.8 to 4.2 μM) (Table 1.1) (Pinto et al. 2019; Le Fol et al. 2017).

BPF can bind to both ERα and ERβ, and *in silico* data suggest that, like BPA, it has a higher affinity for ERβ (Goldinger et al. 2015). The IC50 values of BPF for ERRγ and GPER1 were 0.13 and > 100 μM in the HeLa and SK-BR3 cell lines (Cao et al. 2017; Okada et al. 2008) (Table 1.1). BPF was less estrogenic than BPA in terms of ERE binding in the human breast cancer MCF-7 cell line (Kitamura et al. 2015). In zebrafish (*Danio rerio*) cell lines, the IC50 values for ERα, Erβ1 and Erβ2 were 5.8, 5.4 and 2.4 μM (Le Fol et al. 2017) (Table 1.1). In zebrafish larvae, estrogenic activity of BPF and BPA was reported at 5 and 10 μM, suggesting higher estrogenic activity of BPF than BPA *in vivo* (Le Fol et al. 2017).

TGSH showed no ERα or ERβ mediated activity or antagonism in HepG2 or MCF7 cell lines (Pelch et al. 2019) and was also inactive in a reporter gene assay (Keminer et al. 2020; Bjornsdotter et al. 2017). Likewise, DD-70 was inactive in ERα and ERβ ligand binding assays (Keminer et al. 2020).

BPAF can bind to both ERα and ERβ and the binding potency for ERβ (IC50 = 0.019 μm) was three times greater than ERα (IC50 = 0.054 μm) using a radio ligand binding assay in human HeLa cells (Matsushima et al. 2010) (Table 1.1). BPAF (5 nM) induced ERβ expression in two human breast cancer cell lines, MCF7 and MDA-MB-231 (ERα negative cell line) (Okazaki et al. 2018). In contrast, the affinity was greater for ERα in zebrafish cell lines (Pinto et al. 2019; Cano-Nicolau et al. 2016). The EC50 values for ERα, Erβ1 and Erβ2 were 0.084. 0.76 and 0.9 μm in zebrafish cell lines (Pinto et al. 2019) (Table 1.1). Upregulation of ERα mRNA expression was observed following exposure to BPAF (0.5 μM) for 8h in male medaka (Yamaguchi et al. 2015) and in zebrafish larvae after 7 days of exposure (Chen et al. 2018). Exposure to 1 μM BPA or BPAF resulted in 36 and 43-fold upregulation of aromatase gene, CYP19A1B, in brains of 7 day old zebrafish larvae (Cano-Nicolau et al. 2016). BPAF is a full agonist of ERα in reporter gene assays (Skledar et al. 2019, Matsushima et al. 2010), while acting as an antagonist of ERβ (Kojima et al. 2019; Matsushima et al. 2010). The agonistic activity of BPAF towards ERα was greater than BPA in several cell lines and yeast assays (Skledar et al. 2019; Pelch et al. 2019; Fic et al. 2014; Teng et al. 2013). BPAF was the most potent among replacement compounds and BPA in terms of induction of ERE-mediated transcription (Mesnage et al. 2017; Kitamura et al. 2005). In addition to binding to nuclear ERs, BPAF bound to GPER1 in two human breast cancer cell lines, MCF7 and SKBR3, and increased GPER1 mRNA expression in mouse embryonic stem cell-derived cardiomyocytes (Yang et al. 2020; Cao et al. 2017). The binding affinity of BPAF for GPER1 was 3 μM (Cao et al. 2017).

While fewer studies have investigated the estrogenic activity of BPSIP, this replacement compound (10 μM) was found to have ERα-mediated activity in ER transfected HepG2 cells and the IC50 values for ERα and Erβ were 2.01 and 1.33 μM *in silico* (Goldinger et al. 2015) (Table

1.1). BPSIP had no ERβ antagonism in MCF7 cells (Pelch et al. 2019) and was inactive in a reporter gene assay (Keminer et al. 2020; Bjornsdotter et al. 2017). In contrast, BPSIP (50 μg/mL) upregulated the mRNA expression of ERα and ERβ and increased the estrogen to testosterone (E2/T) ratio in male zebrafish. In general, the endocrine disrupting properties were less potent than BPA in zebrafish (Lee et al. 2018).

Table 1.1. Half maximal inhibitory concentration (IC50) and half effective maximal concentration (EC50) of BPA and the five replacement compounds for estrogen receptors in human and zebrafish cell lines. '-' indicates no data available.

Chemicals	Human cell lines IC50 (μM)				Zebrafish cell lines EC50 (μM)		
	Erα	**ERβ**	**ERRγ**	**GPER1**	**Erα**	**ERβ1**	**ERβ2**
BPA	1.03[a]	0.9[a]	0.01[b]	0.63[c]	0.47-0.81[e,f]	3.3-5.5 [e,f]	2.8-4.2 [e,f]
BPF	-	-	0.13[b]	>100[d]	5.8[e]	5.4[e]	2.4[e]
TGSH	-	-	-	-	-	-	-
DD-70	-	-	-	-	-	-	-
BPAF	0.054[a]	0.019[a]	0.358[b]	3[d]	0.084[f]	0.76[f]	0.9[f]

[a]Matsushima et al. 2010
[b]Okada et al. 2008
[c]Thomas and Dong 2006
[d]Cao et al. 2017
[e]Le Fol et al. 2017
[f]Pinto et al. 2019

1.2.5.2 Vitellogenin induction

Vitellogenin (VTG) has been widely used as a biomarker for estrogenic endocrine disrupting compounds in the environment. VTG, an egg yolk protein precursor, is synthesized in the liver after stimulation by estrogen after which it is transported to maturing oocytes through the blood stream (Sumpter and Jobling 1995). Given the dependency upon estrogen for VTG synthesis, low plasma concentrations and mRNA expression of VTG are observed in males and

juveniles of oviparous species. BPA (10 and 100 µM) increased VTG expression in primary hepatocytes of embryonic chicken (Ma et al. 2015) and upregulated VTG mRNA expression in zebrafish embryos (Chow et al. 2013).

BPF upregulated VTG mRNA expression in a concentration dependent manner starting from 10 µg/L in male medaka and zebrafish, but no change was observed in females (Yang et al. 2016; Yamaguchi et al. 2015). Long term exposure to BPF (0.1 to 25 µg/L) increased VTG mRNA expression and protein content in the liver of zebrafish, and was more estrogenic than BPA after 7 days exposure (Qiu et al 2009; Moreman et al. 2017; Shi et al. 2015; LeFol et al. 2017). One of the other replacement compounds, BPAF, increased mRNA expression and plasma VTG at concentrations of 25 µg/L and 0.5 mg/L, respectively, in male zebrafish following long-term exposure (Shi et al. 2015; Song et al. 2014; Yang et al. 2014). There are no data available for TGSH, DD-70 and BPSIP on vitellogenin induction.

1.2.5.3 Thyroid hormone pathway

Thyroid hormone (TH) signalling plays a major role in metabolic regulation, growth and development. TH signalling is divided into two pathways, genomic and non-genomic. In genomic signalling, triiodothyronine (T3), the active form of TH, binds to nuclear receptors, TRα or TRβ, and the complex binds to a thyroid response element within target genes to activate or repress gene expression (Anyetei-Anum et al. 2018). In non-genomic signalling, T3 interacts with integrin receptors on the cell membrane and activates signalling pathways (Mullur et al. 2014).

Even though BPA is mainly regarded as a xenoestrogen, studies have found that BPA can also interfere with TH signaling as it is structurally similar to T3. BPA (0.01-100 µM) can bind

to both TRs, repress TRβ activity in cell lines (Sheng et al. 2012; Moriyama 2002) and block T3 from binding to TRs and integrin receptors (Sheng et al. 2012; Moriyama et al. 2002). Low dose (0.001 μM) BPA exposure resulted in the upregulation of genes involved in thyroid hormone synthesis and transcription regulation in a thyroid cell line and downregulated TRβ mRNA expression in a pituitary cell line (Lee et al. 2017; Gentilcore et al. 2013). *In vivo* studies examining the effects of low dose BPA on TH signaling reported that *in utero* exposure to BPA (0.6 μg/pup) in rats resulted in elevated serum TH levels in males and females (Zoeller et al., 2005). Similarly, increases in TH levels were observed in zebrafish exposed to BPA (0.4 mg/L) (Lee et al. 2019). In tadpoles (*Xenopus laevis*), BPA downregulated expression of TRα and TRβ and inhibited tail resorption (Iwamuro et al. 2006) and blocked TRβ binding in *Xenopus laevis* oocytes (Heimeier et al. 2009). The results from these studies suggest that BPA mainly acts as a TR antagonist in the presence of T3 and as a TR agonist in the absence of T3.

Similar to BPA, BPF antagonized T3-induced gene transcription in tadpoles (Zhu et al. 2018). There was an increase in serum T3 concentrations and upregulation of genes involved in TH synthesis and transport in zebrafish exposed to BPF (2 mg/L) (Lee et al. 2019). BPF had greater binding potency to TRβ than TRα, but the potency was less than BPA (Zhang et al. 2018). Another BPA replacement, BPAF, also upregulated the expression of genes involved in thyroid synthesis in a thyroid cell line (Lee et al. 2017). In zebrafish, exposure to BPAF caused upregulation of TH synthesis and the expression of transport genes and downregulation of TRα (Tang et al. 2015). BPAF also caused a decrease in whole body T3 levels in zebrafish larvae (Tang et al. 2015). There are no data available for TGSH, DD-70 and BPSIP on thyroid signalling pathway.

1.2.5.4 Hepatic lipid regulation

Lipids are structural components of the cell membrane and precursors of bile acids and steroid hormones. Changes in hepatic lipid metabolism are associated with several disorders, such as non-alcoholic fatty liver disease (steatosis) and cholestasis. Cholesterol and fatty acid synthesis are controlled by sterol regulatory element binding proteins (SREBPs), which are regulators of lipid synthesis (Eberle et al. 2004). Two specific nuclear receptors, liver X receptor (LXR) and farnesoid X receptor (FXR), are primarily involved in maintaining lipid homeostasis by regulating the expression of SREBPs and other genes involved in lipid metabolism (Nakagawa and Shimano 2018).

In addition to endocrine activities, BPA can alter lipid synthesis and regulation. In HepaRG cells, BPA (5 nM) induced hepatic steatosis but the expression of lipid metabolism genes were unchanged (Bucher et al. 2017). Long-term exposure to BPA (50 μg/kg/day) in adult mice resulted in upregulation of hepatic genes related to cholesterol (SREBP) and lipid synthesis and upregulated expression of genes related to bile acid synthesis (Marmugi et al. 2014; 2012). Mice exposed to BPA had elevated plasma cholesterol levels and lipid accumulation in the liver (Marmugi et al. 2012). Perinatal exposure to BPA (10 μg/ml) led to an increase in lipogenic gene and protein expression, and an increase in triglyceride levels. In the same study, there was lipid accumulation in the liver and hepatocytes were condensed in mice exposed to BPA (Lin et al. 2019). Strakovsky et al. (2015) found that perinatal exposure to BPA caused sex-specific changes. In males, there was a decrease in the expression of genes related to triglyceride synthesis, whereas the same genes were upregulated in females. In both males and females, plasma free fatty acid levels were elevated. Similarly, expression of genes associated with lipid

synthesis, metabolism and fatty acid oxidation were upregulated following low dose exposure to BPA in rare minnows (*Gobiocypris rarus*) (Guan et al. 2018).

Perinatal exposure to BPF (100 ng/g bw/day) in male mice resulted in changes in hepatic lipid metabolites along with an increase in lipid accumulation in the liver (Meng et al. 2019a). In HepG2 cells, BPF (10 μM) caused a similar increase in lipid content as BPAF; however, BPAF upregulated genes related to lipogenesis, fatty acid β oxidation, and lipid nuclear receptors (LXR and FXR) (Liu et al. 2020). There was an increase in lipid accumulation in adipose cells following exposure to BPAF (0.1 μM) and the metabolite, BPAF-G (1 μM), along with an increase in gene expression related to fatty acid synthesis (Skledar et al. 2019). BPAF exposure (100 ng/g bw/day) led to a decrease in the expression of genes related to hepatic fatty acid and triglyceride synthesis, whereas fatty acid β oxidation genes were upregulated (Meng et al. 2019b). There are no data available for the effects of TGSH, DD-70 and BPSIP on lipid regulation.

Table 1.2. Effects of BPA, BPF and BPAF on plasma cholesterol, lipid accumulation and triglyceride levels in *in vivo* and *in vitro* studies. '-' indicates no data available.

Chemical	Model	Plasma cholesterol	Lipid accumulation	Triglyceride
BPA	Mouse	Increase	Increase	Increase
BPF	Mouse	-	Increase	-
BPAF	Cell line	-	Increase	-

1.2.6 Toxicity of Bipshenols in Birds

Exposure to EDCs can have adverse effects in avian species. For example, DDT caused feminization of male herring gull embryos leading to a decrease in population (Halldin et al. 1999). Studies looking at the effects of bisphenols in birds have mainly focused on changes in gonad morphology and development in embryonic chickens following *in ovo* exposures. Estrogen is the differentiating hormone for gonadal development in birds and developmental exposure to xenoestrogens can have serious adverse effects (Giesy et al. 2003). *In ovo* exposure to BPA (200 μg/g egg) in chickens resulted in feminization of the left testis in 55% of the samples on embryonic day 19 (E19). Similarly, Jessl et al. (2018) noted a decrease in cortex thickness (by 26%) and surface area of the left ovaries, whereas there was an increase in cortex thickness by up to 62% in the left testis in chicken embryos at concentrations of ≥ 75 μg/g egg BPA . In adult quail exposed to BPA (200 μg/g egg), there was no feminization of the gonads in males (Halldin et al. 2001). Overall, data suggest that birds are more vulnerable to the endocrine disrupting effects of BPA during embryonic development.

In ovo exposure to BPF and BPAF (210 nmol/g egg) in chickens resulted in an increase in cortex thickness in the left testis that was similar to the ovary and following BPAF exposure, there were cells resembling oogonia in the left testis. Furthermore, BPAF caused an increase in gallbladder somatic index (Mentor et al. 2020). Hepatic expression of genes related to bile acid synthesis and cholesterol homeostasis were upregulated in mid-incubation embryonic chickens (E11) following *in ovo* exposure to 180 μg/g TGSH, suggesting a disruption in the bile acid pathway by bisphenol replacement compounds. The TGSH study did not look at the morphological changes in gonad development, but there was a 10-fold increase in the expression of apolipoprotein II, an estrogen responsive gene, at mid-incubation. The expression of VTG was

not modulated by TGSH in chicken embryos (Crump et al. 2018). BPAF and TGSH egg injection studies indicate the potential of BPA replacement compounds to target other pathways in addition to estrogen signalling in developing chicken embryos.

1.3 Thesis Overview

1.3.1 Rationale for Thesis

Avian toxicity testing involves *in vivo* studies to determine mortality or other apical endpoints. *In vivo* tests are usually conducted on laboratory models (i.e. chickens or quails) but can also be performed on wild species such as mallard ducks. Toxicity testing is undergoing a shift from whole animal, *in vivo* studies to mechanistic-based *in vitro* studies. This shift has led to the emergence of *in vitro* methods to predict adverse effects, and screen and prioritize chemicals for further testing. Primary embryonic hepatocytes from chicken (CEH) and double-crested cormorant (DCEH) are the main avian *in vitro* liver models for chemical screening and prioritization used in Environment and Climate Change Canada's Molecular Toxicology lab. The chicken (*Gallus domesticus*) represents a laboratory model for avian toxicology studies as its physiology, development and genetics are well characterized, and fertilized chicken eggs are commercially available year-round. However, chickens are often more sensitive to the toxic effects of chemicals compared to wild bird species and thus may not represent ideal sentinels for risk assessment. Double-crested cormorants (*Phalacrocorax auritus*; DCCO) are piscivorous, colonial water birds that occupy a high trophic position in the aquatic food web and are therefore used as wildlife indicator species in freshwater (e.g. Great Lakes) and marine environments across Canada.

Some of the shortcomings of these primary hepatocyte models are that they undergo dedifferentiation and necessitate animal use for culture. The immortalized chicken hepatic cell line, leghorn male hepatoma (LMH), is a possible animal free alternative that has been used for a few toxicity studies, but the metabolic activity of this cell line is unknown. The metabolic activity of the LMH cell line needs to be characterized to determine its utility for toxicity testing. In addition to the aforementioned drawbacks of primary culture, for wild species it is difficult to obtain eggs from the field. Development of an immortalized DCCO hepatic cell line with metabolic competence would diminish the need to use DCEH for toxicity testing.

BPA replacement compounds have been identified as high priority chemicals for environmental risk assessment by Canada's Chemicals Management Plan. BPA replacement compounds have similar structures, chemical properties and applications as BPA. The production and use of replacement compounds are increasing and are likely to surpass BPA in certain applications like thermal paper in the future. There are limited studies evaluating the toxicity of BPA replacement compounds in avian species and the results from existing studies indicate that replacement compounds could have similar toxicity as BPA. Previous studies have found that birds are vulnerable to the adverse effects of endocrine disrupting compounds in the environment. This thesis directly addresses the need to identify and characterize the five BPA replacements compounds that may be a toxicological concern for birds and prioritize those with greatest potential for harm for further testing.

1.3.2 Thesis Objectives and Chapter Objectives

The overall goals of this thesis are to: 1) generate evidence to support the use of the LMH cell line and a double-crested cormorant hepatic cell line, DCH22, as alternatives to primary hepatocytes for avian ecotoxicological screening; 2) generate novel ecotoxicological data for

screening and prioritizing five BPA replacement compounds using cell culture and *in vitro* toxicogenomics approaches; 3) generate *in vivo* ecotoxicity data using an avian early-life stage model and toxicogenomics approaches for two prioritized BPA replacement compounds. The specific objectives addressed in each chapter are:

Chapter 2

- ✓ To investigate the metabolic competency of the LMH cell line in order to determine if it is a suitable alternative to primary hepatocytes for chemical screening
- ✓ To compare metabolic activity and gene expression in LMH cells cultured as 2D monolayers and 3D spheroids by measuring: CYP1A activity, CYP1A4/5 mRNA expression, and AhR mediated gene expression

Chapter 3

- ✓ To compare CYP1A metabolism-dependent bioactivation of chemicals in LMH cells cultured as 2D monolayers or 3D spheroids following exposure to the environmental mutagen, benzo(a)pyrene, by measuring: CYP1A activity, CYP1A4/5 and DNA damage response mRNA expression, and DNA double-strand breaks

Chapter 4

- ✓ To develop and characterize a continuous DCH22 hepatic cell line for screening chemicals by examining: markers of hepatocytes, CYP1A and CYP3A activity, and the expression of genes associated with phase I and II metabolism

Chapter 5

- ✓ To compare the effects of the five BPA alternatives on cell viability and gene expression in CEH and DCEH, and to prioritize the replacements for further testing

Chapter 6

- ✓ To screen the five BPA replacement compounds in LMH 3D spheroids and to prioritize them for further testing by comparing cytotoxicity and gene expression
- ✓ To prioritize BPA replacements for dose-response gene expression

Chapter 7

- ✓ To determine the effects of early-life stage *in ovo* DD-70 and BPAF exposure on viability, development and hepatic gene expression at two distinct stages of embryonic development; mid-incubation (day 11) and pipping (day 20).

1.4 References

Abu-Absi SF, Friend JR, Hansen LK, Hu WS. 2002. Structural polarity and functional bile canaliculi in rat hepatocyte spheroids. *Experimental Cell Research* 274:56-67. DOI: 10.1006/excr.2001.5467.

Alexander-Dann B, Pruteanu LL, Oerton E, Sharma N, Berindan-Neagoe I, Modos D, Bender A. 2018. Developments in toxicogenomics: understanding and predicting compound-induced toxicity from gene expression data. *Molecular Omics* 14:218-236. DOI: 10.1039/c8mo00042e.

Almeida S, Raposo A, Almeida-Gonzalez M, Carrascosa C. 2018. Bisphenol A: Food Exposure and Impact on Human Health. *Comprehensive Reviews in Food Science and Food Safety* 17:1503-1517. DOI: 10.1111/1541-4337.12388.

Aninat C, Piton A, Glaise D, Le Charpentier T, Langouet S, Morel F, Guguen-Guillouzo C, Guillouzo A. 2006. Expression of cytochromes P450, conjugating enzymes and nuclear receptors in human hepatoma HepaRG cells. *Drug Metabolism and Disposition* 34:75-83. DOI: 10.1124/dmd.105.006759.

Antherieu S, Chesne C, Li RY, Guguen-Guillouzo C, Guillouzo A. 2012. Optimization of the HepaRG cell model for drug metabolism and toxicity studies. *Toxicology in Vitro* 26:1278-1285. DOI: 10.1016/j.tiv.2012.05.008.

Anyetei-Anum CS, Roggero VR, Allison LA. 2018. Thyroid hormone receptor localization in target tissues. *Journal of Endocrinology* 237:R19-R34. DOI: 10.1530/joe-17-0708.

Anzenbacher P, Anzenbacherova E. 2001. Cytochromes P450 and metabolism of xenobiotics. *Cellular and Molecular Life Sciences* 58:737-747. DOI: 10.1007/pl00000897.

Augspurger TP, Tillitt DE, Bursian SJ, Fitzgerald SD, Hinton DE, Di Giulio RT. 2008.Embryo toxicity of 2,3,7,8-tetrachlorodibenzo-p-dioxin to the wood duck (Aix sponsa). *Archives of Environmental Contamination and Toxicology* 55(4):659-669. DOI: 10.1007/s00244-008-9198-2.

Bell CC, Hendriks DFG, Moro SML, Ellis E, Walsh J, Renblom A, Puigvert LF, Dankers ACA, Jacobs F, Snoeys J, Sison-Young RL, Jenkins RE, Nordling A, Mkrtchian S, Park BK, Kitteringham NR, Goldring CEP, Lauschke VM, Ingelman-Sundberg M. 2016. Characterization of primary human hepatocyte spheroids as a model system for drug-induced liver injury, liver function and disease. *Scientific Reports* 6. DOI: 10.1038/srep25187.

Bjornsdotter MK, de Boer J, Ballesteros-Gomez A. 2017. Bisphenol A and replacements in thermal paper: A review. *Chemosphere* 182:691-706. DOI: 10.1016/j.chemosphere.2017.05.070.

Bjornstrom L, Sjoberg M. 2005. Mechanisms of estrogen receptor signaling: Convergence of genomic and nongenomic actions on target genes. *Molecular Endocrinology* 19:833-842. DOI: 10.1210/me.2004-0486.

Blay V, Tolani B, Ho SP, Arkin MR. 2020. High-Throughput Screening: today's biochemical and cell-based approaches. *Drug Discovery Today* 25:1807-1821. DOI: 10.1016/j.drudis.2020.07.024.

Boess F, Kamber M, Romer S, Gasser R, Muller D, Albertini S, Suter L. 2003. Gene expression in two hepatic cell lines, cultured primary hepatocytes, and liver slices compared to the in vivo liver gene expression in rats: Possible implications for toxicogenomics use of in vitro systems. *Toxicological Sciences* 73:386-402. DOI: 10.1093/toxsci/kfg064.

Boucher JG, Gagne R, Rowan-Carroll A, Boudreau A, Yauk CL, Atlas E. 2016. Bisphenol A and Bisphenol S Induce Distinct Transcriptional Profiles in Differentiating Human Primary Preadipocytes. *Plos One* 11. DOI: 10.1371/journal.pone.0163318.

Bourdon-Lacombe JA, Moffat ID, Deveau M, Husain M, Auerbach S, Krewski D, Thomas RS, Bushel PR, Williams A, Yauk CL. 2015. Technical guide for applications of gene expression profiling in human health risk assessment of environmental chemicals. *Regulatory Toxicology and Pharmacology* 72:292-309. DOI: 10.1016/j.yrtph.2015.04.010.

Brown CM, Reisfeld B, Mayeno AN. 2008. Cytochromes p450: A structure-based summary of biotransformations using representative substrates. *Drug Metabolism Reviews* 40:1-100. DOI: 10.1080/03602530701836662.

Burra P. 2013. Liver abnormalities and endocrine diseases. *Best Practice & Research Clinical Gastroenterology* 27:553-563. DOI: 10.1016/j.bpg.2013.06.014.

Cabaton N, Chagnon MC, Lhuguenot JC, Cravedi JP, Zalko D. 2006. Disposition and metabolic profiling of bisphenol F in pregnant and nonpregnant rats. *Journal of Agricultural and Food Chemistry* 54:10307-10314. DOI: 10.1021/jf062250q.

Cano-Nicolau J, Valliant C, Pellegrini E, Charlier TD, Kah O, Coumailleau P. 2016. Estrogenic Effects of Several BPA Analogs in the Developing Zebrafish Brain. *Frontiers in Neuroscience* 10:14. DOI: 10.3389/fnins.2016.00112.

Cao LY, Ren XM, Li CH, Zhang J, Qin WP, Yang Y, Wan B, Guo LH. 2017. Bisphenol AF and Bisphenol B Exert Higher Estrogenic Effects than Bisphenol A via G Protein-Coupled Estrogen Receptor Pathway. *Environmental Science & Technology* 51:11423-11430. DOI: 10.1021/acs.est.7b03336.

Carere C, Costantini D, Sorace A, Santucci D, Alleva E. 2010. Bird populations as sentinels of endocrine disrupting chemicals. Annali dell'Istituto superiore di sanità 46:81-88. DOI: 10.4415/ANN_10_01_10.

Casals-Casas C, Desvergne B. 2011. Endocrine Disruptors: From Endocrine to Metabolic Disruption. *Annual Review of Physiology, Vol 73* 73:135-162. DOI: 10.1146/annurev-physiol-012110-142200.

Chen P, Wang Q, Chen M, Yang J, Wang R, Zhong W, Zhu L, Yang L. 2018. Antagonistic Estrogenic Effects Displayed by Bisphenol AF and Perfluorooctanoic Acid on Zebrafish (Danio rerio) at an Early Developmental Stage. *Environmental science & technology letters, 5*, 655-661. DOI: 10.1021/acs.estlett.8b00559

Chen D, Hale RC. 2010. A global review of polybrominated diphenyl ether flame retardant contamination in birds. *Environment International* 36:800-811. DOI: 10.1016/j.envint.2010.05.013.

Chen D, Kannan K, Tan HL, Zheng ZG, Feng YL, Wu Y, Widelka M. 2016. Bisphenol Analogues Other Than BPA: Environmental Occurrence, Human Exposure, and Toxicity-A Review. *Environmental Science & Technology* 50:5438-5453. DOI: 10.1021/acs.est.5b05387.

Chhabra RS, Bucher JR, Wolfe M, Portier C. 2003. Toxicity characterization of environmental chemicals by the US National Toxicology Program: an overview. *International Journal of Hygiene and Environmental Health* 206:437-445. DOI: 10.1078/1438-4639-00240.

Chow WS, Chan WKL, Chan KM. 2013. Toxicity assessment and vitellogenin expression in zebrafish (Danio rerio) embryos and larvae acutely exposed to bisphenol A, endosulfan, heptachlor, methoxychlor and tetrabromobisphenol A. *Journal of Applied Toxicology* 33:670-678. DOI: 10.1002/jat.2723.

Corrales J, Kristofco LA, Steele WB, Yates BS, Breed CS, Williams ES, Brooks BW. 2015. Global Assessment of Bisphenol A in the Environment: Review and Analysis of Its Occurrence and Bioaccumulation. *Dose-Response* 13. DOI: 10.1177/1559325815598308.

Crump D, Chiu S, Williams KL. 2018. Bis-(3-allyl-4-hydroxyphenyl) Sulfone Decreases Embryonic Viability and Alters Hepatic mRNA Expression at Two Distinct Developmental Stages in Chicken Embryos Exposed Via Egg Injection. *Environmental Toxicology and Chemistry* 37:530-537. DOI: 10.1002/etc.3990.

Crump D, Farhat A, Chiu S, Williams KL, Jones SP, Langlois VS. 2016. Use of a Novel Double-Crested Cormorant ToxChip PCR Array and the EROD Assay to Determine Effects of Environmental Contaminants in Primary Hepatocytes. *Environmental Science & Technology* 50:3265-3274. DOI: 10.1021/acs.est.5b06181.

Custer CM, Custer TW, Schoenfuss HL, Poganski BH, Solem L. 2012. Exposure and effects of perfluoroalkyl compounds on tree swallows nesting at Lake Johanna in east central Minnesota, USA. Reproductive toxicology (Elmsford, NY) 33:556-562. DOI: 10.1016/j.reprotox.2011.01.005.

Daneshian M, Kamp H, Hengstler J, Leist M, van de Water B. 2016. Highlight report: Launch of a large integrated European in vitro toxicology project: EU-ToxRisk. *Archives of Toxicology* 90:1021-1024. DOI: 10.1007/s00204-016-1698-7.

Diamanti-Kandarakis E, Bourguignon JP, Giudice LC, Hauser R, Prins GS, Soto AM, Zoeller RT, Gore AC. 2009. Endocrine-Disrupting Chemicals: An Endocrine Society Scientific Statement. *Endocrine Reviews* 30:293-342. DOI: 10.1210/er.2009-0002.

Eberle D, Hegarty B, Bossard P, Ferre P, Foufelle F. 2004. SREBP transcription factors: master regulators of lipid homeostasis. *Biochimie* 86:839-848. DOI: 10.1016/j.biochi.2004.09.018.

ECHA. 2020. Bisphenol S has replaced bisphenol A in thermal paper.

ECHA. 2018. 4,4'-[2,2,2-trifluoro-1-(trifluoromethyl)ethylidene]diphenol; bisphenol AF. https://echa.europa.eu/substance-information/-/substanceinfo/100.014.579

Edmondson R, Broglie JJ, Adcock AF, Yang LJ. 2014. Three-Dimensional Cell Culture Systems and Their Applications in Drug Discovery and Cell-Based Biosensors. *Assay and Drug Development Technologies* 12:207-218. DOI: 10.1089/adt.2014.573.

Edwards PJ, Leopold A, Beavers JB, Springer TA, Chapman P, Maynard SK, Hubbard P. 2017. More for Less: Analysis of the Performance of Avian Acute Oral Guideline OECD 223 from Empirical Data. *Integrated Environmental Assessment and Management* 13:906-914. DOI: 10.1002/ieam.1930.

Elferink MGL, Olinga P, Draaisma AL, Merema MT, Bauerschmidt S, Polman J, Schoonen WG, Groothuis GMM. 2008. Microarray analysis in rat liver slices correctly predicts in vivo hepatotoxicity. *Toxicology and Applied Pharmacology* 229:300-309. DOI: 10.1016/j.taap.2008.01.037.

EPA. 2015. Bisphenol A alternatives in thermal paper. https://www.epa.gov/sites/production/files/2015-08/documents/bpa_final.pdf

Farhat A, Crump D, Bidinosti L, Boulanger E, Basu N, Hecker M, Head JA. 2020. An Early-Life Stage Alternative Testing Strategy for Assessing the Impacts of Environmental Chemicals in Birds. *Environmental Toxicology and Chemistry* 39:141-154. DOI: 10.1002/etc.4582.

Farhat A, Crump D, Porter E, Chiu S, Letcher RJ, Su GY, Kennedy SW. 2014. Time-dependent effects of the flame retardant tris (1,3-dichloro-2-propyl) phosphate (TDCPP) on mRNA expression, in vitro and in ovo, reveal optimal sampling times for rapidly metabolized compounds. *Environmental Toxicology and Chemistry* 33:2842-2849. DOI: 10.1002/etc.2755.

Fic A, Zegura B, Gramec D, Masic LP. 2014. Estrogenic and androgenic activities of TBBA and TBMEPH, metabolites of novel brominated flame retardants, and selected bisphenols, using the XenoScreen XL YES/YAS assay. *Chemosphere* 112:362-369. DOI: 10.1016/j.chemosphere.2014.04.080.

Filipsson AF, Sand S, Nilsson J, Victorin K. 2003. The benchmark dose method - Review of available models, and recommendations for application in health risk assessment. *Critical Reviews in Toxicology* 33:505-542. DOI: 10.1080/10408440390242360.

Fuentes N, Silveyra P. 2019. Estrogen receptor signaling mechanisms. *Intracellular Signalling Proteins* 116:135-170. DOI: 10.1016/bs.apcsb.2019.01.001.

Gatzidou ET, Zira AN, Theocharis SE. 2007. Toxicogenomics: a pivotal piece in the puzzle of toxicological research. *Journal of Applied Toxicology* 27:302-309. DOI: 10.1002/jat.1248.

Gentilcore D, Porreca I, Rizzo F, Ganbaatar E, Carchia E, Mallardo M, De Felice M, Ambrosino C. 2013. Bisphenol A interferes with thyroid specific gene expression. *Toxicology* 304:21-31. DOI: 10.1016/j.tox.2012.12.001.

Gerets HHJ, Tilmant K, Gerin B, Chanteux H, Depelchin BO, Dhalluin S, Atienzar FA. 2012. Characterization of primary human hepatocytes, HepG2 cells, and HepaRG cells at the mRNA level and CYP activity in response to inducers and their predictivity for the detection of human hepatotoxins. *Cell Biology and Toxicology* 28:69-87. DOI: 10.1007/s10565-011-9208-4.

Giesy JP, Feyk LA, Jones PD, Kannan K, Sanderson T. 2003. Review of the effects of endocrine-disrupting chemicals in birds. *Pure and Applied Chemistry* 75:2287-2303. DOI: 10.1351/pac200375112287.

Gilani SH, Alibhai Y. 1990. Teratogenicity of metals to chick embryos. *Journal of Toxicology and Environmental Health* 30(1):23-31. DOI:10.1080/15287399009531407.

Goldinger DM, Demierre AL, Zoller O, Rupp H, Reinhard H, Magnin R, Becker TW, Bourqui-Pittet M. 2015. Endocrine activity of alternatives to BPA found in thermal paper in Switzerland. *Regulatory Toxicology and Pharmacology* 71:453-462. DOI: 10.1016/j.yrtph.2015.01.002.

Gore AC, Chappell VA, Fenton SE, Flaws JA, Nadal A, Prins GS, Toppari J, Zoeller RT. 2015. EDC-2: The Endocrine Society's Second Scientific Statement on Endocrine-Disrupting Chemicals. *Endocrine Reviews* 36:E1-E150. DOI: 10.1210/er.2015-1010.

Government of Canada. 2010. Questions and answers on Bisphenol A and the Chemicals Management Plan. https://www.canada.ca/en/health-canada/services/chemical-substances/fact-sheets/questions-answers-bisphenol-a-chemicals-management-plan.html#d

Government of Canada. 2019. National Reporting to CSD-18/19 Thematic Profile on Chemicals. https://sustainabledevelopment.un.org/content/documents/dsd/dsd_aofw_ni/ni_pdfs/NationalReports/canada/Chemicals.pdf

Guan Y, Zhang T, He J, Jia J, Zhu L, Wang Z. 2019. Bisphenol A disturbed the lipid metabolism mediated by sterol regulatory element binding protein 1 in rare minnow Gobiocypris rarus. *Aquatic Toxicology* 207:179-186. doi: 10.1016/j.aquatox.2018.12.011.

Guengerich FP. 2006. Cytochrome P450s and other enzymes in drug metabolism and toxicity. *Aaps Journal* 8:E101-E111. DOI: 10.1208/aapsj080112.

Guigueno MF, Fernie KJ. 2017. Birds and flame retardants: A review of the toxic effects on birds of historical and novel flame retardants. *Environmental Research* 154:398-424. DOI: 10.1016/j.envres.2016.12.033.

Hahn ME. 2002. Aryl hydrocarbon receptors: diversity and evolution. *Chemico-Biological Interactions* 141:131-160. DOI: 10.1016/s0009-2797(02)00070-4.

Halldin K, Berg C, Bergman A, Brandt I, Brunstrom B. 2001. Distribution of bisphenol A and tetrabromobisphenol A in quail eggs, embryos and laying birds and studies on reproduction variables in adults following in ovo exposure. *Archives of Toxicology* 75:597-603. DOI: 10.1007/s002040100277.

Halldin K, Berg C, Brandt I, Brunstrom B. 1999. Sexual behavior in Japanese quail as a test end point for endocrine disruption: Effects of in Ovo exposure to ethinylestradiol and diethylstilbestrol. *Environmental Health Perspectives* 107:861-866. DOI: 10.1289/ehp.99107861.

Hamadeh HK, Bushel P, Paules R, Afshari CA. 2001. Discovery in toxicology: Mediation by gene expression array technology. *Journal of Biochemical and Molecular Toxicology* 15:231-242. DOI: 10.1002/jbt.10006.abs.

Handschin C, Podvinec M, Meyer UA. 2000. CXR, a chicken xenobiotic-sensing orphan nuclear receptor, is related to both mammalian pregnane X receptor (PXR) and constitutive androstane receptor (CAR). *Proceedings of the National Academy of Sciences of the United States of America* 97:10769-10774. DOI: 10.1073/pnas.97.20.10769.

Hartung T. 2009. Toxicology for the twenty-first century. *Nature* 460:208-212. DOI: 10.1038/460208a.

Hartung T, Daston G. 2009. Are *In Vitro* Tests Suitable for Regulatory Use? *Toxicological Sciences* Volume 111 (2): 233–237. DOI:10.1093/toxsci/kfp149

Heimeier RA, Shi YB. 2010. Amphibian metamorphosis as a model for studying endocrine disruption on vertebrate development: Effect of bisphenol A on thyroid hormone action. *General and Comparative Endocrinology* 168:181-189. DOI: 10.1016/j.ygcen.2010.02.016.

Hewitt NJ, Lechon MJG, Houston JB, Hallifax D, Brown HS, Maurel P, Kenna JG, Gustavsson L, Lohmann C, Skonberg C, Guillouzo A, Tuschl G, Li AP, LeCluyse E, Groothuis GMM, Hengstler JG. 2007. Primary hepatocytes: Current understanding of the regulation of metabolic enzymes and transporter proteins, and pharmaceutical practice for the use of hepatocytes in metabolism, enzyme induction, transporter, clearance, and hepatotoxicity studies. *Drug Metabolism Reviews* 39:159-234. DOI: 10.1080/03602530601093489.

Hill EF, Hoffman DJ. 1984. Avian Models for Toxicity Testing. *Journal of the American College of Toxicology* 3(6):357-376. DOI: 10.3109/10915818409104398

Hilton GM, Odenkirchen E, Panger M, Waleko G, Lowit A, Clippinger AJ. 2019. Evaluation of the avian acute oral and sub-acute dietary toxicity test for pesticide registration. *Regulatory Toxicology and Pharmacology* 105:30-35. DOI: 10.1016/j.yrtph.2019.03.013.

Honkakoski P, Sueyoshi T, Negishi M. 2003. Drug-activated nuclear receptors CAR and PXR. *Annals of Medicine* 35:172-182. DOI: 10.1080/07853890310008224.

Huss D, Poynter G, Lansford R. 2008. Japanese quail (Coturnix japonica) as a laboratory animal model. *Lab Anim (NY)* 37(11):513-519. DOI: 10.1038/laban1108-513.

Imamura Y, Mukohara T, Shimono Y, Funakoshi Y, Chayahara N, Toyoda M, Kiyota N, Takao S, Kono S, Nakatsura T, Minami H. 2015. Comparison of 2D-and 3D-culture models as drug-testing platforms in breast cancer. *Oncology Reports* 33:1837-1843. DOI: 10.3892/or.2015.3767.

Jessl L, Lenz R, Massing FG, Scheider J, Oehlmann J. 2018. Effects of estrogens and antiestrogens on gonadal sex differentiation and embryonic development in the domestic fowl (Gallus gallus domesticus). *Peerj* 6. DOI: 10.7717/peerj.5094.

Johnson GE, Soeteman-Hernandez LG, Gollapudi BB, Bodger OG, Dearfield KL, Heflich RH, Hixon JG, Lovell DP, MacGregor JT, Pottenger LH, Thompson CM, Abraham L, Thybaud V, Tanir JY, Zeiger E, van Benthem J, White PA. 2014. Derivation of Point of Departure (PoD) Estimates in Genetic Toxicology Studies and Their Potential Applications in Risk Assessment. *Environmental and Molecular Mutagenesis* 55:609-623. DOI: 10.1002/em.21870.

Kavlock RJ, Austin CP, Tice RR. 2009. Toxicity Testing in the 21st Century: Implications for Human Health Risk Assessment. *Risk Analysis* 29:485-487. DOI: 10.1111/j.1539-6924.2008.01168.x.

Kienhuis AS, Wortelboer HM, Hoflack JC, Moonen EJ, Kleinjans JCS, van Ommen B, van Delft JHM, Stierum RH. 2006. Comparison of coumarin-induced toxicity between sandwich-cultured primary rat hepatocytes and rats in vivo: A toxicogenomics approach. *Drug Metabolism and Disposition* 34:2083-2090. DOI: 10.1124/dmd.106.011262.

Kime DE, Nash JP, Scott AP. 1999. Vitellogenesis as a biomarker of reproductive disruption by xenobiotics. *Aquaculture* 177:345-352. DOI: 10.1016/s0044-8486(99)00097-6.

Kitamura S, Suzuki T, Sanoh S, Kohta R, Jinno N, Sugihara K, Yoshihara S, Fujimoto N, Watanabe H, Ohta S. 2005a. Comparative study of the endocrine-disrupting activity of bisphenol A and 19 related compounds. *Toxicological Sciences* 84:249-259. DOI: 10.1093/toxsci/kfi074.

Kitamura S, Suzuki T, Sanoh S, Kohta R, Jinno N, Sugihara K, Yoshihara S, Fujimoto N, Watanabe H, Ohta S. 2005b. Comparative study of the endocrine-disrupting activity of bisphenol A and 19 related compounds. *Toxicological Sciences* 84:249-259. DOI: 10.1093/toxsci/kfi074.

Kojima H, Takeuchi S, Sanoh S, Okuda K, Kitamura S, Uramaru N, Sugihara K, Yoshinari K. 2019. Profiling of bisphenol A and eight its analogues on transcriptional activity via human nuclear receptors. *Toxicology* 413:48-55. DOI: 10.1016/j.tox.2018.12.001.

Krewski D, Acosta D, Andersen M, Anderson H, Bailar JC, Boekelheide K, Brent R, Charnley G, Cheung VG, Green S, Kelsey KT, Kerkvliet NI, Li AA, McCray L, Meyer O, Patterson RD, Pennie W, Scala RA, Solomon GM, Stephens M, Yager J, Zeise L, Staff Comm Toxicity Testing A. 2010. Toxicity Testing in the 21st century: A vision and a strategy. *Journal of Toxicology and Environmental Health-Part B-Critical Reviews* 13:51-138. DOI: 10.1080/10937404.2010.483176.

Krishnan AV, Stathis P, Permuth SF, Tokes L, Feldman D. 1993. Bisphenol A-an estrogenic substance is released from polycarbonate flasks during autoclaving. *Endocrinology* 132:2279-2286. DOI: 10.1210/en.132.6.2279.

Kurebayashi H, Nagatsuka SI, Nemoto H, Noguchi H, Ohno Y. 2005. Disposition of low doses of C-14-bisphenol A in male, female, pregnant, fetal, and neonatal rats. *Archives of Toxicology* 79:243-252. DOI: 10.1007/s00204-004-0628-2.

Kurosawa T, Hiroi H, Tsutsumi O, Ishikawa T, Osuga Y, Fujiwara T, Inoue S, Muramatsu M, Momoeda M, Taketani Y. 2002. The activity of bisphenol A depends on both the estrogen receptor subtype and the cell type. *Endocrine Journal* 49(4):465-71. DOI: 10.1507/endocrj.49.465.

Lauschke VM, Shafagh RZ, Hendriks DFG, Ingelman-Sundberg M. 2019. 3D Primary Hepatocyte Culture Systems for Analyses of Liver Diseases, Drug Metabolism, and Toxicity: Emerging Culture Paradigms and Applications. *Biotechnology Journal* 14. DOI: 10.1002/biot.201800347.

Le Fol V, Ait-Aissa S, Sonavane M, Porcher JM, Balaguer P, Cravedi JP, Zalko D, Brion F. 2017. In vitro and in vivo estrogenic activity of BPA, BPF and BPS in zebrafish-specific assays. *Ecotoxicology and Environmental Safety* 142:150-156. DOI: 10.1016/j.ecoenv.2017.04.009.

Lee S, Kim C, Shin H, Kho Y, Choi K. 2019. Comparison of thyroid hormone disruption potentials by bisphenols A, S, F, and Z in embryo-larval zebrafish. *Chemosphere* 221:115-123. DOI: 10.1016/j.chemosphere.2019.01.019.

Lee S, Kim C, Youn H, Choi K. 2017. Thyroid hormone disrupting potentials of bisphenol A and its analogues - in vitro comparison study employing rat pituitary (GH3) and thyroid follicular (FRTL-5) cells. *Toxicology in Vitro* 40:297-304. DOI: 10.1016/j.tiv.2017.02.004.

Lerche-Langrand C, Toutain HJ. 2000. Precision-cut liver slices: characteristics and use for in vitro pharmaco-toxicology. *Toxicology* 153:221-253. DOI: 10.1016/s0300-483x(00)00316-4.

Li M, Yang YJ, Yang Y, Yin J, Zhang J, Feng YX, Shao B. 2013. Biotransformation of Bisphenol AF to Its Major Glucuronide Metabolite Reduces Estrogenic Activity. *Plos One* 8. DOI: 10.1371/journal.pone.0083170.

Li MC, Gao XN, Tan L, Miao YF, Fan WT, Gao ZS, Liu SH, Ding CC, Shi XZ, Song SQ. 2020. Effects of bisphenol A at the safe reference dose on abdominal fat deposition in aged hens. *Ecotoxicology and Environmental Safety* 206. DOI: 10.1016/j.ecoenv.2020.111398.

Liao CY, Liu F, Moon HB, Yamashita N, Yun SH, Kannan K. 2012. Bisphenol Analogues in Sediments from Industrialized Areas in the United States, Japan, and Korea: Spatial and Temporal Distributions. *Environmental Science & Technology* 46:11558-11565. DOI: 10.1021/es303191g.

Lin R, Jia Y, Wu FJ, Meng Y, Sun Q, Jia LH. 2019. Combined Exposure to Fructose and Bisphenol A Exacerbates Abnormal Lipid Metabolism in Liver of Developmental Male Rats. *International Journal of Environmental Research and Public Health* 16. DOI: 10.3390/ijerph16214152.

Lundholm C.E. 1997. DDE-induced eggshell thinning in birds: Effects of p,p′-DDE on the calcium and prostaglandin metabolism of the eggshell gland. *Comparative Biochemistry and Physiology - Part C: Toxicology & Pharmacology* 118: 113–128. DOI: 10.1016/s0742-8413(97)00105-9.

Malarkey DE, Johnson K, Ryan L, Boorman G, Maronpot RR. 2005. New insights into functional aspects of liver morphology. *Toxicologic Pathology* 33:27-34. DOI: 10.1080/01926230590881826.

Marmugi A, Lasserre F, Beuzelin D, Ducheix S, Huc L, Polizzi A, Chetivaux M, Pineau T, Martin P, Guillou H, Mselli-Lakhal L. 2014. Adverse effects of long-term exposure to bisphenol A during adulthood leading to hyperglycaemia and hypercholesterolemia in mice. *Toxicology* 325:133-143. DOI: 10.1016/j.tox.2014.08.006

Marmugi A, Ducheix S, Lasserre F, Polizzi A, Paris A, Priymenko N, Bertrand-Michel J, Pineau T, Guillou H, Martin PGP, Mselli-Lakhal L. 2012. Low doses of bisphenol a induce gene expression related to lipid synthesis and trigger triglyceride accumulation in adult mouse liver. *Hepatology* 55:395-407. DOI: 10.1002/hep.24685.

Mathijs K, Kienhuis AS, Brauers KJJ, Jennen DGJ, Lahoz A, Kleinjans JCS, van Delft JHM. 2009. Assessing the Metabolic Competence of Sandwich-Cultured Mouse Primary Hepatocytes. *Drug Metabolism and Disposition* 37:1305-1311. DOI: 10.1124/dmd.108.025775.

Matsushima A, Liu XH, Okada H, Shimohigashi M, Shimohigashi Y. 2010. Bisphenol AF Is a Full Agonist for the Estrogen Receptor ER alpha but a Highly Specific Antagonist for ER beta. *Environmental Health Perspectives* 118:1267-1272. DOI: 10.1289/ehp.0901819.

Matthews JB, Twomey K, Zacharewski TR. 2001. In vitro and in vivo interactions of bisphenol A and its metabolite, bisphenol A glucuronide, with estrogen receptors alpha and beta. *Chemical Research in Toxicology* 14:149-157. DOI: 10.1021/tx0001833.

Mayr LM, Bojanic D. 2009. Novel trends in high-throughput screening. *Current Opinion in Pharmacology* 9:580-588. DOI: 10.1016/j.coph.2009.08.004.

Meng ZY, Tian SN, Yan J, Jia M, Yan S, Li RS, Zhang RK, Zhu WT, Zhou ZQ. 2019. Effects of perinatal exposure to BPA, BPF and BPAF on liver function in male mouse offspring involving in oxidative damage and metabolic disorder. *Environmental Pollution* 247:935-943. DOI: 10.1016/j.envpol.2019.01.116.

Mentor A, Wänn M, Brunström B, Jönsson M, Mattsson A. 2020 . Bisphenol AF and Bisphenol F Induce Similar Feminizing Effects in Chicken Embryo Testis as Bisphenol A. *Toxicological Sciences* 178(2):239-250. DOI: 10.1093/toxsci/kfaa152.

Mesnage R, Phedonos A, Arno M, Balu S, Corton JC, Antoniou MN. 2017. Transcriptome Profiling Reveals Bisphenol A Alternatives Activate Estrogen Receptor Alpha in Human Breast Cancer Cells. *Toxicological Sciences* 158:431-443. DOI: 10.1093/toxsci/kfx101.

Moreman J, Lee O, Trznadel M, David A, Kudoh T, Tyler CR. 2017. Acute Toxicity, Teratogenic, and Estrogenic Effects of Bisphenol A and Its Alternative Replacements Bisphenol S, Bisphenol F, and Bisphenol AF in Zebrafish Embryo-Larvae. *Environmental Science & Technology* 51:12796-12805. DOI: 10.1021/acs.est.7b03283.

Moriyama K, Tagami T, Akamizu T, Usui T, Saijo M, Kanamoto N, Hataya Y, Shimatsu A, Kuzuya H, Nakao K. 2002. Thyroid hormone action is disrupted by bisphenol A as an antagonist. *Journal of Clinical Endocrinology & Metabolism* 87:5185-5190. DOI: 10.1210/jc.2002-020209.

Mullur R, Liu YY, Brent GA. 2014. Thyroid hormone regulation of metabolism. *Physiological Reviews* 94:355-382. DOI: 10.1152/physrev.00030.2013.

Nachman RM, Fox SD, Golden WC, Sibinga E, Groopman JD, Lees PSJ. 2015. Serial Free Bisphenol A and Bisphenol A Glucuronide Concentrations in Neonates. *Journal of Pediatrics* 167:64-69. DOI: 10.1016/j.jpeds.2015.03.036.

Nadal A, Ropero AB, Laribi O, Maillet M, Fuentes E, Soria B. 2000. Nongenomic actions of estrogens and xenoestrogens by binding at a plasma membrane receptor unrelated to estrogen receptor alpha and estrogen receptor beta. *Proceedings of the National Academy of Sciences of the United States of America* 97:11603-11608. DOI: 10.1073/pnas.97.21.11603.

Nakagawa Y, Shimano H. 2018. CREBH Regulates Systemic Glucose and Lipid Metabolism. *International Journal of Molecular Sciences* 19(5):1396. DOI: 10.3390/ijms19051396.

Nakayama K, Iwata H, Kim EY, Tashiro K, Tanabe S. 2006. Gene expression profiling in common cormorant liver with an oligo array: Assessing the potential toxic effects of environmental contaminants. *Environmental Science & Technology* 40:1076-1083. DOI: 10.1021/es051386m.

NIH. 2019. Toxiclogy in the 21st Century (Tox21). https://ncats.nih.gov/tox21

NTP. 2008. Chemical profile of Bisphenol AF. https://ntp.niehs.nih.gov/ntp/htdocs/chem_background/exsumpdf/bisphenolaf_093008_508.pdf

OECD.2016. *Test No. 223: Avian Acute Oral Toxicity Test*, OECD Guidelines for the Testing of Chemicals, Section 2, OECD Publishing, Paris, https://doi.org/10.1787/9789264264519-en

OECD. 1984a. *Test No. 205: Avian Dietary Toxicity Test*, OECD Guidelines for the Testing of Chemicals, Section 2, OECD Publishing, Paris, https://doi.org/10.1787/9789264070004-en.

OECD. 1984b. *Test No. 206: Avian Reproduction Test*, OECD Guidelines for the Testing of Chemicals, Section 2, OECD Publishing, Paris, https://doi.org/10.1787/9789264070028-en.

Okada H, Tokunaga T, Liu XH, Takayanagi S, Matsushima A, Shimohigashi Y. 2008. Direct evidence revealing structural elements essential for the high binding ability of bisphenol A to human estrogen-related receptor-gamma. *Environmental Health Perspectives* 116:32-38. DOI: 10.1289/ehp.10587.

Okazaki H, Hirao-Suzuki M, Takeda S, Takemoto Y, Mizunoe R, Haraguchi K, Watanabe K, Takiguchi M, Aramaki H. 2018. Bisphenol AF as an activator of human estrogen receptor β1 (ERβ1) in breast cancer cell lines. *Journal of Toxicological Sciences* 43(5):321-327. DOI: 10.2131/jts.43.321.

Palma E, Doornebal EJ, Chokshi S. 2019. Precision-cut liver slices: a versatile tool to advance liver research. *Hepatology International* 13:51-57. DOI: 10.1007/s12072-018-9913-7.

Pan YN, Deng M, Li J, Du BB, Lan SY, Liang XX, Zeng LX. 2020. Occurrence and Maternal Transfer of Multiple Bisphenols, Including an Emerging Derivative with Unexpectedly High Concentrations, in the Human Maternal-Fetal-Placental Unit. *Environmental Science & Technology* 54:3476-3486. DOI: 10.1021/acs.est.0c00206.

Parfett CL, Desaulniers D. 2017. A Tox21 Approach to Altered Epigenetic Landscapes: Assessing Epigenetic Toxicity Pathways Leading to Altered Gene Expression and Oncogenic Transformation In Vitro. *International Journal of Molecular Sciences* 18. DOI: 10.3390/ijms18061179.

Pelch K, Wignall JA, Goldstone AE, Ross PK, Blain RB, Shapiro AJ, Holmgren SD, Hsieh JH, Svoboda D, Auerbach SS, Parham FM, Masten SA, Walker V, Rooney A, Thayer KA. 2019. A scoping review of the health and toxicological activity of bisphenol A (BPA) structural analogues and functional alternatives. *Toxicology* 424. DOI: 10.1016/j.tox.2019.06.006.

Pinto C, Hao RX, Grimaldi M, Thrikawala S, Boulahtouf A, Ait-Aissa S, Brion F, Gustafsson JA, Balaguer P, Bondesson M. 2019. Differential activity of BPA, BPAF and BPC on zebrafish estrogen receptors in vitro and in vivo. *Toxicology and Applied Pharmacology* 380. DOI: 10.1016/j.taap.2019.114709.

Pottenger LH, Domoradzki JY, Markham DA, Hansen SC, Cagen SZ, Waechter JM. 2000. The relative bioavailability and metabolism of bisphenol A in rats is dependent upon the route of administration. *Toxicological Sciences* 54:3-18. DOI: 10.1093/toxsci/54.1.3.

Qiu WH, Fang MJ, Liu JY, Fu CX, Zheng CM, Chen B, Wang KJ. 2019. In vivo actions of Bisphenol F on the reproductive neuroendocrine system after long-term exposure in zebrafish. *Science of the Total Environment* 665:995-1002. DOI: 10.1016/j.scitotenv.2019.02.154.

Ramaiahgari SC, den Braver MW, Herpers B, Terpstra V, Commandeur JNM, van de Water B, Price LS. 2014. A 3D in vitro model of differentiated HepG2 cell spheroids with improved liver-like properties for repeated dose high-throughput toxicity studies. *Archives of Toxicology* 88:1083-1095. DOI: 10.1007/s00204-014-1215-9.

Ramaiahgari SC, Waidyanatha S, Dixon D, DeVito MJ, Paules RS, Ferguson SS. 2017. Three-Dimensional (3D) HepaRG Spheroid Model With Physiologically Relevant Xenobiotic Metabolism Competence and Hepatocyte Functionality for Liver Toxicity Screening. *Toxicological Sciences* 159:124-136. DOI: 10.1093/toxsci/kfx122.

Rochester JR, Bolden AL. 2015. Bisphenol S and F: A Systematic Review and Comparison of the Hormonal Activity of Bisphenol A Substitutes. *Environmental Health Perspectives* 123:643-650. DOI: 10.1289/ehp.1408989.

Roggen EL. 2011. In vitro toxicity testing in the twenty-first century. *Frontiers in Pharmacology* 2. DOI: 10.3389/fphar.2011.00003.

Rubin BS. 2011. Bisphenol A: An endocrine disruptor with widespread exposure and multiple effects. *Journal of Steroid Biochemistry and Molecular Biology* 127:27-34. DOI: 10.1016/j.jsbmb.2011.05.002.

Schoeters G. 2010. The REACH perspective: toward a new concept of toxicity testing. *Journal of Toxicology and Environmental Health-Part B-Critical Reviews* 13:232-241. DOI: 10.1080/10937404.2010.483938.

Sheng ZG, Tang Y, Liu YX, Yuan Y, Zhao BQ, Chao XJ, Zhu BZ. 2012. Low concentrations of bisphenol a suppress thyroid hormone receptor transcription through a nongenomic mechanism. *Toxicology and Applied Pharmacology* 259:133-142. DOI: 10.1016/j.taap.2011.12.018.

Shi JC, Jiao ZH, Zheng S, Li M, Zhang J, Feng YX, Yin J, Shao B. 2015. Long-term effects of Bisphenol AF (BPAF) on hormonal balance and genes of hypothalamus-pituitary-gonad axis and liver of zebrafish (Danio rerio), and the impact on offspring. *Chemosphere* 128:252-257. DOI: 10.1016/j.chemosphere.2015.01.060.

Shukla SJ, Huang RL, Austin CP, Xia MH. 2010. The future of toxicity testing: a focus on in vitro methods using a quantitative high-throughput screening platform. *Drug Discovery Today* 15:997-1007. DOI: 10.1016/j.drudis.2010.07.007.

Siracusa JS, Yin L, Measel E, Liang SX, Yu XZ. 2018. Effects of bisphenol A and its analogs on reproductive health: A mini review. *Reproductive Toxicology* 79:96-123. DOI: 10.1016/j.reprotox.2018.06.005.

Skledar DG, Carino A, Trontelj J, Troberg J, Distrutti E, Marchianò S, Tomašič T, Zega A, Finel M, Fiorucci S, Mašič LP. 2019. Endocrine activities and adipogenic effects of bisphenol AF and its main metabolite. *Chemosphere.* 215:870-880. DOI: 10.1016/j.chemosphere.2018.10.129.

Smits JEG, Fernie KJ. 2013. Avian wildlife as sentinels of ecosystem health. *Comparative Immunology Microbiology and Infectious Diseases* 36:333-342. DOI: 10.1016/j.cimid.2012.11.007.

Soldatow VY, LeCluyse EL, Griffith LG, Rusyn I. 2013. In vitro models for liver toxicity testing. *Toxicology Research* 2:23-39. DOI: 10.1039/c2tx20051a.

Strakovsky RS, Wang H, Engeseth NJ, Flaws JA, Helferich WG, Pan YX, Lezmi S. 2015. Developmental bisphenol A (BPA) exposure leads to sex-specific modification of hepatic gene expression and epigenome at birth that may exacerbate high-fat diet-induced hepatic steatosis. *Toxicology and Applied Pharmacology* 284:101-112. DOI: 10.1016/j.taap.2015.02.021.

Sumpter JP, Jobling S. 1995. Vitellogenesis as a biomarker for estrogenic contamination of the aquatic environment. *Environmental Health Perspectives* 103:173-178. DOI: 10.2307/3432529.

Takayanagi S, Tokunaga T, Liu XH, Okada H, Matsushima A, Shimohigashi Y. 2006. Endocrine disruptor bisphenol A strongly binds to human estrogen-related receptor gamma (ERR gamma) with high constitutive activity. *Toxicology Letters* 167:95-105. DOI: 10.1016/j.toxlet.2006.08.012.

Tang TL, Yang Y, Chen YW, Tang WH, Wang FQ, Diao XP. 2015. Thyroid Disruption in Zebrafish Larvae by Short-Term Exposure to Bisphenol AF. *International Journal of Environmental Research and Public Health* 12:13069-13084. DOI: 10.3390/ijerph121013069.

Teng C, Goodwin B, Shockley K, Xia MH, Huang RL, Norris J, Merrick BA, Jetten AM, Austin CP, Tice RR. 2013. Bisphenol A affects androgen receptor function via multiple mechanisms. *Chemico-Biological Interactions* 203:556-564. DOI: 10.1016/j.cbi.2013.03.013.

Thayer KA, Taylor KW, Garantziotis S, Schurman SH, Kissling GE, Hunt D, Herbert B, Church R, Jankowich R, Churchwell MI, Scheri RC, Birnbaum LS, Bucher JR. 2016. Bisphenol A, Bisphenol S, and 4-Hydroxyphenyl 4-Isoprooxyphenylsulfone (BPSIP) in Urine and Blood of Cashiers. *Environmental Health Perspectives* 124:437-444. DOI: 10.1289/ehp.1409427.

Thomas P, Dong J. 2006. Binding and activation of the seven-transmembrane estrogen receptor GPR30 by environmental estrogens: A potential novel mechanism of endocrine disruption. *Journal of Steroid Biochemistry and Molecular Biology* 102:175-179. DOI: 10.1016/j.jsbmb.2006.09.017.

Thomas RS, Philbert MA, Auerbach SS, Wetmore BA, Devito MJ, Cote I, Rowlands JC, Whelan MP, Hays SM, Andersen ME, Meek ME, Reiter LW, Lambert JC, Clewell HJ, Stephens ML, Zhao QJ, Wesselkamper SC, Flowers L, Carney EW, Pastoor TP, Petersen DD, Yauk CL, Nong A. 2013. Incorporating New Technologies Into Toxicity Testing and Risk Assessment: Moving From 21st Century Vision to a Data-Driven Framework. *Toxicological Sciences* 136:4-18. DOI: 10.1093/toxsci/kft178.

Tohme M, Prud'homme SM, Boulahtouf A, Samarut E, Brunet F, Bernard L, Bourguet W, Gibert Y, Balaguer P, Laudet V. 2014. Estrogen-related receptor gamma is an in vivo receptor of bisphenol A. *Faseb Journal* 28:3124-3133. DOI: 10.1096/fj.13-240465.

Tremblay, A. M., & Giguère, V. 2007. The NR3B subgroup: an ovERRview. *Nuclear receptor signaling*, *5*, e009. DOI: 10.1621/nrs.05009

Vandenberg LN, Maffini MV, Sonnenschein C, Rubin BS, Soto AM. 2009. Bisphenol-A and the Great Divide: A Review of Controversies in the Field of Endocrine Disruption. *Endocrine Reviews* 30:75-95. DOI: 10.1210/er.2008-0021.

Vinken M, Hengstler JG. 2018. Characterization of hepatocyte-based in vitro systems for reliable toxicity testing. *Archives of Toxicology* 92:2981-2986. DOI: 10.1007/s00204-018-2297-6.

Vokel W, Colnot T, Csanady GA, Filser JG, Dekant W. 2002. Metabolism and kinetics of bisphenol A in humans at low doses following oral administration. *Chemical Research in Toxicology* 15:1281-1287. DOI: 10.1021/tx025548t.

Vos JG, Dybing E, Greim HA, Ladefoged O, Lambré C, Tarazona JV, Brandt I, Vethaak AD. 2000. Health Effects of Endocrine-Disrupting Chemicals on Wildlife, with Special Reference to the European Situation. Critical reviews in toxicology 30:71-133. DOI: 10.1080/10408440091159176.

Waidyanatha S, Mathews JM, Patel PR, Black SR, Snyder RW, Fennell TR. 2015. Disposition of bisphenol AF, a bisphenol A analogue, in hepatocytes in vitro and in male and female Harlan Sprague-Dawley rats and B6C3F1/N mice following oral and intravenous administration. *Xenobiotica* 45:811-819. DOI: 10.3109/00498254.2015.1021732.

Wang Q, Chen M, Shan GQ, Chen PY, Cui S, Yi SJ, Zhu LY. 2017. Bioaccumulation and biomagnification of emerging bisphenol analogues in aquatic organisms from Taihu Lake, China. *Science of the Total Environment* 598:814-820. DOI: 10.1016/j.scitotenv.2017.04.167.

Wanson JC, Drochmans P, Mosselmans R, Ronveaux MF. 1977. Adult rat hepatocytes in primary monolayer culture-ultrastructual characteristics of intercellular contacts and cell membrane differentiations. *Journal of Cell Biology* 74:858-877. DOI: 10.1083/jcb.74.3.858.

Waters MD, Fostel JM. 2004. Toxicogenomics and systems toxicology: Aims and prospects. *Nature Reviews Genetics* 5:936-948. DOI: 10.1038/nrg1493.

Yamaguchi A, Ishibashi H, Arizono K, Tominaga N. 2015. In vivo and in silico analyses of estrogenic potential of bisphenol analogs in medaka (Oryzias latipes) and common carp (Cyprinus carpio). *Ecotoxicology and Environmental Safety* 120:198-205. DOI: 10.1016/j.ecoenv.2015.06.014.

Yamazaki E, Yamashita N, Taniyasu S, Lam J, Lam PKS, Moon HB, Jeong Y, Kannan P, Achyuthan H, Munuswamy N, Kannan K. 2015. Bisphenol A and other bisphenol analogues including BPS and BPF in surface water samples from Japan, China, Korea and India. *Ecotoxicology and Environmental Safety* 122:565-572. DOI: 10.1016/j.ecoenv.2015.09.029.

Yang XX, Liu YC, Li J, Chen MJ, Peng D, Liang Y, Song MY, Zhang J, Jiang GB. 2016. Exposure to Bisphenol AF disrupts sex hormone levels and vitellogenin expression in zebrafish. *Environmental Toxicology* 31:285-294. DOI: 10.1002/tox.22043.

Yang YJ, Guan J, Yin J, Shao B, Li H. 2014. Urinary levels of bisphenol analogues in residents living near a manufacturing plant in south China. *Chemosphere* 112:481-486. DOI: 10.1016/j.chemosphere.2014.05.004.

Yoshihara S, Makishima M, Suzuki N, Ohta S. 2001. Metabolic activation of bisphenol A by rat liver S9 fraction. *Toxicological Sciences* 62:221-227. DOI: 10.1093/toxsci/62.2.221.

Zhang YF, Ren XM, Li YY, Yao XF, Li CH, Qin ZF, Guo LH. 2018. Bisphenol A alternatives bisphenol S and bisphenol F interfere with thyroid hormone signaling pathway in vitro and in vivo. *Environmental Pollution* 237:1072-1079. DOI: 10.1016/j.envpol.2017.11.027.

Zhu M, Chen XY, Li YY, Yin NY, Faiola F, Qin ZF, Wei WJ. 2018. Bisphenol F Disrupts Thyroid Hormone Signaling and Postembryonic Development in Xenopus laevis. *Environmental Science & Technology* 52:1602-1611. DOI: 10.1021/acs.est.7b06270.

Zoeller RT, Bansal R, Parris C. 2005. Bisphenol-A, an environmental contaminant that acts as a thyroid hormone receptor antagonist in vitro, increases serum thyroxine, and alters RC3/neurogranin expression in the developing rat brain. *Endocrinology* 146:607-612. DOI: 10.1210/en.2004-1018.

Chapter 2: Evaluating Aryl Hydrocarbon Receptor Response in LMH 3D Spheroids

Modified from: Sharin T, Crump D, O'Brien JM. 2020. *Environmental Toxicology and Chemistry* 39:1693-1701. DOI: 10.1002/etc.4783.

2.1 Abstract

In the present study, we investigated whether the immortalized chicken hepatocellular carcinoma cell line, LMH, had a comparable aryl hydrocarbon receptor (AhR) response to primary chicken embryonic hepatocytes (CEH) when used in a well-established assay for chemical screening and prioritization. LMH cells were grown as two-dimensional (2D) confluent cells and 3D spheroids in order to determine the optimal cell culture states for chemical screening. Cytochrome P450 1A4 and 1A5 (CYP1A) activity and gene expression were compared between CEH and LMH grown in two culture states following exposure to the dioxin-like compound 3,3',4,4',5-pentachlorobiphenyl (PCB-126). CYP1A activity was measured using the ethoxyresorufin-*O*-deethylase (EROD) assay and changes in mRNA expression associated with the AhR pathway were determined using a custom-designed PCR array. Among LMH cell culture states (i.e. 2D vs 3D), EROD induction was observed only in 3D LMH spheroids. Similarly, 3D spheroids had the greatest number of changes in AhR-related genes compared to confluent cells. Overall, these results suggest that LMH cells grown as 3D spheroids have a metabolic and gene expression profile that is comparable to CEH, and may represent a suitable animal free alternative for *in vitro* screening of chemicals.

2.2 Introduction

To date, primary chicken embryonic hepatocytes (CEH) have been the most common *in vitro* model for avian toxicity testing (Hervé et al. 2009; Egloff et al. 2011; Crump et al. 2012; Crump et al. 2017). The preparation of CEH requires the use of animals and a considerable time commitment. For example, chicken embryos need to be artificially incubated for 19 d and then hepatocyte preparation requires approximately 6h, after which cells are acclimatized for 24h prior to chemical administration. Additionally, primary hepatocytes loose metabolic functions within 48-72h post-isolation (Soldatow et al. 2013). Immortalized hepatic cell lines may represent a viable alternative to primary hepatocytes because they are amenable for high throughput screening applications and could provide insight on cellular mechanisms of action of chemicals. However, many immortalized hepatic cell lines have limited activity of phase I and II metabolizing enzymes, and other key hepatic enzymes (Tolosa et al. 2016).

The standard method of culturing primary and immortalized hepatocytes as two-dimensional (2D) monolayers on culture vessels alters their morphology and microenvironment compared to in vivo conditions. Hepatocytes grown as monolayers are elongated and flattened, which decreases intercellular interactions (Hamilton et al. 2001). Three-dimensional (3D) hepatocyte culture is a better representation of the in vivo microenvironment. Hepatocytes grown as 3D spheroids have increased interactions with adjacent cells and similar morphology to hepatocytes in the liver (Edmondson et al. 2014). Spheroids retain bile canalicular functionality and expression of hepatic secretory proteins and phase I and II enzymes (Ramaiahgari et al. 2017; Gunness et al. 2013). Culturing hepatocytes in 3D provides more realistic cellular morphology and microenvironment than 2D cell culture for *in vitro* toxicity testing.

The chicken leghorn male hepatoma cell line, LMH, might be a useful immortalized alternative to primary hepatocytes for screening chemicals of potential hazard to avian species. The LMH cell line was derived from liver tumours excised from a male leghorn chicken exposed to the carcinogen diethyl nitrosamine (Kawaguchi et al. 1987). LMH cells have characteristics of hepatocytes including numerous endoplasmic reticulum, free ribosomes, microvilli in the plasma membrane, biliary canaliculus-like structures, and desmosomes. They have been primarily used to study the propagation of viruses such as avian reovirus (Heggen-Peay et al. 2002) and laryngotracheitis virus (Schnitzlein et al. 1994) and bacterial pathogens such as *Campylobacter jejuni* (Larson et al. 2008). Little is known about the metabolic activity of the LMH cell line.

The aim of the present study was to determine if the LMH cell line represents a suitable alternative to primary CEH for chemical screening and prioritization for avian toxicity testing. We began this investigation by measuring enzyme and gene expression activities that are regulated by the aryl hydrocarbon receptor (AhR), since this is a major xenobiotic response pathway. The metabolic activity of CYP1A, and expression of CYP1A4 and CYP1A5 genes were investigated following exposure of LMH cells to a known AhR agonist, 3,3',4,4',5-pentachlorobiphenyl (PCB-126). LMH exposures were conducted under 2 distinct culture conditions: 1) cells grown as a monolayer to confluency and; 2) three-dimensional spheroids, to identify the optimal conditions for chemical screening applications. We hypothesized that LMH cells grown as 3D spheroids would have greater metabolic activity and more CEH-like gene expression due to increased cellular communication and complex architecture compared to confluent cells.

2.3 Materials and Methods

2.3.1 Cell culture and dosing

The LMH cell line (ATCC-CRL2117) was purchased from Cedarlane Laboratories. All culturing reagents were purchased from Sigma-Aldrich. Cells were thawed and maintained in DMEM/F-12 medium supplemented with 10% fetal bovine serum (HI-FBS), 100 U/mL of penicillin and 10 000 µg/mL of streptomycin at 37°C with 5% CO_2. Cells were grown in 0.2% gelatin-coated T75 flasks (Corning Inc) to enhance attachment. Fresh medium was provided every 24 to 48 h and cells were sub-cultured when ~75% of the cells attached to the bottom of the flask. Cells were detached from the flask by the addition of 3 mL trypsin-EDTA for 3 min, followed by centrifugation at 125 x g for 3 min, and the resulting pellet was distributed into 4 flasks. Cells were considered confluent when 70-80% of the cells attached to the flask after a minimum of two passages. Confluent cells from passages 3 or 4 were used for all experiments and approximately 40 000 confluent cells in 250 µL of medium were plated in each well in flat bottom 96 well microplates (Corning). Confluents cells were dosed 24 h after plating. 3D spheroids were grown in ultra low attachment (ULA) round bottom 96 well microplates (Corning), which prevents cells from attaching to the surface, from passage 3 or 4 confluent cells. 10 000 cells in 250 µL of medium per well were seeded for spheroids and grown for 7 d prior to experimentation. Medium was changed everyday by removing 200 µL and adding 200 µL of fresh medium to each well.

Primary chicken embryonic hepatocyte (CEH) cultures were used as a positive control for the determination of EROD activity and gene expression. Fertilized, unincubated white leghorn chicken eggs were obtained from the Canadian Food Inspection Agency. The eggs were artificially incubated at 37°C and 60% humidity in a Petersime incubator. Chicken embryos

(n=15; 2 days pre-hatch) were euthanized by cervical decapitation and CEH were cultured as described previously (Kennedy et al. 1993; Crump et al. 2012). All procedures involving the handling of animals were conducted according to protocols approved by Environment and Climate Change Canada's Wildlife Eastern Animal Care Committee. CEH were plated in flat bottom 96 well microplate and incubated for 24h at 37.5°C and 5% CO_2 prior to dosing.

For exposure experiments, CEH and LMH cells (confluent and 3D-spheroids) were dosed with 1.25 µL dimethyl sulfoxide (DMSO (0.5%); Sigma-Aldrich) vehicle control or 3,3',4,4',5-pentachlorobiphenyl (PCB-126; Cas # 57465-28-8, 99% purity; Sigma-Aldrich) dissolved in DMSO to attain nominal in-well concentrations of 0.01 to 100 nM PCB-126 in 250 µL of medium per well. The cells were incubated for 24h and viability was determined immediately after the exposure period. Cells used for EROD analysis were flash frozen on dry ice and stored at -80°C. Cells for gene expression analysis were frozen and stored at -80°C after medium was removed by aspiration.

2.3.2 Cell viability

Cell viability was determined using the ViaLight plus kit (Lonza Group) for confluent cells, or the CellTiter-Glo 3D Cell Viability Assay (Promega Corporation) in spheroids. CellTiter-Glo 3D cell viability assay has a stronger lysis buffer, thus more suitable for spheroids. Both assays measure adenosine triphosphate (ATP) in metabolically active cells using luminescence. Assays were performed according to the manufacturer's protocol. Briefly, confluent cells were lysed with 50 µL of lysis buffer for 10 min at room temperature, and 100 µL of ATP monitoring reagent (AMR) was added to each well for 2 min. For the spheroids, 100 µL of lysis buffer was added per well and shaken for 10 min at room temperature before 100 µL of ATP reagent was added to each well and incubated for 30 min at 37°C. Luminescence was

measured using a Luminoskan Ascent luminometer (Thermo Fisher Scientific). Three technical replicate wells per dose group were analyzed.

2.3.3 EROD assay

EROD activity was determined as described previously with minor modifications (Kennedy and Jones, 1994). Briefly, 25 µL of 7-ethoxyresorufin was added for 12 min at 37.5°C followed by 12.5 µL of nicotinamide adenine dinucleotide phosphate (NADPH) for 7 min at 37.5°C. The reaction was stopped by the addition of cold fluorescamine at room temperature for 15 min. The presence of the EROD product, resorufin, was measured at an excitation wavelength of 530 nm and an emission wavelength of 590 nm and total protein concentration was measured at an excitation wavelength of 400 nm and emission wavelength of 460 nm using a DTX 880 multimode detector (Beckman Coulter). Triplicate plates with three technical replicate wells per plate were analyzed and EROD activity is reported as pmol resorufin/min/mg protein.

2.3.4 RNA isolation and complementary DNA synthesis

RNA was isolated from cells using RNeasy 96 kits (Qiagen) following the manufacturers' protocol. To ensure sufficient RNA quantity, two spheroid replicates were combined before extraction. RNA concentration was determined using a Nanodrop 2000 (ThermoFisher Scientific). Approximately 100 ng and 300 ng of RNA was reverse transcribed using the QuantiTect Reverse Transcription kit (Qiagen) for the CYP1A4 and CYP1A5 RT-PCR assay and the AhR PCR array, respectively.

2.3.5 Real-time RT-PCR

Customized chicken-specific RT^2 primers, CYP1A4 (PPG01289B-200), CYP1A5 (PPG02188A-200), and EEF1A1 (PPG00093A-200), were purchased from Qiagen; primer sequences are proprietary. The PCR reaction mixture for each sample consisted of 12.5 μL RT^2 SYBR Green mastermix (Qiagen), 1 μL of primer, 1 μL of cDNA, and 10.5 μL of RNAase-free water per well. Controls for no template (NTC) were included for each gene. The thermocycler program consisted of an enzyme activation step at 95°C for 10 min, followed by 40 cycles of 30s at 95°C, 1 min at 60°C. RT-PCR was performed using the Strategene MxPro 3005P instrument (Agilent).

2.3.6 Aryl hydrocarbon receptor pathway PCR array

A customized AhR pathway PCR array (Qiagen) was used to measure the expression of 27 dioxin-responsive genes (Table S2.1; Farmahin et al. 2016). cDNA was mixed with RT^2 SYBR Green Mastermix (Qiagen) before aliquoting 25 μL of the mixture to the PCR array. PCR arrays were amplified using a Strategene MxPro 3005P instrument (Agilent). PCR cycling conditions were 95°C for 10 min followed by 40 cycles of 95°C for 15s and 60°C for 1 min. No amplification was detected in any of the genomic DNA contamination control wells. The positive PCR control and reverse transcription control met the appropriate quality control/quality assurance criteria (Qiagen).

2.3.7 Data analysis

Cell viability data were log transformed and fit to a nonlinear regression curve (log (agonist) vs. response) to determine the median lethal concentration (LC50). Nonlinear regression and two-tailed t-test were performed using GraphPad Prism Ver. 6.07.

EROD activity data were fit to a modified Gaussian curve to determine the half maximal effective concentration (EC50), as described previously for hepatocytes treated with PCB-126 (Kennedy et al.1993). EROD curves were generated from three separate cell culture plates per cell type. Significant differences in activity between treatment and control were determined with two-way ANOVA ($p \leq 0.05$), where cell-type and dose were the two independent variables, followed by Tukey's HSD post hoc test using GraphPad Prism Ver. 6.07 (Tables S2.2 and 2.3).

Real-time RT-PCR data were analysed using the $2^{-\Delta Ct}$ method (Schmittgen and Livak 2008). For the CYP1A4 and CYP1A5 dose response experiments, data were normalized to the reference gene, EEF1A1. For the AhR pathway array experiments, data were normalized to the reference gene on the array, RPL4. The expression of the reference gene did not change significantly between treatment groups. Genes on the AhR array with missing Ct values, or Ct values above 35 in more than 25% of all samples were removed from analysis. Any remaining missing Ct values were set to Ct = 35. Fold change was determined relative to the respective DMSO control group for each cell type.

Dose-response data for CYP1A4 and CYP1A5 were fit to a multifactor generalized least-squares linear model to account for unequal variance between dose groups, using the *gls* function from the *nlme* library in R (Ver 3.2.5; R Development Core Team 2012). Dose and culture method were set as the independent variables, with interactions included, and an unequal variance structure between dose groups. Pairwise comparisons between dose groups and culture methods were performed using generalized linear hypothesis tests using the *glht* function from the *multcomp* library in R. The resulting p-values were adjusted using the Holm method.

A simpler ANOVA model was used for the AhR array analysis, since only a single dose was considered per culture method. Prior to ANOVA analysis, fold change data were log2-

transformed to account for unequal variance. The resulting p-values from pairwise comparisons between control and treated groups for all genes were adjusted using the Benjamini-Hochberg method with the false discovery rate (FDR) fixed at 5%. Hierarchical clustering was performed on the set of genes that had significant differential expression using the *heatmap2* function of the *gplots* library in R. Clustering was based on the Euclidian distance.

2.4 Results

2.4.1 Cell morphology

Confluent LMH cells had polygonal bodies and about 90% of the cells adhered to the plate (Figure 2.1A). When grown in ULA wells, LMH cells self-assembled and formed tight spheroids with relatively smooth edges by 24h without any exogenous extracellular matrix. Spheroids were grown for 7 d and had no visible necrotic core (Figure 2.1B). CEH had polygonal bodies but were flat and elongated after attachment at 24h (Figure 2.1C).

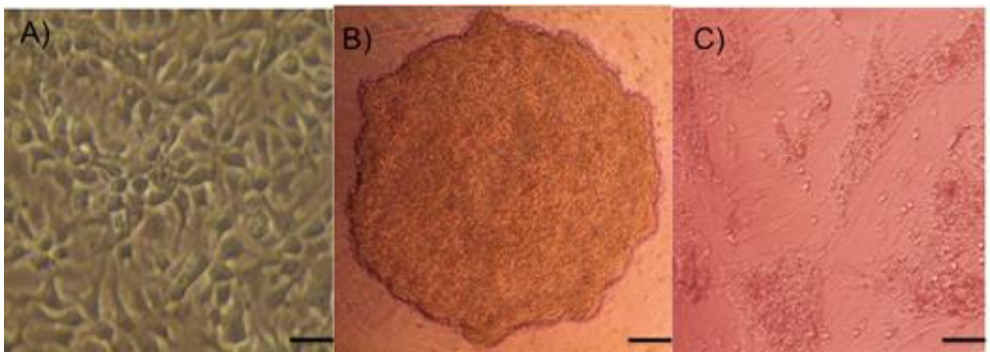

Figure 2.1. LMH cells in two culture conditions grown in 96-well plates: A) confluent cells, B) 3D spheroid, and C) chicken embryonic hepatocytes (CEH). Scale bar 50µM.

2.4.2 Cell viability

Dose-dependent decreases in cell viability were observed for both culture conditions following exposure to PCB-126 for 24h. The LC50 values (± SEM) for each culture type are presented in Table 2.1. There were no significant differences in LC50 values among the two culture conditions based on a two-tailed t-test.

Table 2.1. EC50 ± SEM values for LMH cells grown in the two culture conditions exposed to PCB-126 for 24h.

Culture condition	**EC_{50} (nM)**
Confluent	47.02 ± 23.8
Spheroid	61.1 ± 27

2.4.3 EROD activity in LMH cells

The EROD assay was used to measure catalytic CYP1A activity (measured as pmol resorufin/min/mg protein) in LMH cells grown in both culture conditions following exposure to PCB-126. PCB-126 did not induce EROD activity in confluent cells. EROD activity was induced in spheroids with an EC50 value of 0.09 ± 0.04 nM (Figure 2.2). For comparative purposes, CEH exposed to PCB-126 were used as a control. CEH had higher maximum EROD activity, but the EC50 was similar to that observed in spheroids; 0.05 ± 0.002 nM (Figure 2.2). The decrease in EROD activity observed at higher concentrations of PCB-126 is typical of the EROD assay, and is explained by the competitive inhibition of CYP1A by ligands of the receptor (Petrulis and Bunce 1999) and/or a decrease in cell viability (Table 2.1).

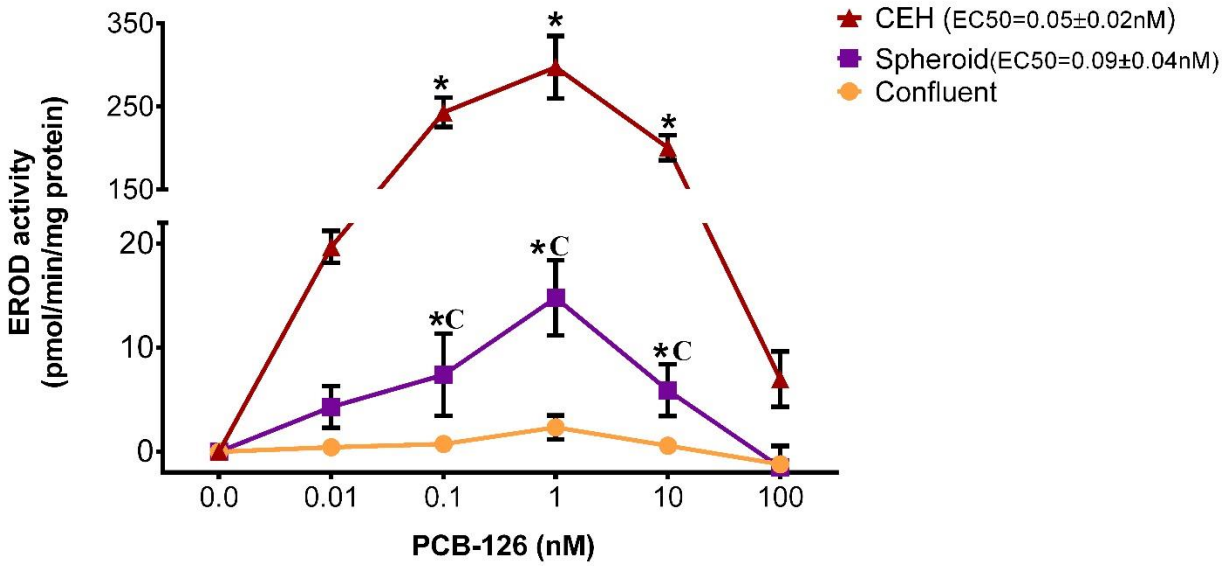

Figure 2.2. Concentration-dependent effects of PCB-126 on EROD activity in LMH 2D confluent cells and 3D spheroids, and CEH after 24h exposure. Data are presented as mean and error bars represent SEM, $p \leq 0.05$. Data were analyzed with a 2-way ANOVA and Tukey's HSD test for LMH cells. '*' denotes differences compared to untreated cells, 'C' indicates differences between confluent and spheroid cells.

2.4.4 CYP1A4 and CYP1A5 mRNA expression

PCB-126 exposure induced CYP1A4 and CYP1A5 mRNA expression in a concentration-dependent manner in confluent and spheroid cultures (Figure 2.3). Maximal induction values for CYP1A4 in confluent cells and spheroid cells were 26.8 and 48.9-fold, respectively. Maximal CYP1A5 induction in confluent and spheroid cells was 40.9- and 88.8-fold, respectively (Figure 2.3). The up-regulation of CYP1A4 was significant at 0.1 and 10 nM, while CYP1A5 was significant compared to the control at all doses in both confluent and spheroid cells. Among the two culture conditions, spheroids had significantly higher fold-changes in CYP1A4 and CYP1A5 mRNA expression compared to confluent LMH cells. CEH had significantly higher induction of

CYP1A4, maximal fold change 216.5, whereas spheroids had a greater induction of CYP1A5 compared to CEH. All possible statistical comparisons between CYP1A4 and CYP1A5 gene expression for confluent, spheroid, and CEH are presented in the supplemental information (Table S2.4 and S2.5).

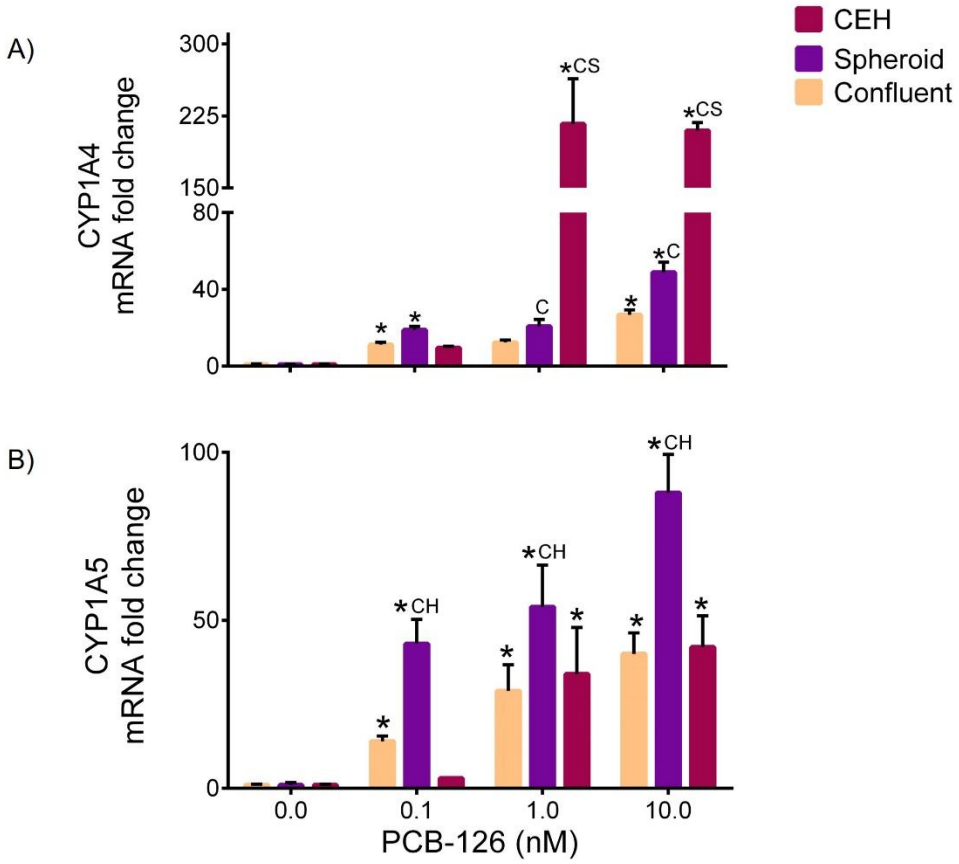

Figure 2.3. Concentration-dependent effects of PCB-126 exposure on A) CYP1A4 and B) CYP1A5 mRNA expression in LMH 2D confluent cells and 3D spheroids, and CEH after 24h. Data are presented as mean +SEM, $p \leq 0.05$. Data were analyzed using multifactor generalized least-squares linear model. * denotes a significant difference compared to DMSO-treated cells, 'C' indicates a significant difference compared to confluent cells at the same dose, 'S' indicates a

significant difference compared to spheroid at the same dose, 'H' indicates a significant difference compared to CEH at the same dose.

2.4.5 Aryl hydrocarbon receptor (AhR) pathway array

Based on EROD activity and CYP1A mRNA expression data, the lowest concentration to induce CYP1A4 and CYP1A5 expression, 0.1 nM PCB-126, was selected to explore additional toxicogenomics effects in LMH cells grown in two culture conditions using a custom-designed chicken AhR PCR array. The custom array measures the expression of 27 genes from several biological pathways that have been shown to be dysregulated by AhR agonists (Farmahin et al. 2016). Six genes from the array, ATP12A, FGF19, IAPP, CWH43, CYP24A1 and PODXL, were omitted from downstream data analysis because they had low expression (Ct values ≥ 35) in the two culture conditions. Twelve genes were significantly dysregulated relative to controls (fold-change ≥ 1.5 and FDR-adjusted p-value ≤ 0.05) in LMH confluent and spheroids, and CEH .The relative fold-changes of these genes are shown in Table 2.2 and visualized in a heatmap in Figure 2.4.

Hierarchical clustering revealed that spheroids clustered closer to CEH compared to confluent cells (Figure 2.4). Similarly, clustering of genes that were solely significant in LMH cells (i.e. when genes that were only significant in CEH were omitted) revealed that spheroid LMH and CEH clustered distinctly from confluent LMH (Figure S2.1). PCB-126 exposure only resulted in the significant up-regulation of three genes in confluent cells: CYP1A5, TGM2 and TIPARP. In confluent cells, average CYP1A4 induction was 6.56-fold, but was highly variable and therefore not significant (Table 2.2). In contrast, seven genes on the array were dysregulated in 3D spheroids exposed to 0.1 nM PCB-126. Genes associated with xenobiotic metabolism (CYP1A4, CYP1A5), keratin metabolism (KRT20), phenylalanine catabolism (PAH), protein

function (TIPARP, EEF1A1), and intercellular signalling (AREGB) were up-regulated, except for EEF1A1, which was down-regulated in spheroids (Table 2.2). For genes up-regulated in both LMH culture states (i.e. CYP1A5, TIPARP), the fold change induction was greater in spheroids (Table 2). The majority of the dysregulated genes in Table 2.2 were directionally consistent when comparing spheroids to CEH and for the three genes significantly modulated in both spheroids and CEH, two genes (CYP1A4, CYP1A5) had considerably higher induction in CEH, whereas TIPARP fold changes were similar between cell types (Table 2.2, Figure 2.4). Overall, 3D spheroids had a more CEH-like response compared to confluent cells based on gene expression following exposure to 0.1 nM PCB-126.

Table 2.2. Mean fold changes (n=3 replicates/cell type) of significant target genes on the AhR pathway array following exposure to 0.1 nM PCB-126 in LMH 2D confluent cells and 3D spheroids, and CEH. Fold changes were calculated relative to the respective DMSO control group. Significant fold changes (fold change ≥1.5, $p \leq 0.05$) are in bold.

	Fold Change		
Genes	Confluent	Spheroid	CEH
AREGB	1.41	**2.27**	1.45
CYP1A4	6.56	**2.53**	**214.28**
CYP1A5	**6.26**	**6.45**	**18.00**
CYP1B1	1.49	3.01	**2.54**
EEF1A1	1.06	**-3.11**	-1.52
FABP3	1.29	1.10	**2.36**
IGFBP4	1.19	1.03	**-1.86**
KRT20	1.64	**1.90**	1.93
PAH	1.26	**1.85**	2.07
TGM2	**2.82**	2.51	**2.47**
THRSP	1.28	2.54	**-4.40**
TIPARP	**2.21**	**3.27**	**2.86**

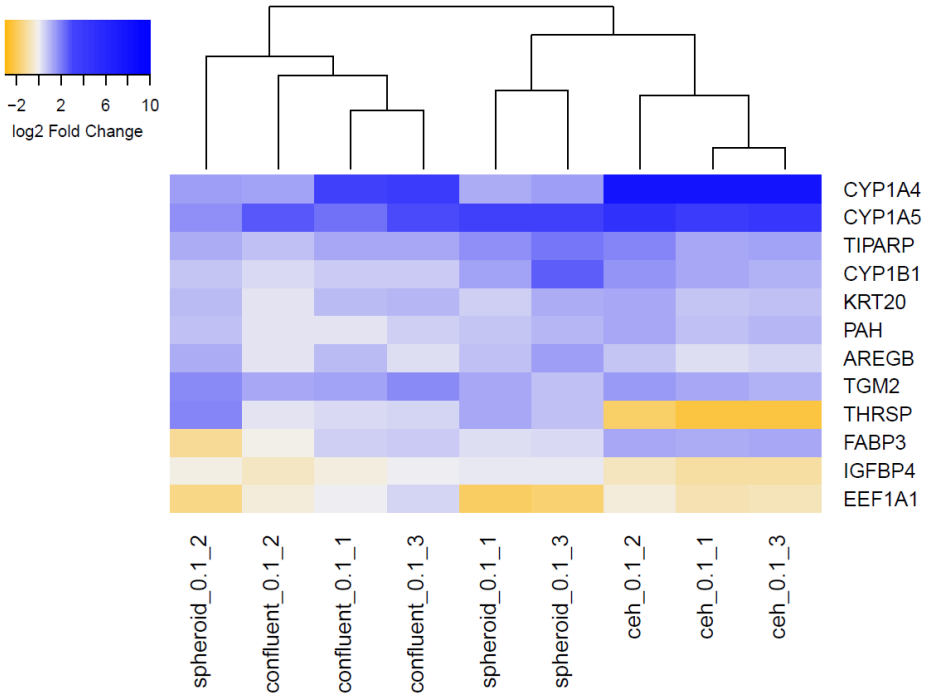

Figure 2.4. Heatmap of significant gene changes on the chicken AhR pathway PCR array for LMH 2D confluent cells and 3D spheroids, and CEH exposed to 0.1 nM PCB-126 for 24h, hierarchically clustered by gene expression and cell culture condition. Blue represents up-regulation and yellow represents down-regulation. The scale represents the log2 fold change.

2.5 Discussion

As toxicity testing shifts focus towards *in vitro* approaches, cell lines need to be properly characterized to ensure that these models adequately represent *in vivo* conditions. Common problems associated with immortalized cells for such applications include loss of activity of metabolizing enzymes, transcription factors, and hepatic specific proteins (Gunness et al. 2013). Expression of functional phase I metabolizing enzymes is of particular importance for cell lines used for chemical screening. 3D culturing using various techniques, such as hanging drops and scaffolds, have been proposed as ways to overcome poor metabolic responsiveness associated

with cells grown as 2D monolayers. Spheroid culturing techniques have proven to be of particular interest due to their relative simplicity and effectiveness. For example, culturing cells using low attachment surfaces and a liquid overlay technique improved enzyme activity in the immortalized human hepatic cell lines, HepaRG (Ramaiahghari et al. 2017) and C3A (Gaskell et al. 2016), and the rainbow trout hepatic cell line, RTL-W1 (Lammel et al. 2019). In the present study, we compared AhR-related metabolic enzyme activity (EROD) and gene expression in chicken LMH cells exposed to PCB-126 when grown in various culture states, including 3D spheroids. Our results indicated that LMH cells grown as spheroids had superior metabolic and gene expression responses to PCB-126 exposure compared to cells grown in a monolayer. Although characterization of additional pathways is still required, these findings suggest that LMH 3D spheroids may represent a suitable animal-free alternative for screening chemicals for potential toxicity to avian species.

2.5.1 PCB-126-induced cytotoxicity

Although several studies have reported differences in cell viability following chemical exposure between 2D and 3D cultured cells, we found that the LC50 values were statistically indistinguishable between confluent and spheroid LMH cells exposed to PCB-126. Conversely, in a previous study, no decrease in cell viability was observed following exposure to ≤ 3000 nM PCB-126 in primary CEH (Manning et al. 2013); a concentration well above LC50 values for the LMH cells (~50-60 nM). It is important to note that differences in cell viability have been rather inconsistent in the literature. Studies comparing cell viability in hepatocyte monolayer and spheroid cultures found that spheroids required a higher (Walker et al. 2000) or lower (Ott et al. 2017) concentration to induce cytotoxicity compared to confluent cells. A chemotherapy drug had similar cytotoxicity in confluent and spheroid cultures of the prostrate adenocarcinoma cell

line, LNCaP (Takagi et al. 2007). The difficulty in comparing LC50 values between confluent and spheroid cultures arises from the different viability endpoints measured, and differences between cell lines. The nature of a spheroid cluster could also impact cell viability results as dye uptake could be variable between compact and loose spheroids (Walzl et al. 2014). The inconsistency in viability data highlights the need for more studies comparing different viability endpoints in the same cell line following exposure to the same chemical.

2.5.2 AhR-related metabolic response was greater in spheroids

In avian species, two proteins of the cytochrome P450 superfamily of enzymes, CYP1A4 and CYP1A5, are, in part, responsible for the phase I metabolism of many environmental toxins, including polychlorinated biphenyls (PCBs), which act via the AhR. Our results demonstrated that 3D spheroids had a greater metabolic response to PCB-126 than 2D confluent cells. 3D spheroids showed a dose-dependent induction in EROD activity, whereas no EROD induction was observed in 2D confluent cells. The EROD EC50 values for spheroids and CEH were similar (0.09 and 0.05 nM) even though the maximal activity values were different (CEH EROD activity was much higher). PCB-126 has been shown to induce CYP1A4 activity, measured as EROD induction, in primary embryonic hepatocytes of several avian species in earlier studies (Head et al. 2009; Jones et al. 2014; Crump et al. 2015). In agreement with our findings, several studies reported greater expression of CYP1A in 3D spheroids compared to 2D monolayers for numerous cell lines (Nakamura et al. 2011; Takahasi et al. 2015; Ramaiahghari et al. 2015; Terashima et al. 2015). In 3D spheroids, the architecture of hepatocytes more closely resembles in vivo conditions due to increased cell-cell connections, resulting in an increase in expression of liver specific enzymes and transcription factors (Soldatow et al. 2013). The increase in transcription factors, such as hepatic nuclear factor 4α, improves cytochrome P450 functions in

spheroids (Chang and Hughes-Fulford 2014). Additionally, the loss of activity of certain cytochrome P450 enzymes has been reported in various immortalized cell lines (Castell et al. 2006; Gerets et al. 2012; Soldatow et al. 2013), even though discrepancies exist depending on the enzyme. This reduced activity in immortalized cells was related to a decrease in transcription of several cytochrome P450 enzymes and liver enriched transcription factors (Rodriguez-Antona et al. 2012).

In contrast to the EROD activity data, CYP1A4 and CYP1A5 mRNA levels were up-regulated in both LMH cell culture conditions. However, the degree of induction was culture-dependent. For both genes, the greatest induction was observed for 3D spheroids: ~42- and 89-fold maximal induction levels of CYP1A4 and CYP1A5 compared to ~27- and 41-fold in confluent cells. These findings are in agreement with the EROD activity data and the lack of EROD response for confluent LMH cells may, in part, be associated with the variable sensitivities of the two assays (i.e. EROD vs. qPCR). Previous studies comparing CYP1A activity and mRNA expression found qPCR to be more sensitive than the EROD assay (Vanden Huevel et al. 1994; Rees et al. 2003). CYP1A4 induction was greater in CEH than spheroids, whereas the opposite was reported for CYP1A5 (i.e. greater in spheroids). Previous studies reported a more pronounced induction of CYP1A4 compared to CYP1A5 in CEH after exposure to perfluoroalkyl compounds (Hickey et al. 2009) and brominated flame retardants (Su et al. 2016). Based on the CYP1A4 and CYP1A5 gene expression data, LMH spheroids have a more pronounced CYP1A5 response compared to CYP1A4.

2.5.3 Gene expression profiles in spheroids similar to primary CEH

The AhR pathway PCR array permitted a deeper gene expression evaluation of the impacts of PCB-126 exposure in confluent cells and 3D spheroids. The array comprises genes

from 18 biological pathways allowing further resolution of those that are impacted at the gene expression level. Overall, spheroids had a more pronounced gene expression response than confluent cells following exposure to an AhR agonist. Cluster analysis was performed to visually organize the gene expression data and revealed that the pathways affected in spheroids were similar to those in CEH and, importantly, different from confluent cells. Genes involved in xenobiotic metabolism, protein function, intercellular signalling, keratin filament organization and phenylalanine catabolism were altered in spheroids. Previous studies reported up-regulation of genes involved in xenobiotic metabolism (Ramaiahghari et al. 2017; Bell et al. 2018), keratin filament (Tostões et al. 2012), cell proliferation and adhesion (Brophy et al. 2009), and protein function (Bell et al. 2016) in immortalized hepatocytes cultured as spheroids. There are no studies looking at phenylalanine catabolism pathways in hepatic spheroid cultures. Phenylalanine catabolism has been found to be elevated in hepatocellular carcinoma (Huang et al. 2013) and therefore modulation of a gene associated with this pathway in LMH spheroids is plausible. The changes in gene expression between CEH and spheroids were similar, except for CYP1A4 and CYP1A5, which had significantly higher fold changes in CEH. The higher fold changes of CYP1A4 and CYP1A5 are probably due to increased expression of CYPs in CEH compared to immortalized hepatocytes (Rodriguez-Antona et al. 2002). The thyroid hormone pathway gene, THRSP, was significantly down-regulated in CEH compared to spheroids. This suggests that thyroid hormone response may be different in LMH spheroids compared to CEH and more characterization of this pathway in LMH spheroids is required. The diverse gene set altered by PCB-126 exposure demonstrates that spheroids have a) metabolizing capability, b) complex cellular signalling, and c) similar gene expression signatures as CEH.

Genes from three pathways were altered in confluent cells: xenobiotic metabolism, protein function and apoptosis. Two of these pathways, xenobiotic metabolism and protein function, were also modulated in spheroids. The gene altered in each pathway was the same as that observed in spheroids. The apoptosis gene, TGM2, was significantly up-regulated in confluent cells but not in spheroids. The abnormal morphology of confluent cells can result in an increase in apoptosis (Tibbitt and Anseth 2009). Overall, confluent cells have decreased AhR-related gene expression compared to spheroids.

In summary, this is the first study to culture LMH cells as 3D spheroids and evaluate metabolic competence compared to 2D confluent cells. LMH spheroids demonstrated enhanced CYP1A metabolic activity and CYP1A4 and CYP1A5 mRNA expression compared to 2D monolayer confluent cells. Moreover, the expression of dioxin-responsive genes involved in metabolic function, protein function, and cellular signalling were more responsive in spheroids and similar to CEH. Confluent LMH cells demonstrated weak metabolic competence, and thus, may not be appropriate for chemical screening applications. The 3D spheroids are more physiologically relevant than 2D monolayers for *in vitro* toxicity testing and therefore may represent a viable alternative to primary avian hepatocytes, currently the standard method in our laboratory. Additionally, unlike primary hepatocytes, LMH spheroids do not require animal utilization and thus, could bridge the gap between 2D cell culture and *in vivo* models for chemical screening applications.

Acknowledgements

This work was supported by funds from three sources within Environment and Climate Change Canada: 1) Chemicals Management Plan (CMP); 2) Strategic Technology Applications of Genomics for the Environment (STAGE); and 3) the Ecotoxicology and Wildlife Health Division.

2.6 References

Bell CC, Dankers ACA, Lauschke VM, Sison-Young R, Jenkins R, Rowe C, Goldring CE, Park K, Regan SL, Walker T, Schofield C, et al. 2018. Comparison of hepatic 2D sandwich cultures and 3D spheroids for long-term toxicity applications: A Multicenter Study. *Toxicological Sciences* 162:655-666. DOI: 10.1093/toxsci/kfx289.

Bell CC, Hendriks DFG, Moro SML, Ellis E, Walsh J, Renblom A, Puigvert LF, Dankers ACA, Jacobs F, Snoeys J, et al. 2016. Characterization of primary human hepatocyte spheroids as a model system for drug-induced liver injury, liver function and disease. *Scientific Reports* 6. DOI: 10.1038/srep25187.

Brophy CM, Luebke-Wheeler JL, Amiot BP, Khan H, Remmel RP, Rinaldo P, Nyberg SL. 2009. Rat hepatocyte spheroids formed by rocked technique maintain differentiated hepatocyte gene expression and function. *Hepatology* 49:578-586. DOI: 10.1002/hep.22674.

Castell JV, Jover R, Martinez-Jimenez CP, Gomez-Lechon MJ. 2006. Hepatocyte cell lines: their use, scope and limitations in drug metabolism studies. *Expert Opinion on Drug Metabolism & Toxicology* 2:183-212. DOI: 10.1517/17425255.2.2.183.

Chang TT, Hughes-Fulford M. 2014. Molecular. mechanisms underlying the enhanced functions of three-dimensional hepatocyte aggregates. *Biomaterials* 35:2162-2171. DOI: 10.1016/j.biomaterials.2013.11.063.

Crump D, Chiu S, Kennedy SW. 2012. Effects of Tris(1,3-dichloro-2-propyl) phosphate and Tris(1-chloropropyl) phosphate on cytotoxicity and mRNA expression in primary cultures of

avian hepatocytes and neuronal cells. *Toxicological Sciences* 126:140-148. DOI: 10.1093/toxsci/kfs015.

Crump D, Williams KL, Chiu S, Letcher RJ, Periard L, Kennedy SW. 2015. Biochemical and transcriptomic effects of herring gull egg extracts from variably contaminated colonies of the laurentian Great Lakes in chicken hepatocytes. *Environmental Science & Technology* 49:10190-10198. DOI: 10.1021/acs.est.5b02745.

Crump D, Williams KL, Chiu S, Zhang YF, Martin JW. 2017. Athabasca oil sands petcoke extract elicits biochemical and transcriptomic effects in avian hepatocytes. *Environmental Science & Technology* 51:5783-5792. DOI: 10.1021/acs.est.7b00767.

Duval K, Grover H, Han LH, Mou Y, Pegoraro AF, Fredberg J, Chen Z. 2017. Modeling physiological events in 2D vs. 3D cell culture. *Physiology* 32:266-277. DOI: 10.1152/physiol.00036.2016.

Edmondson R, Broglie JJ, Adcock AF, Yang LJ. 2014. Three-dimensional cell culture systems and their applications in drug discovery and cell-based biosensors. *Assay and Drug Development Technologies* 12:207-218. DOI: 10.1089/adt.2014.573.

Egloff C, Crump D, Chiu S, Manning G, McLaren KK, Cassone CG, Letcher RJ, Gauthier LT, Kennedy SW. 2011. In vitro and in ovo effects of four brominated flame retardants on toxicity and hepatic mRNA expression in chicken embryos. *Toxicology Letters* 207:25-33. DOI: 10.1016/j.toxlet.2011.08.015.

Farmahin R, Crump D, O'Brien JM, Jones SP, Kennedy SW. 2016. Time-dependent transcriptomic and biochemical responses of 6-formylindolo 3,2-b carbazole (FICZ) and 2,3,7,8-tetrachlorodibenzo-p-dioxin (TCDD) are explained by AHR activation time. *Biochemical Pharmacology* 115:134-143. DOI: 10.1016/j.bcp.2016.06.005.

Gaskell H, Sharma P, Colley HE, Murdoch C, Williams DP, Webb SD. 2016. Characterization of a functional C3A liver spheroid model. *Toxicology Research-UK* 5:1053-1065. DOI: 10.1039/c6tx00101g.

Gerets HHJ, Tilmant K, Gerin B, Chanteux H, Depelchin BO, Dhalluin S, Atienzar FA. 2012. Characterization of primary human hepatocytes, HepG2 cells, and HepaRG cells at the mRNA

level and CYP activity in response to inducers and their predictivity for the detection of human hepatotoxins. *Cell Biology and Toxicology* 28:69-87. DOI: 10.1007/s10565-011-9208-4.

Gripon P, Rumin S, Urban S, Le Seyec J, Glaise D, Cannie I, Guyomard C, Lucas J, Trepo C, Guguen-Guillouzo C. 2002. Infection of a human hepatoma cell line by hepatitis B virus. *P Natl Acad Sci USA* 99:15655-15660. DOI: 10.1073/pnas.232137699.

Gunness P, Mueller D, Shevchenko V, Heinzle E, Ingelman-Sundberg M, Noor F. 2013. 3D organotypic cultures of human HepaRG cells: A Tool for In Vitro Toxicity Studies. *Toxicological Sciences* 133:67-78. DOI: 10.1093/toxsci/kft021.

Hamilton G, Westmoreland C, George E. 2001. Effects of medium composition on the morphology and function of rat hepatocytes cultured as spheroids and monolayers. *In Vitro Cellular & Developmental Biology – Animal* 37:656-667.

Head JA, Kennedy SW. 2010. Correlation between an in vitro and an in vivo measure of dioxin sensitivity in birds. *Ecotoxicology* 19:377-382. DOI: 10.1007/s10646-009-0421-3.

Heggen-Peay CL, Cheema MA, Ali RA, Schat KA, Qureshi MA. 2002. Interactions of poult enteritis and mortality syndrome-associated reovirus with various cell types in vitro. *Poultry Science* 81:1661-1667. DOI: 10.1093/ps/81.11.1661.

Herve JC, Crump D, Jones SP, Mundy LJ, Giesy JP, Zwiernik MJ, Bursian SJ, Jones PD, Wiseman SB, Wan Y, et al. 2010. Cytochrome P4501A Induction by 2,3,7,8-tetrachlorodibenzo-p-dioxin and two chlorinated dibenzofurans in primary hepatocyte cultures of three avian species. *Toxicological Sciences* 113:380-391. DOI: 10.1093/toxsci/kfp270.

Hickey NJ, Crump D, Jones SP, Kennedy SW (2009). Effects of 18 perfluoroalkyl compounds on mRNA expression in chicken embryo hepatocyte cultures. *Toxicological Sciences* 111(2), 311–320. doi:10.1093/toxsci/kfp160

Huang Q, Tan YX, Yin PY, Ye GZ, Gao P, Lu X, Wang HY, Xu GW. 2013. Metabolic characterization of hepatocellular carcinoma using nontargeted tissue metabolomics. *Cancer Research* 73:4992-5002. DOI: 10.1158/0008-5472.can-13-0308.

Jones SP, Farmahin R, Kennedy SW. 2014. Ethoxyresorufin-O-deethylase (EROD) induction by TCDD, PeCDF and PCB 126 in bobwhite quail hepatocytes. *Ecotoxicology* 23:802-808. DOI: 10.1007/s10646-014-1218-6.

Kawaguchi T, Nomura K, Hirayama Y, Kitagawa T. 1987. Establishment and characterization of a chicken hepatocellular carcinoma cell line, LMH. *Cancer Research* 47:4460-4464.

Kennedy SW, Jones SP. 1994. Simultaneous measurement of cytochrome P4501A catalytic activity and total protein-concentration with a fluorescence plate reader. *Analytical Biochemistry* 222:217-223. DOI: 10.1006/abio.1994.1476.

Kennedy SW, Lorenzen A, James CA, Collins BT. 1993. Ethoxyresorufin-o-deethylase and porphyrin analysis in chicken-embryo hepatocyte cultures with a fluorescence multiwall plate reader. *Analytical Biochemistry* 211:102-112. DOI: 10.1006/abio.1993.1239.

Lammel T, Tsoukatou G, Jellinek J, Sturve J. 2019. Development of three-dimensional (3D) spheroid cultures of the continuous rainbow trout liver cell line RTL-W1. *Ecotoxicology and Environmental Safety* 167:250-258. DOI: 10.1016/j.ecoenv.2018.10.009.

Larson CL, Shah DH, Dhillon AS, Call DR, Ahn S, Haldorson GJ, Davitt C, Konkel ME. 2008. Campylobacter jejuni invade chicken LMH cells inefficiently and stimulate differential expression of the chicken CXCLi1 and CXCLi2 cytokines. *Microbiology-Sgm* 154:3835-3847. DOI: 10.1099/mic.0.2008/021279-0.

Liu H, Nie FH, Lin HY, Ma Y, Ju XH, Chen JJ, Gooneratne R. 2016. Developmental toxicity, EROD, and CYP1A mRNA expression in zebrafish embryos exposed to dioxin-like PCB126. *Environmental Toxicology* 31:201-210. DOI: 10.1002/tox.22035.

Manning GE, Mundy LJ, Crump D, Jones SP, Chiu S, Klein J, Konstantinov A, Potter D, Kennedy SW. 2013. Cytochrome P4501A induction in avian hepatocyte cultures exposed to polychlorinated biphenyls: Comparisons with AHR1-mediated reporter gene activity and in ovo toxicity. *Toxicology and Applied Pharmacology* 266(1): 38-47. DOI: 10.1016/j.taap.2012.10.030

Mittler F, Obeid P, Rulina AV, Haguet V, Gidrol X, Balakirev MY. 2017. High-content monitoring of drug effects in a 3D spheroid model. *Frontiers in Oncology* 7:19. DOI: 10.3389/fonc.2017.00293.

Mueller D, Kramer L, Hoffmann E, Klein S, Noor F. 2014. 3D organotypic HepaRG cultures as in vitro model for acute and repeated dose toxicity studies. *Toxicology in Vitro* 28:104-112. DOI: 10.1016/j.tiv.2013.06.024.

Nakamura K, Kato N, Aizawa K, Mizutani R, Yamauchi J, Tanoue A. 2011. Expression of albumin and cytochrome P450 enzymes in HepG2 cells cultured with a nanotechnology-based culture plate with microfabricated scaffold. *Journal of Toxicological Sciences* 36:625-633.

Ott LM, Ramachandran K, Stehno-Bittel L. 2017. An automated multiplexed hepatotoxicity and CYP induction assay using HepaRG cells in 2D and 3D. *Slas Discovery* 22:614-625. DOI: 10.1177/2472555217701058.

Petrulis JR, Chen GS, Benn S, LaMarre J, Bunce NJ. 2001. Application of the ethoxyresorufin-O-deethylase (EROD) assay to mixtures of halogenated aromatic compounds. *Toxicology Letters*16:177-184. DOI: 10.1002/tox.1022.

Ramaiahgari SC, den Braver MW, Herpers B, Terpstra V, Commandeur JNM, van de Water B, Price LS. 2014. A 3D in vitro model of differentiated HepG2 cell spheroids with improved liver-like properties for repeated dose high-throughput toxicity studies. *Archives of Toxicology* 88:1083-1095. DOI: 10.1007/s00204-014-1215-9.

Ramaiahgari SC, Waidyanatha S, Dixon D, DeVito MJ, Paules RS, Ferguson SS. 2017. Three-dimensional (3D) HepaRG spheroid model with physiologically relevant xenobiotic metabolism competence and hepatocyte functionality for liver toxicity screening. *Toxicological Sciences* 159:124-136. DOI: 10.1093/toxsci/kfx122.

Rodriguez-Antona C, Donato MT, Boobis A, Edwards RJ, Watts PS, Castell JV, Gomez-Lechon MJ. 2002. Cytochrome P450 expression in human hepatocytes and hepatoma cell lines: molecular mechanisms that determine lower expression in cultured cells. *Xenobiotica* 32:505-520. DOI: 10.1080/00498250210128675.

Schmittgen TD, Livak KJ. 2008. Analyzing real-time PCR data by the comparative C-T method. *Nature Protocols* 3:1101-1108. DOI: 10.1038/nprot.2008.73.

Schnitzlein WM, Radzevicius J, Tripathy DN. 1994. Propagation of infectious laryngotracheitis virus in an avian liver-cell line. *Avian Diseases* 38:211-217. DOI: 10.2307/1591939.

Shin DS, Seo H, Yang JY, Joo J, Im SH, Kim SS, Kim SK, Bae MA. 2018. Quantitative evaluation of cytochrome P450 3A4 inhibition and hepatotoxicity in HepaRG 3-D spheroids. *International Journal of Toxicology* 37:393-403. DOI: 10.1177/1091581818780149.

Soldatow VY, LeCluyse EL, Griffith LG, Rusyn I. 2013. In vitro models for liver toxicity testing. *Toxicological Research* 2:23-39. DOI: 10.1039/c2tx20051a.

Su G, Letcher RJ, Crump D, Farmahin R, Giesy JP, Kennedy SW. 2016. Sunlight irradiation of highly brominated polyphenyl ethers generates polybenzofuran products that alter dioxin-responsive mRNA expression in chicken hepatocytes. *Environmental Science & Technology*, 50(5), 2318-27. doi: 10.1021/acs.est.5b04939

Takagi A, Watanabe M, Ishii Y, Morita J, Hirokawa Y, Matsuzaki T, Shiraishi T. 2007. Three-dimensional cellular spheroid formation provides human prostate tumor cells with tissue-like features. *Anticancer Res* 27:45-53.

Takahashi Y, Hori Y, Yamamoto T, Urashima T, Ohara Y, Tanaka H. 2015. 3D spheroid cultures improve the metabolic gene expression profiles of HepaRG cells. *Bioscience Reports* 35. DOI: 10.1042/bsr20150034.

Terashima J, Goto S, Hattori H, Hoshi S, Ushirokawa M, Kudo K, Habano W, Ozawa S. 2015. CYP1A1 and CYP1A2 expression levels are differentially regulated in three-dimensional spheroids of liver cancer cells compared to two-dimensional monolayer cultures. *Drug Metabolism and Pharmacokinetics* 30:434-440. DOI: 10.1016/j.dmpk.2015.10.001.

Thomas CH, Collier JH, Sfeir CS, Healy KE. 2002. Engineering gene expression and protein synthesis by modulation of nuclear shape. *Proc Natl Acad Sci USA* 99:1972-1977. DOI: 10.1073/pnas.032668799.

Tibbitt MW and Anseth KW. 2009. Hydrogels as extracellular matrx mimics for 3D cell culture. *Biotechnology & Bioengineering* 103(4): 655-663. DOI: 10.1002/bit.22361.

Tolosa L, Gomez-Lechon MJ, Lopez S, Guzman C, Castell JV, Donato MT, Jover R. 2016. Human upcyte hepatocytes: Characterization of the hepatic phenotype and evaluation for acute and long-term hepatotoxicity routine testing. *Toxicological Sciences* 152:214-229. DOI: 10.1093/toxsci/kfw078.

Tostoes RM, Leite SB, Serra M, Jensen J, Bjorquist P, Carrondo MJT, Brito C, Alves PM. 2012. Human liver cell spheroids in extended perfusion bioreactor culture for repeated-dose drug testing. *Hepatology* 55:1227-1236. DOI: 10.1002/hep.24760.

Vandenheuvel JP, Clark GC, Kohn MC, Tritscher AM, Greenlee WF, Lucier GW, Bell DA. 1994. Dioxin-responsive genes-examination of dose response relationships using quantative reverse transcriptase-polymerase chain reaction. *Cancer Res*earch 54:62-68.

Walker TM, Rhodes PC, Westmoreland C. 2000. The differential cytotoxicity of methotrexate in rat hepatocyte monolayer and spheroid cultures. *Toxicology in Vitro* 14:475-485. DOI: 10.1016/s0887-2333(00)00036-9.

Walzl A, Unger C, Kramer N, Unterleuthner D, Scherzer M, Hengstschlager M, Schwanzer-Pfeiffer D, Dolznig H. 2014. The Resazurin Reduction Assay Can Distinguish Cytotoxic from Cytostatic Compounds in Spheroid Screening Assays. *Journal of Biomolecular Screening* 19:1047-1059. DOI: 10.1177/1087057114532352.

Yamauchi K, Sakamoto A, Nishiyama N, Shimada N. 2005. Identification of thyroid hormone-responsive genes in a chicken hepatoma cell line, LMH. *Zoological Science* 22:1131-1135. DOI: 10.2108/zsj.22.1131.

Zeigerer A, Wuttke A, Marsico G, Seifert S, Kalaidzidis Y, Zerial M. 2017. Functional properties of hepatocytes in vitro are correlated with cell polarity maintenance. *Experimental Cell Research* 350:242-252. DOI: 10.1016/j.yexcr.2016.11.027.

Chapter 3. Concentration- and Time-Dependent Induction of CYP1A and DNA Damage Response by Benzo(a)pyrene in LMH 3D Spheroids

Modified from: Sharin T, Gyasi H, Jones SP, Crump D, O'Brien JM. 2021. *Environmental and Molecular Mutagenesis* 62(5): 319-327. DOI: 10.1002/em.22433

3.1 Abstract

In vitro liver toxicity tests performed using immortalized cell lines cultured as two dimensional (2D) monolayer cells have limited CYP450 activity and may be inadequate for screening chemicals that require activation to exert toxicity. Metabolic competence is greatly improved using three-dimensional (3D) cell culture. In this study, CYP1A induction, and subsequent DNA damage response induced by benzo(a)pyrene (BaP) were compared in 2D monolayer cells and 3D spheroids of the chicken hepatic cell line, LMH. Cells were exposed to BaP (0.1-100 µM) for different durations: 4, 8, 24, 35 or 48h. CYP1A activity, mRNA expression of CYP1A and DNA damage response genes, and phosphorylation of H2A histone family member X (γH2AX) were determined using the EROD assay, a customized PCR array, and flow cytometry, respectively. EROD activity was significantly induced at 8h and achieved maximal induction at 24h in 3D spheroids; earlier time points than for 2D cells. In 3D spheroids, BaP exposure resulted in a concentration-dependent increase in CYP1A4 gene expression beginning at 8h followed by upregulation of DNA damage response genes at 24h. In contrast, CYP1A4 mRNA induction was only observed at 48h in 2D monolayers. CYP1A5 mRNA was induced at an earlier time point in 2D cells (8h) but maximum induction was greater in 3D spheroids. An increase in γH2AX was observed at 24h in spheroids; this endpoint was not evaluated in 2D monolayer cells. These results suggest that BaP metabolism precedes the DNA damage response and occurs earlier in 3D spheroids. This study demonstrates that LMH 3D

spheroids could be a suitable metabolically-competent *in vitro* model to measure genotoxicity of chemicals that require metabolic activation by CYP1A.

3.2 Introduction

Hepatocytes, the most abundant cell type in the liver, are responsible for xenobiotic metabolism, which has an important influence on the ultimate toxicity of chemicals (Sevior et al. 2012). Metabolism of chemicals usually generates metabolites that are less toxic; however in certain cases, metabolism can result in the biotransformation and formation of intermediate reactive metabolites that elicit increased toxicity (Gomez-Lechon et al. 2015). Many environmental carcinogens are mutagenic following metabolic activation. For example, the prototypical polycyclic aromatic hydrocarbon, benzo(a)pyrene (BaP), is metabolized by CYP1A to benzo(a)pyrene-7,8-dihydrodiol-9,10-epoxide (BPDE), a highly reactive metabolite that can bind to DNA and form bulky adducts (Schwarz et al. 2001). Due to the critical role of xenobiotic metabolism, it is important that any hepatocyte model used for toxicity testing maintain this functionality.

In vitro genotoxicity assays are typically performed in cell lines without metabolizing enzymes such as the human lymphoblastoid (TK6) and chicken bursal lymphoma (DT-40), which, on their own, are inadequate to determine the toxicity of chemicals requiring metabolic activation (Buick et al. 2015; Ooka et al. 2016). An exogenous source of metabolic enzymes (e.g. S9) is required to detect metabolism-dependent endpoints in these cell models. However, hepatic cell lines and culturing techniques that retain metabolic activity are becoming more common for studying promutagens (Guo et al. 2020). One such method is three-dimensional (3D) culturing. Hepatic cell lines are commonly cultured as 2D monolayers, which fails to recapitulate the cellular architecture resulting in poor metabolic competence and abnormal gene expression

profiles (Tolosa et al. 2016; Hamilton et al. 2001). 3D cell culturing techniques, such as growing cells as spheroids, enhances intercellular interactions and better represents *in vivo* conditions (Edmondson et al. 2014). Even immortalized hepatocytes, which typically have poor metabolic activity, have improved metabolic competence when cultured as spheroids, including increased CYP450 and other metabolizing enzyme activity (Sharin et al. 2020; Lammel et al. 2019; Ramaiahgari et al. 2017; Gunness et al. 2013).

In avian ecotoxicology testing, the most common *in vitro* model is chicken embryonic hepatocytes (CEH), which retain liver-specific functions including metabolic activity but only for a short period of time (~48-72h) (Soldatow et al. 2013). Furthermore, CEH culture requires animal use and there is increasing demand to incorporate animal free approaches to reduce the animals required for toxicity testing (Pfuhler et al. 2009). The immortalized chicken hepatic cell line, LMH, is an alternative *in vitro* model for screening chemicals for avian toxicity testing. In a previous study, LMH cells cultured as 3D spheroids had improved CYP1A activity and corresponding mRNA expression along with the altered expression of additional aryl hydrocarbon receptor (AhR)-regulated genes (Sharin et al. 2020). The objective of the present study was to determine if CYP1A metabolism-dependent genotoxic endpoints could be detected in LMH cells cultured as 2D monolayers or 3D spheroids exposed to BaP. Metabolic activity was determined by measuring CYP1A activity and gene expression. The DNA damage response was determined by measuring DNA damage response gene expression and phosphorylation of H2AX (γH2AX). To determine if upregulated metabolic activity preceded the DNA damage response, these endpoints were measured across multiple time points.

3.3 Materials and Methods

3.3.1 Cell culture and treatment

The LMH cell line (CRL-2117) was acquired from Cedarlane and cultured as described elsewhere (Sharin et al. 2020). For 3D spheroids, 10 000 cells in 250 µL of media were added to each well of ultra low attachment (ULA) round bottom 96 well microplates (Corning). Media from spheroid culture was changed everyday by removing 200 µL and adding 200 µL of fresh medium to each well. Spheroids were grown for 5d before chemical administration.

For all exposure experiments, LMH cells (2D monolayers and 3D spheroids) were treated with 1.25 µL dimethyl sulfoxide (DMSO (0.5%); Sigma-Aldrich) or BaP (Cas # 50-32-8, 96% purity; Sigma-Aldrich) dissolved in DMSO to attain nominal in-well concentrations of 0.1, 1, 10 or 100 µM in 250 µL of media per well. The cells were incubated for 4, 8, 24, 35 or 48h. Cell viability and γH2AX were measured immediately after the exposure period. Cells for the 7-ethoxy-resorufin-*O*-deethylase (EROD) and gene expression assays were flash frozen on dry ice and stored at -80°C.

3.3.2 Cell viability and EROD assay

Cell viability was determined using CellTiter-Glo and CellTiter-Glo 3D (Promega) assays following the manufacturer's protocol. Briefly, 100 µL of lysis buffer was added per well for both culture states. After the addition of lysis buffer, spheroids were shaken on a plate shaker (ThermoFisher Scientific) for 2 min at room temperature. For both monolayer cells and spheroids, 100 µL of ATP reagent was added to each well and incubated for 30 min at 37°C and transferred to a 96 well white clear flat bottom plate (Nunc). Luminescence was measured using

a Luminoskan Ascent luminometer (ThermoFisher Scientific) and three technical replicate wells per dose group were analyzed.

CYP1A activity was determined using the EROD assay as described previously (Sharin et al. 2020). The presence of the EROD product, resorufin, was measured at an excitation wavelength of 530 nm and an emission wavelength of 590 nm. The total protein concentration in each well was measured at an excitation wavelength of 400 nm and emission wavelength of 460 nm using a DTX 880 multimode detector (Beckman Coulter). Triplicate plates with three technical replicate wells per plate were analyzed and CYP1A activity is reported as pmol resorufin/min/mg protein.

3.3.3 RNA isolation and complementary DNA synthesis

RNA was isolated from cells using the RNeasy 96 kits (Qiagen) according to the manufacturer's protocol. For both culture conditions, two replicates were combined prior to extraction to ensure sufficient RNA yield (n=3/treatment group). RNA concentration was determined using the QIAxpert (Qiagen). Approximately 100 ng of RNA was reverse transcribed using the QuantiTect Reverse Transcription kit (Qiagen) following the manufacturer's instructions.

3.3.4 PCR Array

A customized chicken PCR array was used to measure the expression of genes involved in metabolism, cell cycle, and DNA damage response. The array consisted of eight target genes, a reference gene, EEF1A1, and no template control (NTC) (Table S3.1). The primers were purchased from Qiagen and thus, the primer sequences are proprietary. In each well of a white 384 well microplate (Roche), 0.5 μL of primer and 5.25 μL of RNase free water were added to

each well followed by the addition of 0.5 µL of cDNA and 6.25 µL of RT2 SYBR Green Mastermix (Qiagen) for a total volume of 12.5 µL per well. PCR cycling conditions were 95°C for 10 min followed by 45 cycles of 95°C for 15 s and 60°C for 1 min on the LightCycler 480 Real-Time PCR System (Roche).

3.3.5 γH2AX assay

γH2AX was measured in LMH spheroids using the MultiFlow DNA Damage Kit—p53, γH2AX, Phospho-Histone H3 (Litron Laboratories) according to the manufacturer's directions with minor modifications. Briefly, media was removed after the desired exposure period, 250 µL of MacsQuant running buffer was added to each well and spheroids were disrupted via pipetting fifteen times. Next, 25 µL of samples were removed from each well, added to a new 96-well plate containing 50 µL/well of pre-aliquoted labelling solution, and incubated for 30 min at room temperature in the dark. Following incubation, 50 µL of samples from each well were removed, added to another 96 well round bottom plate containing 200 µl of MacsQuant running buffer to ensure sufficient cell count per samples and cells were analyzed immediately. 20 µl of sample was collected for each run and four to six replicates per dose group were analyzed. The p53 and phosphor-histone H3 endpoints were not reported in the present study (due to poor antibody binding in LMH cells).

3.3.6 Data Analysis

Cell viability data were log transformed and fit to a nonlinear regression curve (log (agonist) vs. response) using least squares (ordinary) fit to determine the median lethal concentration (LC50). Nonlinear regression, 2-way ANOVA and Sidak's multiple comparisons of LC50 values were performed using GraphPad Prism Ver. 6.07.

EROD curves were generated from three separate cell culture plates per cell type. Significant differences in activity between treatment and control were determined with two-way ANOVA ($p \leq 0.05$), where cell-type and dose were the two independent variables, followed by Tukey's HSD test using GraphPad Prism Ver. 6.07.

Real-time RT-PCR data were analysed using the $2^{-\Delta Ct}$ method (Schmittgen and Livak 2008). Target gene Ct values were normalized to the Ct values of the reference gene, EEF1A1. Fold change was determined relative to the respective DMSO control group for each cell type and time point. Prior to ANOVA analysis, fold change data were log2-transformed to account for unequal variance. The resulting p-values from pairwise comparisons between control and treated groups for all genes were adjusted using the Benjamini-Hochberg method with the false discovery rate (FDR) fixed at 5%.

Flow cytometry data were analyzed using FlowJo software (v10 for Windows). After removing apoptotic events, nuclei that positively stained for both peridinin-chlorophyll-protein (PerCP) and allophycocyanin (APC) were selected by gating on a dot-plot from the DNA content histogram. Shifts in cell cycle values were determined by gating on cell populations corresponding to G1, S, and G2/M according to linear histogram plots. Mean APC fluorescence values for each region of the cell cycle were normalized to the solvent control (DMSO) and expressed as fold change. Significant differences in γH2AX in cell cycle phases between treatment and control were determined with two-way ANOVA ($p \leq 0.05$), where concentration and time points were the variables, followed by Tukey's HSD using GraphPad Prism Ver. 6.07.

The dose-response modelling program PROAST (online ver. 70.1, Dutch National Institute for Public Health and the Environment, (RIVM)) was used to determine benchmark dose (BMD) and confidence intervals for gene expression and γH2AX. Data were modeled for

continuous response with time point as covariate and benchmark response (BMR; CES in PROAST) was selected as endpoint specific. Data were fitted to a number of models and model averaging was used to determine the benchmark dose response (BMD; corresponds to critical effect dose (CED) in PROAST) and BMDL (lower bound of the BMD confidence interval) and the BMDU (upper bound of the BMD confidence interval). BMD range plots were created using GraphPad Prism Ver. 6.07.

3.4 Results

3.4.1 Cell viability

Cell viability was not significantly affected at 8h. The viability of LMH 2D monolayers and 3D spheroids significantly decreased following exposure to BaP (100 µM) at 24 and 48h (Figure S3.1). However, there was no significant difference in cell viability between 2D monolayers and 3D spheroids.

3.4.2 CYP1A activity

CYP1A activity was determined at the 8, 24 and 48h time points using the EROD assay (measured as pmol resorufin/min/mg protein) in 2D monolayer cells and 3D spheroids following exposure to BaP. In 2D monolayer cells, BaP did not induce CYP1A activity at 8h. However, CYP1A activity was significantly induced after 24h with maximal activity occurring at 48h (Figure 3.1A). In contrast, CYP1A activity was significantly induced at 8h in spheroids (at 10 and 100 µM BaP). Maximal activity was observed at 24h followed by a decrease at 48h (Figure 3.1B). In general, 3D spheroids had higher CYP1A activity at all three time points compared to 2D monolayer cells.

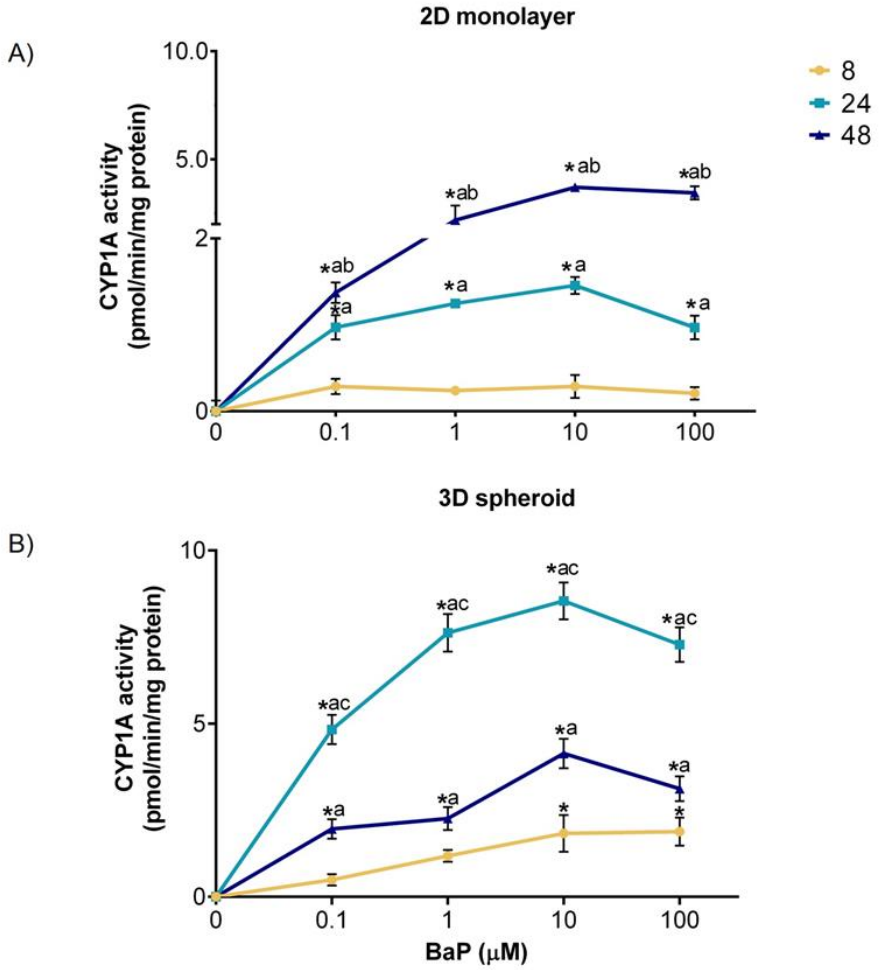

Figure 3.1. Concentration- and time-dependent effects of benzo(a)pyrene (BaP) on CYP1A activity (measured by EROD) in LMH cells cultured as A) 2D monolayer cells and B) 3D spheroids following 8, 24 and 48h exposure. Data are presented as mean and error bars represent SEM, $p \leq 0.05$. Data were analyzed with a 2-way ANOVA and Tukey's HSD test. "*" denotes difference compared to untreated cells, "a" indicates difference from 8h; "b" denotes difference from 24h and "c" represents difference from 48h.

3.3 Gene expression

Gene expression was determined at the 4, 8, 24 and 48h time points. No significant effects on gene expression were observed after 4h in either culture condition, so data from this time point are not shown.

In 2D monolayer cells, significant changes in gene expression were only observed for three of the eight genes measured: CYP1A4, CYP1A5, and GADD45. Significant concentration-dependent upregulation of CYP1A4 expression occurred only at 48h (max = 4.08-log2fold). In contrast, expression of CYP1A5 was upregulated at 8h (max= 2.41-log2fold), which was sustained through 24h and 48h, where the highest upregulation was observed (max = 3.83-log2fold). Only one of the cell cycle regulation and DNA damage response genes, GADD45, was upregulated (1.44-log2fold) at the highest concentration (100 µM) at 48h (Table 3.1).

Table 3.1. Concentration- and time-dependent effects of benzo(a)pyrene (BaP) exposure on gene expression in 2D monolayer cells. Fold changes were calculated relative to the respective DMSO control group. Significant fold changes (log2 fold change ≥ 0.58 and ≤ -0.58, adjp ≤ 0.05) are in bold and yellow.

		Log2 Fold Change							
Time point (h)	Concentration (μM)	CDKN1A	CYP1A4	CYP1A5	DDB2	GADD45	POLB	POLK	XPC
8	0	0.00	0.00	0.00	0.00	0.00	0.00	0.00	0.00
	0.1	-0.20	0.22	-0.23	0.44	0.29	-1.04	-1.93	0.45
	1	0.30	0.11	1.27	-1.46	0.50	0.08	-0.12	0.58
	10	0.30	0.36	**1.82**	0.39	0.10	0.78	0.00	0.34
	100	1.19	0.99	**2.41**	0.23	0.71	0.97	0.46	0.61
24	0	0.00	0.00	0.00	0.00	0.00	0.00	0.00	0.00
	0.1	0.51	-0.03	-0.44	0.71	0.66	0.20	-0.23	0.60
	1	1.60	2.06	0.10	0.74	1.31	0.81	0.97	0.86
	10	1.21	2.04	1.19	1.35	1.81	1.17	0.53	0.55
	100	0.92	2.24	**2.77**	0.98	0.96	0.42	0.77	0.46
48	0	0.00	0.00	0.00	0.00	0.00	0.00	0.00	0.00
	0.1	0.25	1.25	0.76	0.26	0.33	-0.59	0.00	-0.62
	1	0.56	**2.10**	0.26	-0.39	0.52	-0.10	0.22	-0.81
	10	0.93	**3.24**	**2.85**	0.53	1.09	0.50	0.82	-0.12
	100	0.99	**4.08**	**3.83**	0.30	**1.44**	0.80	1.61	-0.22

In contrast to 2D cells, all eight metabolism, cell cycle and DNA damage response genes were significantly upregulated in 3D spheroids treated with BaP. There was a significant concentration-dependent upregulation of CYP1A4 expression starting from 8h and maximal upregulation (5.71-log2fold) occurred at 24h. CYP1A5 was not significantly affected at 8h but was maximally upregulated at 24h (5.47-log2fold) and remained significant at 48h. The expression of both CYP1A4 and CYP1A5 was lower (~3.4-4.1) at 48h compared to 24h (Table 3.2).

Upregulation of one cell cycle gene, CDKN1A, and all four DNA damage response genes, DDB2, POLB, POLK and XPC, were observed at 24h and was sustained at 48h. All of these genes had maximum induction at 48h, except for POLB which was maximally induced at 24h (max log2FC = 3.8, 2.7, 2.4, 2.6 and 3.3 for CDKN1A, DDB2, POLB, POLK and XPC,

respectively). Concentration-dependent upregulation of GADD45 (max = 4.2-log2fold) occurred only at 48h (Table 3.2).

BMD modeling was conducted to compare the gene expression dose-response in both cell models (Figure S3.2). Generally, the confidence intervals were relatively wide (several orders of magnitude), with the lower confidence limit (BMDL) extrapolated several orders of magnitude below the lowest dose used in this study. The dose-response modeling also demonstrated the general lack of DNA damage response gene induction in 2D monolayers cells, and the earlier CY1A4 response at 8h followed by the DNA damage response gene response after 48h in 3D spheroids. However, due the overlapping confidence intervals, limited conclusions could be drawn about the relative potency of BaP for inducing each gene (Figure S3.2).

Table 3.2. Concentration- and time-dependent effects of benzo(a)pyrene (BaP) exposure on gene expression in 3D spheroids. Fold changes were calculated relative to the respective DMSO control group. Significant fold changes (log2 fold change ≥ 0.58 and ≤ -0.58, adjp ≤ 0.05) are in bold and yellow.

		Log2 Fold Change							
Time point (h)	Concentration (μM)	CDKN1A	CYP1A4	CYP1A5	DDB2	GADD45	POLB	POLK	XPC
8	0	0.00	0.00	0.00	0.00	0.00	0.00	0.00	0.00
	0.1	1.03	0.55	-0.62	-0.35	-0.01	1.14	-0.02	-0.44
	1	0.82	**2.88**	-0.20	0.81	-0.33	1.57	0.32	0.98
	10	0.57	**3.07**	-0.18	0.93	-0.58	0.64	-1.23	0.32
	100	0.88	**3.65**	0.99	0.73	0.44	1.49	0.25	1.20
24	0	0.00	0.00	0.00	0.00	0.00	0.00	0.00	0.00
	0.1	**1.44**	**1.46**	**1.87**	**1.54**	0.09	**2.42**	1.00	**1.97**
	1	0.12	**2.89**	**3.11**	**1.59**	0.06	**0.93**	0.33	**2.10**
	10	**1.32**	**5.09**	**5.35**	**2.49**	1.27	**1.56**	**1.41**	**2.15**
	100	**1.86**	**5.71**	**5.47**	0.80	1.86	0.73	0.44	**2.47**
48	0	0.00	0.00	0.00	0.00	0.00	0.00	0.00	0.00
	0.1	1.46	-0.05	0.87	0.95	**2.50**	**1.23**	**1.10**	0.96
	1	1.57	0.76	**2.55**	1.26	**2.76**	**2.03**	**1.66**	**1.35**
	10	**2.13**	**2.26**	**3.98**	**2.39**	**3.31**	**1.92**	**2.56**	**2.01**
	100	**3.84**	**3.47**	**4.14**	**2.70**	**4.16**	**1.83**	**2.38**	**3.29**

3.4 DNA damage (γH2AX)

The induction of double strand breaks (DSBs) by BaP was measured at 8, 24 and 35h in the nuclei of 3D spheroids through the detection of γH2AX formation using flow cytometry. γH2AX occurs following DSBs and is an early marker of DNA damage (Watters et al. 2009). γH2AX was not determined in 2D monolayer cells due to delayed CYP1A activity and CYP1A4 mRNA expression, as well as a lack of response in DNA damage response genes. In 3D spheroids, an increase in γH2AX (1.5-fold) was observed at the highest concentration (100 µM) at 24h (Figure 3.2A). When nuclei were separated by cell cycle, the increase in γH2AX signal was detected in nuclei from the S and G2/M phases, and was significant at 10 and 100 µM at 24h, and sustained at a lower level through 35h (Figure 3.2 B-D). A Cell cycle arrest was observed in G1 nuclei, with a concurrent decrease in G2/M nuclei. This was significant at 8h, was maximal at 24h, and disappeared at 35h (Figure S3.3). There was no difference in S-phase at any time points and a decrease in cells was observed in G2/M checkpoint at 8 and 24h.

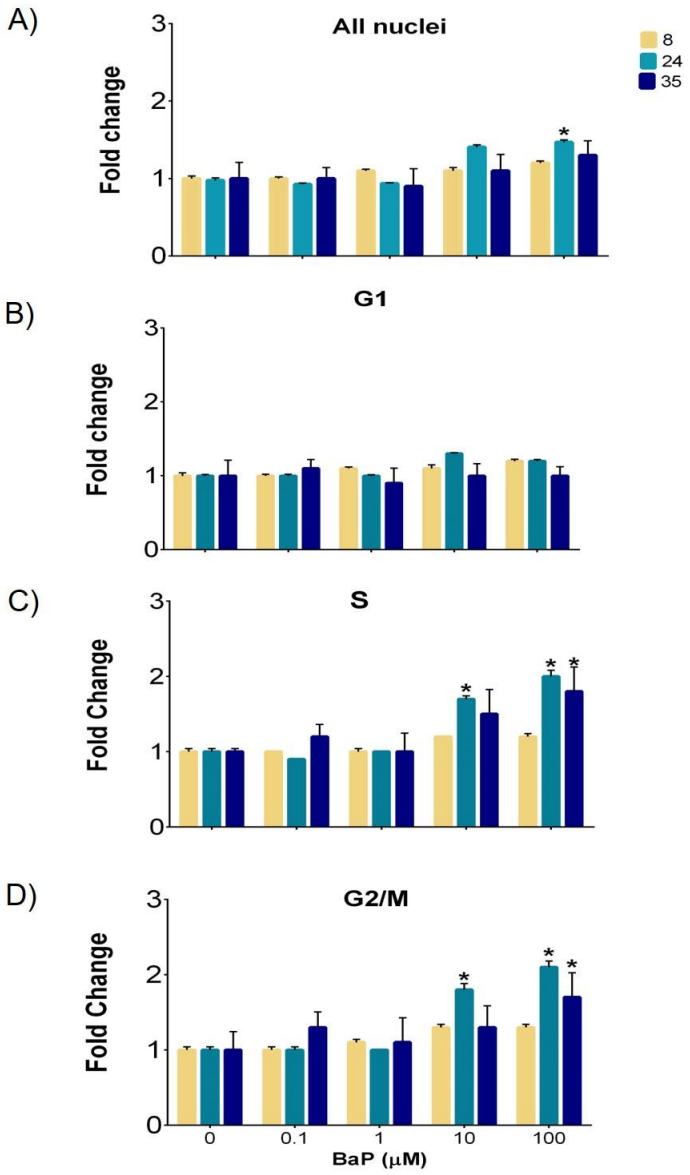

Figure 3.2. Concentration- and time-dependent effects of benzo(a)pyrene exposure (BaP) on H2AX phosphorylation (γH2AX) in 3D spheroids after 8, 24 and 35h. Data are presented as mean +SEM, $p \leq 0.05$. γH2AX data analyzed with a 2-way ANOVA and Tukey's HSD.

3.5 Discussion

Immortalized hepatic cell lines cultured as 2D monolayers are used to determine metabolism-dependent toxicity of chemicals. However, culturing cells in 2D causes them to have dedifferentiated cellular architecture resulting in weak activity of phase I metabolizing enzymes (Mandon et al. 2019). Metabolic competence in immortalized hepatocytes is critical to determine the toxicity of metabolically activated chemicals. Culturing immortalized hepatocytes as 3D spheroids permits hepatocytes to maintain their polygonal shape and cellular contacts, which improves metabolic competence, hepatic functions and response to chemicals (Pampaloni and Stelzer 2013; Elliot and Yuan 2010). The chicken LMH cell line is a potential *in vitro* model for screening chemicals in avian toxicity testing. The present study evaluated the utility of the chicken LMH cell line for detecting metabolism-dependent genotoxic endpoints and compared these endpoints between 2D monolayer cells and 3D spheroids. LMH 2D monolayers and 3D spheroids were exposed to BaP at multiple concentrations and time points to determine changes in CYP1A activity, DNA damage and gene expression. Overall, we found that LMH cells cultured as spheroids had superior CYP1A activity and DNA damage response compared to cells grown as a monolayer.

3.5.1 CYP1A induction precedes DNA damage response, and is more pronounced in 3D spheroids

Exposure to BaP induced CYP1A activity and CYP1A4 and CYP1A5 gene expression in both 2D monolayer cells and 3D spheroids. CYP1A induction and mRNA expression were greater in 3D spheroids across all concentrations and occurred at earlier time points than 2D monolayer cells (Figure 3.1, Tables 3.2 and 3.3). Although CYP1A5 mRNA was not significantly induced until 24h in 3D spheroids, the maximum induction was higher in 3D

spheroids and the BMD values of CYP1A4 and CYP1A5 in spheroids were lower than in monolayer cells. This suggests that these genes were upregulated at lower concentrations and earlier time points (Table S3.3). There was no change in CYP1A4 and CYP1A5 expression at 4h, presumably due to the low uptake of BaP in cells at this time point. Rodd et al. (2017) visualized the uptake of BaP in 3D spheroids of the fish liver cell line, PLHC-1, and found that BaP was fully dispersed in spheroids within 6h of exposure and CYP1A1 expression increased around 6h. CYP1A activity and upregulation of CYP1A4 or CYP1A5 mRNA expression were the only significant effects detected at 8h in both 2D and 3D cultures. In a previous study, LMH spheroids had higher CYP1A activity and CYP1A4 and CYP1A5 expression than 2D monolayer cells following exposure to PCB-126 (Sharin et al. 2020). CYP1A1 expression was 14-fold higher in HepG2 spheroids compared to 2D monolayer cells after 24h BaP exposure (Stampar et al. 2019). In LMH monolayer cells and spheroids, upregulation of CYP1A4 and CYP1A5 occurred before the expression of cell cycle and DNA damage response genes (Tables 3.2 and 3.3), suggesting that BaP is metabolized prior to DNA damage. Based on CYP1A activity and CYP1A4 and CYP1A5 gene expression, LMH 2D monolayer cells and 3D spheroids may both metabolize BaP, however spheroids appear to have enhanced metabolic capacity.

3.5.2 γH2AX observed after CYP1A induction in 3D spheroids

BaP causes an increase in DSBs and γH2AX and impairs DNA synthesis at replication forks resulting in cell cycle arrest at S-phase and G2/M checkpoint after it is metabolized to the reactive metabolite, BPDE (Tung et al. 2013; Hamouchene et al. 2011; van Delft et al. 2010). The formation of γH2AX was only significantly upregulated after 24h of BaP exposure in 3D spheroids, which is later than the significant upregulation of CYP1A activity and mRNA expression at 8h (Figures 3.2, Table 3.3). This increase in γH2AX was most pronounced in cells

in the S and G2/M phases of the cell cycle at both 24 and 35h (Figure 3.2), which indicates that DNA damage primarily occurred in replicating cells. Shortly after the induction of DSBs, histone H2AX is phosphorylated at serine 139 (γH2AX) (Watters et al. 2009), which serves as a signal for DNA damage repair (Burma et al. 2001). Markers of DNA damage like γ-H2AX accumulate in S-phase cells in response to genotoxicants (Freisner et al. 2005). DSBs were observed after 24h exposure to BaP in HepG2 cells cultured as 3D spheroids and 2D monolayers; however, the concentration of BaP required to induce DSBs in spheroids was lower than monolayer cells (Stampar et al. 2019). Similar to the current study, BaP treatment in HepaRG and HepG2 cells resulted in an increase in γH2AX at 24h, which decreased at 48h (Quesnot et al. 2016; van Delft et al. 2010). These findings indicate that the increased γH2AX in LMH spheroids is likely due to CYP1A-activated BaP causing DSB in replicating cells.

3.5.3 Increased γH2AX levels coincides with expression of DNA damage response genes

Elevated levels of γH2AX in spheroids coincided with the upregulation of all of the cell-cycle and DNA damage response genes measured in this study (Table 3.2). CDKN1A expression usually increases in response to DNA damage, which blocks the progression of cells from S-phase permitting DNA damage repair (Guo et al. 1999). In another study, BaP (40μM) upregulated expression of CDKN1A in HepG2 spheroids at 24h (Stampar et al. 2019). The genes, DDB2 and XPC, act as early DNA damage sensors, recognize γH2AX and initiate nucleotide excision repair (NER) (Ray et al. 2013). Consistent with an early DNA damage repair response, both DDB2 and XPC were upregulated starting at 24h by BaP in LMH spheroids (Table 3.3). DDB2 was upregulated in HepG2 following BaP-DNA adduct formation in HepG2 cells (vanDelft et al. 2010). Exposure to BPDE for 24h resulted in concentration-dependent upregulation of DDB2 and XPC in VH10tert and endothelial cells (Kress et al. 2019; Christmann

et al. 2016). In another study, BPDE upregulated the expression of CDKN1A, GADD45, DDB2 and XPC in TK-6 cells (Piberger et al. 2003). Along with CDKN1A, DDB2 and XPC, DNA polymerase β (POLB) was also upregulated in spheroids by BaP starting at 24h in the present study. POLB is involved in base excision repair (BER) and incorporates the correct bases at the site of DNA single strand breaks (Martin et al. 2010). In some cases, DNA single strand breaks are a by-product of NER during repair of bulky DNA adducts similar to the adducts created by BaP (Kress et al. 2019). Along with the previously mentioned DNA damage repair genes, concentration-dependent upregulation of POLK and GADD45 expression occurred at 48h. DNA polymerase κ (POLK) is involved in translesion synthesis and incorporates the correct base opposite the BPDE adducts (Rechkoblit et al. 2017). The upregulation of POLK at a later time point is consistent with its involvement in late stage NER. The cell cycle and DNA damage repair gene, GADD45, interacts with XPC and is involved in NER and BER (Niehrs and Schafer 2012). In addition, GADD45 interacts with cyclin dependent kinases to induce G2/M arrest (Tamura et al. 2013). In contrast to the current study, BaP upregulated GADD45 expression in HepG2/C3A spheroids from 24 to 96h (Stampar et al. 2020). The delayed expression of GADD45 suggests that in LMH spheroids, GADD45 maybe more involved in G2/M arrest than early NER response.

In contrast to spheroids, GADD45 was the only cell cycle and DNA damage response gene that was upregulated in 2D monolayer cells, and only at 48h at the highest dose tested (Figure 3.2). This demonstrates that an orchestrated DNA damage response was not induced in 2D monolayer cells after exposure to BaP at the time points tested. This is likely because BaP was not sufficiently metabolized at earlier time points to induce significant DNA damage, as suggested by the reduced EROD activity and CYP1A mRNA expression in these cells. The later

induction of GADD45 suggests BaP may be starting to cause DNA damage after 48h, but measurements of γH2AX and DNA damage response genes at later time points (60 and 72h) is required to confirm this.

In conclusion, the significant induction of CYP1A activity and gene expression following BaP exposure was detected earlier in 3D spheroids than 2D monolayer cells. This suggests that the metabolism of BaP to its reactive metabolite is slower in monolayer cells due to weak CYP1A activity. There was an increase in γH2AX, which was detected only after CYP1A induction in 3D spheroids. Changes in DNA damage repair genes were observed around the same time as the γH2AX increase in spheroids and these genes remained active at a later time point. These results demonstrate that LMH spheroids have superior sensitivity for detecting CYP1A metabolism-dependent genotoxicity of chemicals and may be a relevant metabolically competent *in vitro* model for avian toxicology.

Acknowledgements

This work was supported by funds from three sources within Environment and Climate Change Canada: 1) Chemicals Management Plan (CMP); 2) Strategic Technology Applications of Genomics for the Environment (STAGE); and 3) the Ecotoxicology and Wildlife Health Division.

3.6 References

Buick JK, Moffat I, Williams A, Swartz CD, Recio L, Hyduke DR, Li HH, Fornace AJ, Aubrecht J, Yauk CL. 2015. Integration of metabolic activation with a predictive toxicogenomics signature to classify genotoxic versus nongenotoxic chemicals in human TK6 cells. *Environmental and Molecular Mutagenesis* 56:520-534. DOI: 10.1002/em.21940.

Burma S, Chen BP, Murphy M, Kurimasa A, Chen DJ. 2001. ATM phosphorylates histone H2AX in response to DNA double-strand breaks. *Journal of Biological Chemistry* 276:42462-42467. DOI: 10.1074/jbc.C100466200.

Christmann M, Boisseau C, Kitzinger R, Berac C, Allmann S, Sommer T, Aasland D, Kaina B, Tomicic MT. 2016. Adaptive upregulation of DNA repair genes following benzo(a)pyrene diol epoxide protects against cell death at the expense of mutations. *Nucleic Acids Research* 44:10727-10743. DOI: 10.1093/nar/gkw873.

Elliott NT, Yuan F. 2011. A Review of Three-Dimensional In Vitro Tissue Models for Drug Discovery and Transport Studies. *Journal of Pharmaceutical Sciences* 100:59-74. DOI: 10.1002/jps.22257.

Filipsson AF, Sand S, Nilsson J, Victorin K. 2003. The benchmark dose method - Review of available models, and recommendations for application in health risk assessment. *Critical Reviews in Toxicology* 33:505-542. DOI: 10.1080/10408440390242360.

Friesner JD, Liu B, Culligan K, Britt AB. 2005. "Ionizing radiation-dependent gamma-H2AX focus formation requires ataxia telangiectasia mutated and ataxia telangiectasia mutated and rad3-related" (vol 16, pg 2566, 2005). *Molecular Biology of the Cell* 16:3454-3454. DOI: 10.1091/mbc.E01-10-0890.

Gomez-Lechon MJ, Tolosa L, Donato MT. 2016. Metabolic activation and drug-induced liver injury: in vitro approaches for the safety risk assessment of new drugs. *Journal of Applied Toxicology* 36:752-768. DOI: 10.1002/jat.3277.

Gunness P, Mueller D, Shevchenko V, Heinzle E, Ingelman-Sundberg M, Noor F. 2013. 3D Organotypic Cultures of Human HepaRG Cells: A Tool for In Vitro Toxicity Studies. *Toxicological Sciences* 133:67-78. DOI: 10.1093/toxsci/kft021.

Guo XQ, Seo JE, Li XL, Mei N. 2020. Genetic toxicity assessment using liver cell models: past, present, and future. *Journal of Toxicology and Environmental Health-Part B-Critical Reviews* 23:27-50. DOI: 10.1080/10937404.2019.1692744.

Hamilton G, Westmoreland C, George E. 2001. Effects of medium composition on the morphology and function of rat hepatocytes cultured as spheroids and monolayers. *In Vitro Cellular & Developmental Biology-Animal* 37:656-667.

Hamouchene H, Arlt VM, Giddings I, Phillips DH. 2011. Influence of cell cycle on responses of MCF-7 cells to benzo a pyrene. *Bmc Genomics* 12. DOI: 10.1186/1471-2164-12-333.

Kress JM, Di Dio L, Heck L, Pulliero A, Izzotti A, Laarmann K, Fritz G, Kaina B. 2019. Human primary endothelial cells are impaired in nucleotide excision repair and sensitive to benzo a pyrene compared with smooth muscle cells and pericytes. *Scientific Reports* 9. DOI: 10.1038/s41598-019-49953-w.

Lammel T, Tsoukatou G, Jellinek J, Sturve J. 2019. Development of three-dimensional (3D) spheroid cultures of the continuous rainbow trout liver cell line RTL-W1. *Ecotoxicology and Environmental Safety* 167:250-258. DOI: 10.1016/j.ecoenv.2018.10.009.

Mandon M, Huet S, Dubreil E, Fessard V, Le Hegarat L. 2019. Three-dimensional HepaRG spheroids as a liver model to study human genotoxicity in vitro with the single cell gel electrophoresis assay. *Scientific Reports* 9. DOI: 10.1038/s41598-019-47114-7.

Niehrs C, Schafer A. 2012. Active DNA demethylation by Gadd45 and DNA repair. *Trends in Cell Biology* 22:220-227. DOI: 10.1016/j.tcb.2012.01.002.

Ooka M, Takazawa H, Takeda S, Hirota K. 2016. Cytotoxic and genotoxic profiles of benzo a pyrene and N-nitrosodimethylamine demonstrated using DNA repair deficient DT40 cells with metabolic activation. *Chemosphere* 144:1901-1907. DOI: 10.1016/j.chemosphere.2015.10.085.

Pfuhler S, Kirkland D, Kasper P, Hayashi M, Vanparys P, Carmichael P, Dertinger S, Eastmond D, Elhajouji A, Krul C, Rothfuss A, Schoening G, Smith A, Speit G, Thomas C, van Benthem J, Corvi R. 2009. Reduction of use of animals in regulatory genotoxicity testing: Identification and implementation opportunities-Report from an ECVAM workshop. *Mutation Research-Genetic Toxicology and Environmental Mutagenesis* 680:31-42. DOI: 10.1016/j.mrgentox.2009.09.002.

Piberger AL, Kruger CT, Strauch BM, Schneider B, Hartwig A. 2018. BPDE-induced genotoxicity: relationship between DNA adducts, mutagenicity in the in vitro PIG-A assay, and the transcriptional response to DNA damage in TK6 cells. *Archives of Toxicology* 92:541-551. DOI: 10.1007/s00204-017-2003-0.

Quesnot N, Rondel K, Audebert M, Martinais S, Glaise D, Morel F, Loyer P, Robin MA. 2016. Evaluation of genotoxicity using automated detection of gamma H2AX in metabolically competent HepaRG cells. *Mutagenesis* 31:43-50. DOI: 10.1093/mutage/gev059.

Ramaiahgari SC, Waidyanatha S, Dixon D, DeVito MJ, Paules RS, Ferguson SS. 2017. Three-Dimensional (3D) HepaRG Spheroid Model With Physiologically Relevant Xenobiotic Metabolism Competence and Hepatocyte Functionality for Liver Toxicity Screening. *Toxicological Sciences* 159:124-136. DOI: 10.1093/toxsci/kfx122.

Ray A, Milum K, Battu A, Wani G, Wani AA. 2013. NER initiation factors, DDB2 and XPC, regulate UV radiation response by recruiting ATR and ATM kinases to DNA damage sites. *DNA Repair* 12:273-283. DOI: 10.1016/j.dnarep.2013.01.003.

Rodd AL, Messier NJ, Vaslet CA, Kane AB. 2017. A 3D fish liver model for aquatic toxicology: Morphological changes and Cyp1a induction in PLHC-1 microtissues after repeated benzo(a)pyrene exposures. *Aquatic Toxicology* 186:134-144. DOI: 10.1016/j.aquatox.2017.02.018.

Schmittgen TD, Livak KJ. 2008. Analyzing real-time PCR data by the comparative C-T method. *Nature Protocols* 3:1101-1108. DOI: 10.1038/nprot.2008.73.

Schwarz D, Kisselev P, Cascorbi I, Schunck WH, Roots I. 2001. Differential metabolism of benzo a pyrene and benzo a pyrene-7,8-dihydrodiol by human CYP1A1 variants. *Carcinogenesis* 22:453-459. DOI: 10.1093/carcin/22.3.453.

Sevior DK, Pelkonen O, Ahokas JT. 2012. Hepatocytes: The powerhouse of biotransformation. *International Journal of Biochemistry & Cell Biology* 44:257-261. DOI: 10.1016/j.biocel.2011.11.011.

Sharin T, Crump D, O'Brien JM. 2020. Evaluation of the Aryl Hydrocarbon Receptor Response in LMH 3D Spheroids. *Environmental Toxicology and Chemistry* 39:1693-1701. DOI: 10.1002/etc.4783.

Soldatow VY, LeCluyse EL, Griffith LG, Rusyn I. 2013. In vitro models for liver toxicity testing. *Toxicology Research* 2:23-39. DOI: 10.1039/c2tx20051a.

Stampar M, Tomc J, Filipic M, Zegura B. 2019. Development of in vitro 3D cell model from hepatocellular carcinoma (HepG2) cell line and its application for genotoxicity testing. *Archives of Toxicology* 93:3321-3333. DOI: 10.1007/s00204-019-02576-6.

Tamura RE, de Vasconcellos JF, Sarkar D, Libermann TA, Fisher PB, Zerbini LF. 2012. GADD45 Proteins: Central Players in Tumorigenesis. *Current Molecular Medicine* 12:634-651.

Tung JN, Wu HH, Chiang CC, Tsai YY, Chou MC, Lee H, Cheng YW. 2010. An association between BPDE-like DNA adduct levels and CYP1A1 and GSTM1 polymorphisma in pterygium. *Molecular Vision* 16:623-629.

van Delft JHM, Mathijs K, Staal YCM, van Herwijnen MHM, Brauers KJJ, Boorsma A, Kleinjans JCS. 2010. Time Series Analysis of Benzo A Pyrene-Induced Transcriptome Changes Suggests That a Network of Transcription Factors Regulates the Effects on Functional Gene Sets. *Toxicological Sciences* 117:381-392. DOI: 10.1093/toxsci/kfq214.

Watters GP, Smart DJ, Harvey JS, Austin CA. 2009. H2AX phosphorylation as a genotoxicity endpoint. *Mutation Research-Genetic Toxicology and Environmental Mutagenesis* 679:50-58. DOI: 10.1016/j.mrgentox.2009.07.007.

Chapter 4. Development and Characterization of a Double-Crested Cormorant Hepatic Cell Line for Chemical Screening

4.1 Abstract

There are currently no available cell lines for the ecologically relevant colonial waterbird species, the double-crested cormorant (DCCO). DCCOs are high trophic level aquatic birds that are used for routine contaminant monitoring programs in the Laurentian Great Lakes and marine coasts of Canada. Developing a DCCO cell line for *in vitro* toxicological screening will ideally provide improved understanding of the effects of environmental chemicals given the large differences in sensitivity between laboratory and wild avian species. In this study, an immortalized DCCO hepatic cell line, DCH22, was established from the liver of a day 22 embryo as a potential alternative to primary double-crested cormorant embryonic hepatocytes (DCEH) for chemical screening. DCH22 cells were cultured for over a year and had hepatocyte-like morphology. Exposure to PCB-126 induced CYP1A activity in DCH22 cells cultured as 2D monolayers and 3D spheroids. Induction of CYP3A activity was observed following exposure to metyrapone in 2D monolayer cells. Preliminary results suggest that DCH22 cells have CYP1A and CYP3A activity supporting their potential use as an alternative to primary DCEH for chemical screening.

4.2 Introduction

There is an international demand for faster, focused, ethical, and economic toxicity testing tools and a move towards mechanistic toxicology. High-throughput, *in vitro* approaches can help meet the demands of the shifting toxicity testing paradigm (Judson et al. 2013). Primary embryonic hepatocyte culture is a commonly used *in vitro* model for avian toxicity testing (e.g.

Mundy et al. 2019; Page-Lariviere et al. 2018). However, it is difficult to obtain eggs of avian wildlife species for the preparation of primary embryonic hepatocytes. Furthermore, primary hepatocytes have limited proliferation and metabolic activity, they can only be maintained for a few days, and they require the use of animals (Soldatow et al. 2013). Thus, it is a challenge to screen large numbers of chemicals using primary hepatocyte culture. Immortalized cell lines can be cultured indefinitely, permit the generation of large amounts of mechanistic and dose-response data, and reduce/replace the use of animals (Astashkina et al. 2012). Advancements in cell culturing techniques, such as three-dimensional (3D) culture systems, have made immortalized cell lines more relevant for toxicity testing as cells cultured in 3D systems are more predictive of cellular responses to chemicals (Ravi et al. 2004).

There are two commercially available avian hepatic cell lines, both derived from chicken (*Gallus gallus domesticus*), a key laboratory model for avian toxicity testing. Currently, there are no hepatic cell lines available for ecologically relevant avian species, such as the double-crested cormorant (*Phalacrocorax auritus*; DCCO). DCCOs are piscivorous, colonial waterbirds that occupy a high trophic position in the aquatic food web and are therefore, used as wildlife indicator species in freshwater (e.g. Great Lakes) and marine environments across Canada (Harris et al. 2005; Ludwig et al. 1996). Primary double-crested cormorant embryonic hepatocytes (DCEH) are used to screen chemicals and compare toxicity of chemicals between laboratory and wildlife species; e.g., chicken and double-crested cormorants (Mundy et al. 2019; Page-Lariviere et al. 2018; Crump et al. 2016). A cell line for an ecologically relevant model avian species may represent a better predictor of the *in vitro* toxic effects of environmental chemicals, since previous studies have found that chickens are more sensitive to a range of chemicals than wildlife species (Norden et al. 2016; Head et al. 2008). The objectives of this

study were to develop a continuous hepatic cell line from DCCO and to evaluate its utility as an alternative to DCEH for chemical screening.

4.3 Materials and Methods

4.3.1 Hepatocyte isolation and cell line development

Fertilized, unincubated DCCO eggs were collected from ground nests containing one or two eggs from a nesting colony in Batchawana Bay, Lake Superior (46°52'8.89"N; 84°26'49.45"W) that has low concentrations of legacy persistent organic pollutants and chemicals of emerging concern (Shane DeSolla, Environment and Climate Change Canada, personal communication). DCCO eggs were transported in foam-lined coolers to the National Wildlife Research Centre in Ottawa and incubated according to methods described previously (Powell et al. 1997) within 48h of collection. Briefly, DCCO eggs were artificially incubated by placing the eggs horizontally in a Petersime incubator (Model XI) at 37.5°C and 60% relative humidity. All procedures involving the handling of animals were conducted according to protocols approved by Environment and Climate Change Canada's Wildlife Eastern Animal Care Committee. An embryonic day 22 female DCCO was euthanized by decapitation and the liver was dissected and rinsed in HEPES buffer. Subsequently, the liver was placed in a petri dish with 10 mL collagenase solution, sliced into small pieces, transferred to a tube and digested at 37°C for 5 min. The resulting solution was centrifuged at 500 g for 5 min, the supernatant and red blood cells were removed, and cells were suspended in 5 mL collagenase solution and centrifuged again at 250 g for 4 min. After the collagenase solution was aspirated, 10 mL of 2% bovine serum albumin (BSA) solution was added to the pellet and centrifuged at 250 g for 4 min. The resulting pellet weighed 0.43 g and was suspended in DMEM/F12 solution supplemented with 10% fetal bovine serum (HI-FBS), 100 U/mL of penicillin and 10 000 μg/mL of

streptomycin, 0.1% DMSO, 0.5 µg/mL insulin, 0.1 µM hydrocortisone, and 0.5µM dexamethasone. All reagents were purchased from Sigma-Aldrich. Hepatocytes (viability 70% stained with Trypan blue) were plated at a high density – eight million cells in a 100 mm petri dish (Nunc) coated with 0.2% gelatin – and cultured at 37°C with 5% CO_2. Media was changed as required and cells were passaged (1:2 or 1:3 dilution) by adding 3 mL trypsin-EDTA to the dish for 3 min and centrifuging at 250 g for 3 min. From passage 5, cells had hepatocyte-like morphology and formed small clusters. After 6 passages (~1.5 months in culture), the culture media was modified. Hepatocyte maturation/maintenance media consisted of DMEM/F12 media supplemented with 10% HI-FBS, 1% penicillin/streptomycin, 0.5% DMSO, 1% insulin transferrin selenium (ITS) solution and 1 µM hydrocortisone. The media was changed every 48h and passaged when cells reached 80 to 90% confluency.

4.3.2 2D monolayer and 3D spheroid cultures

For chemical exposure and experiments, modified maintanance media (DMEM/F12 media supplemented with 10% HI-FBS, 1100 U/mL of penicillin and 10 000 µg/mL of streptomycin, 1% insulin transferrin selenium (ITS) solution, and 1 µM hydrocortisone) was used to culture cells. 40 000 confluent cells in 250 µL of media were plated in each well of flat bottom 96 well microplates (Corning). Confluent cells were dosed 24h after plating. For 3D spheroids, 10 000 cells in 250 µL of medium per well were added to each well of a 96 well ultra low attachment (ULA) microplate (Corning). Medium was changed daily by removing 200 µL existing medium and adding 200 µL of fresh medium to each well. Spheroids were cultured for 4 days prior to chemical administration.

4.3.3 EROD and CYP3A assays

For the ethoxyresorufin-*O*-deethylase (EROD) assay, DCH22 (2D monolayers and 3D spheroids) were dosed with 1.25 µl of the dimethyl sulfoxide (DMSO (0.5%); Sigma-Aldrich) vehicle control or 3,3',4,4',5-pentachlorobiphenyl (PCB-126; CAS # 57465-28-8, 99% purity; Sigma Aldrich) dissolved in DMSO to attain nominal in-well concentrations of 0.01-100 nM PCB-126 in 250 µL of medium per well. The cells were incubated for 24h, media was aspirated, and plates were flash frozen on dry ice and stored at -80°C. EROD activity was determined as described previously (Sharin et al. 2020). The presence of the EROD product, resorufin, was measured at an excitation wavelength of 530 nm and an emission wavelength of 590 nm and total protein concentration was measured at an excitation wavelength of 400 nm and emission wavelength of 460 nm using a DTX 880 multimode detector (Beckman Coulter, Brea, CA). Triplicate plates with three technical replicate wells per plate were analyzed and EROD activity was reported as pmol resorufin/min/mg protein. Significant differences in activity between treatment and control were determined with two-way ANOVA, where cell-type and dose were the two independent variables, followed by Tukey's HSD test using GraphPad Prism Ver. 6.07.

For the CYP3A assay, DCH22 cells (2D monolayers only) were dosed with 1.25 µl of the dimethyl sulfoxide (DMSO (0.5%); Sigma Aldrich) vehicle control or 2-methyl-1,2-di-3-pyridyl-1-propanone (metyrapone; Cas # 54-36-4, 98% purity; Sigma-Aldrich) dissolved in DMSO to yield nominal in-well concentrations of 1 to 1000 µM metyrapone in 250 µL of medium per well. CYP3A activity was measured using the P450-Glo CYP3A4 Assay and Screening System (Promega) following the manufacturer's instructions. Briefly, 12.5 µL of 4X CYP3A4 reaction mixture was added to each well, mixed for 1 min on a plate shaker, and incubated for 10 min at 37°C. After this incubation, 25 µl of 2X NADPH regeneration system was added to all wells and

incubated for an additional 10 min at 37°C. 50 µl luciferin detection reagent was added to all wells, mixed for 1 min on a plate shaker and incubated for 20 min at 37°C. Luminescence was measured using a Luminoskan Ascent luminometer (Thermo Fisher Scientific). Five technical replicate wells per dose group were analyzed and CYP3A activity was reported as relative luminescence units (RLU). Significant differences from control were determined with one-way ANOVA followed by Dunnett's test using GraphPad Prism Ver. 6.07.

4.4 Results and Discussion

There is a lack of toxicity data for ecologically relevant indicator species such as DCCOs, which are naturally exposed to chemicals in the environment. DCCOs have been used as a model wildlife species to monitor the prevalence and effects of contaminants in aquatic ecosystems (Harris et al. 2005; Ludwig et al. 1996). The liver is the primary site of xenobiotic metabolism and biotransformation, and is an important organ for toxicity testing (Malarkey et al. 2005). Currently, there are no immortalized hepatic cell lines available for DCCO and thus, when conducting *in vitro* screening approaches for this species, primary hepatocytes must be used. The goal of this study was to derive an immortalized DCCO hepatic cell line, DCH22, and characterize CYP1A and CYP3A metabolic activity to evaluate whether it could be used as an alternative to primary DCEH for chemical screening.

DCH22 cells were continuously cultured for over a year and thus, can be considered immortalized. After five passages, the morphology of 2D confluent monolayer cells was predominantly flat polygonal cells that grew in clusters. DCH22 cells self-assembled and formed tight spheroids with relatively smooth edges by 24h without any exogenous extracellular matrix in ULA 96 well microplates (Figure 4.1)

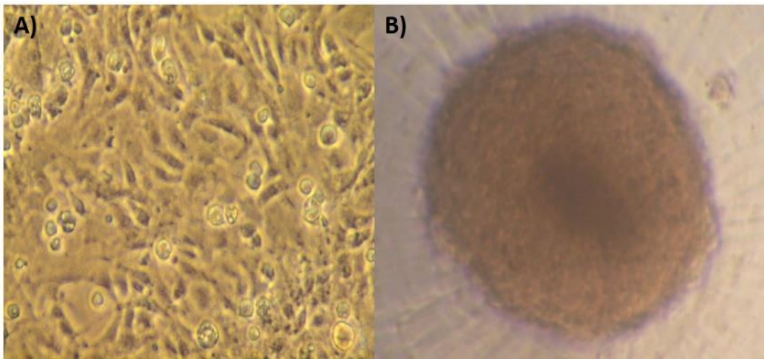

Figure 4.1. DCH22 cells in two culture conditions grown in 96-well plates: A) 2D monolayer confluent cells, and B) 3D spheroid.

4.4.1 PCB-126 induced CYP1A activity in 2D monolayer cells and 3D spheroids

Induction of EROD activity in birds is a widely used and accepted biomarker of exposure to chemicals that induce CYP1A activity via aryl hydrocarbon receptor (AhR) binding (Farmahin et al. 2016). PCB-126 is a dioxin-like compound, which binds to the AhR and upregulates the expression of CYP1A (Silkworth et al. 2005). Exposure to PCB-126 for 24h led to an increase in CYP1A induction in both 2D confluent cells and 3D spheroids (Figure 4.2). CYP1A activity induction was lower in 2D monolayer cells compared to 3D spheroids. The decrease in CYP1A activity observed at higher concentrations of PCB-126 is due to the competitive inhibition of CYP1A inducers (Petrulis and Bunce, 1999). In previous studies, cells cultured as 3D spheroids had higher activity of CYP1A compared to 2D monolayer cells using the EROD assay in cell lines from several species (Sharin et al. 2020; Uchea et al. 2015; Zeiger et al. 2001). The induction of CYP1A activity in DCH22 spheroids followed a similar pattern as DCEH, but the activity was much higher in DCEH (Crump et al. 2016).

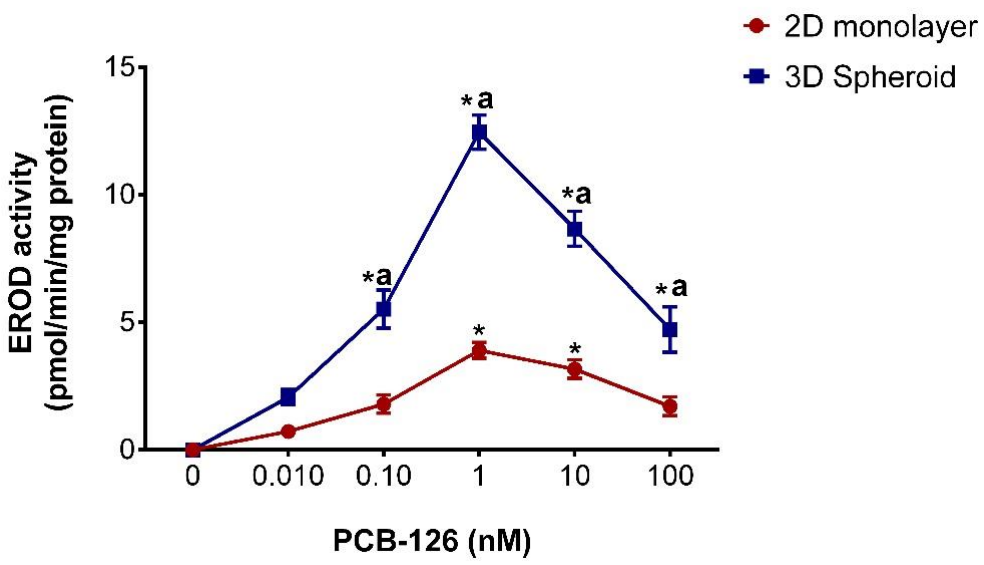

Figure 4.2. Concentration-dependent effects of PCB-126 exposure on EROD activity in DCH22 2D monolayer cells and 3D spheroids after 24h exposure. Data are presented as mean and error bars represent SEM, $p \leq 0.05$. Data were analyzed with a 2-way ANOVA and Tukey's HSD test. "*" denotes significant differences compared to untreated cells, 'a' indicates significant differences between 2D monolayer cells and 3D spheroids.

4.4.2 Metyrapone induced CYP3A activity in 2D monolayer cells

CYP3A metabolizes a vast number of chemicals with various chemical structures and is the predominant CYP450 in the mammalian liver (Ourlin et al 2000). CYP3A activity increased in DCH22 2D monolayer cells upon exposure to increasing concentrations of metyrapone (Figure 4.3). Metyrapone, a glucocorticoid synthesis inhibitor, is an inducer of CYP3A expression in human and rat hepatocytes, and activates the pregnane X receptor (PXR) (Harvey et al. 2000; Wright et al. 1996). There is no available information on the induction of CYP3A by metyrapone in DCEH and thus, a comparison to primary hepatocytes of this species was not possible. In a previous study, metyrapone upregulated mRNA expression of CYP3A37 in the immortalized

chicken hepatic cell line, LMH (Ourlin et al. 2000). The activity of CYP3A in 3D spheroids following exposure to metyrapone will be determined in future studies.

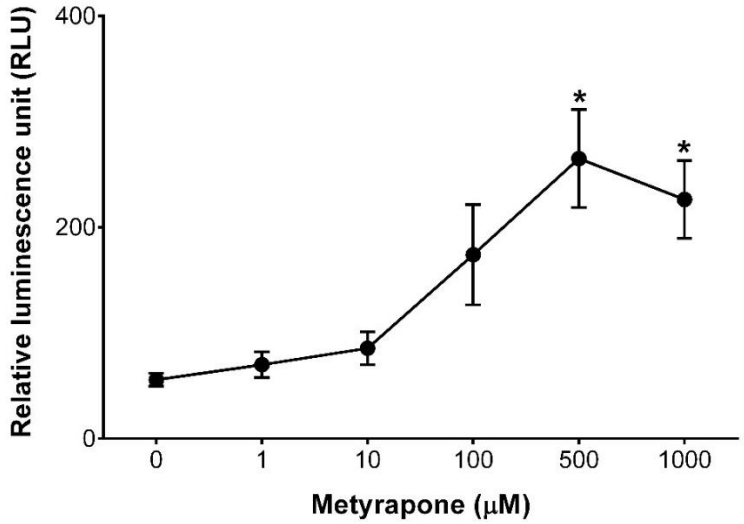

Figure 4.3. Concentration-dependent effects of metyrapone on CYP3A activity (measured as relative luminescence units [RLU]) in DCH22 2D monolayer cells after 24h exposure. Data are presented as mean and error bars represent SEM, $p \leq 0.05$. "*" denotes significant differences compared to untreated cells.

The increase in CYP1A and CYP3A activity in 2D monolayer cells following exposure to PCB-126 and metyrapone, respectively, indicates that the DCH22 cell line has metabolic competence. CYP1A and CYP3A activity in DCH22 cells cultured as 2D monolayers and 3D spheroids need to be further characterized by exposure to pharmaceutical chemicals, whose metabolism by CYP450s are extensively studied. DCH22 cells will be exposed to the CYP1A substrates, omeprazole and phenacetin, and the CYP3A substrates, midazolam and carbamazepine (Ramaiahgari et al. 2017; Bell et al. 2016; Yamashita et al. 2002). DCH22 will also be treated with environmental chemicals that are known to induce CYP1A or CYP3A activity in DCCO such as benzo(a)pyrene and hexabromocyclododecane. Species-specific RT-

qPCR will be used to measure changes in mRNA expression of CYP1A4, CYP3A7, SULT1E1 and UGT1A1 following exposure to the standard CYP1A and CYP3A inducers and environmental chemicals mentioned earlier. Hepatocytes will also be characterized by measuring albumin and α-1-antitrypsin using commercially available ELISA kits for chicken as there are no ELISA kits available for DCCO. Synthesis of both albumin and α-1-antitrypsin occurs in the liver and therefore, they are considered to be effective markers of hepatocyte specific functions (Toba et al. 2020; Gomez-Mariano et al. 2020; Bell et al. 2016). The planned experiments for full characterization of this cell line, DCH22, were not completed due to COVID19-related restrictions on lab work at the National Wildlife Research Centre. Based on the results of CYP1A and CYP3A activity, mRNA expression of key metabolizing enzymes, and the presence of hepatocyte-specific markers, we can evaluate whether the DCH22 cell line can be used as an alternative to DCEH for chemical screening.

4.5 References

Astashkina A, Mann B, Grainger DW. 2012. A critical evaluation of in vitro cell culture models for high-throughput drug screening and toxicity. *Pharmacology & Therapeutics* 134:82-106. DOI: 10.1016/j.pharmthera.2012.01.001.

Bell CC, Hendriks DFG, Moro SML, Ellis E, Walsh J, Renblom A, Puigvert LF, Dankers ACA, Jacobs F, Snoeys J, Sison-Young RL, Jenkins RE, Nordling A, Mkrtchian S, Park BK, Kitteringham NR, Goldring CEP, Lauschke VM, Ingelman-Sundberg M. 2016. Characterization of primary human hepatocyte spheroids as a model system for drug-induced liver injury, liver function and disease. *Scientific Reports* 6. DOI: 10.1038/srep25187.

Crump D, Farhat A, Chiu S, Williams KL, Jones SP, Langlois VS. 2016. Use of a Novel Double-Crested Cormorant ToxChip PCR Array and the EROD Assay to Determine Effects of Environmental Contaminants in Primary Hepatocytes. *Environmental Science & Technology* 50:3265-3274. DOI: 10.1021/acs.est.5b06181.

Farmahin R, Crump D, O'Brien JM, Jones SP, Kennedy SW. 2016. Time-dependent transcriptomic and biochemical responses of 6-formylindolo 3,2-b carbazole (FICZ) and 2,3,7,8-tetrachlorodibenzo-p-dioxin (TCDD) are explained by AHR activation time. *Biochemical Pharmacology* 115:134-143. DOI: 10.1016/j.bcp.2016.06.005

Gomez-Mariano G, Matamala N, Martinez S, Justo I, Marcacuzco A, Jimenez C, Monzon S, Cuesta I, Garfia C, Martinez MT, Huch M, de Castro IP, Posada M, Janciauskiene S, Martinez-Delgado B. 2020. Liver organoids reproduce alpha-1 antitrypsin deficiency-related liver disease. *Hepatology International* 14:127-137. DOI: 10.1007/s12072-019-10007-y.

Harvey JL, Paine AJ, Maurel P, Wright MC. 2000. Effect of the adrenal 11-beta-hydroxylase inhibitor metyrapone on human hepatic cytochrome P-450 expression: induction of cytochrome P-450 3A4. *Drug Metabolism and Disposition* 28 (1) 96-101.

Head JA, Hahn ME, Kennedy SW. 2008. Key amino acids in the aryl hydrocarbon receptor predict dioxin sensitivity in avian species. *Environmental Science & Technology* 42:7535-7541. DOI: 10.1021/es801082a.

Judson R, Kavlock R, Martin M, Reif D, Houck K, Knudsen T, Richard A, Tice RR, Whelan M, Xia MH, Huang RL, Austin C, Daston G, Hartung T, Fowle JR, Wooge W, Tong WD, Dix D. 2013. Perspectives on Validation of High-Throughput Assays Supporting 21st Century Toxicity Testing. *Altex-Alternatives to Animal Experimentation* 30:51-66. DOI: 10.14573/altex.2013.1.051.

Ludwig JP, KuritaMatsuba H, Auman HJ, Ludwig ME, Summer CL, Glesy JP, Tillitt DE, Jones PD. 1996. Deformities, PCBs, and TCDD-Equivalents in double-crested cormorants (Phalacrocorax auritus) and Caspian terns (Hydroprogne caspia) of the upper Great Lakes 1986-1991: Testing a cause-effect hypothesis. *Journal of Great Lakes Research* 22:172-197. DOI: 10.1016/s0380-1330(96)70948-6.

Malarkey DE, Johnson K, Ryan L, Boorman G, Maronpot RR. 2005. New insights into functional aspects of liver morphology. *Toxicologic Pathology* 33:27-34. DOI: 10.1080/01926230590881826.

Mundy LJ, Williams KL, Chiu S, Pauli BD, Crump D. 2019. Extracts of Passive Samplers Deployed in Variably Contaminated Wetlands in the Athabasca Oil Sands Region Elicit Biochemical and Transcriptomic Effects in Avian Hepatocytes. *Environmental Science & Technology* 53:9192-9202. DOI: 10.1021/acs.est.9b02066.

Norden M, Berger U, Engwall M. 2016. Developmental toxicity of PFOS and PFOA in great cormorant (Phalacrocorax carbo sinensis), herring gull (Larus argentatus) and chicken (Gallus gallus domesticus). *Environmental Science and Pollution Research* 23:10855-10862. DOI: 10.1007/s11356-016-6285-1.

Ourlin JC, Baader M, Fraser D, Halpert JR, Meyer UA. 2000. Cloning and functional expression of a first inducible avian cytochrome P450 of the CYP3A subfamily (CYP3A37). *Archives of Biochemistry and Biophysics* 373:375-384. DOI: 10.1006/abbi.1999.1566.

Page-Lariviere F, Chiu S, Jones SP, Farhat A, Crump D, O'Brien JM. 2018. Prioritization of 10 organic flame retardants using an avian hepatocyte toxicogenomic assay. *Environmental Toxicology & Chemistry* 37:3134-3144. DOI: 10.1002/etc.4260.

Petrulis, J. R., and Bunce, N.J. (1999). Competitive inhibition by inducer as a confounding factor in the use of the ethoxyresorufin-O-deethylase (EROD) assay to estimate exposure to dioxin-like compounds. *Toxicology Letters*, 105(3):251-260. doi: 10.1016/S0378-4274(99)00005-3

Powell DC, Aulerich RJ, Meadows JC, Tillitt DE, Stromborg KL, Kubiak TJ, Giesy JP. Bursian SJ. 1997. Organochlorine Contaminants in Double-Crested Cormorants from Green Bay,Wisconsin: II. Effects of an Extract Derived from Cormorant Eggs on the Chicken Embryo. *Archives of Environmental Contamination and Toxicology* 32 (3), 316−322.

Ramaiahgari SC, den Braver MW, Herpers B, Terpstra V, Commandeur JNM, van de Water B, Price LS. 2014. A 3D in vitro model of differentiated HepG2 cell spheroids with improved liver-like properties for repeated dose high-throughput toxicity studies. *Archives of Toxicology* 88:1083-1095. DOI: 10.1007/s00204-014-1215-9.

Ramaiahgari SC, Waidyanatha S, Dixon D, DeVito MJ, Paules RS, Ferguson SS. 2017. Three-Dimensional (3D) HepaRG Spheroid Model With Physiologically Relevant Xenobiotic Metabolism Competence and Hepatocyte Functionality for Liver Toxicity Screening. *Toxicological Sciences* 159:124-136. DOI: 10.1093/toxsci/kfx122.

Ravi M, Paramesh V, Kaviya SR, Anuradha E, Solomon FDP. 2015. 3D Cell Culture Systems: Advantages and Applications. *Journal of Cellular Physiology* 230:16-26. DOI: 10.1002/jcp.24683.

Sharin T, Crump D, O'Brien JM. 2020. Evaluation of the Aryl Hydrocarbon Receptor Response in LMH 3D Spheroids. *Environmental Toxicology & Chemistry* 39:1693-1701. DOI: 10.1002/etc.4783.

Silkworth JB, Koganti A, Illouz K, Possolo A, Zhao M, Hamilton SB. 2005. Comparison of TCDD and PCB CYP1A induction sensitivities in fresh hepatocytes from human donors, sprague-dawley rats, and rhesus monkeys and HepG2 cells. *Toxicological Sciences* 87:508-519. DOI: 10.1093/toxsci/kfi261.

Soldatow VY, LeCluyse EL, Griffith LG, Rusyn I. 2013. In vitro models for liver toxicity testing. *Toxicology Research* 2:23-39. DOI: 10.1039/c2tx20051a.

Toba Y, Deguchi S, Mimura N, Sakamoto A, Harada K, Hirata K, Takayama K, Mizuguchi H. 2020. Comparison of commercially available media for hepatic differentiation and hepatocyte maintenance. *Plos One* 15. DOI: 10.1371/journal.pone.0229654.

Uchea C, Owen SF, Chipman JK. 2015. Functional xenobiotic metabolism and efflux transporters in trout hepatocyte spheroid cultures. *Toxicology Research* 4:494-507. DOI: 10.1039/c4tx00160e.

Chapter 5. Toxicity Screening of Bisphenol A Replacement Compounds: Cytotoxicity and mRNA Expression in Primary Hepatocytes of Chicken and Double-Crested Cormorant

Modified from: Sharin T, Williams KL, Chiu S, Crump D, O'Brien JM. 2021. *Environmental Toxicology and Chemistry* 40(5):1368-1378. doi: 10.1002/etc.4985

5.1 Abstract

A market for bisphenol A (BPA) replacement compounds has emerged due to restrictions on the use of BPA. Some of these compounds were detected in the environment, yet little is known about their toxicological properties. In the present study, an avian *in vitro* toxicogenomic approach was used to compare the effects of five BPA alternatives. Cell viability and mRNA expression were compared in primary embryonic hepatocytes of chickens (CEH) and double-crested cormorants (DCEH) exposed to 4,4'-(propane-2,2-diyl) diphenol (BPA), bis (4-hydroxyphenyl) methane (BPF), bis-(3-allyl-4-hydroxyphenyl) sulfone (TGSH), 7-bis (4-hydroxyphenylthio)-3,5-dioxaheptane (DD-70), 2,2-bis (4-hydroxyphenyl) hexafluoropropane (BPAF) and 4-hydroxyphenyl 4-isoprooxyphenylsulfone (BPSIP). Changes in gene expression were determined using two PCR arrays: 1) the species-specific ToxChip, which contains genes representing toxicologically-relevant pathways; and 2) the chicken-specific AestroChip, which measures estrogen responsive genes. 17β estradiol (E2) was used as a control for both arrays in CEH. TGSH, DD-70 and BPAF were most cytotoxic in CEH and DCEH. Some of the replacement compounds changed the expression of genes related to xenobiotic metabolism, bile acid and cholesterol regulation. The rank order based on the number of genes altered on the chicken ToxChip array was TGSH > DD-70 > BPAF = BPF > E2 > BPSIP > BPA. BPSIP altered the greatest number of genes on the cormorant ToxChip array. Based upon the chicken

Aestrochip data, BPSIP and BPF were slightly estrogenic. The results suggest that the replacement compounds have comparable or even greater toxicity than BPA and act via different mechanisms.

5.2 Introduction

Bisphenol A (BPA) is one of the most widely used chemicals for the synthesis of polycarbonate plastics and epoxy resins (Andra et al. 2015). Due to widespread production and use, BPA has been detected in human and wildlife samples (Dekant and Volkel 2008; Corrales et al. 2015). Previous studies have found that BPA can disrupt endocrine functions in several species (Keri et al. 2007; Zoeller et al. 2005; Moriyama et al. 2002; Jessl et al. 2018), which has raised concerns about its safety. The use of BPA in baby bottles has been restricted in Canada and the European Union (Eladak et al. 2015). Consequently, structural analogs of BPA are used as replacement compounds (Andra et al. 2015). While the toxicity of BPA has been extensively studied, the toxicological properties of some of the replacement compounds are poorly characterized.

Five BPA replacement compounds – bisphenol F (BPF), bis-(3-allyl-4-hydroxyphenyl) sulfone (TGSH/TGSA), 7-bis(4-hydroxyphenylthio)-3,5-dioxaheptane (DD-70), bisphenol AF(BPAF) and 4-hydroxyphenyl 4-isoprooxyphenylsulfone (BPSIP/D-8) – were selected for the current study from a list of high priority chemicals identified by Canada's Chemicals Management Plan (Environment and Climate Change Canada and Health Canada 2019). The five replacement compounds contain at least one hydroxyphenyl functional group similar to BPA (Eladak et al. 2015) but have different side groups. The molecular structures and CAS numbers of the five replacement compounds are presented in Table 5.1. These replacement compounds are found in a variety of products such as fibre optics, canned food and thermal paper (Chen et

al. 2016). Like BPA, some of these replacement compounds have been detected in surface water, waste water, sediment and indoor dust samples. BPF and BPAF have been detected in environmental water samples in the range of 5 to 2850 ng/L (Yamazaki et al. 2015) and 0.5 to 246 ng/L, respectively (Chen et al. 2016). Studies have found that BPF altered expression of neurotransmitter metabolism genes and reduced neuronal growth factor in rats (Castro et al. 2015), disrupted thyroid signaling (Huang et al. 2016) and had similar estrogenicity as BPA (Moreman et al. 2017) in zebrafish larvae. Genes involved in lipid homeostasis, xenobiotic metabolism, and cell cycle regulation were modulated in chicken embryos exposed to TGSH (Crump et al. 2018). DD-70 did not bind to estrogen receptors in cell-based assays (Keminer et al. 2020). The marker of estrogen sensitivity in the developing brain of zebrafish, CYP19A1B, was upregulated by BPAF (Cano-Nicolau et al. 2016). Compared to BPA, BPAF was more cytotoxic and estrogenic in the MCF-7 cell line (Mesnage et al. 2017; Kitamura et al. 2005) and zebrafish embryo (Moreman et al. 2017). BPAF is an agonist of estrogen receptor (ER) α and antagonist of ERβ (Matsushima et al. 2010), and also binds to the G protein-coupled estrogen receptor (Cao et al. 2017). BPSIP exposure altered the expression of genes in the hypothalamus-pituitary-gonadal axis and decreased gonadal somatic index in male zebrafish (Lee et al. 2018) and caused developmental abnormalities in zebrafish embryos (Björnsdotter et al. 2017).

BPA and BPF have been detected in liver tissue of the great cormorant (*Phalacrocorax carbo*), a high trophic level avian species (Nakayama et al. 2006), and white-tailed eagle (*Haliaeetus albicilla*), a top predator and sentinel of environmental contamination (Gonzalez-Rubio et al. 2020). In this study, the cytotoxicity and gene expression profiles of the 5 BPA replacement compounds were compared to BPA and 17β estradiol (E2) in primary hepatocytes of chicken (CEH), a laboratory model, and the double-crested cormorant (DCEH), a high trophic

level avian species. E2 was included as a positive control to compare estrogenic effects of the BPA replacement compounds. The gene expression profile across several biological pathways was evaluated using customized species-specific ToxChip PCR arrays (chicken and double-crested cormorant (DCCO)). In addition, a customized chicken-specific, AestroChip was used to determine effects on estrogen responsive gene targets for the five replacement compounds in CEH. This study contributes to the currently limited toxicity data of these five BPA replacement compounds, especially for avian species.

Table 5.1. Common name, CASRN, molecular weight and structure of Bisphenol A and five Bisphenol A replacement compounds.

Name	Common Name	CASRN	Molecular Weight (g/mol)	Structure
4,4'-(propane-2,2-diyl)diphenol	Bisphenol A (BPA)	80-05-7	228.29	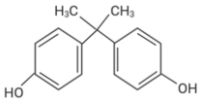
Bis(4-hydroxyphenyl)methane	Bisphenol F (BPF)	620-92-8	200.23	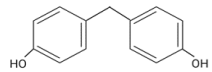
Bis(3-allyl-4-hydroxyphenyl)sulfone	TGSA/TGSH	41481-66-7	330.4	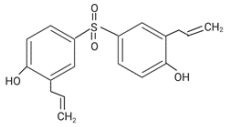
1,7-bis(4-hydroxyphenylthio)-3,5-dioxaheptane	DD-70	93589-69-6	352.47	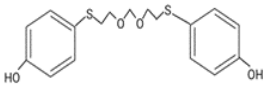
2,2-Bis(4-hydroxyphenyl) hexafluoropropane	Bisphenol AF (BPAF)	1478-61-1	336.23	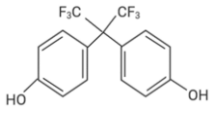
4-hydroxyphenyl 4-isopropoxyphenyl sulfone	BPSIP/D-8	95235-30-6	292.35	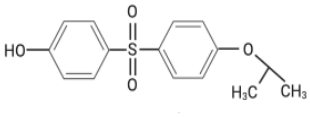

5.3 Materials and Methods

5.3.1 Chemicals

TGSH (96%), BPAF (98%), and BPSIP (98%) were purchased from Santa Cruz Biotechnology, DD-70 (97%) from Toronto Research Chemicals, and BPF (98%), BPA (97%) and E2 (98%) from Sigma-Aldrich. The certificate of analysis provided by the supplier of the chemicals confirmed that the chemicals met quality control specifications. Stock solutions of the chemicals were prepared by dissolution in dimethyl sulfoxide (DMSO; Sigma-Aldrich) to a final concentration of 1 mM, except for E2 (200 μM). The concentrations of the chemicals were not analytically verified, however, all chemicals were miscible with DMSO up to the highest stock concentration of 1mM. Dosing solutions were made by serial dilution of stock solutions in DMSO.

5.3.2 Primary Hepatocyte Isolation

Fertilized, unincubated white leghorn chicken (*Gallus gallus domesticus*) eggs were acquired from the Canadian Food Inspection Agency and artificially incubated (Petersime, Model XI incubator) at 37.5°C and 60% relative humidity. Fertilized, unincubated DCCO eggs were collected from nests containing one or two eggs from Black Rock (46°6'57.06"N, 82°50'3.14"W) in the North Channel of Lake Huron that has previously been shown to have relatively low organohalogen contaminant concentrations (Pagé-Larivière et al. 2018). DCCO eggs were transported in foam-lined coolers to the National Wildlife Research Centre in Ottawa and incubated according to methods described elsewhere (Powell et al. 1997) within 48h of collection. Briefly, eggs were placed horizontally in a Petersime incubator (Model XI) at 37.5°C and 60% relative humidity.

On incubation day 19 or 26 for chicken and DCCO, respectively (2 d prehatch), embryos (n = 25 chicken; n = 15 DCCO) were euthanized by decapitation. All procedures involving the handling of animals were conducted according to protocols approved by Environment and Climate Change Canada's Wildlife Eastern Animal Care Committee. Livers were removed, pooled and primary hepatocytes were cultured as described previously (Kennedy et al. 1993). Briefly, hepatocytes were isolated by collagenase digestion and filtration, followed by Percoll (GE Healthcare) purification and DNase I (Roche Applied Science) treatment. Primary hepatocytes were maintained in Medium 199 (Life Technologies) supplemented with sodium bicarbonate (2.24 g/L), penicillin (60 mg/L), streptomycin (100 mg/L), insulin (1 mg/L), and L-thyroxine (1 mg/L) (all reagents from Sigma-Aldrich). Primary hepatocytes were cultured in clear 48-well flat bottom plates by adding 25 μL of the cell suspension to 500 μL of medium and incubated at 37°C with 5% CO_2 for 24h prior to dosing.

5.3.3 Chemical administration and cell viability

After 24h of incubation, CEH were treated with either one of the five BPA replacement compounds, DMSO (0.5%), BPA or E2 (2.5 μL/well) at nominal concentrations ranging from 0.01 to 300 μM for cell viability. DCEH were treated with the same concentrations of TGSH, DD-70, BPAF and BPSIP. Due to the limited pool of hepatocytes available for the wild avian species, the evaluation of cell viability for BPA was not included in order to prioritize screening of the BPA replacements. For gene expression, CEH were exposed to 30 μM BPF, TGSH, BPSIP and BPA, and 10 μM DD-70, BPAF and E2 based on cell viability data. Four of the BPA replacement compounds were prioritized for comparison between CEH and DCEH in this study due to the difficulty in obtaining DCCO eggs from the field. DCEH were exposed to 10 μM TGSH, DD-70, BPAF and E2, and 30 μM BPSIP for gene expression. CEH and DCEH were

incubated at 37°C with 5% CO_2 for 24h and assayed immediately for cell viability or frozen at –80°C until subsequent RNA isolation.

CEH and DCEH viability (n= 3 replicates/treatment group) was determined using the ViaLight Plus kit (Lonza), following manufacturer's protocol. The kit measures adenosine triphosphate (ATP) in living cells to determine viability. Briefly, after the 24h exposure period, media was aspirated and 100 µL of fresh medium with 50 µL of lysis buffer was added to each well. 100 µL of the mixture from each well was transferred to a 96 well white clear bottom plate (Corning), 100 µL of ATP monitoring reagent was added to each well and incubated for 2 min at room temperature. Luminescence was read with a 1-s integrated reading time using the Luminoskan Ascent luminometer (Thermo Fisher Scientific).

5.3.4 RNA isolation and cDNA synthesis

RNA was extracted from CEH and DCEH using RNeasy 96 kits (Qiagen) following the manufacturer's protocol. Prior to isolation, hepatocytes from two replicate wells were combined to ensure sufficient RNA yield (n= 3 replicates/treatment) and concentration of RNA was determined using the QIAxpert (Qiagen). Approximately 250 ng of RNA was reverse transcribed using the QuantiTect Reverse Transcription kit (Qiagen).

5.3.5 ToxChip and AestroChip PCR Arrays

Custom-designed, species-specific ToxChip PCR arrays were used to determine gene expression perturbations across several toxicity pathways following exposure to the BPA replacement compounds. The chicken-specific ToxChip array (Qiagen; catalog no. CLAG22572, Table S5.1) consists of 43 target genes and 5 controls (Porter et al. 2014). The cormorant-specific ToxChip comprises 44 genes of interest and 4 control genes (Table S5.2) (Crump et al.

2016). Another customized chicken PCR array, the AestroChip, was used to determine the expression of ten estrogen responsive genes in CEH and included a reference gene, elongation factor 1 alpha 1 (EEF1A1), plus a no template control (Table S5.3). Customized chicken-specific RT^2 primers for the AestroChip were purchased from Qiagen; primer sequences are proprietary. The real-time RT-PCR reactions for both arrays were prepared with the RT^2 SYBR Green qPCR Master Mix (Qiagen). The thermal profile was 95°C for 10 min followed by 40 cycles of 95°C for 15 s and 60°C for 1 min and a final extension at 95°C for 1 min. Real-time RT-PCR was performed using a Stratagene Mx3005 instrument (Agilent Technologies).

5.3.6 Data Analysis

Cell viability data were log transformed and fit to a nonlinear regression curve (log (agonist) vs. response) to determine the median lethal concentration (LC50) using GraphPad Prism Ver. 6.07.

ToxChip PCR array cycle threshold (Ct) values were normalized using the trimmed M means (TMM) method in the R Bioconductor package edgeR (Robinson et al. 2010). For the AestroChip PCR array, the Ct values were normalized to the housekeeping gene EEF1A1 using the $2^{-\Delta Ct}$ method (Schmittgen and Livak 2008). Fold change was determined relative to DMSO control group. The fold change data were log2-transformed before ANOVA analysis to account for unequal variance. The resulting p-values between control and treated groups for all genes were adjusted using the Benjamini-Hochberg method with the false discovery rate (FDR) fixed at 5%. Principal component analysis was performed on log2-transformed fold-change data using the *prcomp* function in R with the default settings (R Core Team 2013) and visualized using the *autoplot* function in the *ggplot2* package (Wickham 2016).

5.4 Results and Discussion

5.4.1 TGSH, DD-70 and BPAF were the most cytotoxic BPA replacements

CEH were exposed to 0.01 to 300 μM of the 5 BPA replacement compounds for 24 h to determine LC50 values (Table 5.2, Figure S5.1). Three of the five BPA replacement compounds, TGSH, DD-70 and BPAF, had LC50 values of 35.1 ± 5.2, 13.1 ± 5.0 and 32.9 ± 7.3 μM in CEH, which were lower than the LC50 value of BPA (61.7 ± 43.1 μM) determined in a previous study (Ma et al. 2015). The LC50 value for BPSIP (168.3 ± 74.9 μM) was greater than BPA in CEH. The LC50 value of BPF could not be calculated from the dose range administered (0.01 to 300 μM) because cells were ~100% viable at 100 μM and ~0% viable at 300 μM (Figure S5.1). Therefore, the LC50 is between 100 and 300 μM but could not be calculated based on the curve fitting used for all other chemicals.

Table 5.2. LC50 ± SEM[a] values of BPA and replacement compounds in chicken embryonic hepatocytes (CEH) and double-crested cormorant hepatocytes (DCEH)

	LC50 (μM)	
Common Name	**CEH**	**DCEH**
Bisphenol A (BPA)	61.7±43.1[b]	ND[c]
Bisphenol F (BPF)	N/A[d]	ND
TGSH/TGSA	35.1 ± 5.2	21.0±9.9
DD-70	32.9±7.3	14.3±4.1
Bisphenol AF (BPAF)	13.1±5.0	14.2±5.2
BPSIP/D-8	168.3±74.9	85.9±42.3

[a] Standard error of the mean
[b] Data from Ma et al. 2015
[c] ND, not determined
[d] LC50 value could not be determined based on the concentrations (0.01-300 μM) included in this study

Based on CEH LC50 values, four of the replacement compounds, BPAF, DD-70, TGSH, and BPSIP, were selected for cytotoxicity determination in DCEH (Figure S5.2). BPF was excluded due to low cytotoxicity in CEH. BPF was also one of the least cytotoxic (LC50 >100 μM) among 7 BPA replacement compounds in cell lines (Russo et al. 2018) and also less cytotoxic than BPA in zebrafish embryos (Moreman et al. 2017); a finding consistent with that observed for CEH in the present study. In DCEH, DD-70 and BPAF had similar LC50 values (14.3 ± 4.1 and 14.2 ± 5.2 μM) and for both species, DD-70 and BPAF were the most cytotoxic. There are no previous data on the cytotoxicity of DD-70 for comparative purposes. However, BPAF was also found to be the most cytotoxic among several BPA alternatives in cell lines (Russo et al. 2018), embryonic stem cells (Liang et al. 2020) and zebrafish embryos (Moreman et al. 2017). TGSH and BPSIP had LC50 values of 20.9 ± 9.9 and 85.9 ± 42.3 μM in DCEH; values lower than those observed in CEH (Table 5.2). In a chicken egg injection study, TGSH had a similar LD50 value as BPA (Crump et al. 2018) and no viability data exist for BPSIP. Overall, DCEH were more sensitive to the BPA alternatives compared to CEH in terms of cytotoxicity. Similarly, LC50 values of several organic flame retardants were lower in hepatocytes of DCCO (Page-Lariviere et al. 2018) or herring gulls (Porter et al. 2014) compared to CEH. Even though the DCCO embryos were collected from an area of the Great Lakes basin that has relatively low concentrations of organohalogen contaminants, it is plausible that the reduced cell viability observed in this, and previous studies, compared to chicken hepatocytes, could be associated with the presence of endogenous contaminants and their interaction with the administered chemicals. Therefore, further evidence will be required to confirm species differences in cytotoxic sensitivity to these BPA replacements.

3.2 BPA replacements dysregulated more genes than BPA in CEH

Based on the cell viability data, the highest concentration that did not affect cell viability was selected for gene expression analysis in CEH. Gene expression data are presented in two ways: 1) BPA alternatives with significant gene fold changes and their related pathways on the ToxChip array (Table 5.3) and AestroChip array (Table 5.4), and 2) principal component analysis (Figures 5.1 and 5.2). The reverse transcriptase control and positive PCR control met the appropriate quality control/assurance criteria for the ToxChip and there was no amplification in NTC for the AestroChip. Gene expression results will first be presented for the ToxChip array. BPA replacement compounds altered the expression of at least 5 genes on the ToxChip in CEH, whereas BPA and E2 affected 2 and 8 genes, respectively. Importantly, the five replacement compounds elicited a greater fold change on the ToxChip array in CEH compared to BPA. The rank order of compounds in terms of gene alterations in CEH was TGSH (23) > DD-70 (14) >BPAF (10) = BPF (10) > E2 (8) > BPSIP (5) > BPA (2).

ToxChip gene expression profiles in CEH were reduced to two principal components (Figure 5.1). Principal component 1 (PC1) explained 52.25% of the variability and was influenced by genes involved in bile acid and cholesterol regulation (CYP7B1, FOXA1 and LSS), xenobiotic metabolism (AOC1 and FGA) and the thyroid hormone pathway (THRSP). Principal component 2 (PC2) explained 16.08% of gene expression variability and was influenced by genes involved in xenobiotic metabolism (CYP1A4) and bile acid and cholesterol regulation (FGF19). TGSH, which had the greatest number of dysregulated genes overall, separated furthest away from DMSO and the other replacement compounds along PC1 and PC2. BPF, DD-70 and BPAF clustered together and BPSIP clustered near E2. Surprisingly, BPA had a limited gene expression response compared to the replacements and clustered closest to DMSO.

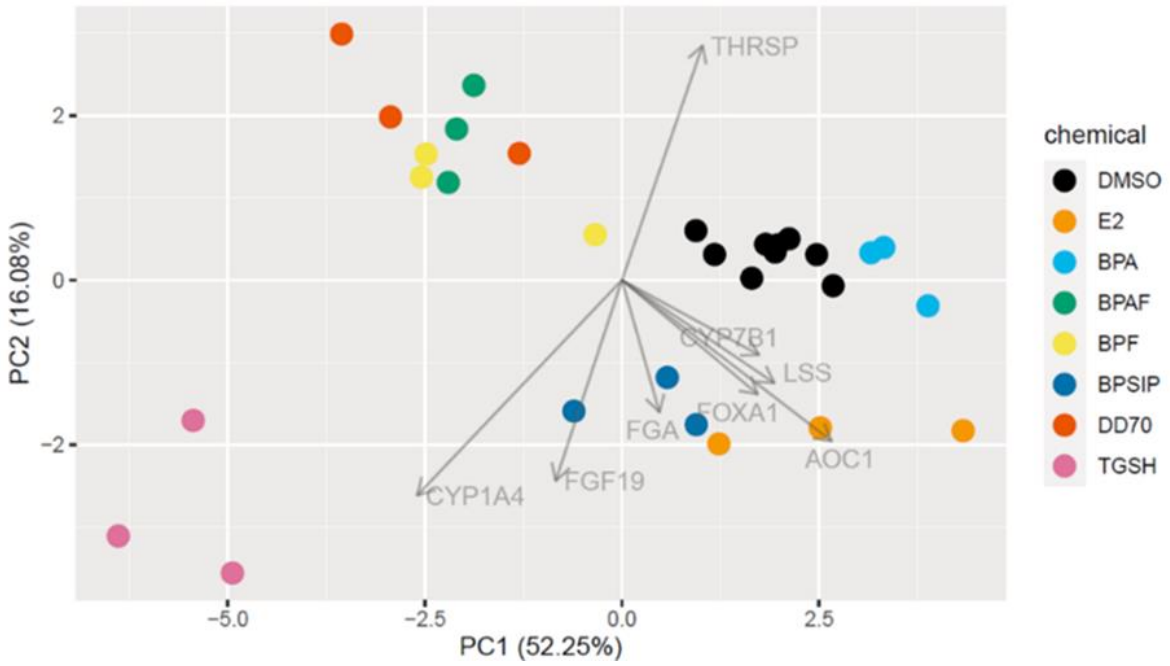

Figure 5.1. Principal component analysis of significant genes on the ToxChip array in CEH following exposure to BPA, BPA replacement compounds (BPF, TGSH, DD-70, BPAF and BPSIP), and 17β estradiol (E2). Data are coloured by chemical. Gene loadings for the most responsive transcripts are depicted by arrows on the graph.

Of the nine pathways on the ToxChip array, xenobiotic metabolism was the most affected by all of the BPA alternatives in CEH (Table 5.3). The fold changes of all genes on the chicken ToxChip array are presented in the supplemental information (Table S5.5). The phase I metabolism gene, CYP1A4, was upregulated (1.2 to 3.9 log2 fold) by the five replacement compounds, while its expression remained unchanged by BPA and E2. Likewise, another BPA alternative, BPS, upregulated the expression of CYP1A4 in CEH (Ma et al. 2015). The expression of CYP1A is mediated by the aryl hydrocarbon receptor (AhR) (Nebert et al. 2014), indicating that the five replacement compounds may act as agonists of this receptor.

Table 5.3. Mean log2 fold change of significantly altered genes on the ToxChip array in chicken embryonic hepatocytes following exposure to 30 μM of BPF, TGSH, BPSIP and BPA, and 10 μM of DD-70, BPAF and E2.

		Log2 fold change[a]						
Pathway	**Gene**	**BPF**	**TGSH**	**DD-70**	**BPAF**	**BPSIP**	**BPA**	**E2**
Bile acid/cholesterol regulation	APOB	**-1.1**	**-1.1**	**-0.7**	-0.3	0.0	0.1	**1.0**
	CYP7B1	-0.4	**-1.4**	**-1.0**	-0.9	0.1	0.7	**1.2**
	FGF19	-1.0	**1.8**	**-1.1**	-0.4	-0.3	-1.3	-0.3
	FOXA1	**-1.4**	**-1.4**	**-1.5**	**-1.4**	0.3	0.2	0.4
	LSS	-0.9	**-1.6**	**-1.9**	**-2.2**	-0.1	0.1	-0.1
Cell cycle	RPL4	0.5	**0.8**	0.3	**0.7**	0.3	-0.4	-0.3
	TP63	-0.6	-0.2	**-0.8**	**-0.9**	-0.4	-0.7	-0.4
DNA repair	GADD45	**-0.9**	**-0.8**	**-1.6**	**-1.1**	-0.1	0.4	0.6
	POLB	-0.7	-0.7	**-0.9**	**-0.9**	-0.1	-0.3	-0.1
Glucose metabolism	G6PC	0.8	0.5	0.2	0.0	-0.1	-0.6	**-1.1**
	PDK4	0.6	**2.1**	0.8	0.3	**1.2**	0.4	0.4
Immune response	IL1B	-0.2	**-0.9**	-0.4	-0.3	0.6	-0.2	-0.6
	LEAP2	**0.7**	**1.7**	0.4	0.6	0.4	-0.6	-0.3
Lipid homeostasis	ACSL5	0.2	**1.0**	0.3	0.1	0.1	-0.6	-0.9
	LBFABP	**0.9**	**0.9**	**1.0**	0.2	0.5	-0.4	**-0.9**
	SCD	**-1.3**	**-1.9**	**-1.4**	**-1.2**	-0.2	-0.1	-1.6
	SLCO1A2	0.2	0.5	**0.6**	0.4	0.2	-0.1	-0.1
Oxidative stress	HMOX1	**-1.1**	-0.7	**-0.8**	-0.3	-0.1	0.4	**1.2**
	MGST3	0.5	**0.6**	0.5	0.2	0.2	-0.7	-1.0
	TXN	0.4	**1.7**	0.2	-0.2	-0.2	-0.5	0.6
Thyroid hormone	IGF1	-0.6	**-2.1**	-0.2	**-1.1**	**-0.9**	0.7	-0.3
	THRSP	-0.2	**-2.7**	-0.2	0.0	**-0.8**	-0.4	**-1.1**
	TTR	-0.1	**-0.8**	0.0	-0.1	-0.2	**0.7**	0.2
Xenobiotic metabolism	AOC1	-1.2	**-2.2**	**-2.5**	**-2.7**	0.0	0.5	0.2
	ALAS1	0.2	**1.3**	0.5	0.3	0.1	-0.2	**0.7**
	CYP1A4	**1.6**	**3.9**	**1.5**	**1.2**	**2.4**	0.1	0.9
	CYP3A7	**-0.6**	**-0.9**	0.1	0.6	-0.4	0.0	0.4
	FGA	-0.3	0.4	-0.6	-0.2	**1.1**	**0.8**	0.5
	SULT1B1	0.0	-0.2	-0.3	0.1	0.3	0.4	**0.7**
	SULT1E1	**0.6**	**0.6**	0.3	-0.1	0.0	-0.6	-0.6

[a] Fold changes calculated relative to the respective DMSO control group. Significant fold changes (log2 fold change ≥ 0.58 and ≤ -0.58, adjp ≤ 0.05) are in bold and upregulated and downregulated genes are in yellow and blue

With the exception of BPSIP, the four other replacement compounds changed at least two genes from the bile acid/cholesterol regulation pathway. TGSH and DD-70 exposure resulted in the alteration of all genes from this pathway (5 genes), followed by BPF and BPAF (2 genes). BPA did not change the expression of a single gene (Table 5.3). FOXA1 and LSS, involved in triglyceride synthesis and production of monosaturated fatty acid from saturated fatty acid (Moya et al. 2012), were downregulated by the four replacement compounds. Another gene that regulates bile acid synthesis and lipid and carbohydrate metabolism (Massafra et al. 2017), FGF19, was upregulated by TGSH (1.8 log2 fold) and downregulated by DD-70 (-1.1 log2 fold). The gene, CYP7B1, which breaks down cholesterol to form bile acid (Stiles et al. 2009) was downregulated by TGSH and DD-70 (-1.4 and -1 log2 fold) and upregulated by E2 (1.2 log2 fold). Cholesterol is essential for cellular function as a component of cell membranes and a precursor of steroid hormones and bile acids (Stiles et al. 2009). Alterations of genes involved in bile acid and cholesterol synthesis could lead to a loss of optimal amount of cholesterol for cellular functions and signaling and cause metabolic disorders like cholestasis (Massafra et al. 2017). In addition to xenobiotic metabolism and bile acid/ cholesterol related genes, TGSH and BPSIP, decreased the expression of the thyroid hormone pathway gene, THRSP (-2.7 and -0.8 log2 fold); a similar directional change observed following E2 exposure (-1.1 log2 fold). THRSP expression is induced by thyroid hormone and estrogen in chickens in order to regulate lipid biosynthesis (Ren et al. 2017), thus playing a key role in metabolism. Exposure to another BPA replacement compound, BPS, resulted in a concordant downregulation of THRSP in CEH (Ma et al. 2015). Disruption of the thyroid hormone pathway could lead to adverse outcomes in avian species because it is critical for growth, development of the nervous system, egg laying, pipping

and heat production (McNabb 2007). The ToxChip results suggest that TGSH and other replacements are more transcriptionally active than BPA in CEH.

In addition to the ToxChip array genes, estrogen responsive genes were also altered by BPF, TGSH, BPAF and BPSIP in CEH, evaluated using the AestroChip array (Table 5.4). The rank order for gene dysregulation was: E2 (5) > BPSIP (3) > BPF (2) =TGSH (2) =BPAF (2) >BPA (1) > DD-70 (0). The fold changes of all genes on the chicken AestroChip array are presented in the supplemental information (Table S5.6). On the AestroChip PCA (Figure 5.2), E2 was furthest separated from DMSO along PC1, which was highly influenced by vitellogenin II (VTG2; 9.3 log2 fold) and apovitellenin (APO; 9.8 log2 fold) (Table 5.4). Among the BPA-related compounds, only BPF and BPSIP separated towards E2 along PC1, although still closer to DMSO. The clustering of BPSIP was influenced by CPT and VCAM, and BPF clustering was influenced by APO.

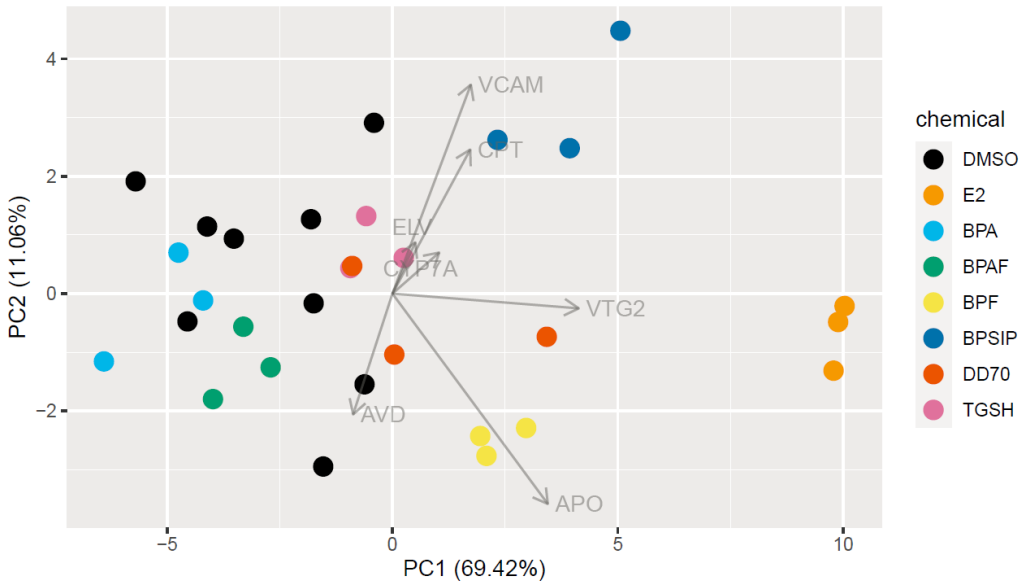

Figure 5.2. Principal component analysis of significant genes on the AestroChip array in CEH following exposure to BPA, BPA replacement compounds (BPF, TGSH, DD-70, BPAF and BPSIP), and 17β estradiol (E2). Data are coloured by chemical. Gene loadings for the most responsive significant transcripts are included on the graph.

The expression of APO was upregulated by one replacement compound, BPF (5.8 log 2 fold), and E2 (9.8 log2 fold). APO is synthesized in the liver and prevents the breakdown of very low-density lipoproteins by lipase during transfer to oocytes from the liver (Bourin et al. 2012). BPF was found to have similar estrogenicity (Moreman et al. 2017) as BPA and increased expression of estrogen receptors (ERα, ERβ) and cytochrome P450 aromatase (CYP19A1A and CYP19A1B) in zebrafish (Qiu et al. 2019). Carnitine palmitoyltransferase 1A (CPT) plays a crucial role in fatty acid oxidation and cell proliferation (Schlaepfer and Joshi 2020). The expression of CPT was found to be regulated by E2 in rats (Campbell et al. 2003) and was upregulated by BPSIP (4.1 log2 fold) in this study. The other gene upregulated by BPSIP was vascular cell adhesion protein 1 (VCAM), which attaches white blood cells to the endothelium, thus playing a role in the immune system (Cook-Mills et al. 2011). In general, gene

dysregulation following BPSIP exposure were directionally concordant with E2 exposure in CEH. To date, there has been only one study, which evaluated the endocrine disrupting properties of BPSIP. In male zebrafish exposed to BPSIP, an increase in ERα, and brain and gonad cytochrome P450 aromatase (converts androgen to estrogen) mRNA expression was observed (Lee et al. 2018). BPAF and BPA downregulated the expression of VTG2 (-2.9 and -2.8-log2 fold). Previous studies reported that BPAF was one of the most estrogenic replacement compounds in the estrogen responsive MCF-7 cell line (Mesnage et al. 2017; Kitamura et al. 2005). In the current study, livers from females and males were pooled when preparing CEH, which could have impacted the overall expression of estrogen responsive genes. Overall, these results suggest that BPF and BPSIP may have some mild estrogenic activity and requires further investigation.

Table 5.4. Mean log2 fold change of significantly altered genes on the AestroChip array in chicken embryonic hepatocytes following exposure to 30 μM of BPF, TGSH, BPSIP, BPA, and 10 μM of DD-70, BPAF and E2.

		Log2 Fold Change[a]						
Pathway	**Genes**	**BPF**	**TGSH**	**DD-70**	**BPAF**	**BPSIP**	**BPA**	**E2**
Estrogen Responsive	APO	**5.8**	1.1	0.4	0.0	1.4	2.2	**9.8**
	CYP7A	1.1	**2.6**	-1.3	-0.2	2.1	1.4	2.8
	ELOVL2	0.0	-0.4	1.1	1.0	2.0	0.3	**1.0**
	AVD	**2.8**	**1.2**	0.0	-1.1	**-2.4**	0.4	**-2.7**
	CPT	1.0	0.7	1.2	**-1.8**	**4.1**	1.0	**3.2**
	VCAM	-0.6	-0.6	1.6	0.9	**4.5**	-0.5	3.4
	VTG2	1.6	0.9	1.8	**-2.9**	1.5	**-2.8**	**9.3**

[a] Fold changes were calculated relative to the respective DMSO control group. Significant fold changes (log2 fold change ≥ 0.58 and ≤ -0.58, adjp ≤ 0.05) are in bold and upregulated and downregulated genes are in yellow and blue

3.3 BPA replacements had different gene expression responses in DCEH

In DCEH, PCA revealed that PC1 accounted for 45.96% of the variability, while PC2 accounted for 27.9% (Figure 5.3). PC1 was influenced by MT4, FGF19, LIPC and CYP3A7 and PC2 by POLK and ALDH1A1. PCA clustering of ToxChip genes in DCEH, revealed that BPSIP clustered furthest away from DMSO along PC1 and the rest of the replacement compounds clustered close to DMSO. The clustering of E2 along PC2 was influenced by ALDH1A1 (Figure 3).

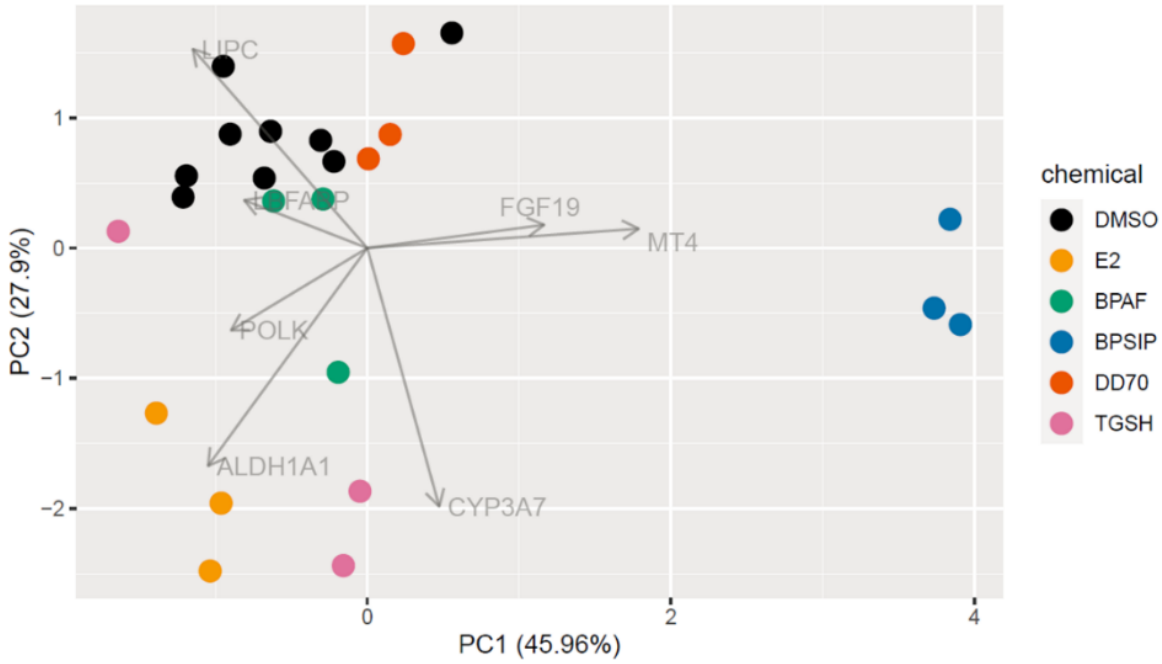

Figure 5.3. Principal component analysis of significant genes on the double-crested cormorant ToxChip array in DCEH following exposure to the BPA replacement compounds, TGSH, DD-70, BPAF and BPSIP, and 17β estradiol (E2). Data are coloured by chemical. Gene loadings for the most responsive significant transcripts are included on the graph.

In DCEH, BPSIP was the most responsive in terms of both the number of altered genes, and the pathways affected (Table 5.5). The fold changes of all genes on the DCCO ToxChip array are presented in the supplemental information (Table S5.7). The rank order for gene dysregulation was: BPSIP (8) > DD-70 (1) = BPAF (1) > TGSH (0). The most altered genes by BPSIP were MT4 (2.4 log2 fold), FGF19 (1.9 log2 fold), LIPC (-1.9 log2 fold), and CYP3A7 (1.5 log2 fold) (Table 5.5). The gene, MT4, stabilizes reactive oxygen species and provides protection against oxidative stress (Sutherland and Stillman 2011). An increase in FGF19 activity can lead to fatty acid and bile acid oxidation (Massafra et al. 2017). The suppression of the gene, LIPC can cause lipid accumulation since it breaks down phospholipids and triglycerides (Connelly and Hegele 1998). There are no studies on the effects of BPSIP on bile acids and cholesterol regulation and future studies are needed to investigate this pathway. BPSIP also upregulated CYP3A7 expression, whereas CYP1A4 was upregulated by BPSIP in CEH. This suggests that the metabolism of BPSIP in CEH and DCEH occurs via different mechanisms. Among these 5 replacement compounds, BPSIP was the least responsive in CEH, which is in contrast to the results for DCEH, suggesting species differences based on in vitro effects.

Table 5.5. Mean log2 fold change of significantly altered genes on the ToxChip array in double-crested cormorant embryonic hepatocytes following exposure to 10 μM TGSH, DD-70, BPAF, and E2, and 30 μM BPSIP

		Log2 Fold Change[a]				
Pathway	**Genes**	**TGSH**	**DD-70**	**BPAF**	**BPSIP**	**E2**
Bile acids/cholesterol regulation	FGF19	0	**0.7**	0.7	**1.9**	0.4
	LIPC	-0.8	-0.1	-0.3	**-1.9**	1.1
DNA Repair	FRZB	-0.4	-0.3	-0.1	**-0.9**	0.1
	POLK	0.3	0.4	0.5	**-1**	0.5
Lipid homeostasis	LBFABP	0.1	0.3	-0.5	**-1.3**	0.3
Oxidative stress	MT4	-0.4	0	-0.7	**2.6**	0.3
Thyroid hormone pathway	TTR	0.2	-0.3	-0.5	**-1.1**	0.2
Xenobiotic metabolism	CYP3A7	2	0.5	**1**	**1.5**	1.4
	ALDH1A1	0.9	-0.7	0	-0.8	**2.1**

[a] Fold changes were calculated relative to the respective DMSO control group. Significant fold changes (log2 fold change ≥ 0.58 and ≤ -0.58, adjp ≤ 0.05) are in bold, upregulated and downregulated genes are in yellow and blue

PCA of the four common BPA replacement compounds in CEH and DCEH showed that gene dysregulation was more pronounced in CEH (Figure 5.4). DCEH samples were close to the control, while in CEH, three of the replacement compounds, TGSH, DD-70 and BPAF, were separated from the control. PC1 was highly influenced by the xenobiotic metabolism gene, CYP1A4. All five of the BPA replacement compounds upregulated CYP1A4 expression in CEH (Table 5.3). In contrast, CYP3A7 expression was upregulated by BPAF and BPSIP in DCEH (Table 5.4) and no changes were observed in CYP1A4 (Table S5.6).

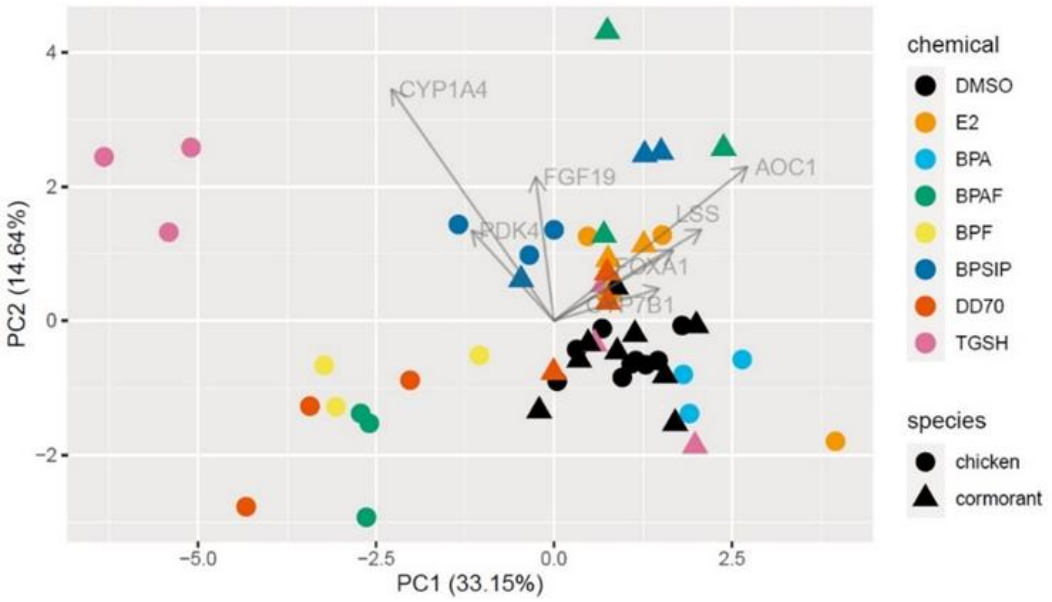

Figure 5.4. Principal component analysis of significant genes from the ToxChip array in CEH and DCEH following exposure to the BPA replacement compounds, TGSH, DD-70, BPAF and BPSIP, and 17β estradiol (E2). Data are coloured by chemical and species represented by shapes. Gene loadings for the most responsive significant transcripts are included on the graph.

The differences in detoxification mechanisms of the replacement compounds between CEH and DCEH could help explain the variability of *in vitro* effects (i.e. cytotoxicity, gene expression). Differences in amino acid sequences within the ligand-binding domain of AhR account for species differences in sensitivity to AhR agonists and induction of CYP1A4 (Farmahin et al. 2014). Chickens are highly sensitive to AhR agonists compared to DCCO due to the substitution of two amino acids within the ligand-binding domain of AhR (Head et al. 2008). Avian CYP3A7 belongs to the CYP3A subfamily of phase I metabolizing enzymes and is regulated by the chicken xenobiotic receptor (CXR), which is similar to the mammalian pregnane X receptor (PXR) (Handschin et al. 2000). Previous studies reported inter-species differences of CYP3A sensitivity in mammals in response to BPA and BPAF; both were ligands

of human PXR but not rat PXR (Sui et al. 2012). Our gene expression data suggest a species-specific difference in the metabolism of these compounds by phase I metabolizing enzymes in primary hepatocytes, which could account for differences in subsequent toxicity. Future studies should include more doses to investigate the differences between cytotoxicity and gene expression and to generate gene expression dose-response curves.

Overall, TGSH, DD-70 and BPAF had the highest cytotoxicity among the BPA replacement compounds in CEH and DCEH, while BPF and BPSIP were less cytotoxic than BPA in CEH. The two BPA alternatives modulated the expression of genes from pathways including xenobiotic metabolism, bile acid/cholesterol regulation and lipid homeostasis and interestingly, altered more ToxChip genes than BPA in CEH. With the exception of DD-70, the four remaining BPA replacements altered the expression of more estrogen responsive genes than BPA in CEH. The inclusion of hepatocytes from two avian species permitted cross-species comparisons and in general, LC50 values were lower and fewer gene expression changes were observed in DCEH. Genes associated with variable pathways were dysregulated indicating potential differences in mechanisms of action compared to BPA for the two species. Future whole-animal studies are required to evaluate individual-level effects of the BPA replacements prioritized in this screening study (e.g. DD-70, BPAF) to contribute to the identification of safe replacements for BPA.

Acknowledgements

This work was supported by funds from three sources within Environment and Climate Change Canada: 1) Chemicals Management Plan (CMP); 2) Strategic Technology Applications of Genomics for the Environment (STAGE); and 3) the Ecotoxicology and Wildlife Health Division.

5.5 References

Andra SS, Charisiadis P, Arora M, van Vliet-Ostaptchouk JV, Makris KC. 2015. Biomonitoring of human exposures to chlorinated derivatives and structural analogs of bisphenol A. *Environment International* 85:352-379. DOI: 10.1016/j.envint.2015.09.011.

Bjornsdotter MK, Jonker W, Legradi J, Kool J, Ballesteros-Gomez A. 2017. Bisphenol A alternatives in thermal paper from the Netherlands, Spain, Sweden and Norway. Screening and potential toxicity. *Science of the Total Environment* 601:210-221. DOI: 10.1016/j.scitotenv.2017.05.171.

Bourin M, Gautron J, Berges M, Hennequet-Antier C, Cabau C, Nys Y, Rehault-Godbert S. 2012. Transcriptomic profiling of proteases and antiproteases in the liver of sexually mature hens in relation to vitellogenesis. *Bmc Genomics* 13. DOI: 10.1186/1471-2164-13-457.

Campbell SE, Mehan KA, Tunstall MA, Febbraio MA, Cameron-Smith D. 2003. 17beta-estradiol upregulates the expression of peroxisome proliferator-activated receptor alpha and lipid oxidative genes in skeletal muscle. *Journal of Molecular Endocrinology* 31(1):37-45. DOI: 10.1677/jme.0.0310037.

Castro B, Sanchez P, Torres JM, Ortega E. 2015. Bisphenol A, bisphenol F and bisphenol S affect differently 5α-reductase expression and dopamine–serotonin systems in the prefrontal cortex of juvenile female rats. *Environmental Research* 142: 281-287. DOI: 10.1016/j.envres.2015.07.001.

Cano-Nicolau J, Valliant C, Pellegrini E, Charlier TD, Kah O, Coumailleau P. 2016. Estrogenic Effects of Several BPA Analogs in the Developing Zebrafish Brain. *Frontiers in Neuroscience* 10. DOI: 10.3389/fnins.2016.00112.

Cao LY, Ren XM, Li CH, Zhang J, Qin WP, Yang Y, Wan B, Guo LH. 2017. Bisphenol AF and Bisphenol B Exert Higher Estrogenic Effects than Bisphenol A via G Protein-Coupled Estrogen Receptor Pathway. *Environmental Science & Technology* 51:11423-11430. DOI: 10.1021/acs.est.7b03336.

Cook-Mills JM, Marchese ME, Abdala-Valencia H. 2011. Vascular Cell Adhesion Molecule-1 Expression and Signaling During Disease: Regulation by Reactive Oxygen Species and Antioxidants. *Antioxidants & Redox Signaling* 15:1607-1638. DOI: 10.1089/ars.2010.3522.

Connelly PW, Hegele RA. 2008. Hepatic lipase deficiency. *Critical Reviews in Clinical Laboratory Sciences* 35(6):547-572. DOI: 10.1080/10408369891234273.

Corrales J, Kristofco LA, Steele WB, Yates BS, Breed CS, Williams ES, Brooks BW. 2015. Global Assessment of Bisphenol A in the Environment: Review and Analysis of Its Occurrence and Bioaccumulation. *Dose-Response* 13. DOI: 10.1177/1559325815598308.

Crump D, Chiu S, Williams KL. 2018. Bis-(3-allyl-4-hydroxyphenyl) sulfone decreases embryonic viability and alters hepatic mRNA expression at two distinct developmental stages in chicken embryos exposed via egg injection. *Environmental Chemistry & Toxicology* 37(2):530-537. DOI: 10.1002/etc.3990

Crump D, Farhat A, Chiu S, Williams KL, Jones SP, Langlois VS. 2016. Use of a Novel Double-Crested Cormorant ToxChip PCR Array and the EROD Assay to Determine Effects of Environmental Contaminants in Primary Hepatocytes. *Environmental Science & Technology* 50:3265-3274. DOI: 10.1021/acs.est.5b06181.

Dekant W, Voelkel W. 2008. Human exposure to bisphenol A by biomonitoring: Methods, results and assessment of environmental exposures. *Toxicology and Applied Pharmacology* 228:114-134. DOI: 10.1016/j.taap.2007.12.008.

Eladak S, Grisin T, Moison D, Guerquin MJ, N'Tumba-Byn T, Pozzi-Gaudin S, Benachi A, Livera G, Rouiller-Fabre V, Habert, R. 2015. A new chapter in the bisphenol A story: bisphenol S and bisphenol F are not safe alternatives to this compound. *Fertility and sterility* 103(1): 11–21. DOI: 10.1016/j.fertnstert.2014.11.005.

Environment and Climate Change Canada and Health Canada. 2019. Identification of Risk Assessment Priorities (IRAP). Last accessed September 2020. https://www.canada.ca/content/dam/eccc/documents/pdf/pded/irap/Identification-of-risk-assessment-priorities-(IRAP).pdf

Farmahin R, Crump D, Kennedy SW. 2014. Sensitivity of avian species to the aryl hydrocarbon receptor ligand 6-formylindolo 3,2-b carbazole (FICZ). *Chemico-Biological Interactions* 221:61-69. DOI: 10.1016/j.cbi.2014.07.009.

Gonzalez-Rubio S, Vike-Jonas K, Gonzalez SV, Ballesteros-Gomez A, Sonne C, Dietz R, Boertmann D, Rasmussen LM, Jaspers VLB, Asimakopoulos AG. 2020. Bioaccumulation potential of bisphenols and benzophenone UV filters: A multiresidue approach in raptor tissues. *Science of the Total Environment* DOI: https://doi.org/10.1016/j.scitotenv.2020.14033

Handschin C, Podvinec M, Meyer UA. 2000. CXR, a chicken xenobiotic-sensing orphan nuclear receptor, is related to both mammalian pregnane X receptor (PXR) and constitutive androstane receptor (CAR). *Proceedings of the National Academy of Sciences of the United States of America* 97:10769-10774. DOI: 10.1073/pnas.97.20.10769.

Head JA, Hahn ME, Kennedy SW. 2008. Key Amino Acids in the Aryl Hydrocarbon Receptor Predict Dioxin Sensitivity in Avian Species. *Environmental Science and Technology* 42(19) 7535–7541. DOI: 10.1021/es801082a.

Huang GM, Tian XF, Fang XD, Ji FJ. 2016. Waterborne exposure to bisphenol F causes thyroid endocrine disruption in zebrafish larvae. *Chemosphere* 147:188-194. DOI: 10.1016/j.chemosphere.2015.12.080.

Jessl L, Lenz R, Massing FG, Scheider J, Oehlmann J. 2018. Effects of estrogens and antiestrogens on gonadal sex differentiation and embryonic development in the domestic fowl (Gallus gallus domesticus). *Peerj* 6. DOI: 10.7717/peerj.5094.

Keminer O, Teigeler M, Kohler M, Wenzel A, Arning J, Kassner F, Windshugel B, Eilebrecht E. 2020. A tiered high-throughput screening approach for evaluation of estrogen and androgen receptor modulation by environmentally relevant bisphenol A substitutes. *Science of the Total Environment* 717. DOI: 10.1016/j.scitotenv.2019.134743.

Kennedy SW, Lorenzen A, James CA, Collins BT. 1993. Ethoxyresorufin-o-deethylase and porphyrin analysis in chicken-embryo hepatocyte cultures with a fluorescence multiwall plate reader. *Analytical Biochemistry* 211:102-112. DOI: 10.1006/abio.1993.1239.

Keri RA, Ho SM, Hunt PA, Knudsen KE, Soto AM, Prins GS. 2007. An evaluation of evidence for the carcinogenic activity of bisphenol A. *Reproductive Toxicology* 24:240-252. DOI: 10.1016/j.reprotox.2007.06.008.

Kitamura S, Suzuki T, Sanoh S, Kohta R, Jinno N, Sugihara K, Yoshihara S, Fujimoto N, Watanabe H, Ohta S. 2005. Comparative study of the endocrine-disrupting activity of bisphenol A and 19 related compounds. *Toxicological Sciences* 84:249-259. DOI: 10.1093/toxsci/kfi074.

Lee J, Park NY, Kho Y, Ji K. 2018. Effects of 4-Hydroxyphenyl 4-Isoprooxyphenylsulfone (BPSIP) Exposure on Reproduction and Endocrine System of Zebrafish. Environmental Science & Technology 52:1506-1513. DOI: 10.1021/acs.est.7b00498.

Liang XX, Yin NY, Liang SX, Yang RJ, Liu SY, Lu YP, Jiang LS, Zhou QF, Jiang GB, Faiola F. 2020. Bisphenol A and several derivatives exert neural toxicity in human neuron-like cells by decreasing neurite length. *Food and Chemical Toxicology* 135. DOI: 10.1016/j.fct.2019.111015.

Ma M, Crump D, Farmahin R, Kennedy SW. 2015. Comparing the effects of tetrabromobisphenol-a, bisphenol a, and their potential alternatives, TBBPA-bis (2,3-dibromopropyl ether) and bisphenol s on cell viability and messenger ribonucleic acid expression in chicken embryonic hepatocytes. *Environmental Toxicology and Chemistry* 34:391-401. DOI: 10.1002/etc.2814.

Massafra V, Milona A, Vos HR, Burgering BMT, van Mil SWC. 2017. Quantitative liver proteomics identifies FGF19 targets that couple metabolism and proliferation. *Plos One* 12. DOI: 10.1371/journal.pone.0171185.

Matsushima A, Liu XH, Okada H, Shimohigashi M, Shimohigashi Y. 2010. Bisphenol AF Is a Full Agonist for the Estrogen Receptor ER alpha but a Highly Specific Antagonist for ER beta. *Environmental Health Perspectives* 118:1267-1272. DOI: 10.1289/ehp.0901819.

McNabb FMA. 2007. The hypothalamic-pituitary-thyroid (HPT) axis in birds and its role in bird development and reproduction. *Critical Reviews in Toxicology* 37:163-193. DOI: 10.1080/10408440601123552.

Mesnage R, Phedonos A, Arno M, Balu S, Corton JC, Antoniou MN. 2017. Transcriptome Profiling Reveals Bisphenol A Alternatives Activate Estrogen Receptor Alpha in Human Breast Cancer Cells. *Toxicological Sciences* 158:431-443. DOI: 10.1093/toxsci/kfx101.

Moreman J, Lee O, Trznadel M, David A, Kudoh T, Tyler CR. 2017. Acute Toxicity, Teratogenic, and Estrogenic Effects of Bisphenol A and Its Alternative Replacements Bisphenol S, Bisphenol F, and Bisphenol AF in Zebrafish Embryo-Larvae. *Environmental Science & Technology* 51:12796-12805. DOI: 10.1021/acs.est.7b03283.

Moriyama K, Tagami T, Akamizu T, Usui T, Saijo M, Kanamoto N, Hataya Y, Shimatsu A, Kuzuya H, Nakao K. 2002. Thyroid hormone action is disrupted by bisphenol A as an antagonist. *Journal of Clinical Endocrinology & Metabolism* 87:5185-5190. DOI: 10.1210/jc.2002-020209.

Moya M, Benet M, Guzman C, Tolosa L, Garcia-Monzon C, Pareja E, Castell JV, Jover R. 2012. Foxa1 reduces lipid accumulation in human hepatocytes and is down-regulated in nonalcoholic fatty liver. *Plos One* 7. DOI: 10.1371/journal.pone.0030014.

Nakayama K, Iwata H, Kim EY, Tashiro K, Tanabe S. 2006. Gene expression profiling in common cormorant liver with an oligo array: Assessing the potential toxic effects of environmental contaminants. *Environmental Science & Technology* 40:1076-1083. DOI: 10.1021/es051386m.

Nebert DW, Dalton TP, Okey AB, Gonzalez FJ. 2004. Role of aryl hydrocarbon receptor-mediated induction of the CYP1 enzymes in environmental toxicity and cancer. *Journal of Biological Chemistry* 279:23847-23850. DOI: 10.1074/jbc.R400004200.

Page-Lariviere F, Chiu S, Jones SP, Farhat A, Crump D, O'Brien JM. 2018. Prioritization of 10 organic flame retardants using an avian hepatocyte toxicogenomic assay. *Environmental Toxicology and Chemistry* 37:3134-3144. DOI: 10.1002/etc.4260.

Porter E, Crump D, Egloff C, Chiu S, Kennedy SW. 2014. Use of an avian hepatocyte assay and the avian toxchip polymerse chain reaction array for testing prioritization of 16 organic flame retardants. *Environmental Toxicology and Chemistry* 33:573-582. DOI: 10.1002/etc.2469.

Powell DC, Aulerich RJ, Meadows JC, Tillitt DE, Stromborg KL, Kubiak TJ, Giesy JP. Bursian SJ. 1997. Organochlorine Contaminants in Double-Crested Cormorants from Green Bay,Wisconsin: II. Effects of an Extract Derived from Cormorant Eggs on the Chicken Embryo. *Archives of Environmental Contamination and Toxicology* 32 (3), 316−322.

Qiu WH, Fang MJ, Liu JY, Fu CX, Zheng CM, Chen B, Wang KJ. 2019. In vivo actions of Bisphenol F on the reproductive neuroendocrine system after long-term exposure in zebrafish. *Science of the Total Environment* 665:995-1002. DOI: 10.1016/j.scitotenv.2019.02.154.

R Core Team. 2013. R: A language and environment for statistical computing.R Foundation for Statistical Computing, Vienna, Austria. http://www.R-project.org/

Ren JX, Xu NY, Zheng H, Tian WH, Li H, Li ZJ, Wang YB, Tian YD, Kang XT, Liu XJ. 2017. Expression of Thyroid Hormone Responsive SPOT 14 Gene Is Regulated by Estrogen in Chicken (Gallus gallus). *Scientific Reports* 7. DOI: 10.1038/s41598-017-08452-6.

Robinson MD, McCarthy DJ, Smyth GK. 2010. edgeR: a Bioconductor package for differential expression analysis of digital gene expression data. *Bioinformatics* 26(1):139-140. DOI: 10.1093/bioinformatics/btp616.

Russo G, Capuozzo A, Barbato F, Irace C, Santamaria R, Grumetto L. 2018. Cytotoxicity of seven bisphenol analogues compared to bisphenol A and relationships with membrane affinity data. *Chemosphere* 201:432-440. DOI: 10.1016/j.chemosphere.2018.03.014.

Schlaepfer IR, Joshi M. 2020. CPT1A-mediated Fat Oxidation, Mechanisms, and Therapeutic Potential. *Endocrinology* 161. DOI: 10.1210/endoer/bqz046.

Schmittgen TD, Livak KJ. 2008. Analyzing real-time PCR data by the comparative C-T method. *Nature Protocols* 3:1101-1108. DOI: 10.1038/nprot.2008.73.

Stiles AR, McDonald JG, Bauman DR, Russell DW. 2009. CYP7B1: One Cytochrome P450, Two Human Genetic Diseases, and Multiple Physiological Functions. *Journal of Biological Chemistry* 284:28485-28489. DOI: 10.1074/jbc.R109.042168.

Sui YP, Ai N, Park SH, Rios-Pilier J, Perkins JT, Welsh WJ, Zhou CC. 2012. Bisphenol A and Its Analogues Activate Human Pregnane X Receptor. *Environmental Health Perspectives* 120:399-405. DOI: 10.1289/ehp.1104426.

Sutherland DEK, Stillman MJ. 2011. The "magic numbers" of metallothionein. *Metallomics* 3:444-463. DOI: 10.1039/c0mt00102c.

Wickham H. 2016 ggplot2: Elegant Graphics for Data Analysis. Springer-Verlag New York.

Yamazaki E, Yamashita N, Taniyasu S, Lam J, Lam PKS, Moon HB, Jeong Y, Kannan P, Achyuthan H, Munuswamy N, Kannan K. 2015. Bisphenol A and other bisphenol analogues including BPS and BPF in surface water samples from Japan, China, Korea and India. *Ecotoxicology and Environmental Safety* 122:565-572. DOI: 10.1016/j.ecoenv.2015.09.029.

Zoeller RT, Bansal R, Parris C. 2005. Bisphenol-A, an environmental contaminant that acts as a thyroid hormone receptor antagonist in vitro, increases serum thyroxine, and alters RC3/neurogranin expression in the developing rat brain. *Endocrinology* 146:607-612. DOI: 10.1210/en.2004-1018.

Chapter 6. Toxicity Screening of Bisphenol A Replacement Compounds: Cytotoxicity and mRNA Expression in LMH 3D Spheroids

6.1 Abstract

Previously, we showed that the chicken LMH cell line grown as 3D spheroids may be a suitable animal free alternative to primary chicken hepatocytes (CEH) for *in vitro* ecotoxicological screening of chemicals. In this study, the cytotoxicity and mRNA expression of Bisphenol A (BPA) and five replacement compounds (BPF, TGSH, DD-70, BPAF, BPSIP), and 17β estradiol (E2) were determined in LMH 3D spheroids. Results were compared to an earlier study that evaluated the same endpoints for these chemicals in CEH. Cytotoxicity and gene expression were determined using ATP concentrations and customized PCR arrays, respectively. The ToxChip array contains genes from toxicologically relevant pathways and the AestroChip array measures estrogen-responsive genes. Concentration-response gene expression perturbations following DD-70 and BPAF exposure were determined using a customized PCR array of select genes from the ToxChip and AestroChip arrays. DD-70 and BPAF were the most cytotoxic replacement compounds. TGSH and DD-70 modulated the greatest number of genes among replacements and BPA on the ToxChip array, although fewer genes compared to CEH. Based on the gene expression profile of E2, BPAF was the most estrogenic followed by BPF, BPSIP and BPA, and more estrogen-responsive genes were modulated in LMH spheroids compared to CEH. Concentration-dependent gene expression revealed that DD-70 and BPAF altered genes related to lipid and bile acid regulation. The cytotoxicity and clustering of the replacements based on gene expression profiles were similar between LMH spheroids and CEH, however LMH spheroids were more sensitive in terms of estrogenic response. In addition to generating novel

gene expression data for five BPA replacement compounds in an *in vitro* avian model, this research also demonstrates that LMH spheroids may represent a useful animal free alternative for ecotoxicological screening.

6.2 Introduction

In recent years toxicity testing has shifted focus towards mechanistic approaches to characterize the toxicity of the large number of chemicals in the environment (Krewski et al. 2009). Primary embryonic hepatocytes are frequently used for avian toxicity testing (Mundy et al. 2019; Porter et al. 2014). Primary hepatocytes have similar gene expression and enzyme activity compared to *in vivo* conditions; however, a loss of biochemical functions occurs shortly after isolation (Fraczek et al. 2013). Advancements in 3D cell culture techniques, such as spheroids, which resemble 3D organization of cells *in vivo*, has become more common in toxicity testing applications (Hellwig et al. 2018; Breslin and Driscoll 2013). Immortalized hepatic cell lines are an animal free alternative to primary hepatocytes and when cultured as spheroids have improved gene expression and metabolic/biochemical activities and are thus, better predictors of toxicity than 2D monolayer cultures (Sharin et al. 2020; Frolich 2018; Takahasi et al. 2015; Ramaiaghari et al. 2014).

Bisphenol A (BPA) replacement compounds are a group of chemicals for which toxicity data are limited. BPA is an industrial chemical used in the production of polycarbonate plastics and epoxy resin in a wide range of consumer products. BPA can bind to endocrine receptors and interfere with other biological pathways, which led to a ban on use in applications including infant products, food packaging and thermal paper (Siracusa et al. 2018; ECHA 2020). Such restrictions have led to the production of "BPA-free" products, many of which contain structural analogs of BPA. The production and use of BPA replacement compounds are increasing globally

and they have been detected in various environmental samples (Chen et al. 2016) yet their toxic effects remain largely unknown. Thus, there is a strong demand to rapidly generate ecotoxicological information for this group of priority compounds.

Here, we apply an *in vitro* transcriptomic approach to generate ecotoxicologial data for five BPA replacement compounds in a 3D cultured avian cell line. The chicken leghorn male hepatoma (LMH) cell line, especially when cultured in 3D spheroids, is a potential alternative to CEH for avian toxicity testing (Sharin et al. 2020). The five BPA replacement compounds chosen for this study are: bisphenol F (BPF), 4,4′-sulfonylbis(2-allylphenol) (TGSH/TGSA), Phenol, 4,4'-[methylenebis(oxy-2,1-ethanediylthio)] bis- (DD-70), bisphenol AF (BPAF), and 4-hydroxyphenyl 4-isopropoxyphenyl sulfone (BPSIP/D-8). Concentrations of BPF and BPAF were similar, and in some locations greater than BPA in sediments and water samples (Yamazaki et al. 2015; Yang et al. 2014; Song et al. 2012). BPF has been detected in wildlife, including the liver of the white-tailed eagle (Gonzalez-Rubio et al. 2020). TGSH was more teratogenic than BPA in zebrafish embryos (Bjornsdotter et al. 2017) and had similar lethality as BPA in chicken embryos (Crump et al. 2018). DD-70 was found to be non-estrogenic in a reporter gene assay (Keminer et al. 2019). Several studies have found BPAF to be more cytotoxic and estrogenic than BPA in several cell lines and species (Mu et al. 2018; Song et al. 2014; Kitamura et al. 2005). BPSIP upregulated mRNA expression of estrogen receptors (Lee et al. 2018) and caused similar developmental abnormalities as BPA in zebrafish embryos (Bjornsdotter et al. 2017). There are limited data on the production, usage, environmental prevalence and potential toxicity of TGSH, DD-70 and BPSIP.

The specific aims of this study were to: 1) generate ecotoxicological data for five BPA replacement compounds in LMH 3D spheroids, including cytotoxicity and perturbations in gene

expression; 2) evaluate whether LMH spheroids were an effective *in vitro* model for avian hepatic toxicity, and a viable alternative to CEH for chemical screening based on comparisons with recently reported results for the same five chemicals in CEH (Sharin et al. in 2021a).

6.3 Materials and Methods

6.3.1 Reagents

BPF (98%), BPA (97%) and 17β estradiol (E2, 98%) were purchased from Sigma-Aldrich, TGSH (96%), BPAF (98%), and BPSIP (98%) from Santa Cruz Biotechnology, and DD-70 (97%) from Toronto Research Chemicals (Table 6.1). The certificate of analysis provided by the supplier of the chemicals confirmed that the chemicals met quality control specifications. Stock solutions of the chemicals were prepared by dissolution in dimethyl sulfoxide (DMSO; Sigma-Aldrich) to a final concentration of 1 mM, except for E2 (200 μM). Dosing solutions were prepared by serial dilution from stock solutions to attain nominal concentrations of 0.1 to 100 μM. All cell culture reagents were purchased from Sigma-Aldrich unless stated otherwise.

6.3.2 Cell culture, dosing and viability

LMH cells were cultured and maintained as previously described (Sharin et al. 2020). For 3D spheroids, cells were seeded at 10 000 cells/well in 250 μl medium/well in ultra-low attachment (ULA) 96 well microplates (Corning) and grown for 4 days. On day 5, spheroids were treated with 0.1 to 300 μM of BPA and the five replacement compounds for cell viability or 30 μM BPF, TGSH, BPSIP and BPA, and 10 μM DD-70, BPAF and E2 for the ToxChip and AestroChip arrays. E2 was used as a positive control for the gene expression evaluation using the ToxChip and AestroChip arrays. LMH spheroids were treated with 0.01, 0.1 and 1 μM of DD-70

and BPAF for dose-response evaluation. Following a 24h exposure, spheroids were assessed for cell viability or stored at -80°C until subsequent gene expression analysis.

For cell viability, the spheroids were treated with BPA and the five replacement compounds for 24h and viability was determined using the CellTiter Glo 3D assay (Promega) following the manufacturer's instructions. Briefly, after the exposure period, 100 μL of assay reagent was added to each well containing spheroids in 100 μL medium and placed on an orbital shaker for lysis. The contents of each well were transferred to a flat clear bottom white 96 well microplate (Nunc) and incubated for 10 min in the dark at room temperature, and luminescence was read using the Luminoskan Ascent Luminometer (ThermoFisher).

6.3.3 RNA isolation and cDNA synthesis

Total RNA was extracted from spheroids using the PureLink RNA Micro Scale kit (ThermoFisher) according to the manufacturer's protocol. Two spheroids per replicate were pooled to ensure sufficient RNA yield. RNA concentration was quantified using a NanoDrop 2000 (ThermoFisher) and 250 ng was reverse transcribed with the Quantitect Reverse Transcription kit (Qiagen) according to the manufacturer's instructions.

6.3.4 PCR arrays

Gene expression was determined using three customized chicken PCR arrays: 1) ToxChip, 2) AestroChip, and 3) ComboChip. The ToxChip array (Qiagen, catalog no. CLAG22572, Table S6.1) comprises 43 target genes covering eight biologically relevant pathways, two reference genes (EEF1A1 and RPL4) and three quality controls (genomic DNA contamination control, reverse-transcription control, and a positive PCR control). The AestroChip array consists of nine estrogen-responsive genes, two reference genes (EEF1A1 and

RPL4) and a no template control (NTC) (Table S6.2). Concentration-dependent gene expression of DD-70 and BPAF were determined using the ComboChip array, which consists of 4 estrogen responsive genes from the AestroChip and 6 genes from the ToxChip array, 2 reference genes (EFF1A1 and RPL4) and NTC (Table S6.3). The RT^2 qPCR primer assays for the AestroChip and ComboChip arrays were purchased from Qiagen, and thus the sequences are proprietary. Real-time RT-PCR reactions were prepared with the RT^2 SYBR Green qPCR Master Mix kit (Qiagen). The thermal profile was 95°C for 10 min followed by 40 cycles of 95°C for 15 s and 60°C for 1 min and a final extension at 95°C for 1 min. Real-time RT-PCR was performed using a Stratagene Mx3005 instrument (Agilent Technologies) and CFX96 Touch Real-Time PCR Detection System (Bio-Rad Laboratories).

6.3.5 Data analysis

To calculate the lethal median concentration (LC50), cell viability data were log transformed and fit to a nonlinear regression curve (log (agonist) vs. response) using least squares (ordinary) on GraphPad Prism Ver. 6.07. 2-way ANOVA and post hoc Sidak comparison of LC50 values in LMH spheroids and CEH (from a previous study) were performed using GraphPad Prism Ver. 6.07.

The reverse transcription, genomic DNA and positive PCR controls met the appropriate quality control/assurance criteria for the ToxChip and there was no amplification in NTC for the AestroChip or the ComboChip. All PCR array Ct values were normalized to the housekeeping gene RPL4 using the $2^{-\Delta Ct}$ method (Schmittgen and Livak 2008). EEF1A1 was omitted as a reference gene due to variabilities in expression in the BPA samples on the AestroChip array. Genes on the ToxChip array with missing Ct values, or Ct values above 35 in more than 25% of all samples were removed from analysis. Fold change was determined relative to the DMSO

control group. The fold change data were log2-transformed before ANOVA analysis to account for unequal variance. The resulting p-values from pairwise comparisons between control and treated groups for all genes were adjusted using the Benjamini-Hochberg method with the false discovery rate (FDR) fixed at 5%. Principal component analysis (PCA) was performed on log2-transformed fold-change data using the prcomp function in R with the default settings (R Core Team 2013) and visualized using the autoplot function in the ggplot2 package (Wickham 2016).

6.4 Results and Discussion

BPA replacements are of emerging concern due to their potential to perturb endocrine systems and other pathways. Environmental contamination of these compounds is expected to increase as BPA is being phased out, yet there is limited information on their toxicological properties (Rosenmai et al. 2014). Therefore, a rapid approach is needed to identify any potential toxicological concerns these replacement compounds may present. Ideally, any approach would also be as ethical as possible in terms of animal utilization. In the present study, we utilized the chicken hepatic cell line, LMH, cultured as spheroids, to screen five BPA replacement compounds. Results using this animal free *in vitro* screening approach were compared to those previously reported for the same five replacement compounds in another *in vitro* model that required animal use, CEH (Sharin et al. 2021a)

Two of the replacement compounds tested, DD-70 and BPAF, were more cytotoxic than BPA based on the LC50 values (Table 6.1). For BPA, the LC50 was 69.35 ± 22.85 µM, which was similar to the LC50 determined in CEH, 61.7 ± 43.1 µM (Ma et al. 2015). Among the replacement compounds, DD-70 and BPAF were the most cytotoxic with LC50 values of 17.23 ± 4.51 and 16.6 ± 4.78 µM, respectively. TGSH had a LC50 value of 57.27 ± 11.70 µM, and the two other replacement compounds included in this study, BPSIP and BPF, had LC50 values of

76.24 ± 24.89 and 81.84 ± 23.92 µM, respectively. BPF was more cytotoxic in LMH spheroids than in CEH (LC50 >300 µM) and the cytotoxicity of TGSH, BPSIP and BPF were similar to BPA. The rank order of the chemicals evaluated in the present study based on LC50 was BPAF ~DD-70 >TGSH ~BPA ~BPSIP ~BPF. BPAF and BPF were one of the most and least cytotoxic, respectively, among several BPA replacement compounds screened in various cell lines (Liu et al. 2020; Russo et al. 2018; Goldinger et al. 2015). No other cell viability data exist for TSGH or DD-70. BPSIP was found to have similar cytotoxicity as BPA in H295R adrenocortical cell line (Goldinger et al. 2015). The LC50 values of BPA (69.35 µM) and BPSIP (76.24 µM) were also similar in LMH spheroids in the present study.

Table 6.1. Common name, CASRN, LC50 (μM) ± SEM and structure of bisphenol A and five bisphenol A replacement compounds.

Common Name	CASRN	LC50 (μM) ± SEM	Structure
Bisphenol A (BPA)	80-05-7	69.35 ± 22.85	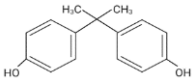
Bisphenol F (BPF)	620-92-8	81.84 ± 23.92	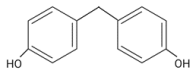
TGSA/TGSH	41481-66-7	57.27 ± 11.70	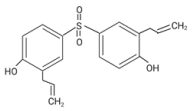
DD-70	93589-69-6	17.23 ± 4.51	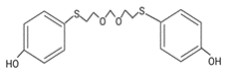
Bisphenol AF (BPAF)	1478-61-1	16.6 ± 4.78	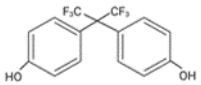
BPSIP/D-8	95235-30-6	76.24 ± 24.89	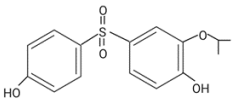

The expression of ToxChip and AestroChip genes in LMH spheroids were combined and reduced to two principal components using PCA (Figure 6.1A). The first principal component (PC1) accounted for 40.5% of the variability and PC2 explained 21.5% of the variability among samples. The key contributors to PC1 were the Aestrochip genes, APO and VTG2, while PC2 clustering was based on ToxChip and AestroChip genes including CYP1A and CPT1A.

Similarly, PCA of combined ToxChip and AestroChip gene expression in CEH showed that PC1 was mainly based on VTG2 and APO, whereas ToxChip genes explained PC2 variability (Figure 6.1B) (Sharin et al. 2021a). In LHM spheroids, BPAF and BPF clustered closely with E2 along PC1, suggesting that that these two compounds may have estrogenic properties. TGSH and DD-70 separated furthest from the DMSO controls along PC2 in LMH spheroids, suggesting non-estrogenic toxicity. In comparison to CEH, BPAF did not cluster with E2, but rather separated along PC2 with TGSH and DD-70. BPF clustered towards E2 in CEH, but not as strongly as in LMH. BPSIP clustered in a similar manner in LMH spheroids and CEH, somewhere in between DMSO controls and E2 along PC1, indicating modest estrogenicity in both models. BPA was more transcriptionally active in LMH spheroids compared to CEH, but was still closest to the DMSO control. This is an important consistency because the more transcriptionally responsive chemicals are those that could potentially replace BPA in various applications.

The modulation of AestroChip genes by BPA and the replacement compounds was greater in LMH spheroids than in CEH. The rank order of dysregulation of APO and VTG2 expression in LMH spheroids was: E2 (6.98 and 6.68-log2), BPAF (6.36 and 4.41-log2), BPF (5.76 and 4.18-log2), BPSIP (3.21 and 3.74-log2), BPA (2.29 and 3.76-log2) and DD-70 (no change and 2.56-log2) (Table S6.4). In CEH, VTG2 was down regulated by BPAF (-2.9 log2) and BPA (-2.8 log2). None of the other replacement compounds altered the expression of VTG2 in CEH (Sharin et al. 2021a). For the preparation of CEH cultures, livers from females and males were pooled, and the evaluation of VTG2 expression in this mixed sex pool could help explain the discrepancy in VTG2 expression between CEH and LMH spheroids. The increased sensitivity of the LMH spheroids to estrogen-responsive genes compared to CEH is likely due to fact that the LMH cell line was established from a male liver. Males are typically more

vulnerable to the adverse effects of xenoestrogens and the induction of estrogen responsive genes (e.g. VTG) are more evident since the basal expression of these genes are low in adult males (Matozzo et al. 2008).

Several BPA replacement compounds had gene expression profiles in LMH that were more similar to E2 compared to BPA. Specifically, BPAF, BPF and BPSIP all had stronger VTG2 and APO induction than BPA. VTG2, a marker of endocrine disruption, is synthesized by the liver in response to estrogen (Woods and Kumar 2011). APO is an egg yolk protein and lipoprotein lipase inhibitor involved in preventing the breakdown of very low-density lipoproteins (Bourin et al. 2012). VTG2 and APO are established markers of xenoestrogen exposure in oviparous species (Li et al. 2020; Heppell et al. 1995) and were the most responsive AestroChip genes for the PCA analysis (Figure 6.1A). Similar to the current study, BPAF was more estrogenic than BPF and BPA in zebrafish embryo-larvae (Moreman et al. 2017) and increased VTG expression in zebrafish liver (Yang et al. 2014). Other studies have found BPAF to be more estrogenic than BPA in several cell lines (Russo et al. 2018; Chen et al. 2016; Fic et al. 2014). BPF exposure resulted in the upregulation of vitellogenin (concordant with the findings in LMH cells in the present study) and aromatase (CYP19A1B) via estrogen receptor binding in zebrafish (LeFol et al. 2017; Cano-Nicolau et al. 2016). TGSH had no significant estrogen receptor binding in reporter gene assays and did not change VTG2 expression in chickens (Bjornsdotter et al. 2017; Crump et al. 2017). Similarly, DD-70 did not bind to the estrogen receptor in reporter gene assays (Keminer et al. 2020). BPSIP was found to alter estradiol concentrations in the human H295R cell line, although it was less estrogenic than BPA (Goldinger et al. 2015; Bjornsdotter et al. 2017). The overall ranking of the compounds on the

AestroChip in terms of VTG2 and APO modulation was: E2 > BPAF >BPF >BPSIP >BPA >DD-70 >TGSH (Table S6.4).

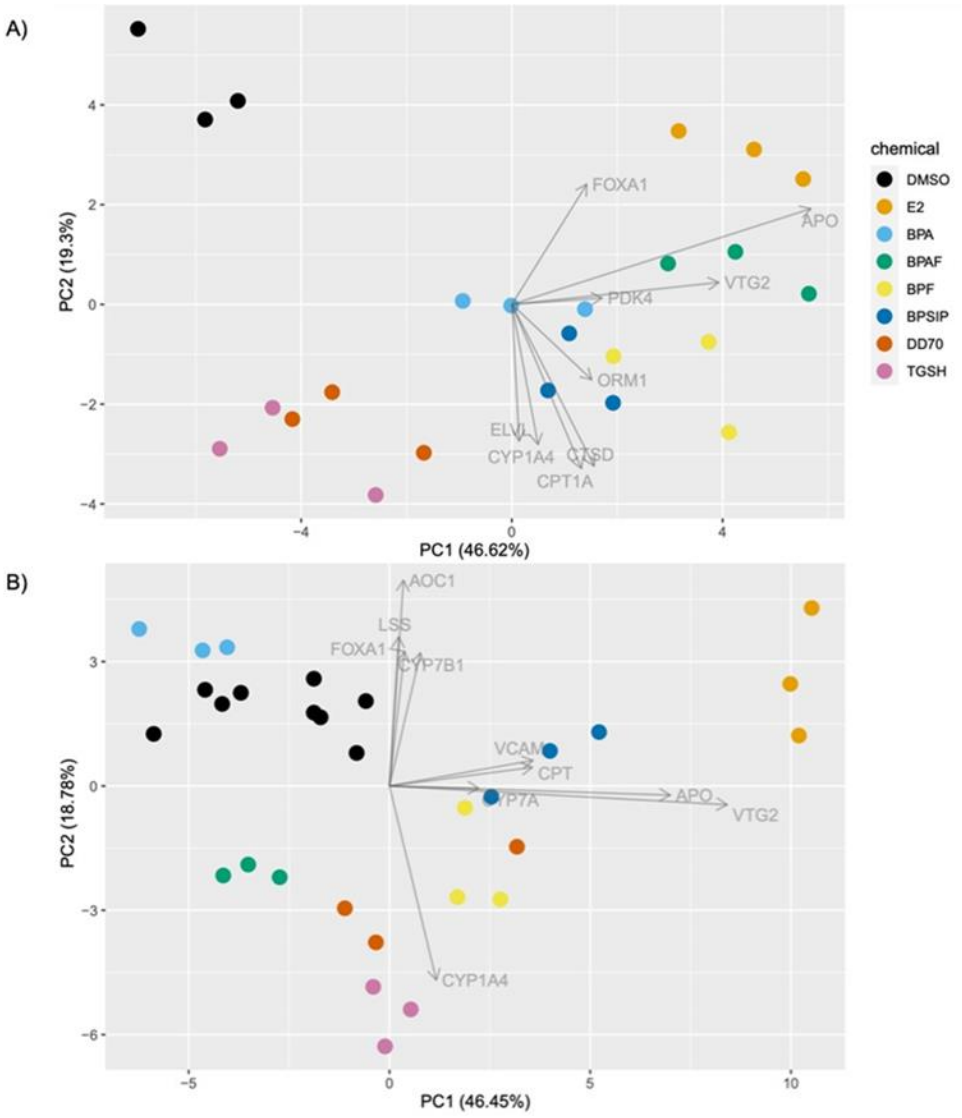

Figure 6.1. Principal component analysis of significant genes on the ToxChip and AestroChip arrays in A) LMH 3D spheroids and B) CEH following exposure to BPA, BPA replacement compounds (BPF, TGSH, DD-70, BPAF and BPSIP), and 17β estradiol (E2). Data are coloured by chemical. Gene loadings for the most responsive transcripts are depicted by arrows on the graph. CEH data are from Sharin et al. (2021a).

In general, all of the compounds led to fewer dysregulated genes on the ToxChip array compared to the AestroChip array in LMH spheroids suggesting that the compounds have minor effects on non-estrogenic pathways. TGSH, DD-70 and BPSIP altered the most genes on the ToxChip array and the expression of CYP1A4 was upregulated by all five replacement compounds, similar to the results in CEH (Sharin et al. 2021a). In the human hepatic cell line, HepG2, BPF and BPAF upregulated the expression of CYP1A1 (Hercog et al. 2019). The transcription of CYP1A4 is regulated by AhR, and therefore, the five replacement compounds are possible AhR agonists (Monostory et al. 2009). The limited response of ToxChip genes in LMH spheroids compared to CEH could be related to developmental stage. That is, CEH are cultured from embryonic livers and developing organs are more vulnerable to chemical toxicity compared to adults (Barton et al. 2005); the LMH cell line was established from an adult. The toxicity of the compounds on the ToxChip in LMH cells cultured as 2D monolayers needs to be investigated in order to determine if the discrepancy in chemical response could be due to different culture conditions. The rank order of the replacement compounds based on number of genes altered on the ToxChip was: DD-70 >TGSH =BPSIP >BPF >BPAF =BPA >E2. The fold changes of genes on the ToxChip array by all of the compounds are in Table S6.5.

DD-70 and BPAF were chosen for further concentration-dependent gene expression analysis using the ComboChip array (Figure 6.2; Table S6.3). DD-70 was selected because it was one of the most cytotoxic replacements, yet appeared to have a non-estrogenic mode of action, based on our clustering results. Moreover, there is very little toxicity data available for DD-70. BPAF was selected due to its high cytotoxicity and because it was more estrogenic than BPA based on our LMH clustering results and in other studies (Russo et al. 2018; Chen et al. 2016; Fic et al. 2014). The genes selected for the array were those that were most dysregulated

from both arrays in CEH. Both DD-70 and BPAF upregulated the expression of CYP1A4, CYP7A1, SCD and POLB (Figure 6.2; Table S6.6). Both compounds upregulated CYP1A4 at an administered concentration of 1 µM, which was sustained at 10 µM on the ToxChip array. Cholesterol 7α-hydroxylase (CYP7A) is the rate-limiting enzyme in bile acid synthesis (Jelinek et al. 1990) and stearoyl-CoA desaturase (SCD) is involved in the synthesis of monounsaturated fatty acids (Piccinin et al. 2019). Another replacement compound, BPS, upregulated the hepatic expression of CYP7B1, which is involved in the alternative pathway of bile acid synthesis in chickens (Crump et al. 2016). In previous studies, BPAF upregulated the expression of SCD and other lipid metabolism genes in HepG2 and 3T3-L1cells (Liu et al. 2020; Skeledar et al. 2015). Polymerase β (POLB) is involved in base excision repair by incorporating the correct base at the site of single stranded breaks (Martin et al. 2010). BPAF (30 µM) induced DNA double strand breaks, upregulated the expression of cell cycle genes, CDKN1A and GADD45, in HepG2 cells (Hercog et al. 2019), and induced single strand breaks at 3 nM in peripheral blood mononuclear cells (Mokra et al. 2017). DD-70 did not change the expression of the estrogen-responsive genes, APO and VTG2, at the doses included on the ComboChip array corroborating results in CEH. Two genes were upregulated solely by DD-70 following evaluation with the ComboChip: FGF19 and FOXA1 (Figure 6.2B; Table S6.6). These gene targets are involved in maintaining bile acid homeostasis (Schumacher and Guo 2019) and bile duct development (Bernado and Keri 2012). Such dysregulation is consistent with another study that found an increase in FGF19 expression in livers of chicken embryos exposed to DD-70 via egg injection (Sharin et al. 2021b). Overall, DD-70 and BPAF exposure may lead to disruption of bile acid and lipid regulation; however further studies are wanrranted to evaluate this.

Specific to BPAF, we observed concentration-dependent increases in APO and CTSD expression starting at 0.01 and 0.1 μM, respectively, while no change in VTG2 expression was observed (Figure 6.2A). On the AestroChip array, 10 μM BPAF upregulated the expression of APO, CTSD and VTG2; therefore in the concentration-dependent study, the threshold concentration for induction of VTG2 by BPAF was not achieved. BPAF strongly binds to both estrogen receptors α (ERα) and β (ERβ), with binding potencies 20 and 48 times greater than BPA (Matsushima et al. 2010). Cathepsin D (CTSD) is a protease that cleaves proteins to activate and deactivate enzymes (Benes et al. 2009) and its expression is mediated by estrogen (Bretschneider et al. 2008). Similar to LMH spheroids, BPAF upregulated CTSD expression in a concentration-dependent (0.01 to 10 μM) manner in the MCF-7 cell line (Li et al. 2014). Overall, BPAF induced estrogen responsive genes in LMH spheroids, while DD-70 was not estrogenic at these lower concentrations evaluated.

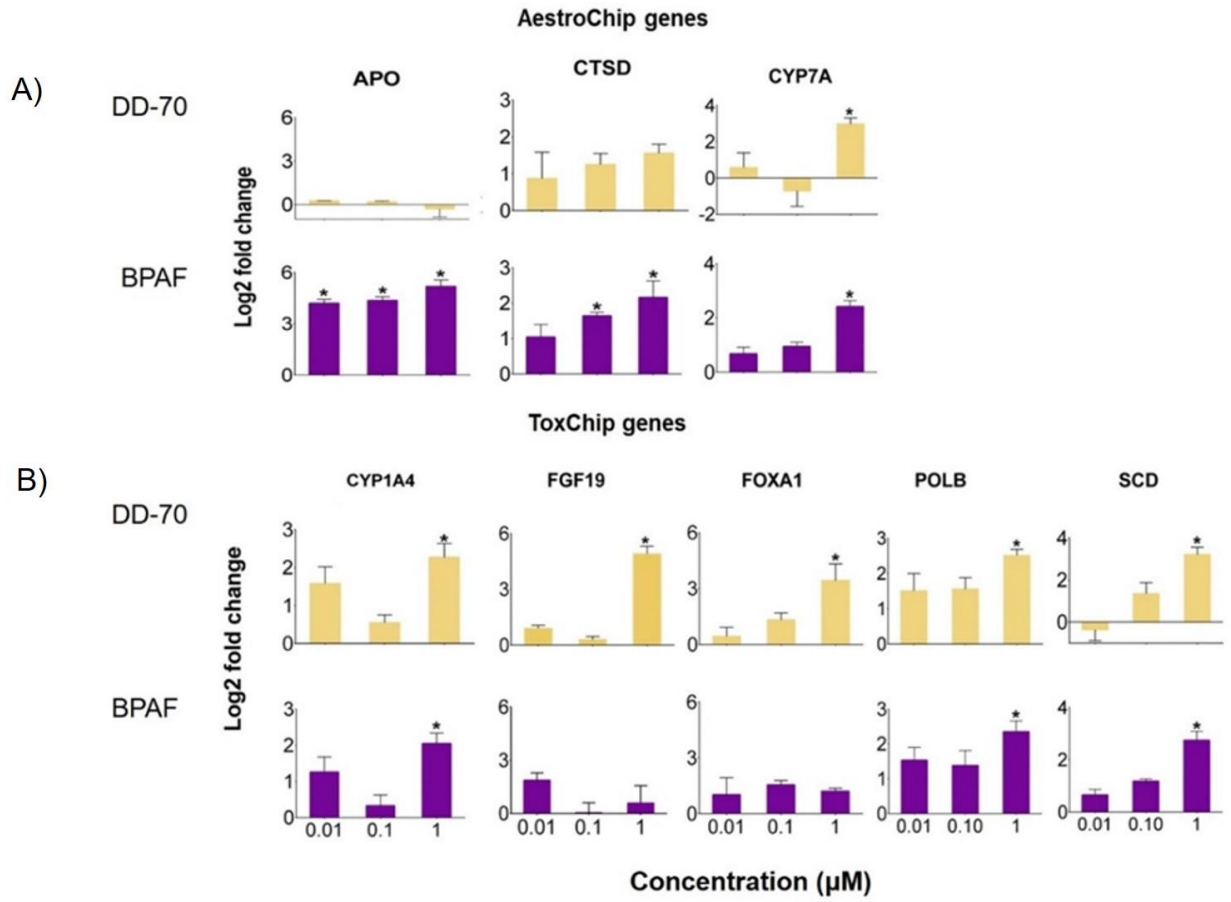

Figure 6.2. Concentration-dependent fold change (log2) in significant expression of selected A) AestroChip and B) ToxChip genes following exposure to DD-70 or BPAF for 24h in LMH spheroids. "*" denotes difference compared to untreated cells.

The use of LMH spheroids permitted a concentration-dependent analysis of DD-70 and BPAF effects, an approach that would have been more logistically challenging with CEH due to the time-consuming nature of the culture and limited availability of primary hepatocytes for a single study. On the ToxChip, DD-70 and BPAF (10 µM) altered 3 and 0 genes related to bile acid and lipid homeostasis, respectively. In contrast, 7 and 3 genes from the same pathways were modulated by DD-70 and BPAF (10 µM) in CEH. At lower doses, the expression of genes associated with this pathway on the ComboChip array were altered, indicating that bile and lipid

genes are modulated by DD-70 and especially BPAF. The results from the ComboChip array emphasize the importance of concentration-dependent analysis in terms of gene expression as some genes were modulated at low doses, while other genes like VTG2 were altered at a higher dose. This dynamic gene expression response, which is reliant on dose, highlights the importance of future studies that incorporate concentration-dependant gene expression analysis when trying to determine the mechanism of action of chemicals and gene expression points of departure.

In summary, the ranking of the five replacement compounds in terms of cytotoxicity was similar in LMH spheroids and CEH. In terms of gene expression, the replacement compounds upregulated CYP1A expression in both models. TGSH and DD-70 were non-estrogenic compared to the other replacements, while BPAF was the most estrogenic replacement based on the gene expression endpoints measured in LMH spheroids. In LMH spheroids, gene alterations on the AestroChip array were more pronounced than in CEH suggesting that LMH may be a more sensitive model for detecting estrogenic activity. The concentration-dependent analysis revealed that DD-70 and BPAF modulated the expression of genes related to bile acid and lipid metabolism pathways. Overall, LMH spheroids represent a useful, animal free model for screening xenoestrogens and a suitable alternative to CEH for avian toxicity testing.

Acknowledgements

This work was supported by funds from three sources within Environment and Climate Change Canada: 1) Chemicals Management Plan (CMP); 2) Strategic Technology Applications of Genomics for the Environment (STAGE); and 3) the Ecotoxicology and Wildlife Health Division.

6.5 References

Barton HA, Cogliano VJ, Flowers L, Valcovic L, Setzer RW, Woodruff TJ. 2005. Assessing susceptibility from early-life exposure to carcinogens. *Environmental Health Perspectives* 113:1125-1133. DOI: 10.1289/ehp.7667.

Benes P, Vetvicka V, Fusek M. 2008. Cathepsin D-Many functions of one aspartic protease. *Critical Reviews in Oncology Hematology* 68:12-28. DOI: 10.1016/j.critrevonc.2008.02.008.

Bernardo GM, Keri RA. 2012. FOXA1: a transcription factor with parallel functions in development and cancer. *Bioscience Reports* 32:113-130. DOI: 10.1042/bsr20110046.

Bjornsdotter MK, Jonker W, Legradi J, Kool J, Ballesteros-Gomez A. 2017. Bisphenol A alternatives in thermal paper from the Netherlands, Spain, Sweden and Norway. Screening and potential toxicity. *Science of the Total Environment* 601:210-221. DOI: 10.1016/j.scitotenv.2017.05.171.

Bourin M, Gautron J, Berges M, Hennequet-Antier C, Cabau C, Nys Y, Rehault-Godbert S. 2012. Transcriptomic profiling of proteases and antiproteases in the liver of sexually mature hens in relation to vitellogenesis. *Bmc Genomics* 13. DOI: 10.1186/1471-2164-13-457.

Breslin S, O'Driscoll L. 2013. Three-dimensional cell culture: the missing link in drug discovery. *Drug Discovery Today* 18:240-249. DOI: 10.1016/j.drudis.2012.10.003.

Bretschneider N, Kangaspeska S, Seifert M, Reid G, Gannon F, Denger S. 2008. E2-mediated cathepsin D (CTSD) activation involves looping of distal enhancer elements. *Molecular Oncology* 2:182-190. DOI: 10.1016/j.molonc.2008.05.004.

Chen D, Kannan K, Tan HL, Zheng ZG, Feng YL, Wu Y, Widelka M. 2016. Bisphenol Analogues Other Than BPA: Environmental Occurrence, Human Exposure, and Toxicity-A Review. *Environmental Science & Technology* 50:5438-5453. DOI: 10.1021/acs.est.5b05387.

Crump D, Chiu S, Williams KL. 2016. Bisphenol A alters embryonic viability, development, gallbladder size, and messenger RNA expression in chicken embryos exposed via egg injection.. *Environmental Toxicology and Chemistry* 35:1541-1549. DOI: 10.1002/etc.3313.

Crump D, Chiu S, Williams KL. 2018. Bis-(3-allyl-4-hydroxyphenyl) Sulfone Decreases Embryonic Viability and Alters Hepatic mRNA Expression at Two Distinct Developmental Stages in Chicken Embryos Exposed Via Egg Injection. *Environmental Toxicology and Chemistry* 37:530-537. DOI: 10.1002/etc.3990.

Dix DJ, Houck KA, Martin MT, Richard AM, Setzer RW, Kavlock RJ. 2007. The ToxCast program for prioritizing toxicity testing of environmental chemicals. *Toxicological Sciences* 95:5-12. DOI: 10.1093/toxsci/kfl103.

ECHA. 2020. Bisphenol S has replaced bisphenol A in thermal paper.

Fic A, Zegura B, Gramec D, Masic LP. 2014. Estrogenic and androgenic activities of TBBA and TBMEPH, metabolites of novel brominated flame retardants, and selected bisphenols, using the XenoScreen XL YES/YAS assay. *Chemosphere* 112:362-369. DOI: 10.1016/j.chemosphere.2014.04.080.

Fraczek J, Bolleyn J, Vanhaecke T, Rogiers V, Vinken M. 2013. Primary hepatocyte cultures for pharmaco-toxicological studies: at the busy crossroad of various anti-dedifferentiation strategies. *Archives of Toxicology* 87:577-610. DOI: 10.1007/s00204-012-0983-3.

Frohlich E. 2018. Comparison of conventional and advanced in vitro models in the toxicity testing of nanoparticles. *Artificial Cells Nanomedicine and Biotechnology* 46:1091-1107. DOI: 10.1080/21691401.2018.1479709.

Goldinger DM, Demierre AL, Zoller O, Rupp H, Reinhard H, Magnin R, Becker TW, Bourqui-Pittet M. 2015. Endocrine activity of alternatives to BPA found in thermal paper in Switzerland. *Regulatory Toxicology and Pharmacology* 71:453-462. DOI: 10.1016/j.yrtph.2015.01.002.

Gonzalez-Rubio S, Vike-Jonas K, Gonzalez SV, Ballesteros-Gomez A, Sonne C, Dietz R, Boertmann D, Rasmussen LM, Jaspers VLB, Asimakopoulos AG. 2020. Bioaccumulation potential of bisphenols and benzophenone UV filters: A multiresidue approach in raptor tissues. *Science of the Total Environment* 741. DOI: 10.1016/j.scitotenv.2020.140330.

Hellwig C, Barenys M, Baumann J, Gassmann K, Casanellas L, Kauer G, Fritsche E. 2018. Culture of human neurospheres in 3D scaffolds for developmental neurotoxicity testing. *Toxicology in Vitro* 52:106-115. DOI: 10.1016/j.tiv.2018.06.002.

Heppell SA, Denslow ND, Folmar LC, Sullivan CV. 1995. Universal assay of vitellogenin as a biomarker for environmental estrogens. *Environmental Health Perspectives* 103:9-15. DOI: 10.2307/3432500.

Hercog K, Maisanaba S, Filipic M, Sollner-Dolenc M, Kac L, Zegura B. 2019. Genotoxic activity of bisphenol A and its analogues bisphenol S, bisphenol F and bisphenol AF and their mixtures in human hepatocellular carcinoma (HepG2) cells. *Science of the Total Environment* 687:267-276. DOI: 10.1016/j.scitotenv.2019.05.486.

Jelinek DF, Andersson S, Slaughter CA, Russell DW. 1990. Cloning and regulation of cholesterol 7-alpha hydroxylase, the rate-limiting enzyme in bile acid synthesis. *Journal of Biological Chemistry* 265:8190-8197.

Keminer O, Teigeler M, Kohler M, Wenzel A, Arning J, Kassner F, Windshugel B, Eilebrecht E. 2020. A tiered high-throughput screening approach for evaluation of estrogen and androgen receptor modulation by environmentally relevant bisphenol A substitutes. *Science of the Total Environment* 717. DOI: 10.1016/j.scitotenv.2019.134743.

Kitamura S, Suzuki T, Sanoh S, Kohta R, Jinno N, Sugihara K, Yoshihara S, Fujimoto N, Watanabe H, Ohta S. 2005. Comparative study of the endocrine-disrupting activity of bisphenol A and 19 related compounds. *Toxicological Sciences* 84:249-259. DOI: 10.1093/toxsci/kfi074.

Krewski D, Andersen ME, Mantus E, Zeise L. 2009. Toxicity Testing in the 21st Century: Implications for Human Health Risk Assessment. *Risk Analysis* 29:474-479. DOI: 10.1111/j.1539-6924.2008.01150.x.

Le Fol V, Ait-Aissa S, Sonavane M, Porcher JM, Balaguer P, Cravedi JP, Zalko D, Brion F. 2017. In vitro and in vivo estrogenic activity of BPA, BPF and BPS in zebrafish-specific assays. *Ecotoxicology and Environmental Safety* 142:150-156. DOI: 10.1016/j.ecoenv.2017.04.009.

Lee J, Park NY, Kho Y, Ji K. 2018. Effects of 4-Hydroxyphenyl 4-Isoprooxyphenylsulfone (BPSIP) Exposure on Reproduction and Endocrine System of Zebrafish. *Environmental Science & Technology* 52:1506-1513. DOI: 10.1021/acs.est.7b00498.

Li MC, Gao XN, Tan L, Miao YF, Fan WT, Gao ZS, Liu SH, Ding CC, Shi XZ, Song SQ. 2020. Effects of bisphenol A at the safe reference dose on abdominal fat deposition in aged hens. *Ecotoxicology and Environmental Safety* 206. DOI: 10.1016/j.ecoenv.2020.111398.

Liu Q, Shao WT, Weng ZK, Zhang X, Ding GP, Xu C, Xu J, Jiang ZY, Gu AH. 2020. In vitro evaluation of the hepatic lipid accumulation of bisphenol analogs: A high-content screening assay. *Toxicology in Vitro* 68. DOI: 10.1016/j.tiv.2020.104959.

Ma M, Crump D, Farmahin R, Kennedy SW. 2015. Comparing the effects of tetrabromobisphenol-a, bisphenol a, and their potential alternatives, TBBPA-bis (2,3-dibromopropyl ether) and bisphenol s on cell viability and messenger ribonucleic acid expression in chicken embryonic hepatocytes. *Environmental Toxicology and Chemistry* 34:391-401. DOI: 10.1002/etc.2814

Martin SA, McCabe N, Mullarkey M, Cummins R, Burgess DJ, Nakabeppu Y, Oka S, Kay E, Lord CJ, Ashworth A. 2010. DNA Polymerases as Potential Therapeutic Targets for Cancers Deficient in the DNA Mismatch Repair Proteins MSH2 or MLH1. *Cancer Cell* 17:235-248. DOI: 10.1016/j.ccr.2009.12.046.

Matsushima A, Liu XH, Okada H, Shimohigashi M, Shimohigashi Y. 2010. Bisphenol AF Is a Full Agonist for the Estrogen Receptor ER alpha but a Highly Specific Antagonist for ER beta. *Environmental Health Perspectives* 118:1267-1272. DOI: 10.1289/ehp.0901819.

Matozzo V, Gagne F, Marin MG, Ricciardi F, Blaise C. 2008. Vitellogenin as a biomarker of exposure to estrogenic compounds in aquatic invertebrates: A review. *Environment International* 34:531-545. DOI: 10.1016/j.envint.2007.09.008.

Mokra K, Kuzminska-Surowaniec A, Wozniak K, Michalowicz J. 2017. Evaluation of DNA-damaging potential of bisphenol A and its selected analogs in human peripheral blood

mononuclear cells (in vitro study). *Food and Chemical Toxicology* 100:62-69. DOI: 10.1016/j.fct.2016.12.003.

Monostory K, Pascussi JM, Kobori L, Dvorak Z. 2009. Hormonal regulation of CYP1A expression. *Drug Metabolism Reviews* 41:547-572. DOI: 10.1080/03602530903112284.

Mu XY, Huang Y, Li XX, Lei YL, Teng MM, Li XF, Wang CJ, Li YR. 2018. Developmental Effects and Estrogenicity of Bisphenol A Alternatives in a Zebrafish Embryo Model. *Environmental Science & Technology* 52:3222-3231. DOI: 10.1021/acs.est.7b06255.

Mundy LJ, Williams KL, Chiu S, Pauli BD, Crump D. 2019. Extracts of Passive Samplers Deployed in Variably Contaminated Wetlands in the Athabasca Oil Sands Region Elicit Biochemical and Transcriptomic Effects in Avian Hepatocytes. *Environmental Science & Technology* 53:9192-9202. DOI: 10.1021/acs.est.9b02066.

Ourlin JC, Baader M, Fraser D, Halpert JR, Meyer UA. 2000. Cloning and functional expression of a first inducible avian cytochrome P450 of the CYP3A subfamily (CYP3A37). *Archives of Biochemistry and Biophysics* 373:375-384. DOI: 10.1006/abbi.1999.1566.

Piccinin E, Cariello M, De Santis S, Ducheix S, Sabba C, Ntambi JM, Moschetta A. 2019. Role of Oleic Acid in the Gut-Liver Axis: From Diet to the Regulation of Its Synthesis via Stearoyl-CoA Desaturase 1 (SCD1). *Nutrients* 11. DOI: 10.3390/nu11102283.

Porter E, Crump D, Egloff C, Chiu S, Kennedy SW. 2014. Use of an avian hepatocyte assay and the avian toxchip polymerse chain reaction array for testing prioritization of 16 organic flame retardants. *Environmental Toxicology and Chemistry* 33:573-582. DOI: 10.1002/etc.2469.

Ramaiahgari SC, den Braver MW, Herpers B, Terpstra V, Commandeur JNM, van de Water B, Price LS. 2014. A 3D in vitro model of differentiated HepG2 cell spheroids with improved liver-like properties for repeated dose high-throughput toxicity studies. *Archives of Toxicology* 88:1083-1095. DOI: 10.1007/s00204-014-1215-9.

Rosenmai AK, Dybdahl M, Pedersen M, van Vugt-Lussenburg BMA, Wedebye EB, Taxvig C, Vinggaard AM. 2014. Are Structural Analogues to Bisphenol A Safe Alternatives? *Toxicological Sciences* 139:35-47. DOI: 10.1093/toxsci/kfu030.

Russo G, Capuozzo A, Barbato F, Irace C, Santamaria R, Grumetto L. 2018. Cytotoxicity of seven bisphenol analogues compared to bisphenol A and relationships with membrane affinity data. *Chemosphere* 201:432-440. DOI: 10.1016/j.chemosphere.2018.03.014.

Schmittgen TD, Livak KJ. 2008. Analyzing real-time PCR data by the comparative C-T method. *Nature Protocols* 3:1101-1108. DOI: 10.1038/nprot.2008.73.

Schumacher JD, Guo GL. 2016. Regulation of Hepatic Stellate Cells and Fibrogenesis by Fibroblast Growth Factors. *Biomed Research International* 2016. DOI: 10.1155/2016/8323747.

Sharin T, Crump D, O'Brien JM. 2020. Evaluation of the Aryl Hydrocarbon Receptor Response in LMH 3D Spheroids. *Environmental Toxicology and Chemistry* 39:1693-1701. DOI: 10.1002/etc.4783.

Sharin T, Williams KL, Chiu S, Crump D, O'Brien JM. 2021a. Toxicity Screening of Bisphenol A Replacement Compounds: Cytotoxicity and mRNA Expression in Primary Hepatocytes of Chicken and Double-Crested Cormorant. *Environmental Toxicology and Chemistry* 40(5):1368-1378. DOI: 10.1002/etc.4985

Sharin T, Gyasi H, Williams KL, Crump D, O'Brien JM. 2021b. Effects of DD-70 and BPAF on mRNA Expression and Developmental Toxicity in Chicken Embryos. *Ecotoxicology and Environmental Safety 2021,* 215(Suppl 1):112140. DOI:10.1016/j.ecoenv.2021.112140

Siracusa JS, Yin L, Measel E, Liang SX, Yu XZ. 2018. Effects of bisphenol A and its analogs on reproductive health: A mini review. *Reproductive Toxicology* 79:96-123. DOI: 10.1016/j.reprotox.2018.06.005.

Song MY, Liang D, Liang Y, Chen MJ, Wang FB, Wang HL, Jiang GB. 2014. Assessing developmental toxicity and estrogenic activity of halogenated bisphenol A on zebrafish (Danio rerio). *Chemosphere* 112:275-281. DOI: 10.1016/j.chemosphere.2014.04.084.

Song SJ, Ruan T, Wang T, Liu RZ, Jiang GB. 2012. Distribution and Preliminary Exposure Assessment of Bisphenol AF (BPAF) in Various Environmental Matrices around a Manufacturing Plant in China. *Environmental Science & Technology* 46:13136-13143. DOI: 10.1021/es303960k.

Takahashi Y, Hori Y, Yamamoto T, Urashima T, Ohara Y, Tanaka H. 2015. 3D spheroid cultures improve the metabolic gene expression profiles of HepaRG cells. *Bioscience Reports* 35. DOI: 10.1042/bsr20150034.

Woods M, Kumar A. 2011. Vitellogenin induction by 17 beta-estradiol and 17 alpha-ethynylestradiol in male murray rainbow fish (Melanotaenia fluviatilis). *Environmental Toxicology and Chemistry* 30:2620-2627. DOI: 10.1002/etc.660.

Yamaguchi A, Ishibashi H, Arizono K, Tominaga N. 2015. In vivo and in silico analyses of estrogenic potential of bisphenol analogs in medaka (Oryzias latipes) and common carp (Cyprinus carpio). *Ecotoxicology and Environmental Safety* 120:198-205. DOI: 10.1016/j.ecoenv.2015.06.014.

Yamazaki E, Yamashita N, Taniyasu S, Lam J, Lam PKS, Moon HB, Jeong Y, Kannan P, Achyuthan H, Munuswamy N, Kannan K. 2015. Bisphenol A and other bisphenol analogues including BPS and BPF in surface water samples from Japan, China, Korea and India. *Ecotoxicology and Environmental Safety* 122:565-572. DOI: 10.1016/j.ecoenv.2015.09.029.

Yang XX, Liu YC, Li J, Chen MJ, Peng D, Liang Y, Song MY, Zhang J, Jiang GB. 2016. Exposure to Bisphenol AF disrupts sex hormone levels and vitellogenin expression in zebrafish. *Environmental Toxicology* 31:285-294. DOI: 10.1002/tox.22043.

Yang YJ, Guan J, Yin J, Shao B, Li H. 2014. Urinary levels of bisphenol analogues in residents living near a manufacturing plant in south China. *Chemosphere* 112:481-486. DOI: 10.1016/j.chemosphere.2014.05.004.

Chapter 7: Effects of DD-70 and BPAF on mRNA Expression and Developmental Toxicity in Chicken Embryos

Modified from: Sharin T, Gyasi H, Williams KL, Crump D, O'Brien JM. 2021. *Ecotoxicology and Environmental Safety* 215:112140. DOI: 10.1016/j.ecoenv.2021.112140.

7.1 Abstract

Concerns about the estrogenic properties of Bisphenol A (BPA) have led to increased efforts to find BPA replacements. 1,7-bis(4-Hydroxyphenylthio)-3,5-dioxaheptane (DD-70) and 4,4′-(Hexafluoroisopropylidene) diphenol (bisphenol AF, BPAF) are two potential chemical substitutes for BPA; however, toxicity data of these chemicals in avian species is limited. To determine effects on avian embryonic viability, development, and hepatic mRNA expression at two distinct developmental periods (mid-incubation [day 11] and term [day 20]), two egg injection studies were performed. Test chemicals were injected into the air cell of unincubated, fertilized chicken eggs at concentrations ranging from 0 to 88.2 µg/g for DD-70 and 0 to 114 µg/g egg for BPAF. Embryonic concentrations of DD-70 and BPAF decreased at mid-incubation and term compared to injected concentrations suggesting embryonic metabolism. Exposure to DD-70 (40.9 and 88.2 µg/g) and BPAF (114 µg/g) significantly decreased embryonic viability at mid-incubation. Exposure to DD-70 (88.2 µg/g) decreased embryo mass and increased gallbladder mass, while 114 µg/g BPAF resulted in increased gallbladder mass in term embryos. Expression of hepatic genes related to xenobiotic metabolism, lipid homeostasis, and response to estrogen were altered at both developmental stages. Given the importance of identifying suitable BPA replacements, the present study provides novel, whole animal avian toxicological data for two replacement compounds, DD-70 and BPAF.

7.2 Introduction

Bisphenol A (BPA), a highly produced chemical used in the production of polycarbonate plastics and epoxy resins (Rubin 2011), can be found ubiquitously within the environment. It has been detected in surface water and sediments (Liao et al. 2012) and in wildlife, including top predators like birds (Nakayama et al. 2006). BPA exposure is associated with cardiovascular problems, diabetes (Ranciere et al. 2015), neurological disruption (Yeo et al. 2013), and reproductive dysfunction (Tomza-Marciniak et al. 2018). In birds, embryonic BPA exposure causes ovary malformations in females, and ovotestes in males (Berg et al. 2001; Jessl et al. 2018). The phenolic structure of BPA as well as *in vivo* and *in vitro* evidence demonstrating interference with estrogen (Andersen et al. 1999), androgen (Teng et al. 2013), and thyroid hormone (Moriyama et al. 2002) receptors highlight its endocrine disrupting potential. As a result, the use of BPA in baby products was banned in Canada in 2010 and the European Union in 2011 (Flint et al. 2012) and several countries have restricted the use of BPA in other consumer products (Bjornsdotter et al. 2017). Accordingly, the use of BPA replacement compounds has increased in recent years in order to manufacture BPA-free products.

BPA replacement compounds are structural analogs of BPA (Pelch et al. 2017). Being similar in structure to BPA makes them suitable for use in polycarbonate plastics and resins (Chen et al. 2016). However, as structural analogs, these compounds have the potential to have similar toxicity profiles as BPA (Rochester and Bolden, 2015). Replacement compounds have been detected in sediments, indoor dust, and rivers (Liao et al 2012). These compounds are commonly found in plastic products, canned food and beverages, and thermal papers (Rosenmai et al. 2014). However, there is scarce information on the toxicological properties of these compounds, especially for avian species. Bisphenol A replacement compounds such as bisphenol

S (BPS) and bisphenol F (BPF) have been shown to induce the expression of estrogen responsive genes both *in vitro* (Richter et al. 2007; Mesnage et al. 2017) and *in vivo* (Yamaguchi et al. 2015; Cano-Nicolau et al. 2016). In a comparative study of the endocrine-disrupting activity of bisphenol A and 19 related compounds, several BPA alternatives altered additional endocrine-related pathways (Kitamura et al. 2005). A previous study in our lab found that BPS exposure affected growth, pipping success, and gallbladder length in chicken embryos (Crump et al. 2016a). Another replacement compound, bis-(3-allyl-4-hydroxyphenyl) sulfone (TGSH), altered the hepatic expression of genes related to lipid homeostasis and xenobiotic metabolism, and had similar effects on chicken embryonic viability as BPA (Crump et al. 2018). Given these findings, identifying safer replacement compounds for BPA is essential given that the production of such alternatives will increase as BPA use diminishes.

1,7-bis (4-Hydroxyphenylthio)-3, 5-dioxaheptane (DD-70) and 4,4'-(hexafluoroisopropylidene) diphenol (Bisphenol AF, BPAF) are two BPA replacement compounds (Table 1). DD-70 is a derivative of BPA primarily found in thermal paper (US Environmental Protection Agency 2015). To our knowledge, no published toxicological studies exist for this chemical. BPAF is found in plastic polymers, thermal paper, electronics and fiber optics (Shi et al. 2016) and is one of more common replacement compounds in use. In a previous study, we looked at the cytotoxicity and gene expression of five BPA replacement compounds in primary hepatocytes of chicken and double-crested cormorants, and DD-70 and BPAF were the most cytotoxic in both species. Furthermore, both compounds altered the expression of genes in several pathways, including bile acid and cholesterol regulation in chicken primary hepatocytes (Sharin et al.in press). BPAF induced the expression of estrogen responsive genes in the Michigan Cancer Foundation-7 **(**MCF-7) cell line (Li et al. 2014) and bound to estrogen

receptors with higher affinity than BPA (Matsushima et al. 2010). Moreover, BPAF acts as an antagonist of androgen receptors (Perera et al. 2017) and was found to be a stronger androgen antagonist than BPA (Kitamura et al. 2005). In addition to endocrine-related disruption, exposure to BPAF resulted in delayed hatching rates and morphological malfunctions in zebrafish (Mu et al. 2018).

Due to the lack of data for DD-70 and potential endocrine disrupting properties of BPAF, these two chemicals were evaluated using an early-life stage, chicken egg injection toxicity test in the present study. Embryonic viability, growth metrics, and accumulation and metabolism of the two compounds in embryonic homogenates were investigated. Additionally, hepatic mRNA expression of genes associated with several critical toxicity pathways (including response to estrogen) were measured using customized PCR arrays. Gene expression and chemical residue analyses were evaluated at mid-incubation (day 11) and term (day 20) in order to compare the hepatic gene expression and parent compound metabolism at two distinct developmental stages. Hepatic competence is established in chicken embryos by day 7 (Sandström and Westman 1971), prior to the two stages evaluated here (i.e. day 11 and 20). The results from this study provide much needed whole-animal data on the developmental toxicity of BPA alternatives in a model avian species. Furthermore, the gene expression data can be used to elucidate potential molecular mechanisms of toxicity.

Table 7.1- Chemical Structures of Bisphenol A (BPA), 1,7-bis (4-Hydroxyphenylthio)-3,5-dioxaheptane (DD-70), and Bisphenol AF (BPAF).

Chemical name	Common name	CAS #	Molecular Structure
4,4'-(propane-2,2-diyl)diphenol	Bisphenol A (BPA)	80-05-7	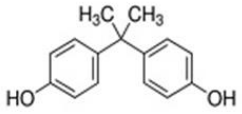
1,7-bis (4-Hydroxyphenylthio)-3,5-dioxaheptane	DD-70	93589-69-6	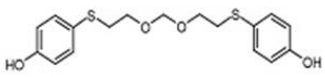
2,2-Bis (4- hydroxyphenyl) hexafluoropropane	Bisphenol AF (BPAF)	1478-61-1	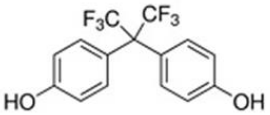

7.3 Materials and Methods

7.3.1 Chemicals and chemical analysis of DD-70 and BPAF

DD-70 (≥ 97.8% purity; CAS number 93589-69-6) was purchased from Toronto Research Chemicals and BPAF (≥ 98% purity; CAS number 1478-61-1) was purchased from Santa-Cruz Biotechnology. Stock solutions and serial dilutions were prepared in dimethyl sulfoxide (DMSO; Sigma Aldrich). The nominal concentrations of DD-70 and BPAF working solutions prepared for the study were 1, 10, 50, and 100 mg/mL dissolved in DMSO; DMSO served as the solvent control. The selected doses are comparable to those of previous chicken egg injection studies conducted with BPA (Berg et al. 2001) and other BPA replacement compounds (Crump et al. 2016a; Crump et al. 2018).

Chemical concentrations of DD-70 and BPAF dosing solutions and embryonic homogenates were determined following US Environmental Protection Agency methods 3545C (Pressurized fluid extraction) and 8321B (Solvent-extractable nonvolatile compounds by high-performance liquid chromatography/thermospray/mass spectrometry [HPLC–TS–MS] or ultraviolet [UV] detection) by Applied Technical Service. Embryonic samples were freeze-dried for 48h using a Labconco FreezeZone 6 Litre Freeze Dry System (Model 77530).Triplicate samples of freeze-dried embryonic homogenates (1 g) from the DMSO control, 10 µg/g DD-70 (nominal) and 100 µg/g BPAF (nominal) dose groups were extracted as described previously (Crump et al. 2018). Briefly samples were extracted with acetonitrile for 16 h and the method limit of detection was 0.001µg/g.

7.3.2 Egg injection, liver collection and morphological measurements

Fertilized, unincubated domestic chicken eggs (n= 211) were obtained from the Canadian Food Inspection Agency. Animal handling procedures were approved by Environment and Climate Change Canada's Wildlife Eastern Animal Care Committee. The following doses (based on the weight of the egg contents) were included for the two separate egg injection studies and chemical concentrations of the stock solutions (see chemical analysis section above) yielded the following concentrations: 1) DD-70 – DMSO control (n= 20), 1.09 µg/g (n= 20), 7.74 µg/g (n= 26), 40.9 µg/g (n= 20), and 88.2 µg/g (n= 25); and 2) BPAF (n= 20/dose group) – 0 (DMSO control), 0.56, 6.21, 54.9, and 114 µg/g. The eggs were weighed, candled, and the chemicals were injected into air cell (~1µL/g egg) based on previously described methods (Crump et al. 2016a). The eggs were incubated at 37.5°C and 60% relative humidity in a Petersime (model XI) incubator.

All embryos were candled at mid-incubation (embryonic day 11) to determine fertility/viability. Egg contents without a visible embryo or vascularization during candling were considered infertile; this was confirmed by opening the eggs and thoroughly examining the contents for any signs of development. A subset of viable embryos from all treatment groups (n = 6/group) was removed from the incubator, euthanized by decapitation, and livers from five embryos were collected for mRNA expression analysis. A single embryo, including all contents (e.g. yolk sac and shell membrane), from each dose was collected for chemical analysis. The remaining viable embryos in each treatment group were returned to the incubator until day 20, according to procedures previously described **(**Farhat et al. 2013; Crump et al. 2016a).

Morphological measurements were taken for embryos on day 20 as described previously (Crump et al. 2016a), except gallbladder mass was recorded in this study instead of gallbladder length. The left liver lobe was collected from all treatment groups (n= 5 for all groups, except 114 µg /g BPAF, where n=3) for mRNA expression analysis. Similar to day 11 embryos, the entire contents of an embryo (i.e. embryo, yolk sac and shell membrane) from each dose group were homogenized and stored in amber glass jars and sent for chemical analysis.

7.3.4 Real-time reverse transcription PCR: screening toxicity pathways & estrogenicity

The effects of DD-70 and BPAF on gene expression in chicken embryo livers were investigated at both embryonic day 11 and day 20, between the DMSO controls and high dose groups (i.e. 88.2 µg/g DD-70 and 114 µg/g BPAF). Gene expression was measured in five liver samples per group for each chemical except 114 µg/g BPAF dose group, where the sample size was 3.

Liver tissue (15-30 mg) was homogenized using the MM301 mixer mill (Retsch), total RNA was isolated using the RNeasy Mini kit (Qiagen) following manufacturer's protocol, and RNA concentration was determined using the Nanodrop 2000 (ThermoFisher Scientific). Approximately 300 ng total RNA was reverse transcribed using the QuantiTect Reverse Transcription kit (Qiagen) and the volume for each reverse transcription was 20µL. Real-time RT-PCR reactions were performed with RT^2 qPCR SYBR Green master mix (Qiagen) following manufacturer's instructions.

Two custom PCR arrays were used in the present study: 1) chicken ToxChip RT^2 Profiler PCR array (Catalogue number: CAPG13982; Qiagen); and 2) chicken Aestrochip array. The ToxChip consists of 43 genes of interest associated with nine biologically relevant pathways, 2 reference genes (EEF1A1 and RPL4), a reverse-transcription control, a genomic DNA contamination control, and a positive PCR control (Table S7.1). The Aestrochip comprises 10 estrogen responsive genes, a reference gene, EEF1A1, and a no template control (Table S7.2). The PCR thermal profile consisted of enzyme activation step at 95°C for 10 min followed by 40 cycles of 95°C for 15 s and 60°C for 1 min and final extension at 95°C for 1 min on Stratagene MX3005P qPCR system (Agilent Technologies).

7.3.5 Data analysis

Significant differences in embryonic viability at mid-incubation, and morphological measurements relative to the control (DMSO) were determined with one-way ANOVA followed by Dunnett's test ($p < 0.05$) using GraphPad Prism (Ver 6.07). Embryonic viability at term was calculated as the number of embryos that survived to day 20 after taking into account mid-incubation removal of viable and nonviable embryos and infertile eggs.

Real-time RT-PCR data were analysed using the $2^{-\Delta Ct}$ method (Schmittgen and Livak 2008). ToxChip and AestroChip array data were normalized to EEF1A1. Fold change (log2) was determined relative to the respective DMSO control group. For each gene, significant changes in expression relative to the DMSO control (≥ 2-fold; $p<0.05$) were determined by Student's t-test followed by a multiple comparison adjustment using the Bonferroni method.

7.4 Results

7.4.1 Chemical analysis of DD-70 and BPAF

Based on chemical analysis of the dosing solutions, the injected concentrations of DD-70 and BPAF were 1.09, 7.74, 40.9 and 88.2 µg/g, and 0.6, 6.21, 54.9, and 114 µg/g, respectively (Table 2). DD-70 and BPAF were below the method limit of detection (0.001 µg/g) in the DMSO control solution. Embryo homogenate concentrations of DD-70 concentrations from the 7.4 µg/g dose group were 4.04 µg/g at mid-incubation and decreased to 0.10 µg/g at term, while BPAF concentrations in the highest dose group (114 µg/g) were 93.1 µg/g at mid-incubation and decreased to 58.8 µg/g at term. The detection of both DD-70 and BPAF in embryos at mid-incubation and subsequent decreased levels in term embryos suggests embryonic uptake and subsequent metabolism/degradation (Table 7.2).

Table 7.2. Injected and embryo homogenate concentrations of 1,7-bis (4-Hydroxyphenylthio)-3,5-dioxaheptane (DD-70) and bisphenol AF (BPAF)[a] and effects on embryonic viability[b]

				Viability (mid)		Viability (term)	
Chemical	Nominal Concentration (µg/g)	Actual Injected (µg/g)	Embryo Homogenate Concentration (µg/g ww ± SD)	Ratio	%	Ratio	%
DD-70	0	<MLOD	<MLOD	17/18	94	10/10	100
	1	1.09	ND	18/18	100	12/12	100
	10	7.74	4.04±0.59(mid) 0.10±0.03 (term)	25/26	96	19/19	100
	50	40.90	ND	12/19	63	5/6	83
	100	88.20	ND	15/24	63	8/9	89
BPAF	0	<MLOD	<MLOD	19/19	100	17/17	100
	1	0.56	ND	18/18	100	12/12	100
	10	6.21	ND	19/20	95	13/13	100
	50	54.90	ND	18/19	95	11/12	92
	100	114.00	93.10±3.67 (mid) 58.80±3.71 (term)	11/14	79	4/5	80

[a]After injection (day 0), embryos (n= 3 technical replicates, standard deviation (SD)) were
[a]After injection (day 0), embryos (n= 3 technical replicates, standard deviation (SD)) were
sampled at mid- incubation (mid, day 11) and term (day 20).
[b]Effects on embryonic viability at mid-incubation (day 11) were determined as the number of viable embryos compared with the total number of fertile eggs. Viability at term (day 20) was determined as the number of embryos that survived to term after mid-incubation removal of viable and nonviable embryos.
ww=wet weight; MLOD= Method limit of detection is 0.001 µg/g wet weight; ND=not determined.

7.4.2 Embryonic viability and morphological measurements

DD-70 (40.9 and 88.2 µg/g) and BPAF (114 µg/g) reduced embryonic viability at mid-incubation to 63 % (both doses) and 79 %, respectively (Figure 7.1). The survival rate for DMSO control of DD-70 and BPAF was 95% and 100 %. Embryonic viability for individuals that survived to term after mid-incubation sampling for DD-70 was 100, 100, 100, 83, and 89% for DMSO, 1.09, 7.74, 40.9 and 88.2 µg/g dose groups. (Table 7.2). The embryonic viability at term for BPAF was 100, 100, 100, 92, and 80% for DMSO, 0.6, 6.21, 54.9, and 114 µg/g dose groups,

respectively (Table 2). The LD50 values and confidence intervals of DD-70 and BPAF were 128.6µg/g (30.94-534.4mg/g) and 210.4 (89.3 and 495.7µg/g), respectively (Figure S1)

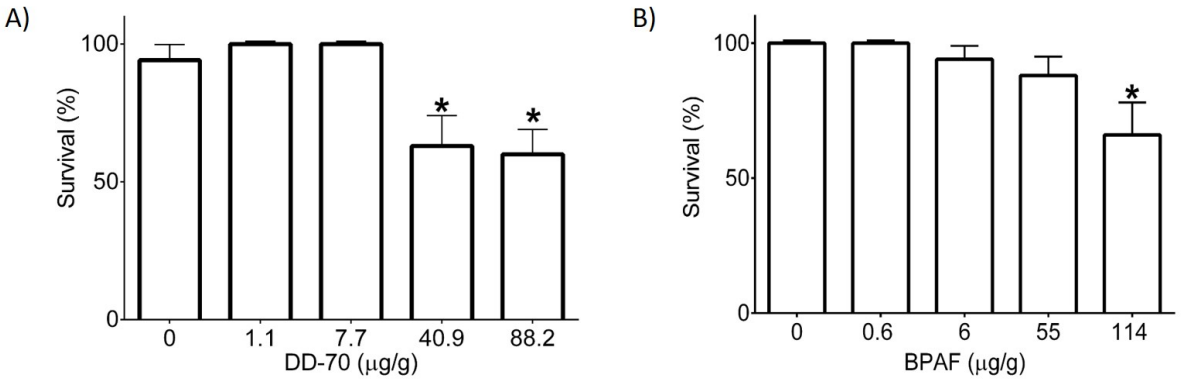

Figure 7.1. Effect of (A) 1,7-bis (4-Hydroxyphenylthio)-3,5-dioxaheptane **(**DD-70), and (B) Bisphenol AF (BPAF) on embryonic viability at mid-incubation (embryonic day 11; n= 14-19). Error bars represent the standard error of the mean (+SEM), and significant changes are indicated relative to dimethyl sulfoxide (DMSO) control. *$p \leq 0.05$; Dunnett's test).

Exposure to the highest dose of DD-70 (88.2 µg/g) resulted in decreased embryonic mass (Figure 7.2a), while the second highest dose (40.9 µg/g) caused a significant increase in gallbladder mass (0.033 ± 0.0023 g; $p \leq 0.05$) compared to the DMSO control group (0.022 ± 0.003 g) (Figure 7.2b). None of the other morphological parameters were altered following DD-70 exposure (Figure S7.2). The majority of the morphometric parameters measured, including embryo mass, were not significantly different from the control in any of the BPAF treatment groups (Figure S7.3). However, gallbladder mass of embryos exposed to the highest dose of BPAF (114µg/g) was significantly greater (0.033 ± 0.005 g; $p \leq 0.05$) compared to the DMSO control group (0.021 ± 0.006 g) (Figure 7.3).

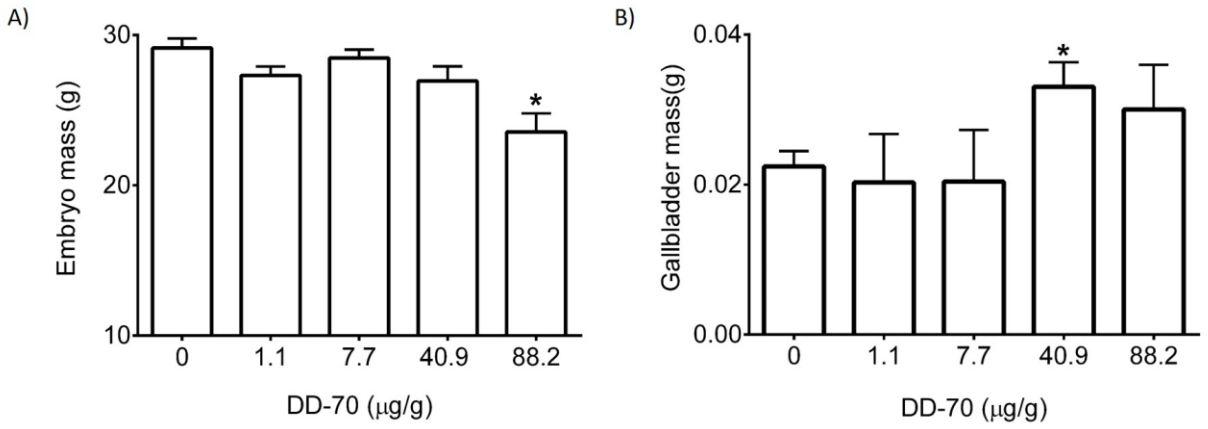

Figure 7.2. Effect of *in ovo* DD-70 exposure on (A) embryo mass, and (B) gallbladder mass for all embryos at term (embryonic day 20; n= 4-19/dose group). Error bars represent the standard error of the mean (+SEM). Data were analyzed with a 1-way ANOVA and Dunnett's test. '*'denotes differences compared to DMSO control.

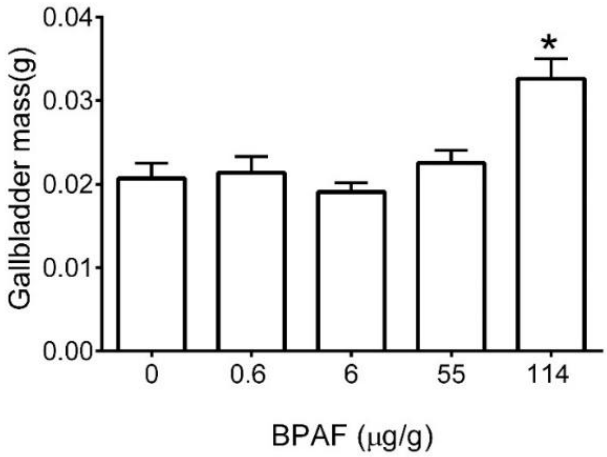

Figure 7.3. Effect of *in ovo* Bisphenol AF (BPAF) exposure on gallbladder mass for all embryos at term (embryonic day 20; n= 5-12/dose group). Error bars represent the standard error of the mean (+SEM). Data were analyzed with a 1-way ANOVA and Dunnett's test. '*'denotes differences compared to DMSO control.

3.3 Gene expression based on the two PCR arrays

Few significant changes in mRNA expression were observed at either time point using the ToxChip PCR array. The most dysregulated gene on the ToxChip array following exposure to DD-70 (88.2 µg/g) was fibroblast growth factor 19 (FGF19), which was significantly upregulated 6.81-log2 fold at mid-incubation and 3.53-log2 fold at term (Table 7.3). From the AestroChip array, 3 genes were significantly altered by DD-70 exposure; apovitellenin-1 (APOV1) was downregulated 4.04-log2 fold at mid-incubation and both avidin (AVD) and carnitine O-palmitoyltransferase 1 (CPT1A) were upregulated at term (1.54 and 1.30–log2 fold) (Table 7.3). Cytochrome P450 A37 (CYP3A7) and CPT1A were significantly upregulated at mid-incubation (2.5-log2 fold) following exposure to the highest dose of BPAF (114 µg/g) (Table 7.3). BPAF exposure did not result in the alteration of any ToxChip genes at term. The fold change, standard deviation and adjusted p-values for all genes on the ToxChip and AestroChip arrays are available in the supplemental information (Table S7.3).

Table 7.3. Hepatic mRNA expression results from chicken embryos exposed to 88.2 µg/g 1,7-bis (4-Hydroxyphenylthio)-3,5-dioxaheptane (DD-70) and 114 µg/g Bisphenol AF determined using two custom PCR arrays [a]

		Log2 fold-change			
Array	Genes	DD-70_M	DD-70_T	BPAF_M	BPAF_T
ToxChip	CYP3A7	-	-	2.50	-
	FGF19	6.81	3.53	-	-
AestroChip	APOV1	-4.04	-	-	-
	AVD	-	1.54	-	-
	CPT1A	-	1.30		-

[a] Gene expression values from ToxChip and AestroChip array are expressed as log2-fold change compared to the DMSO control for mid-incubation and term (n=3-5/chemical; Student's t-test, Bonferroni-adjusted p-value).
M=mid-incubation; T= term; CYP3A7=cytochrome P 450 3A7; FGF19=fibroblast growth factor 19; APOV1=apovitellenin-1; AVD=avidin; CPT1A= carnitine O-palmitoyltransferase 1

To date, there are no whole-animal studies on the toxicological properties of the BPA replacement chemicals, DD-70 and BPAF, for avian species. For DD-70, there is no empirical evidence available on its toxicological potential in any species. Several studies have demonstrated the estrogenic activity of BPAF (Li et al. 2014; Matsushima et al. 2010; Cano-Nicolau et al. 2016). In addition, *in vivo* exposure studies with zebrafish have shown BPAF exposure delays hatching rates and causes morphological malfunctions (Mu et al. 2018). Therefore, indentifying the toxicity of these chemicals is needed given the increased use of BPA replacement compounds as substitute of BPA in various products. By determining the effects of DD-70 and BPAF on embryonic development and hepatic mRNA expression, the present study contributes whole-animal toxicity data for a model avian species and attempts to link changes occurring at a cellular gene expression level to observable adverse phenotypic effects.

The decrease in concentrations of DD-70 and BPAF in embryonic contents between mid-incubation and term suggests that the compounds were metabolized by the developing embryos. The concentration of DD-70 in embryonic contents at mid-incubation (4.04 µg/g) was approximately forty-fold higher than at term (0.10 µg/g). The concentration of BPAF in embryonic contents at mid-incubation (93.1 µg/g) decreased by 1.6-fold in term embryos (58.8 µg/g). In a previous egg injection study, Crump et al. (2016a; 2018) reported low concentrations of two BPA replacements, BPS and TGSH, in developing chicken embryos sampled at term compared to the injected concentrations at day 0. Embryos treated with 207 µg/g of BPS and 48 µg/g of TGSH at day 0, had embryonic concentrations of 1.24 µg/g and 2 µg/g, respectively. Both BPS and TGSH analyses was solely conducted on embryonic contents of term embryos and therefore, it is not possible to compare with the mid-incubation results from the present study. The reduced concentration of DD-70 and BPAF at mid-incubation (day 11) and term (day 20) is

likely due to metabolism as metabolic functions are established on embryonic day 7 (Sandström and Westman 1971). The octanol/water coefficient (log Kow) of DD-70 is 3.34 compared to 4.47 for BPAF (US Environment Protection Agency, 2015) meaning that DD-70 is slightly more hydrophilic. The bio-concentration factor (BCF) of DD-70 was determined to be 75 whereas the BCF value for BPAF is 420 (US Environment Protection Agency, 2015). The hydrophilic nature and low BCF value of DD-70 means it is less likely to accumulate in an organism, which could account for the more efficient metabolism/clearance of DD-70 compared to BPAF.

Both BPA replacement compounds, DD-70 and BPAF decreased chicken embryonic viability. The viability data for DD-70 are comparable to those reported in a chicken TSGH egg injection study, where the mid-incubation viability was 60% after exposure to 48 µg/g TGSH (Crump et al. 2018); viability in DD-70-exposed embryos at 40.9 and 88.2 µg/g was 63%. Exposure of chicken embryos to another BPA replacement compound, BPS, decreased viability to 58% at 207 µg/g on day 22 (Crump et al. 2016). In addition, embryonic viability of chicken embryos decreased to 48% on day 19 after *in ovo* exposure to 67 µg/g BPA (Berg et al. 2001). In contrast, zebrafish embryos exposed to 2 mg/L BPAF resulted in 100% mortality compared to the solvent control group, whereas a dose of 10 mg/L BPA was required to have the same effect, indicating that BPAF was more embryo lethal in fish (Shi et al. 2016). Overall, when determining safe alternatives to BPA these variable toxicological responses to bisphenol replacement compounds among species need to be carefully considered.

Embryonic exposure to the highest dose of DD-70 resulted in a decrease in embryo mass, similar to the effects observed following BPS exposure (Crump et al. 2016a). The decrease in embryonic mass by both DD-70 and BPS suggests that certain bisphenol replacement compounds can impair normal growth in birds. Future studies should evaluate the mechanism(s)

that could impact embryonic mass/growth including the measurement of growth and thyroid hormone levels in plasma. Both DD-70 (second highest dose) and BPAF (highest dose) caused a significant increase in gallbladder mass. A concordant effect on gallbladder size based on length was observed following *in ovo* exposure to BPS (Crump et al. 2016a), suggesting a similar disruption of the enterohepatic system in avian embryos exposed to two different BPA alternatives.

The hepatic transcriptomic response for chicken embryos exposed to DD-70 was slightly more pronounced than BPAF: two of the ToxChip genes and three of the AestroChip genes were dysregulated at the developmental stages evaluated. FGF19, belonging to the lipid/cholesterol metabolism pathway, was upregulated 6.81-log2 fold at mid-incubation and 3.53-log2 fold at term following exposure to 88.2 µg/g DD-70. In a previous chicken egg injection study, FGF19 was also the most highly dysregulated gene following exposure to the BPA alternative, TGSH, with a 17-fold upregulation at mid-incubation in embryos exposed to 180 µg/g and a 10-fold induction at term for embryos exposed to 48µg/g (Crump et al. 2018). In addition, FGF19 was the most highly dysregulated gene (14-fold upregulation) in an *in vitro* chemical screening study of BPS in double-crested cormorants (Crump et al. 2016b). FGF19 is involved with the regulation of the enterohepatic circulation of bile, gallbladder filling and volume, and glucose and lipid metabolism. This growth factor induces protein and glycogen synthesis and suppresses gluconeogenesis in the liver (Jones 2008; Kir et al. 2011). Mice with impaired FGF15 activity, an ortholog of FGF19, had smaller gallbladders due to a decrease in gallbladder filling (Choi et al. 2006). This suggests the dysregulation of FGF19 could alter bile acid homeostasis, which could account for the increase in gallbladder mass in embryos exposed to DD-70.

In addition to FGF19, DD-70 exposure led to the alteration of 3 estrogen-responsive genes: 1) apovitellenin-1 (APOV1), 2) avidin (AVD), and 3) carnitine O-palmitoyltransferase 1 (CPT1A). APOV1 was downregulated at mid-incubation and CPT1A and AVD were upregulated at term. APOV1 is a very low-density lipoprotein synthesized in the liver, which is induced by estrogen in egg-laying hens. It acts as a lipoprotein lipase inhibitor preventing the breakdown of lipoprotein from the liver to the egg yolk (Chan et al. 1980). BPA decreased the expression of several apolipoprotein genes in young mice and altered lipid accumulation in the liver (Ke et al. 2016). A decrease in APOV1 expression suggests possible disruption in lipid metabolism (Wei et al. 2019). AVD is a glycoprotein found in egg white and has antimicrobial properties; its expression is modulated by estrogen (Foye-Jackson et al. 2011). An increase in AVD expression highlights a disruption of estrogen-mediated pathways (Socha and Hrabia, 2018). CPT1A was upregulated following DD-70 exposure but only at term. CPT1A is involved in the rate-limiting step of mitochondrial fatty acid oxidation and lipid metabolism (Strakovsky et al. 2015). Adult rats exposed to BPA during the perinatal stage had increased expression of CPT1A mRNA (Wei et al. 2014). The authors speculated that the increase in CPT1A expression was due to an increase in fatty acid accumulation in the liver. The increase in expression of CPT1A mRNA at term (day 20) suggests abnormal fatty acid metabolism, which could result in impaired bile acid homeostasis. Overall, the dysregulation of three estrogen-responsive genes on the AestroChip following DD-70 exposure highlights potential molecular mechanisms of action that should be further explored. For example, an important consideration for future egg injection studies, especially for those chemicals that may exert toxic effects via bile acid homeostasis disruption, is to quantify total plasma bile acid concentrations. This would provide a link

between an apical measure (gallbladder weight and bile acid concentrations) and a subcellular key event (genes involved in bile acid homeostasis/gallbladder filling).

On the ToxChip array, BPAF altered the expression of a single gene, CYP3A7, which was significantly upregulated at mid-incubation (2.5-log2 fold) (Table 3). CYP3A7, a member of the cytochrome P450 super family of enzymes, is involved in metabolism of xenobiotics and endogenous compounds, including cholesterol and bile acids (Gnerre et al. 2004). In a human hepatoma cell line, BPA increased the expression of CYP3A4, which is 60 % homologous to chicken CYP3A7 and has an essential role in hydroxylation of steroid hormones (Kuzbari et al. 2011; Osselaere et al. 2013). The upregulation of CYP3A7 at mid-incubation could have led to the metabolism of BPAF and impairments in bile acid regulation, which may have played a role in the increase in gallbladder mass on day 20. Excess bile acid can induce CYP3A via the farnesoid X receptor (FXR) and pregnane X receptor (PXR; equivalent to chicken xenobiotic receptor (CXR)) to maintain bile acid homeostasis (Gnerre et al. 2004). None of the genes on the AestroChip were altered by BPAF exposure indicating that in this early-life stage model, the response to estrogen pathway may not be dysregulated. In the current study, it was not possible to determine sex-dependent changes in gene expression due to an insufficient number of males and females in each dose group for DD-70 and BPAF. Future studies on BPA replacement compounds would benefit from an increased sample size to enable the investigation of sex-specific gene expression responses (especially for estrogen responsive genes).

In addition, future whole animal avian studies should include gonadal histology and determination of gonadal somatic index to further evaluate reproductive endpoints, and endocrine disrupting properties of DD-70 and BPAF. Previous studies by Jessl et al. (2018) found reduced cortex thickness in females and increased cortex thickness of male chicken

embryos (day 19) exposed to BPA. Moreover, BPA (200 μg/g egg) caused feminization of the left testis (ovotestis) in male chicken embryos (day 19) (Berg et al. 2001). To serve as a benchmark comparison to known estrogens, another important consideration for future early-life stage avian studies would be to perform an egg injection study with estradiol and BPA that measures the same endpoints (e.g. embryonic viability, growth metrics, gene expression) evaluated in the present study. In addition, to evaluate disruption to the endocrine system at another biological level of organization, quantification of plasma vitellogenin (estrogen biomarker) concentrations could be performed to empirically determine if the gene-level responses observed following DD-70 exposure are reflected at an additional level of biological organization.

Due to concerns about the health effects of BPA, there are associated restrictions on its production and use in consumer goods. BPAF and DD-70 are two BPA replacement compounds, which are currently in use; however, adequate toxicological characterization is not available. Both BPAF and DD-70 reduced embryonic viability in developing chicken embryos and DD-70 was more embryo lethal than BPAF and had similar toxicity as another replacement compound, TGSH. Minimal morphological effects were observed with the exception of gallbladder size (DD-70 and BPAF) and embryonic mass (DD-70) in exposed chicken embryos. Similarly, based on the number of gene targets evaluated by two custom PCR arrays, a minimal hepatic transcriptomic response was observed for either chemical. The present study provides whole-animal toxicological data for an avian species that can be used to inform chemical regulators on the suitability of DD-70 and BPAF as BPA replacement alternatives.

Acknowledgments

The present study was supported by funds from sources within Environment and Climate Change Canada: 1) Chemicals Management Plan; 2) Strategic Technology Applications of Genomics for the Environment; and 3) Ecotoxicology and Wildlife Health Division.

7.6 References

Andersen HR, Andersson AM, Arnold SF, Autrup H, Barfoed M, Beresford NA, Bjerregaard P, Christiansen LB, Gissel B, Hummel R, Jørgensen EB. 1999. Comparison of short-term estrogenicity tests for identification of hormone-disrupting chemicals. *Environmental Health Perspectives* 107(suppl 1):89–108.

Berg C, Halldin K, Brunstrom B. 2001. Effects of bisphenol A and tetrabromobisphenol A on sex organ development in quail and chicken embryos. *Environmental Toxicology & Chemistry* 20(12):2836–2840.

Bjornsdotter MK, de Boer J, Ballesteros-Gomez A. 2017. Bisphenol A and replacements in thermal paper: A review. *Chemosphere* 182:691-706.

Cano-Nicolau J, Valliant C, Pellegrini E, Charlier TD, Kah O, Coumailleau P. 2016. Estrogenic effects of several BPA Analogs in the developing zebrafish brain. *Frontiers in Neurology* 10:112.

Chan L, Bradley WA, Means AR. 1980. Amino acid sequence of the signal peptide of apoVLDL-II, a major apoprotein in avian very low density lipoproteins. *Journal of Biological Chemistry* 255(21):10060-3.

Chen D, Kannan K, Tan H, Zheng Z, Feng YL, Wu Y, Widelka M. 2006. Bisphenol Analogues Other Than BPA: Environmental Occurrence, Human Exposure, and Toxicity—A Review. *Environental Science & Technology* 50:5438−5453. DOI: 10.1021/acs.est.5b05387

Choi M, Moschetta A, Bookout AL, Peng L, Umetani M, Holmstrom SR, Suino-Powell K, Xu HE, Richardson JA, Gerard RD, Mangelsdorf DJ, Kliewer SA. 2006. Identification of a hormonal basis for gallbladder filling. *Nature Medicine* 12 (11): 1253-1255.

Crump D, Chiu S, Williams KL. 2016a. Bisphenol S alters embryonic viability, development, gallbladder size, and messenger RNA expression in chicken embryos exposed via egg injection *Environmental Toxicology & Chemistry* 35:1541–1549.

Crump D, Farhat A, Chiu S, Williams KL, Jones SP, Langlois VS. 2016b. Use of a novel double-crested cormorant ToxChip PCR array and the EROD assay to determine effects of environmental contaminants in primary hepatocytes. *Environental Science & Technology* 50(6):3265-3274.

Crump D, Chiu S, Williams KL. 2018. Bis-(3-allyl-4-hydroxyphenyl) sulfone decreases embryonic viability and alters hepatic mRNA expression at two distinct developmental stages in chicken embryos exposed via egg injection. *Environmental Toxicology & Chemistry* 37(2):530-537.

Farhat A, Crump D, Chiu S, Williams KL, Letcher RJ, Gauthier LT, Kennedy SW. 2013. In ovo effects of 2 organophosphate flame retardants—TCPP and TDCPP—on pipping success, development, mRNA expression, and thyroid hormone levels in chicken embryos. *Toxicological Sciences* 134(1):92-102.

Flint S, Markle T, Thompson S, Wallace E. 2012. Bisphenol A exposure, effects, and policy: a wildlife perspective. *Journal of Environmental Management* 104:19-34.

Foye-Jackson OT, Long JA, Bakst MR, Blomberg LA, Akuffo VG, Silva MV, Guthrie HD, McMurtry JP. 2011. Oviductal expression of avidin, avidin-related protein-2, and progesterone receptor in turkey hens in relation to sperm storage: Effects of oviduct tissue type, sperm presence, and turkey line. *Poultry Science* 90(7):1539-47.

Gnerre C, Blattler S, Kaufmann MR, Looser R, Meyer UA. 2004. Regulation of CYP3A4 by the bile acid receptor FXR: evidence for functional binding sites in the CYP3A4 gene. *Pharmacogenetics* 14(10), 635-645. doi: 10.1097/00008571-200410000-00001.

Ke ZH, Pan JX, Jin LY, Xu HY, Yu TT, Ullah K, Rahman TU, Ren J, Cheng Y, Dong XY, Sheng JZ, Huang HF. 2016. Bisphenol A Exposure May Induce Hepatic Lipid Accumulation via Reprogramming the DNA Methylation Patterns of Genes Involved in Lipid Metabolism. *Scientific Reports* 6:31331.

Kir S, Kliewer SA, Mangelsdorf DJ. 2011. Roles of FGF19 in liver metabolism. *Cold Spring Harbor Symposia on Quantitative Biology* 76:139-144.

Kuzbari, O., Lamb, J. G., Hathaway, L. B., Franklin, M. R., Hammoud, A., & Peterson, C. M. 2011. Bisphenol A alters human CYP3A4 enzyme expression and activity. *Fertility and Sterility* 96(3), S157.

Jessl L, Scheider J, Oehlmann, J. 2018a. The domestic fowl (*Gallus gallus domesticus*) embryo as an alternative for mammalian experiments – Validation of a test method for the detection of endocrine disrupting chemicals. *Chemosphere* 196: 502-513. 10.1016/j.chemosphere.2017.12.131

Jessl L, Lenz R, Massing FG, Scheider J, Oehlmann, J. 2018b. Effects of estrogens and antiestrogens on gonadal sex differentiation and embryonic development in the domestic fowl (*Gallus gallus domesticus*). *PeerJ* 6:e5094.

Jones, S. 2008. Mini-review: endocrine actions of fibroblast growth factor 19. *Molecular Pharmaceutics* 5(1):42-48.

Kitamura S, Suzuki T, Sanoh S, Kohta R, Jinno N, Sugihara K, Yoshihara S, Fujimoto N, Watanabe H, Ohta S. 2005. Comparative study of the endocrine-disrupting activity of bisphenol A and 19 related compounds. *Toxicological Sciences* 84(2):249-259.

Li M, Guo J, Gao WH, Yu JL, Han XY, Zhang J, Shao B. 2014. Bisphenol AF-Induced Endogenous Transcription Is Mediated by ER alpha and ERK1/2 Activation in Human Breast Cancer Cells. *PloS one* 9(4): e94725.

Liao CY, Liu F, Guo Y, Moon HB, Nakata H, Wu Q, Kannan K. 2012. Occurrence of Eight Bisphenol Analogues in Indoor Dust from the United States and Several Asian Countries: Implications for Human Exposure. . *Environental Science & Technology* 46(16):9138-9145.

Matsushima A, Liu XH, Okada H, Shimohigashi M, Shimohigashi Y. 2010. Bisphenol AF Is a Full Agonist for the Estrogen Receptor ER alpha but a Highly Specific Antagonist for ER beta. *Environmental Health Perspectives* 118(9):1267-1272.

Mesnage R, Phedonos A, Arno M, Balu S, Corton JC, Antoniou MN. 2017. Transcriptome Profiling Reveals Bisphenol A Alternatives Activate Estrogen Receptor Alpha in Human Breast Cancer Cells. *Toxicological Sciences* 158(2):431-443.

Moriyama K, Tagami T, Akamizu T, Usui T, Saijo M, Kanamoto N, Hataya Y, Shimatsu A, Kuzuya H, Nakao K. 2002. Thyroid hormone action is disrupted by bisphenol A as an antagonist. *The Journal of Clinical Endocrinology and Metabolism* 87(11):5185-5190.

Mu XY, Huang Y, Li XX, Lei YL, Teng MM, Li XF, Wang CJ, Li YR. 2018. Developmental Effects and Estrogenicity of Bisphenol A Alternatives in a Zebrafish Embryo Model. *Environental Science & Technology* 52(5):3222-3231.

Nakayama K, Iwata H, Kim EY, Tashiro K, Tanabe S. 2006. Gene expression profiling in common cormorant liver with an oligo array: assessing the potential toxic effects of environmental contaminants. *Environental Science & Technology* 40(3):1076-1083.

Osselaere A, De Bock L, Eeckhaut V, De Backer P, Van Bocxlaer J, Boussery K, Croubels S. 2013. Hepatic and intestinal CYP 3A expression and activity in broilers. *J Vet Pharmacology & Therapeutics* 36(6):588-593.

Perera L, Li Y, Coons LA, Houtman R, van Beuningen R, Goodwin B, Auerbach SS, Teng CT. 2017. Binding of bisphenol A, bisphenol AF, and bisphenol S on the androgen receptor: Coregulator recruitment and stimulation of potential interaction sites. *Toxicology In Vitro* 44:287-302.

Pelch KE, Wignall JA, Goldstone AE Ross PK, Blain RB, Shapiro AJ, Holmgren SD, Hsieh J-H, Svoboda D, Auerbach SS, Parham FM, Masten SA, Thayer KA. 2017. NTP Research Report on Biological Activity of Bisphenol A (BPA) Structural Analogues and Functional Alternatives.

NTP RR 4. Technical Report. Research Triangle Park, NC: *National Toxicology Program*. 4: 1-78.

Porter E, Crump D, Egloff C, Chiu S, Kennedy SW. 2014. Use of an avian hepatocyte assay and the avian Toxchip Polymerse chain reaction array for testing prioritization of 16 organic flame retardants. *Environ Toxicol Chem* 33(3):573-582.

Ranciere F, Lyons JG, Loh VHY, Botton J, Galloway T, Wang TG, Shaw JE, Magliano DJ. 2015. Bisphenol A and the risk of cardiometabolic disorders: a systematic review with meta-analysis of the epidemiological evidence. *Environmental Health* 14:23.

Richter CA, Taylor JA, Ruhlen RL, Welshons WV, vom Saal FS. 2007. Estradiol and bisphenol A stimulate androgen receptor and estrogen receptor gene expression in fetal mouse prostate mesenchyme cells. *Environmental Health Perspectives* 115(6):902-908.

Rochester JR and Bolden AL. 2015. Bisphenol S and F: A Systematic Review and Comparison of the Hormonal Activity of Bisphenol A Substitutes. . *Environ Health Perspect* 123(7):643-650.
Rubin BS. 2011. Bisphenol A: an endocrine disruptor with widespread exposure and multiple effects. *J Steroid Biochem Mol Biol* 127(1-2):27-34.

Schmittgen TD and Livak KJ. 2008. Analyzing real-time PCR data by the comparative C(T) method. *Nat Protoc* 3(6):110-1108.

Sandström B, Westman J. 1971. Ultrastructure of the developing chicken liver before hatching. *Z Zellforsch Mikrosk Anat* 117(4):516-525

Sharin T, Williams KL, Chiu S, Crump D, O'Brien JM. (in press). Toxicity of Bisphenol A Replacement Compounds: Cytotoxicity and mRNA Expression in Primary Hepatocytes of Chicken and Double-Crested Cormorant. *Environmental Toxicology and Chemistry* DOI: 10.1002/etc.4985

Shi J, Yang Y, Zhang J, Feng Y, Shao B. 2016. Uptake, depuration and bioconcentration of bisphenol AF (BPAF) in whole-body and tissues of zebrafish (*Danio rerio*). *Ecotoxicology and Environmental Safety* 132:339-344.

Socha JK and Hrabia A. 2018. Alterations in apoptotic markers and egg-specific protein gene expression in the chicken oviduct during pause in laying induced by tamoxifen. *Theriogenology* 1(105):126-134.

Strakovsky RS, Wang H, Engeseth NJ, Flaws JA, Helferich WG, Pan YX, Lezmi S. 2015. Developmental bisphenol A (BPA) exposure leads to sex-specific modification of hepatic gene expression and epigenome at birth that may exacerbate high-fat diet-induced hepatic steatosis. *Toxicology and Applied Pharmacology* 284(2):101-112

Teng C, Goodwin B, Shockley K, Xia MH, Huang RL, Norris J, Merrick BA, Jetten AM, Austin

CP, Tice RR. 2013. Bisphenol A affects androgen receptor function via multiple mechanisms. *Chemico-Biological Interactions* 203(3):556-564.

Tomza-Marciniak A, Stepkowska P, Kuba J, Pilarczyk B. 2018. Effect of bisphenol A on reproductive processes: A review of in vitro, in vivo and epidemiological studies. *Journal of Applied Toxicology* 38(1):51-80.

US Environmental Protection Agency. 2015. Bisphenol A alternatives in thermal paper. Final Report. Available from: https://www.epa.gov/sites/production/files/2015-09/documents/bpa_ch4.pdf

Wei J, Sun X, Chen Y, Li Y, Song L, Zhou Z, Xu B, Lin Y, Xu S. 2014. Perinatal exposure to bisphenol A exacerbates nonalcoholic steatohepatitis-like phenotype in male rat offspring fed on a high-fat diet. *J of Endocrinoogyl* 222(3):313-25.

Wei Z, Li P, Huang S, Lkhagvagarav P, Zhu M, Liang C, Jia C. 2019. Identification of key genes and molecular mechanisms associated with low egg production of broiler breeder hens in ad libitum. *BMC Genomics* 20(1):408.

Yamaguchi A, Ishibashi H, Arizono K, Tominaga N. 2015. In vivo and in silico analyses of estrogenic potential of bisphenol analogs in medaka (Oryzias latipes) and common carp (Cyprinus carpio). *Ecotoxicology and Environmental Safety* 120:198-205.

Yeo M, Berglund K, Hanna M, Guo JU, Kittur J, Torres MD, Abramowitz J, Busciglio J, Gao Y, Birnbaumer L, Liedtke WB. 2013. Bisphenol A delays the perinatal chloride shift in cortical neurons by epigenetic effects on the Kcc2 promoter. *PNAS* 110(11):4315-4320.

8.0 General Conclusions

The major goals of this thesis were to: 1) determine the applicability of the chicken Leghorn male hepatoma (LMH) and double-crested cormorant hepatocyte (DCH22) cell lines for ecotoxicological screening of chemicals; 2) generate and compare toxicity data for five bisphenol A (BPA) replacement compounds using three different *in vitro* models; and 3) use the data generated from *in vitro* models to prioritize the replacement compounds for *in vivo* testing. The metabolic competence and ability to detect metabolism-mediated genotoxicity in the LMH cell line were investigated. An immortalized hepatic cell line derived from a double-crested cormorant embryo, DCH22, was established for avian toxicity screening. Cytotoxicity and modulation of target genes following exposure to five BPA replacement compounds were compared in primary embryonic hepatocytes of chicken (CEH) and double-crested cormorant (DCEH), and the LMH cell line. Lastly, two of the replacement compounds were prioritized for *in vitro* concentration-dependent gene expression analysis and *in vivo* chicken egg injection studies. In addressing these important research questions, this thesis sought to achieve the objectives that were outlined in the introductory chapter. More specifically, to:

1) generate evidence to support the use of the LMH and DCH22 cell lines as alternatives to primary hepatocytes for avian ecotoxicological screening

2) generate novel ecotoxicological data for screening and prioritizing five BPA replacement compounds using cell culture and *in vitro* toxicogenomics approaches

3) generate *in vivo* ecotoxicity data using an avian early-stage alternative testing strategy and toxicogenomics for two prioritized BPA replacement compounds

8.1 Chapter Summaries Based on Objectives

8.1.1 Generate evidence to support the use of LMH and DCH22 cell lines as alternatives to primary hepatocytes for avian ecotoxicological screening

The research objectives of Chapters 2 and 3 were to evaluate a) metabolic competency and b) metabolism-dependent genotoxic endpoints in the LMH cell line cultured as 2D confluent monolayers or 3D spheroids. To do this, two well-characterized environmental contaminants were selected for LMH exposure studies: 3,3′,4,4′,5-pentachlorobiphenyl (PCB-126) and benzo(a)pyrene (BaP). PCB-126 is a potent aryl hydrocarbon receptor (AhR) agonist, which is metabolized very slowly resulting in sustained activation of AhR and CYP1A (NTP 2006). Similarly, BaP is an AhR agonist and activates CYP1A. However, the induction of CYP1A by BaP produces a DNA-reactive metabolite, benzo(a)pyrene diol epoxide (BPDE), that causes DNA-damage and activates DNA damage response pathways (Tung et al. 2014). Thus, these two compounds were selected for determining the metabolic competence and ability to detect metabolism-dependent genotoxicity of the LMH cell line, respectively. Both PCB-126 and BaP upregulated the expression of CYP1A4 and CYP1A5 mRNA, and CYP1A activity (measured using the 7-ethoxy-resorufin-O-deethylase [EROD] assay) in LMH cells cultured as 2D confluent monolayers and 3D spheroids, but the expression/activity was greater in 3D spheroids. In addition, CYP1A activity was induced at an earlier time point in 3D spheroids than 2D confluent monolayers by BaP. The activity of CYP1A in 3D spheroids was lower than CEH; however, EC50 values of CYP1A activity (0.09 ± 0.04 nM in LMH spheroids vs. 0.05 ± 0.02 nM in CEH) and the expression profile of other AhR related genes were similar to CEH. Even though the metabolism of BaP to BPDE was not directly measured in this thesis, there was a concentration-dependent increase in γH2AX levels indicating the presence of DNA double-

strand breaks in 3D spheroids. Furthermore, a concurrent upregulation of DNA damage response genes was observed, suggesting metabolism of BaP to BPDE and resulting DNA double strand breaks. The results from Chapters 2 and 3 provide evidence of: 1) metabolic competency; and 2) CYP1A metabolism dependent bioactivation of chemicals with regards to genotoxic endpoints in the LMH cell line cultured as 3D spheroids.

In Chapter 4, an immortalized DCCO cell line, DCH22, was developed as a possible alternative to primary double-crested cormorant embryonic hepatocytes for *in vitro* chemical screening. *In vitro* avian toxicity data are often generated using a chicken primary hepatocyte model. However, studies have found chicken to be more sensitive to toxicants than most wild species (Head et al. 2008), and therefore, the lab model may not be as suitable for screening for the ecotoxicological effects of priority chemicals. There are few studies that screen chemicals for toxic effects in wild avian species, which are exposed in the natural environment. Primary hepatocytes from DCCO have been used as an ecologically relevant alternative for chemical screening, but it is difficult to obtain eggs for primary culture. There are currently no cell lines available for DCCO. Thus, a DCCO hepatic cell line, DCH22, was established from an embryonic day 22 double-crested cormorant embryo and the cell line was continuously cultured for a year. Similar to the LMH results, exposure to PCB-126 induced greater CYP1A activity in the DCH22 cell line cultured as 3D spheroids compared to 2D confluent monolayers. DCH22 confluent monolayers treated with metyrapone, an inducer of CYP3A expression in human and rat hepatocytes (Harvey et al. 2000), resulted in an increase in CYP3A activity. Future research is warranted to investigate CYP3A activity in DCH22 3D spheroids. In addition, CYP1A, CYP2E and CYP3A activities in 2D confluent monolayer cells and 3D spheroids needs to be further determined by treating the cells with other CYP1A, CYP2E and CYP3A inducers such as

β napthoflavone, buproprion and midazolam. Albumin and α-1-antitrypsin, markers of hepatocytes, will be determined using ELISA. Overall, the DCH22 cell line still needs to be further characterized for Phase I and II enzyme gene expression and to evaluate the cellular characteristics of the hepatocytes. However, the establishment of a hepatic cell line for an ecologically relevant species shows promise for future screening applications once additional characterization of hepatocyte specific functions are conducted.

8.1.2 Generate novel ecotoxicological data for screening and prioritizing of five BPA replacement compounds using cell culture and in vitro toxicogenomics approaches

The research objectives of Chapters 5 and 6 were to screen five BPA replacement compounds, BPF, TGSH, DD-70, BPAF and BPSIP, for effects on cytotoxicity and gene expression in CEH, LMH spheroids, and DCEH. Cytotoxicity of the replacement compounds was compared to BPA in CEH and LMH spheroids. BPF was the least cytotoxic compound in both CEH and LMH spheroids among the replacement compounds and BPA. The cytotoxicity of BPF was not evaluated in DCEH due to low cytotoxicity in CEH. TGSH, DD-70 and BPAF were the most cytotoxic replacement compounds in all three models. BPSIP was moderately cytotoxic in all three models and had similar cytotoxicity as BPA in CEH and LMH spheroids. The relative cytotoxicity of all five replacements compounds in each of the cell models is summarized in Table 8.1.

Table 8.1. Ranking of the relative cytotoxicity, ToxChip and AestroChip gene expression of BPA replacement compounds and BPA in CEH, LMH spheroids and DCEH.

Compound	Cytotoxicity			ToxChip			AestroChip		
	CEH	LMH	DCEH	CEH	LMH	DCEH	CEH	LMH	DCEH
BPA	Moderate	Moderate	ND	Low	Low	ND	Low	Moderate	ND
BPF	Low	Low	ND	Low	Moderate	ND	Moderate	High	ND
TGSH	High	High	High	High	High	Low	Low	Low	ND
BPAF	High	High	High	Moderate	Low	Low	Low	High	ND
DD-70	High	High	High	High	Moderate	Low	Low	Low	ND
BPSIP	Moderate	Moderate	Moderate	Low	Moderate	Moderate	Moderate	High	ND

"ND" indicates not determined

Changes in gene expression were explored using two PCR arrays: 1) species-specific ToxChips (chicken and DCCO); and 2) a chicken-specific AestroChip. The ToxChip measures the expression of genes associated with nine toxicologically relevant pathways including xenobiotic metabolism, lipid homeostasis and the thyroid hormone pathway. The relative potency of BPA and the five BPA replacement compounds with respect to the induction of pathways on the ToxChip and AestroChip arrays are summarized in Table 8.1. These relative rankings were calculated based on the Euclidean distance of each treatment group from the DMSO control using the average log2 fold change data of each cell type and array, followed by pooling the Euclidean distances of each *in vitro* model for each array. Then, the 50th and 75th percentiles of the pool were calculated. Treatment groups with a Euclidean distance less than or equal to the 50th percentile were assigned as "low", groups between the 50th and 75th percentile were ranked as "medium", and groups greater than the 75th percentile were ranked as "high".

Generally, the replacement compounds changed the expression of a greater number of genes on the ToxChip array in CEH compared to LMH spheroids or DCEH at the same concentrations. For example, TGSH altered the expression of genes in all pathways included on the ToxChip for CEH, but modulated fewer genes in LMH spheroids, and had no effect in

DCEH. The difference in sensitivity between CEH and DCEH was expected. As previously discussed, many studies have shown that the chicken is generally more sensitive to toxicants than wild species (Head et al. 2008). The discrepancy between CEH and the LMH cell line could be the result of several factors. The primary factor may be that the LMH cell line originated from a chemically transformed hepatocellular carcinoma that has been propagated for many years (Kawaguchi et al 1987), and may have diverged significantly from its hepatocyte origins. Another important factor may be the sex and life stage of origin; CEH were cultured from a pool of embryonic livers from both males and females while the LMH cell line was derived from a single adult male liver. The toxicity of a chemical usually depends on the life stage at the time of exposure and in many species, early-life stages are the most vulnerable (Barton et al. 2005; Birnbaum and Fenton 2003). However, these differences in sensitivity were not reflected in the cytotoxicity response in either cell line, suggesting that the pathways on the ToxChip array represent model-specific sub-lethal effects.

With regard to the relative responses of specific compounds, BPA interestingly altered the least number of genes on the ToxChip in both CEH and LMH spheroids (and was not tested in DCEH). This indicates that the BPA replacement compounds included in this thesis have greater non-estrogenic toxicity than BPA. BPF changed the expression of ten genes associated with different pathways on the ToxChip in CEH and two genes in LMH spheroids. BPF was not evaluated in DCEH due to the low cytotoxicity reported in CEH. TGSH was the most potent compound in CEH. TGSH altered fewer ToxChip genes in LMH but with greater fold-change values, resulting in a “high” relative potency call in LMH. Like other compounds, TGSH had minimal ToxChip effects in DCEH. DD-70 induced a strong to moderate response in both chicken models, but had minimal effects in DCEH. BPAF altered a moderate number of

ToxChip genes related to several pathways in CEH but elicited minimal change in LMH spheroids and DCEH. Finally, BPSIP induced a moderate response in CEH but a relatively weak response in LMH. Interestingly, BPSIP was the most transcriptionally active compound in DCEH. Toxicity data on BPSIP is extremely limited compared to BPA. BPSIP altered mRNA expression of ERα and ERβ in zebrafish and was mildly estrogenic compared to BPA (Lee et al. 2018).

Some perturbed pathways in common emerged across multiple BPA replacement compounds. Both TGSH and DD-70, which were the most potent compounds in CEH, and all the replacements except BPSIP, affected genes involved in bile acid/cholesterol regulation. For TGSH, this was only observed in CEH, but for DD-70 this pathway was dysregulated in CEH, LMH and DCEH. Bile acid is involved in the elimination of lipids, and mediates cholesterol, glucose and energy homeostasis. Therefore, the bile acid pool is tightly regulated in the liver and alteration in bile acid regulation can have adverse effects like cholestasis (Staels and Foncesca 2009). Two compounds, TGSH and BPSIP, also dysregulated genes in the thyroid hormone pathway in CEH (and in DCEH for BPSIP). Thyroid hormone is involved in growth, development and homeothermy in birds, and disruptions in this pathway can lead to decreased egg production and pipping, as well as changes in lipid regulation and nervous system development (McNabb 2007).

In LMH spheroids, DD-70 and BPAF were selected for concentration-dependent gene expression due to high cytotoxicity in CEH, LMH and DCEH. DD-70 altered the expression of a higher number of ToxChip genes at lower concentrations compared to the concentration used for comparison between the two models. It would helpful for future studies to include concentration-

dependent gene expression analysis in LMH spheroids in order to compare non-estrogenic endpoint induction between models.

Using an estrogen pathway-specific PCR array, the AestroChip, we generated evidence that several BPA replacement compound may be equally, if not more, estrogenic than BPA. These results are summarized in Table 8.1. The AestroChip array consists of estrogen-responsive genes including two genes that are considered molecular markers of xenoestrogen exposure in oviparous wildlife, apovitellenin (APO) and vitellogenin 2 (VTG2). Generally, BPA, BPF, BPAF and BPSIP were more active in terms of dysregulation of the AestroChip genes in LMH spheroids compared to CEH (Table 8.1). The LMH cell line originates from a male, as opposed to a mixed sex pool for hepatocyte preparation, which could help explain the increased response of LMH cells to the BPA replacements. Since the liver from males and females were combined (in an unknown ratio) during the preparation of CEH cultures, it may complicate the determination of estrogenic effects of the compounds. Males are typically more vulnerable to the adverse effects of xenoestrogens and the induction of estrogen responsive genes (e.g. VTG) are more evident since the basal expression of these genes are lower in males. For example, serum concentrations of BPA were higher in male compared to female rats and metabolism of BPA was slower in males (Caporossi and Papaleo 2015).

Regarding the chemical-specific Aestrochip responses, BPA dysregulated the expression of both APO and VTG2 in LMH spheroids, but the magnitude of change was smaller than BPF, BPAF and BPSIP. BPF is potentially a mild estrogenic replacement compound based on the changes in expression of AestroChip genes, especially APO and VTG2. BPF exposure upregulated the expression of APO in CEH and both APO and VTG2 in LMH spheroids. Based on the AestroChip results, TGSH is a non-estrogenic replacement compound in both CEH and

LMH spheroids. DD-70 did not alter the expression of APO or VTG2 in CEH but upregulated VTG2 in LMH spheroids. BPAF was the only replacement compound along with BPA to modulate the expression of VTG2 in CEH. In LMH spheroids, BPAF was the most estrogenic compound after E2 based on changes in APO and VTG2 expression. BPSIP did not elicit APO or VTG2 expression in CEH but upregulated other estrogen responsive genes. In LMH spheroids, BPSIP upregulated both APO and VTG2, and may have estrogenic potential. BPF and BPAF are replacement compounds with potential estrogenic activities in CEH and LMH spheroids, and TGSH is non-estrogenic in both models.

8.1.3 Generate in vivo ecotoxicity data using an avian early-life stage test and toxicogenomics approaches for prioritized BPA replacement compounds

Based on the cytotoxicity, ToxChip and AestroChip gene expression data, two replacement compounds were prioritized for early-life stage *in vivo* testing: DD-70 and BPAF. DD-70 and BPAF were the most cytotoxic replacements in CEH, LMH and DCEH. DD-70 altered the expression of genes on the ToxChip and is likely non-estrogenic. BPAF was the most estrogenic compound on the AestroChip in LMH spheroids. The research objective of Chapter 7 was to generate *in vivo* data such as embryo mortality, morphometrics and hepatic gene expression for DD-70 and BPAF. Fertilized chicken eggs were injected with DD-70 or BPAF, at concentrations based on previous chicken egg injection studies with BPA and other replacements (Crump et al. 2017; Berg 2001). Both DD-70 and BPAF were metabolized as concentrations of the compounds were lower in whole embryo homogenates collected at termination (1 day pre-hatch) compared to mid-incubation embryos. DD-70 was more embryo lethal than BPAF and decreased embryo mass, while both compounds caused an increase in gallbladder mass. In terms of gene expression, DD-70 altered the expression of more genes than BPAF. On the ToxChip

array, DD-70 induced the expression of FGF19, involved in the bile acid pathway at both developmental stages. The change in FGF19 is consistent with the changes observed in CEH, LMH spheroids and DCEH (Chapters 5 and 6). BPAF upregulated the expression of the xenobiotic metabolizing enzyme, CYP3A7, at mid-incubation. On the AestroChip array, DD-70 down regulated the expression of an estrogen-mediated gene, APOV1, at mid-incubation and upregulated two genes at termination, whereas BPAF did not change the expression of any estrogen-responsive genes at either developmental stage. This is in contrast to the AestroChip results where BPAF was the most estrogenic replacement compound in CEH and LMH spheroids (Chapters 5 and 6). Due to the small sample size, livers from female and male embryos were pooled, making it difficult to interpret the endocrine disrupting properties of DD-70 and BPAF. For example, DMSO control livers were from 4 females and 1 male while BPAF treated livers were from 2 females and 1 male at termination (1 day pre-hatch). Overall, DD-70 had a greater impact on lethality, morphometric endpoints and gene expression than BPAF.

8.2 Future Directions

8.2.1 Further Characterization of the LMH and DCH22 Cell Lines

Results from this thesis demonstrate that LMH cells cultured as 3D spheroids have CYP1A activity that is induced by dioxin-like compounds and can activate promutagens like BaP. The activity and mRNA expression of only one type of CYP450 was studied, CYP1Al; however, there are other CYP450s, e.g. CYP2C and CYP3A, which play important roles in chicken xenobiotic metabolism (Watanabe et al. 2013). There is limited information available on the activity of CYP2C and CYP3A in the LMH cell line. In a previous study, LMH cells cultured as 2D monolayer cells had weak mRNA expression of CYP2C45 (the main isoform of CYP2C in chickens) and CYP3A37 (main isoform of CYP3A in chickens) following exposure to

phenobarbital and a high concentration (1mM) of metyrapone (Ourlin et al. 2000). In order to characterize the metabolic competence of the LMH and DDC22 cell lines, the activity and mRNA expression of CYP2C and CYP3A need to be investigated.

Phase II enzymes like uridine diphosphate-glucuronosyltransferase (UGT), sulfotransferase (SULT), glutathione-S-transferase (GST), N-acetyltransferase also play an important role in the metabolism of chemicals. UGT and SULT are the main phase II enzymes that detoxify xenobiotics and endogenous compounds such as bile acid and steroid hormones (Jancova et al. 2010). Similar to CYP1A metabolism, sulfonation of compounds like N-hydroxy arylamines can result in DNA reactive metabolites (Gamage et al. 2006). Results from the ToxChip array in LMH spheroids (Chapter 6) indicate mRNA expression of phase II enzymes, especially SULT1E1 and possibly SULT1B1 and UGT1A9. The characterization of the DCH22 cell line in Chapter 4 focuses mainly on the metabolic capacity of phase I enzymes (CYP1A, CYP2C and CYP3A). Thus, future studies need to determine the mRNA expression and enzyme activity of the main isoforms of UGT and SULT after exposure to well-established inducers in the LMH and DCH22 cell lines cultured as 2D monolayers and 3D spheroids to gain insight into phase II metabolism of the cell lines. The determination of phase I and II enzymes will provide better perspective on the metabolic competence of the two cell lines.

The metabolism and toxicity of many chemicals are mediated by nuclear receptors, which are ligand-activated transcription factors involved in regulating expression of genes associated with a wide variety of pathways (Woods et al. 2007). In avian species, two nuclear receptors are mainly involved in xenobiotic metabolism, AhR and chicken xenobiotic receptor (CXR). AhR mediated expression of genes associated with several pathways was investigated using the customized AhR array in LMH cells cultured as 2D monolayer cells and 3D spheroids in Chapter

2 and demonstrated that the AhR gene expression profile of LMH spheroids was similar to CEH. The expression of the phase I metabolizing enzymes, CYP2C and CYP3A, is mediated by the CXR, which is analogous to the mammalian pregnane X receptor (PXR) and constitutive androstane receptor (Handschin et al. 2004). Thus, future studies should assess CXR mediated gene expression in the LMH cell line cultured as 2D monolayers and 3D spheroids. DCCOs likely have a homolog of CXR but there is no information on the receptor(s) involved in the expression of CYP2C and CYP3A. Since nuclear receptors play key roles in xenobiotic metabolism, the presence and functionality of AhR and CXR are important for the application of the LMH and DCH22 cell lines for avian toxicity testing.

Nuclear receptors are also the main targets of endocrine disrupting compounds (EDCs) and impairments in nuclear receptors account for the adverse effects of many EDCs. The interaction of nuclear receptors and EDCs is important for understanding the mechanisms of action of EDCs (Toporova and Balaguer 2020). The actions of xenoestrogens, like BPA, are mediated mostly via binding to estrogen receptors (ER). Based on the modulation of genes on the AestroChip by the replacement compounds, the LMH cell line expresses ER; however, whether the cell line is ERα or ERβ positive requires further analysis. In Chapters 5 and 6, there were differences in the modulation of genes on the AestroChip by the five replacement compounds in CEH and LMH spheroids. The binding of the replacement compounds to ER could account for the differences in modulation of estrogen-responsive genes. The affinity of bisphenol replacement compounds to ER could be determined using competitive ligand-binding assays in the LMH cell line, which could help determine the estrogenic potential of bisphenols and other xenoestrogens.

8.2.2 Appropriate Avian In Vitro Model and Method for Identifying Estrogenic Compounds

This thesis utilized two avian *in vitro* models, CEH and LMH spheroids, to examine the estrogenic effects of bisphenol replacement compounds using the AestroChip array. There were some inconsistencies in estrogen-responsive gene expression between the two models. For example, the direction of fold change in VTG2 expression was different in the two models for some compounds. BPAF and BPA downregulated the expression of VTG2 in CEH, whereas it was upregulated by both compounds in LMH spheroids. Upregulation of VTG2 by BPAF and BPA in LMH spheroids is in agreement with previous *in vitro* and *in vivo* studies in various species (Yamaguchi et al. 2015; Shi et al. 2015; Ma et al. 2015), suggesting it may be a more reliable model to determine estrogenicity than CEH. This is likely due to the male origin of the LMH cell line. If CEH are to be used for screening EDCs, it is recommended to only collect livers from males prior to culture.

The AestroChip was used to determine the estrogenic profile of the five replacement compounds. The genes on the AestroChip were selected based on an ethinylestradiol study in Japanese quail (Coturnix japonica). The array consisted of two genes that are highly responsive to estrogen exposure in oviparous species, APO and VTG2, and the mechanisms of action of these two genes in response to estrogen are well-studied. However, for some of the genes on the array, the mechanism behind estrogen-mediated activity is unknown. For example, the expression of avidin (AVD) in the oviduct of chickens and quails is induced by estrogen and progesterone (Korpela et al. 1981) but the mechanism of action of AVD in the liver is unknown. The AestroChip enabled the assessment of the estrogenic potential of the replacement compounds but could be improved by including estrogen receptor genes (e.g. ESR1 (ERα), ESR2 (ERβ)) and other genes that are well-known markers of estrogen exposure. For example,

the expression of signal transducer and activator of transcription 3 (STAT3) is regulated by ERα and is induced by E2 in the liver (Palmisano et al. 2018).

8.2.3 Future Screening of BPA Replacements for Avian Ecotoxicity

This thesis utilized changes in gene expression to screen several BPA replacement compounds for potential ecotoxicological concern. Changes in gene expression, measured *in vitro*, provide an indication of the plausible adverse effects in an organ or individual. Insights into mechanism of action and adverse effects of chemicals can be gained by integrating changes in gene expression to higher level of biological organization (Titz et al. 2014). Frameworks such as the adverse outcome pathway (AOP) can be used for linking molecular events to changes in the individual and population (Ankley et al. 2009). One of the toxicological concerns regarding BPA replacement compounds is estrogenic adverse effects, since BPA is considered to be an estrogenic compound (Pinto et al. 2019). Results from this thesis suggest that BPA replacements like BPAF and BPF could impair estrogen signalling pathways. Previous studies have found that BPA replacements bind to ER and modulate the expression of VTG (Pinto et al. 2019; Lee et al. 2018; LeFol et al. 2017). An AOP for the VTG pathway exists for fish and demonstrates quantitatively that disruption of VTG synthesis can be linked to an apical endpoint, reduced fecundity, and ultimately a decrease in population (Ankley et al. 2020). There are limited data for avian species associated with the ER antagonism AOP. A future BPA and 17β-estradiol egg injection study is required to generate data on different endpoints such as hepatic VTG gene expression, plasma VTG concentration and gonad histology, which could be used to expand the ER antagonism AOP (AOP:30, AOP-Wiki) for avian species. This will provide information on key events, which can be measured *in vitro* to identify adverse effects of other BPA replacement compounds.

One of the findings of this thesis was that all of the replacement compounds evaluated altered the expression of genes related to cholesterol and bile acid synthesis in CEH, LMH spheroids and DCEH. Furthermore, gallbladder mass was increased by DD-70 and BPAF in chicken embryos with a concomitant increase in the expression of genes associated with gallbladder filling and volume. An AOP exists for cholestasis, which demonstrates the link between key receptors and genes involved at the cellular level (e.g. inhibition of bile transporter export pump (BSEP) resulting in upregulation of organic solute transport genes) to changes in enzyme activity and bile accumulation that ultimately lead to the adverse outcome of liver cholestasis (Vinken et al. 2013). This AOP can be used to assess *in vitro* receptor binding and changes in the expression of genes following exposure to BPA replacement compounds that can be linked to cholestasis.

8.3 Concluding Remarks

This thesis addressed the need for characterizing avian hepatic cell lines for *in vitro* chemical screening and generating avian toxicity data for five BPA replacement compounds. The chicken LMH cell line, cultured as 3D spheroids, had improved metabolic activity and was a better alternative for chemical screening compared to LMH cells grown in 2D monolayer culture. Non-estrogenic and estrogenic activity varied among the replacement compounds and this likely relates to the differences in chemical structures. Some replacement compounds (BPF, BPAF, and BPSIP) are potentially more estrogenic than BPA while others (TGSH and DD-70) appear non-estrogenic but impair other critical pathways such as bile acid and cholesterol regulation. These *in vitro* data were used to prioritize two compounds, DD-70 and BPAF, for further *in vivo* testing where the generated data are more amendable to traditional risk assessment. One of the most significant contributions of this thesis was the demonstration that LMH spheroids may provide a

rapid, animal free alternative model for generating toxicological and estrogenicity data to support the prioritization and ecological risk assessment of BPA replacements and other compounds.

8.4 References

Ankley GT, Bennett RS, Erickson RJ, Hoff DJ, Hornung MW, Johnson RD, Mount DR, Nichols JW, Russom CL, Schmieder PK, Serrrano JA, Tietge JE, Villeneuve DL. 2010. Adverse outcome pathways: A conceptual framework to support ecotoxicology research and risk assessment. *Environmental Toxicology and Chemistry* 29:730-741. DOI: 10.1002/etc.34.

Ankley GT, Blackwell BR, Cavallin JE, Doering JA, Feifarek DJ, Jensen KM, Kahl MD, LaLone CA, Poole ST, Randolph EC, Saari TW, Villeneuve DL. 2020. Adverse Outcome Pathway Network-Based Assessment of the Interactive Effects of an Androgen Receptor Agonist and an Aromatase Inhibitor on Fish Endocrine Function. *Environmental Toxicology and Chemistry* 39:913-922. DOI: 10.1002/etc.4668.

Barton HA, Cogliano VJ, Flowers L, Valcovic L, Setzer RW, Woodruff TJ. 2005. Assessing susceptibility from early-life exposure to carcinogens. *Environmental Health Perspectives* 113:1125-1133. DOI: 10.1289/ehp.7667.

Birnbaum LS, Fenton SE. Cancer and developmental exposure to endocrine disruptors. *Environmental Health Perspectives* 111(4):389-94. DOI:10.1289/ehp.5686

Berg C, Halldin K, Fridolfsson AK, Brandt I, Brunstrom B. 1999. The avian egg as a test system for endocrine disrupters: effects of diethylstilbestrol and ethynylestradiol on sex organ development. *Science of the Total Environment* 233:57-66. DOI: 10.1016/s0048-9697(99)00179-5.

Caporossi L, Papaleo B. 2015. Exposure to bisphenol A and gender differences: from rodents to humans evidences and hypothesis about the health effects. *Journal of Xenobiotics* 5:15-19. DOI: 10.4081/xeno.2015.5264.

Crump D, Chiu S, Williams KL. 2018. Bis-(3-allyl-4-hydroxyphenyl) Sulfone Decreases Embryonic Viability and Alters Hepatic mRNA Expression at Two Distinct Developmental Stages in Chicken Embryos Exposed Via Egg Injection. *Environmental Toxicology and Chemistry* 37:530-537. DOI: 10.1002/etc.3990.

Gamage N, Barnett A, Hempel N, Duggleby RG, Windmill KF, Martin JL, McManus ME. 2006. Human sulfotransferases and their role in chemical metabolism. *Toxicological Sciences* 90:5-22. DOI: 10.1093/toxsci/kfj061.

Handschin C, Podvinec M, Meyer UA. 2000. CXR, a chicken xenobiotic-sensing orphan nuclear receptor, is related to both mammalian pregnane X receptor (PXR) and constitutive androstane receptor (CAR). *Proceedings of the National Academy of Sciences of the United States of America* 97:10769-10774. DOI: 10.1073/pnas.97.20.10769.

Harvey JL, Paine AJ, Maurel P, Wright MC. 2000. Effect of the adrenal 11-beta-hydroxylase inhibitor metyrapone on human hepatic cytochrome P-450 expression: induction of cytochrome P-450 3A4. *Drug Metabolism and Disposition* 28 (1) 96-101.

Head JA, Hahn ME, Kennedy SW. 2008. Key amino acids in the aryl hydrocarbon receptor predict dioxin sensitivity in avian species. *Environmental Science & Technology* 42:7535-7541. DOI: 10.1021/es801082a.

Head JA, Kennedy SW. 2010. Correlation between an in vitro and an in vivo measure of dioxin sensitivity in birds. *Ecotoxicology* 19:377-382. DOI: 10.1007/s10646-009-0421-3.

Jancova P, Anzenbacher P, Anzenbacherova E. 2010. PHASE II DRUG METABOLIZING ENZYMES. *Biomedical Papers-Olomouc* 154:103-116. DOI: 10.5507/bp.2010.017.

Kawaguchi T, Nomura K, Hirayama Y, Kitagawa T. 1987. Establishment and characterization of a chicken hepatocellular carcinoma cell line, LMH. *Cancer Research* 47:4460-4464.

Korpela JK, Elo HA, Tuohimaa PJ. 1981. Avidin induction by estrogen and progesterone in the immature oviduct of chicken, Japanese quail, duck, and gull. *General and Comparative Endocrinology* 44:230-232. DOI: 10.1016/0016-6480(81)90253-7.

Le Fol V, Ait-Aissa S, Sonavane M, Porcher JM, Balaguer P, Cravedi JP, Zalko D, Brion F. 2017. In vitro and in vivo estrogenic activity of BPA, BPF and BPS in zebrafish-specific assays. *Ecotoxicology and Environmental Safety* 142:150-156. DOI: 10.1016/j.ecoenv.2017.04.009.

Lee J, Park NY, Kho Y, Ji K. 2018. Effects of 4-Hydroxyphenyl 4-Isoprooxyphenylsulfone (BPSIP) Exposure on Reproduction and Endocrine System of Zebrafish. *Environmental Science & Technology* 52:1506-1513. DOI: 10.1021/acs.est.7b00498.

Ma M, Crump D, Farmahin R, Kennedy SW. 2015. Comparing the effects of tetrabromobisphenol-a, bisphenol a, and their potential alternatives, TBBPA-bis (2,3-dibromopropyl ether) and bisphenol s on cell viability and messenger ribonucleic acid expression in chicken embryonic hepatocytes. *Environmental Toxicology and Chemistry* 34:391-401. DOI: 10.1002/etc.2814.

McNabb FMA. 2007. The hypothalamic-pituitary-thyroid (HPT) axis in birds and its role in bird development and reproduction. *Critical Reviews in Toxicology* 37:163-193. DOI: 10.1080/10408440601123552.

National Toxicology Program. 2006. NTP toxicology and carcinogenesis studies of 3,3',4,4',5-pentachlorobiphenyl (PCB 126) (CAS No. 57465-28-8) in female Harlan Sprague-Dawley rats (Gavage Studies). *National Toxicol Program Technical Report Series*. 520:4-246.

Ourlin JC, Baader M, Fraser D, Halpert JR, Meyer UA. 2000. Cloning and functional expression of a first inducible avian cytochrome P450 of the CYP3A subfamily (CYP3A37). *Archives of Biochemistry and Biophysics* 373:375-384. DOI: 10.1006/abbi.1999.1566.

Palmisano, B. T., Zhu, L., & Stafford, J. M. 2017. Role of Estrogens in the Regulation of Liver Lipid Metabolism. *Advances in experimental medicine and biology*, *1043*, 227–256. DOI:10.1007/978-3-319-70178-3_12

Pinto C, Hao RX, Grimaldi M, Thrikawala S, Boulahtouf A, Ait-Aissa S, Brion F, Gustafsson JA, Balaguer P, Bondesson M. 2019. Differential activity of BPA, BPAF and BPC on zebrafish estrogen receptors in vitro and in vivo. *Toxicology and Applied Pharmacology* 380. DOI: 10.1016/j.taap.2019.114709.

Shi JC, Jiao ZH, Zheng S, Li M, Zhang J, Feng YX, Yin J, Shao B. 2015. Long-term effects of Bisphenol AF (BPAF) on hormonal balance and genes of hypothalamus-pituitary-gonad axis and liver of zebrafish (Danio rerio), and the impact on offspring. *Chemosphere* 128:252-257. DOI: 10.1016/j.chemosphere.2015.01.060.

Titz B, Elamin A, Martin F, Schneider T, Dijon S, Ivanov NV, Hoeng J, Peitsch MC. 2014. Proteomics for systems toxicology. *Computational and Structural Biotechnology Journal* 11:73-90. DOI: 10.1016/j.csbj.2014.08.004.

Toporova L, Balaguer P. 2020. Nuclear receptors are the major targets of endocrine disrupting chemicals. *Molecular and Cellular Endocrinology* 502. DOI: 10.1016/j.mce.2019.110665.

Vinken M, Landesmann B, Goumenou M, Vinken S, Shah I, Jaeschke H, Willett C, Whelan M, Rogiers V. 2013. Development of an Adverse Outcome Pathway From Drug-Mediated Bile Salt Export Pump Inhibition to Cholestatic Liver Injury. *Toxicological Sciences* 136:97-106. DOI: 10.1093/toxsci/kft177.

Watanabe KP, Kawai YK, Ikenaka Y, Kawata M, Ikushiro SI, Sakaki T, Ishizuka M. 2013. Avian Cytochrome P450 (CYP) 1-3 Family Genes: Isoforms, Evolutionary Relationships, and mRNA Expression in Chicken Liver. *Plos One* 8. DOI: 10.1371/journal.pone.0075689.

Woods CG, Heuvel JPV, Rusyn I. 2007. Genomic profiling in nuclear receptor-mediated toxicity. *Toxicologic Pathology* 35:474-494. DOI: 10.1080/01926230701311351.

Yamaguchi A, Ishibashi H, Arizono K, Tominaga N. 2015. In vivo and in silico analyses of estrogenic potential of bisphenol analogs in medaka (Oryzias latipes) and common carp (Cyprinus carpio). *Ecotoxicology and Environmental Safety* 120:198-205. DOI: 10.1016/j.ecoenv.2015.06.014.

Appendix

Supplemental Information

A1. Chapter 2: Evaluating Aryl Hydrocarbon Receptor Response in LMH 3D Spheroids

Table S2.1. List of genes on the chicken AhR array (catalogue number CAPG12083, Qiagen)

Description	Symbol	Refseq #
ATPase, H+/K+ transporting, nongastric, alpha polypeptide	ATP12A	NM_001030909
UDP-GlcNAc:betaGal beta-1,3-N-acetylglucosaminyltransferase 7	B3GNT7	XM_422738
Cell wall biogenesis 43 C-terminal homolog (S. cerevisiae)	CWH43	XM_420716
Cytochrome P450 1A4	CYP1A4	NM_205147
Cytochrome P450, family 1, subfamily A, polypeptide 5	CYP1A5	NM_205146
Cytochrome P450, family 1, subfamily B, polypeptide 1	CYP1B1	XM_419515
Fibroblast growth factor 19	FGF19	NM_204674
Fibroblast growth factor binding protein 1	FGFBP1	XM_420773
Frizzled-related protein	FRZB	NM_204772
Kelch domain containing 8B	KLHDC8B	XM_414393
Keratin 20	KRT20	XM_418168
Matrix Gla protein	MGP	NM_205044
Matrix metallopeptidase 7 (matrilysin, uterine)	MMP7	NM_001006278
Phenylalanine hydroxylase	PAH	NM_001001298
Regucalcin	RGN	NM_204729
Transglutaminase 2 (C polypeptide, protein-glutamine-gamma-glutamyltransferase)	TGM2	NM_205448
TCDD-inducible poly(ADP-ribose) polymerase	TIPARP	XM_422828
Islet amyloid polypeptide	IAPP	NM_205397
Similar to type VII collagen	COL7A1	XM_425157
EF-hand calcium binding domain 4B	EFCAB4B	XM_421040
Amphiregulin B	AREGB	NM_001031537
Cytochrome P450, family 24, subfamily A, polypeptide 1	CYP24A1	NM_204979
Dapper, antagonist of beta-catenin, homolog 2 (Xenopus laevis)	DACT2	XM_419602
Podocalyxin-like	PODXL	XM_416475
Fatty acid binding protein 3, muscle and heart (mammary-derived growth inhibitor)	FABP3	NM_001030889
Insulin-like growth factor binding protein 4	IGFBP4	NM_204353
Thyroid hormone responsive (SPOT14 homolog, rat)	THRSP	NM_213577
Eukaryotic translation elongation factor 1 alpha 1	EEF1A1	NM_204157
Ribosomal protein L4	RPL4	NM_001007479
Chicken Genomic DNA Contamination	GGDC	SA_00517

Reverse Transcription Control	RTC	SA_00104
Positive PCR Control	PPC	SA_00103

Table S2.2 Summary of 2-way Anova and Tukey's HSD results in 2D confluent cells and 3D spheroids after exposure to PCB-126 compared to DMSO control

Source of Variation	% of total variation	P value	P value	Significant?	
Interaction	19.97	0.0004	***	Yes	
Row Factor	42.86	< 0.0001	****	Yes	
Column Factor	23.27	< 0.0001	****	Yes	
ANOVA table	SS	DF	MS	F (DFn, DFd)	P value
Interaction	168.6	5	33.71	F (5, 24) = 6.895	P = 0.0004
Row Factor	361.8	5	72.35	F (5, 24) = 14.80	P < 0.0001
Column Factor	196.5	1	196.5	F (1, 24) = 40.18	P < 0.0001
Residual	117.3	24	4.889		
Tukey's multiple comparisons test	Mean Diff.	95% CI of diff.	Significant?	Summary	Adjusted P Value
Confluent					
0.0 vs. 0.01	-0.4333	-5.501 to 4.634	No	ns	0.9998
0.0 vs. 0.1	-0.7333	-5.801 to 4.334	No	ns	0.9974
0.0 vs. 1	-2.333	-7.401 to 2.734	No	ns	0.7129
0.0 vs. 10	-0.5667	-5.634 to 4.501	No	ns	0.9993
0.0 vs. 100	1.2	-3.868 to 6.268	No	ns	0.9759
Spheroid					
0.0 vs. 0.01	-4.3	-9.368 to 0.7677	No	ns	0.1299
0.0 vs. 0.1	-7.4	-12.47 to -2.332	Yes	**	0.0018
0.0 vs. 1	-14.8	-19.87 to -9.732	Yes	****	< 0.0001
0.0 vs. 10	-5.9	-10.97 to -0.8323	Yes	*	0.016
0.0 vs. 100	1.5	-3.568 to 6.568	No	ns	0.9388

Table 2.3 Summary of 2-way Anova and Sidak's comparison results between 2D confluent cells and 3D spheroids.

Source of Variation	% of total variation	P value	P value summary	Significant?	
Interaction	20.47	0.0001	***	Yes	
Row Factor	43.93	< 0.0001	****	Yes	
Column Factor	23.86	< 0.0001	****	Yes	
ANOVA table	SS	DF	MS	F (DFn, DFd)	P value
Interaction	168.6	5	33.71	F (5, 24) = 8.366	P = 0.0001
Row Factor	361.8	5	72.35	F (5, 24) = 17.96	P < 0.0001
Column Factor	196.5	1	196.5	F (1, 24) = 48.76	P < 0.0001
Residual	96.71	24	4.03		
Sidak's multiple comparisons test Confluent - Spheroid	Mean Diff.	95% CI of diff.	Significant?	Summary	Adjusted P Value
0.0	0	-4.697 to 4.697	No	ns	> 0.9999
0.01	-3.867	-8.564 to 0.8308	No	ns	0.1504
0.1	-6.667	-11.36 to -1.969	Yes	**	0.0027
1	-12.47	-17.16 to -7.769	Yes	****	< 0.0001
10	-5.333	-10.03 to -0.6359	Yes	*	0.02
100	0.3	-4.397 to 4.997	No	ns	> 0.9999

Table S2.4. Comparisons of CYP1A4 gene expression between LMH 2D confluent cells and 3D spheroids, and CEH following exposure to PCB-126 using generalized linear hypothesis tests. Resulting p-values were adjusted using Holm method. "*" denotes p <0.05; SE: standard error; c: confluent; s: spheroids; CEH: chicken embryonic hepatocytes

Comparison	Difference	SE	p_value	adj_p_values	Significance
c0.1-c0	10.24	1.37	6.48E-14	7.78E-13	*
c1-c0	11.41	27.36	6.77E-01	1.00E+00	
c10-c0	25.76	5.98	1.67E-05	1.17E-04	*
s0.1-s0	17.92	1.45	0.00E+00	0.00E+00	*
s1-s0	19.82	27.37	4.69E-01	1.00E+00	
s10-s0	47.87	6.01	1.55E-15	2.18E-14	*
CEH0.1-CEH0	8.59	1.45	3.53E-09	3.88E-08	*
CEH1-CEH0	215.51	27.37	3.33E-15	4.33E-14	*
CEH10-CEH0	208.58	6.01	0.00E+00	0.00E+00	*
s0.1-c0.1	7.68	1.93	6.94E-05	4.17E-04	*
CEH0.1-c0.1	-1.65	1.93	3.93E-01	1.00E+00	
CEH0.1-s0.1	-9.33	1.93	1.35E-06	1.08E-05	*
s1-c1	8.40	38.70	8.28E-01	1.00E+00	
CEH1-c1	204.10	38.70	1.33E-07	1.33E-06	*
CEH1-s1	195.70	38.70	4.26E-07	3.83E-06	*
s10-c10	22.11	8.46	9.00E-03	4.50E-02	*
CEH10-c10	182.82	8.46	0.00E+00	0.00E+00	*
CEH10-s10	160.72	8.46	0.00E+00	0.00E+00	*

Tab. S2.5 Comparisons of CYP1A5 gene expression between LMH 2D confluent cells and 3D spheroids, and CEH following exposure to PCB-126 using generalized linear hypothesis tests. Resulting p-values were adjusted using Holm method. "*" denotes p <0.05; SE: standard error; c: confluent; s: spheroids; CEH: chicken embryonic hepatocytes

Contrast	Difference	SE	p_value	adj_p_values	Significance
c0.1-c0	13.51	2.51	7.03E-08	6.33E-07	*
c1-c0	28.64	6.73	2.07E-05	1.45E-04	*
c10-c0	39.90	5.37	1.06E-13	1.28E-12	*
s0.1-s0	42.25	2.56	0.00E+00	0.00E+00	*
s1-s0	53.77	6.75	1.55E-15	2.18E-14	*
s10-s0	87.84	5.39	0.00E+00	0.00E+00	*
CEH0.1-CEH0	2.77	2.56	2.79E-01	8.37E-01	
CEH1-CEH0	33.94	6.75	4.86E-07	3.89E-06	*
CEH10-CEH0	40.99	5.39	2.98E-14	3.87E-13	*
s0.1-c0.1	28.74	3.54	4.44E-16	6.66E-15	*
CEH0.1-c0.1	-10.74	3.54	2.45E-03	1.47E-02	*
CEH0.1-s0.1	-39.48	3.54	0.00E+00	0.00E+00	*
s1-c1	25.13	9.51	8.25E-03	4.12E-02	*
CEH1-c1	5.31	9.51	5.77E-01	1.00E+00	
CEH1-s1	-19.82	9.51	3.72E-02	1.49E-01	
s10-c10	47.93	7.59	2.73E-10	3.00E-09	*
CEH10-c10	1.08	7.59	8.87E-01	1.00E+00	
CEH10-s10	-46.85	7.59	6.80E-10	6.80E-09	*

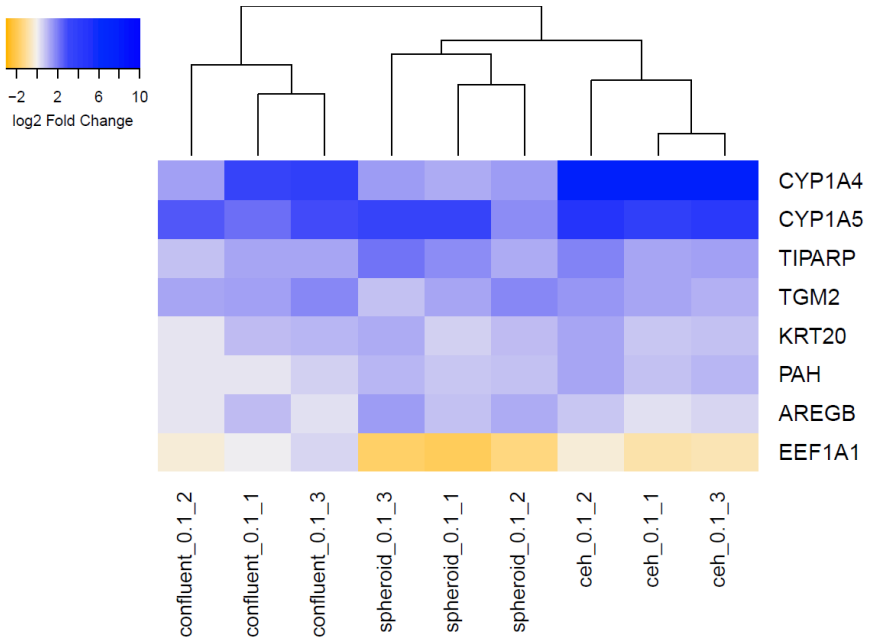

Figure S2.1. Heatmap of significant gene changes on the chicken AhR pathway PCR array for LMH cells exposed to 0.1 nM PCB-126 for 24h, hierarchically clustered by gene expression. Blue represents up-regulation and yellow represents down-regulation. The scale represents the log2 fold change.

A2. Chapter 3: Concentration- and Time-Dependent Induction of CYP1A and DNA Damage Response by Benzo(a)pyrene in LMH 3D Spheroids

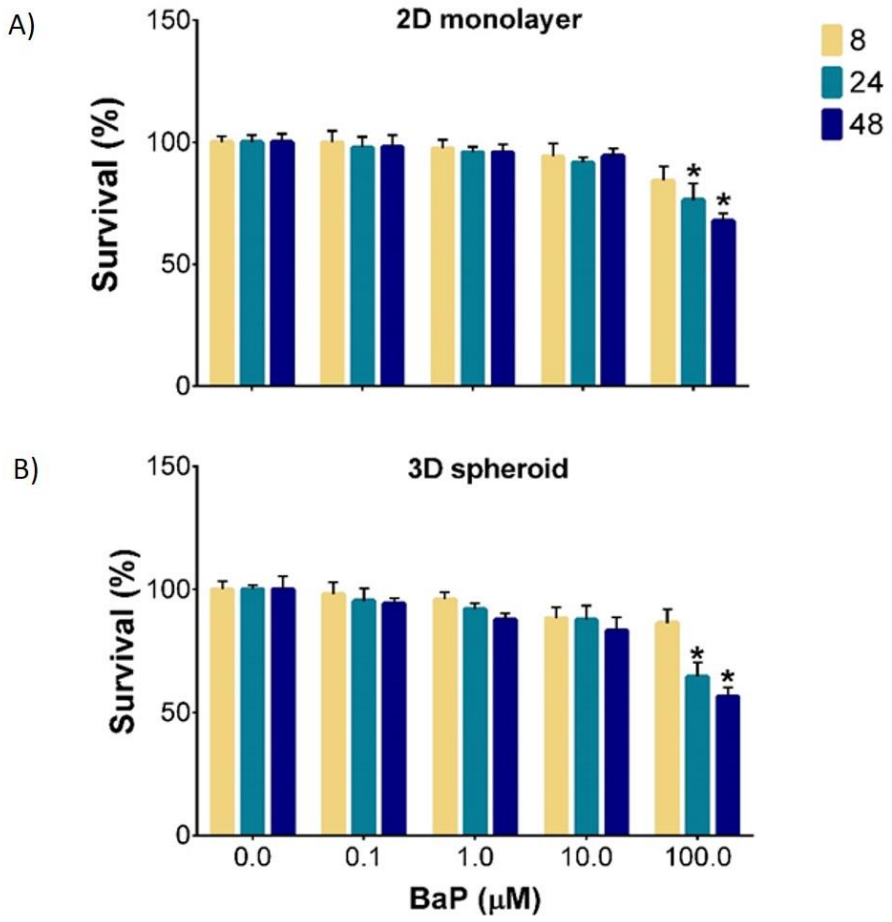

Figure S3.1. Concentration dependent effects of benzo(a)pyrene on cell viability in LMH A) 2D monolayer cells and B) 3D spheroids after 8, 24 and 48h exposure. '*' denotes significant difference from untreated cells.

Table S3.1 List of genes on the chicken DNA damage PCR array

Description	Symbol	RefSeq
Cytochrome P450 Family 1 Subfamily A Member 4	CYP1A4	NM_205147
Cytochrome P450 Family 1 Subfamily A Member 5	CYP1A5	NM_205146
Cyclin Dependent Kinase Inhibitor 1A	CDKN1A	NM_204396
Growth Arrest And DNA Damage Inducible Alpha	GADD45	NM_001044678
Damage Specific DNA Binding Protein 2	DDB2	NM_001039301
DNA Polymerase Beta	POLB	XM_004947614
DNA Polymerase Kappa	POLK	NM_204183
Xeroderma Pigmentosum Group C-Complementing Protein	XPC	NM_204853
Eukaryotic Translation Elongation Factor 1 Alpha 1	EEF1A1	NM_204157
60S ribosomal protein L4	RPL4	NM_001007479

Table S3.2. FDR adjusted P-value of gene expression in LMH 2D monolayer cells after exposure to BaP.

		FDR adjusted p-value							
Experiment	Concentration	CDKN1A	CYP1A4	CYP1A5	DDB2	GADD45	POLB	POLK	XPC
BaP_Conf_4	0.1	0.809	0.814	0.797	0.566	0.903	0.727	0.250	0.890
BaP_Conf_4	1	0.727	0.731	0.693	0.708	0.727	0.920	0.955	0.914
BaP_Conf_4	10	0.595	0.955	0.844	0.865	0.955	0.565	0.068	0.187
BaP_Conf_4	100	**0.031**	0.845	0.565	0.988	0.914	0.164	0.565	0.071
BaP_Conf_8	0.1	0.838	0.903	0.838	0.865	0.833	0.693	0.214	0.438
BaP_Conf_8	1	0.745	0.955	0.107	0.565	0.708	0.968	0.955	0.283
BaP_Conf_8	10	0.745	0.838	**0.031**	0.885	0.954	0.745	1.000	0.602
BaP_Conf_8	100	0.082	0.565	**0.005**	0.934	0.565	0.708	0.833	0.243
BaP_Conf_24	0.1	0.693	0.983	0.791	0.595	0.708	0.865	0.874	0.708
BaP_Conf_24	1	0.068	0.068	0.955	0.573	0.366	0.418	0.418	0.547
BaP_Conf_24	10	0.173	0.068	0.376	0.194	0.164	0.173	0.708	0.708
BaP_Conf_24	100	0.357	0.055	**0.030**	0.420	0.565	0.727	0.565	0.745
BaP_Conf_48	0.1	0.740	0.173	0.438	0.845	0.727	0.677	1.000	0.595
BaP_Conf_48	1	0.380	**0.031**	0.826	0.771	0.565	0.954	0.849	0.438
BaP_Conf_48	10	0.091	**0.002**	**0.002**	0.708	0.107	0.708	0.399	0.924
BaP_Conf_48	100	0.071	**0.000**	**0.000**	0.833	**0.046**	0.547	0.066	0.855

Table S3.3. FDR adjusted P-value of gene expression in LMH spheroids after exposure to BaP

		FDR adjusted p-value							
Experiment	Concentration	CDKN1A	CYP1A4	CYP1A5	DDB2	GADD45	POLB	POLK	XPC
BaP_Sph_4	0.1	0.708	0.858	0.669	0.868	0.403	0.725	0.943	0.967
BaP_Sph_4	1	0.669	0.433	0.385	0.494	0.494	0.708	0.443	0.740
BaP_Sph_4	10	0.920	0.965	0.669	0.740	0.793	0.708	0.613	0.935
BaP_Sph_4	100	0.869	0.773	0.578	0.954	0.954	0.708	0.806	0.888
BaP_Sph_8	0.1	0.057	0.195	0.331	0.667	0.982	0.140	0.967	0.634
BaP_Sph_8	1	0.115	**0.000**	0.790	0.205	0.663	0.051	0.685	0.194
BaP_Sph_8	10	0.276	**0.000**	0.816	0.148	0.354	0.443	0.059	0.725
BaP_Sph_8	100	0.094	**0.000**	0.107	0.264	0.497	0.059	0.740	0.109
BaP_Sph_24	0.1	**0.022**	**0.012**	**0.005**	**0.022**	0.953	**0.000**	0.101	**0.000**
BaP_Sph_24	1	0.869	**0.000**	**0.000**	**0.019**	0.965	**0.026**	0.667	**0.000**
BaP_Sph_24	10	**0.033**	**0.000**	**0.000**	**0.001**	0.168	**0.001**	**0.026**	**0.000**
BaP_Sph_24	100	**0.005**	**0.000**	**0.000**	0.202	0.051	0.071	0.497	**0.000**
BaP_Sph_48	0.1	0.101	0.954	0.354	0.148	**0.003**	**0.007**	**0.041**	0.134
BaP_Sph_48	1	0.082	0.232	**0.010**	0.063	**0.002**	**0.000**	**0.004**	**0.043**
BaP_Sph_48	10	**0.024**	**0.002**	**0.000**	**0.002**	**0.000**	**0.000**	**0.000**	**0.005**
BaP_Sph_48	100	**0.000**	**0.000**	**0.000**	**0.001**	**0.000**	**0.000**	**0.000**	**0.000**

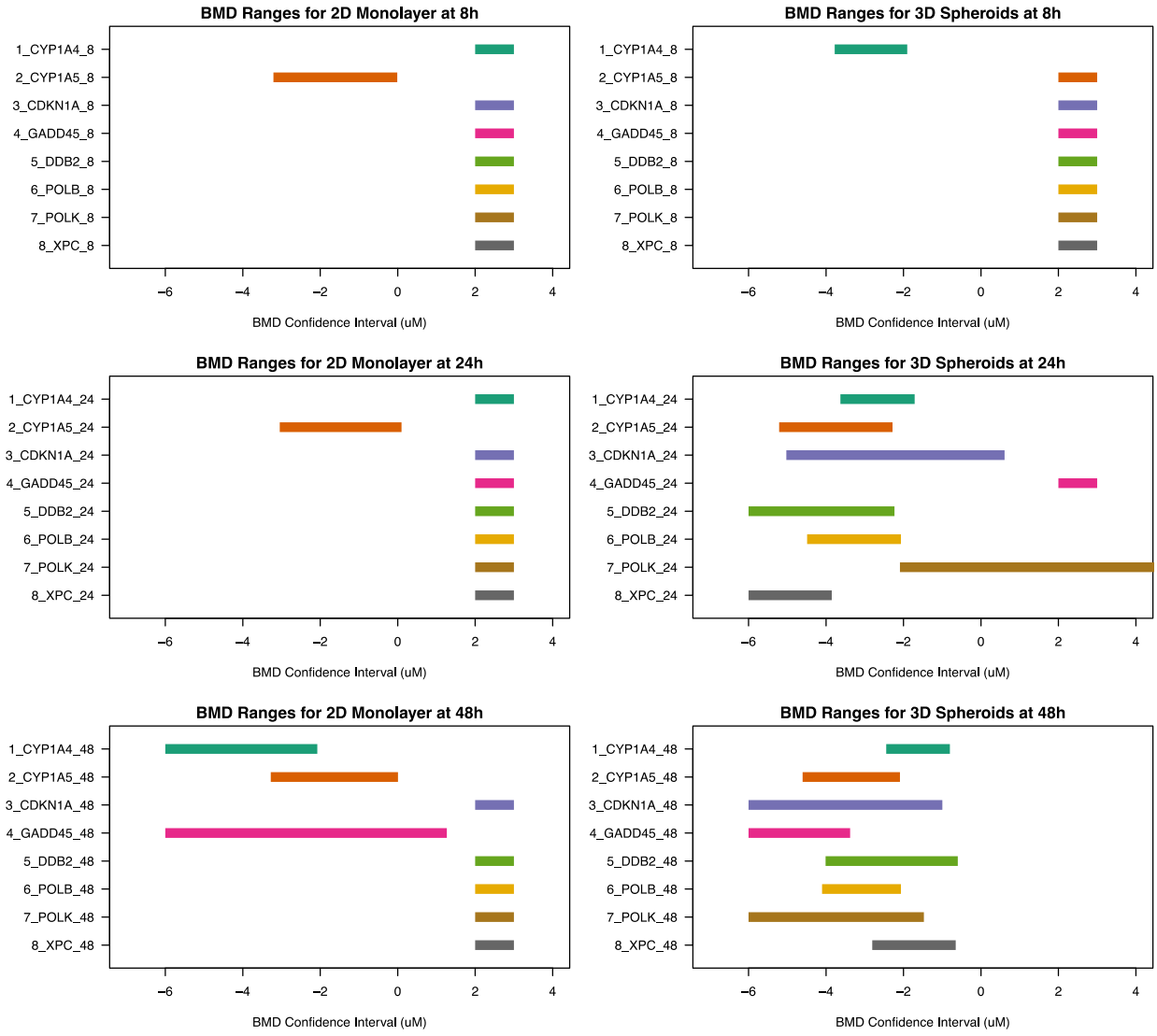

Figure S3.2. BMD ranges (BMDL-BMDU) for the expression of eight genes across three time points (8, 24 and 48h) after expsoure to benzo(a)pyrene (BPA) in LMH 2D monolayer and 3D spheroids. BMD ranges determined using PROAST (v.70.1).

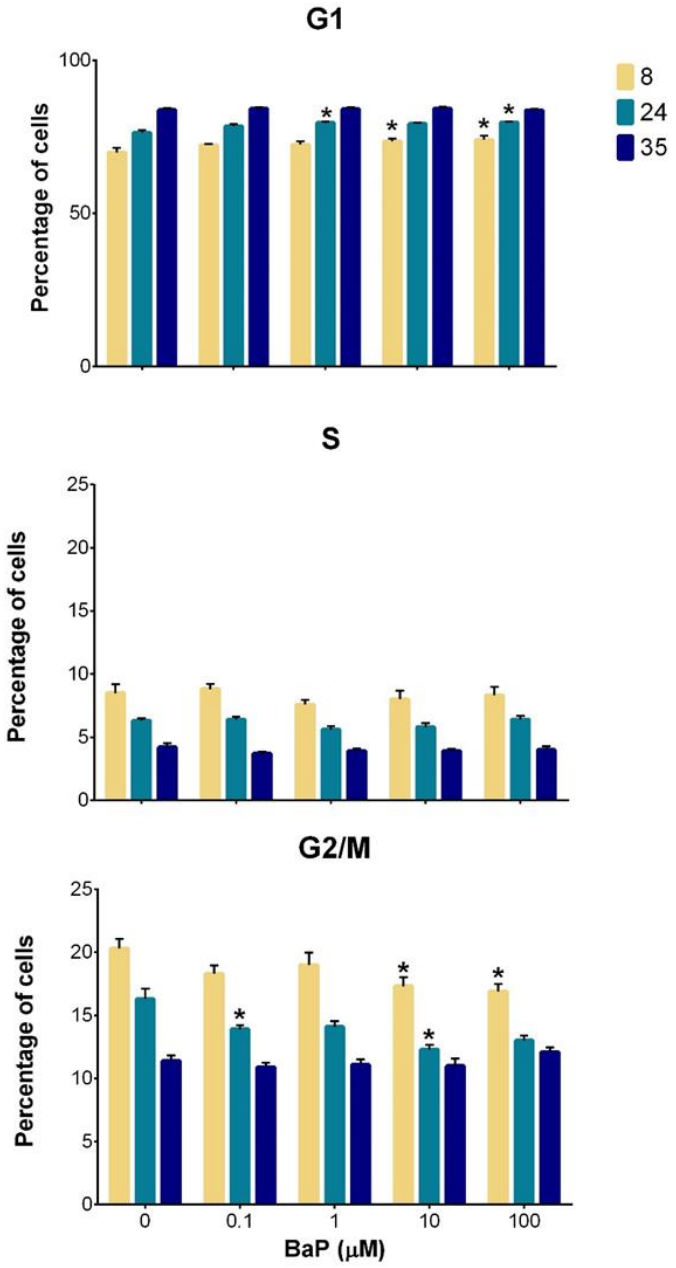

Figure S3.3. Percentage of cells in G1, S and G2/M phases of the cell cycle after exposure to benzo(a)pyrene for 8, 24 or 35h. "*" denotes difference from control.

A3. Chapter 5: Toxicity Screening of Bisphenol A Replacement Compounds: Cytotoxicity and mRNA Expression in Primary Hepatocytes of Chicken and Double-Crested Cormorant

Table S5.2. List of Pathways and Genes on the Chicken ToxChip Array (Qiagen catalogue # CLAG22572).

Pathway	Description	Symbol	RefSeq
Bile acids/cholesterol regulation	Cytochrome P450, family 7, subfamily B, polypeptide 1	CYP7B1	XM_418276
	Fibroblast growth factor 19	FGF19	NM_204674
	Forkhead box A1	FOXA1	XM_004941922
	Apolipoprotein B (including Ag(x) antigen)	APOB	NM_001044633
	Lanosterol synthase (2,3-oxidosqualene-lanosterol cyclase)	LSS	NM_001006514
Cell cycle	Cdk inhibitor CIP1 (p21)	CDKN1A	NM_204396
	Tumor protein p63	TP63	NM_204351
	Amine oxidase, copper containing 1	AOC1	XM_015281151
DNA repair	Growth arrest and DNA-damage-inducible, alpha	GADD45A	NM_001044678
	O-6-methylguanine-DNA methyltransferase	MGMT	XM_421823
	MutS homolog 2, colon cancer, nonpolyposis type 1 (E. coli)	MSH2	XM_426110
	Polymerase (DNA directed), beta	POLB	XM_004947614
	Polymerase (DNA directed) kappa	POLK	NM_204183
Glucose metabolism	Pyruvate dehydrogenase kinase, isozyme 4	PDK4	NM_001199909
	Glucose-6-phosphatase-like	G6pc	XM_003642817
Immune response	Basic leucine zipper transcription factor, ATF-like 3	BATF3	XM_419428
	Interleukin 16 (lymphocyte chemoattractant factor)	IL16	NM_204352
	Liver expressed antimicrobial peptide 2	LEAP2	NM_001001606
	Interleukin 1, beta	IL1B	NM_204524
	Nitric oxide synthase 2, inducible	NOS2	NM_204961
Lipid homeostasis	Acyl-CoA synthetase long-chain family member 5	ACSL5	NM_001031237
	Solute carrier organic anion transporter family, member 1A2	SLCO1A2	XM_416421
	Stearoyl-CoA desaturase (delta-9-desaturase)	SCD	NM_204890
	Liver basic fatty acid binding protein	LBFABP	NM_204634

Oxidative stress	Thioredoxin	TXN	NM_205453
	Carbonic anhydrase III-like (LOC420209)	CA3B	NM_001277410.1
	Metallothionein 4	MT4	NM_205275
	Heme oxygenase 1	HMOX1	NM_205344
	Microsomal glutathione S-transferase 3	MGST3	NM_001277533
Thyroid hormone pathway	Crystallin, alpha B	CRYAB	NM_205176
	Transthyretin	TTR	NM_205335
	Thyroid hormone responsive (SPOT14 homolog, rat)	THRSP	NM_213577
Xenobiotic metabolism	Insulin-like growth factor 1 (somatomedin C)	IGF1	NM_001004384
	Cytochrome P450 A 37	CYP3A7	NM_001001751
	Cytochrome P450 1A4	CYP1A4	NM_205147
	UDP glucuronosyltransferase 1 family, polypeptide A9	UGT1A9	XM_001234353
	Sulfotransferase family, cytosolic, 1B, member 1	SULT1B1	NM_204545
	Sulfotransferase family 1E, estrogen-preferring, member 1	SULT1E1	XM_420616
	Aminolevulinate, delta-, synthase 1	ALAS1	NM_001018012
	Fibrinogen alpha chain	FGA	NM_001271911
	Methionine adenosyltransferase I, alpha	MAT1A	NM_001199519
	N-acetyltransferase 2 (arylamine N-acetyltransferase)	NAT2	XM_001232799
	Aldehyde dehydrogenase 1 family, member A1	ALDH1A1	NM_204577
Control	Eukaryotic translation elongation factor 1 alpha 1	EEF1A1	NM_204157
	Ribosomal protein L4	RPL4	NM_001007479
	Chicken Genomic DNA Contamination	GGDC	SA_00517
	Reverse Transcription Control	RTC	SA_00104
	Positive PCR Control	PPC	SA_00103

Table S5.3. List of Pathways and Genes on the Double-Crested Cormorant ToxChip Array

Pathway	Description	Symbol	GenBank #
Bile acids/cholesterol regulation	Fibroblast growth factor 19	FGF19	KT886904.1
	Cytochrome P450, family 7, subfamily B, polypeptide 1	CYP7B1	KT886919.1
	Apolipoprotein B	APOB	-
	Lanosterol synthase (2,3-oxidosqualene-lanosterol cyclase)	LSS	-
	Forkhead box A1	FOXA1	-
	Lipase, hepatic	LIPC	-
Calcium regulation	Regucalcin	RGN	KT886902.1
Cell cycle	E3 ubiquitin-protein ligase	MDM2	KT886914.1
	O-6-methylguanine-DNA methyltransferase	MGMT	-
	Cyclin-dependent kinase inhibitor 1A	CDKN1A	-
	Amine oxidase, copper containing 1	AOC1	-
	Frizzled-related protein	FRZB	-
	Beta-2-microglobulin	M2B	-
DNA repair	MutS homolog 2	MSH2	-
	Polymerase (DNA directed), beta	POLB	-
	Polymerase (DNA) kappa	POLK	-
Glucose metabolism	Pyruvate dehydrogenase kinase, isozyme 4	PDK4	KT886905.1
	Glucose-6-phosphatase-like	G6PC	-
	Hexokinase 1	HK1	-
Immune response	Basic leucine zipper transcription factor, ATF-like 3	BATF3	-
	Interleukin 16 (lymphocyte chemoattractant factor)	IL16	KT886907.1
	Nuclear receptor coactivator 3	NCOA3	KT886912.1
	Liver expressed antimicrobial peptide 2	LEAP2	-
	Nitric oxide synthase 2, inducible	NOS2	-
Lipid homeostasis	3-hydroxy-3-methylglutaryl-Coenzyme A reductase	HMGCR	KT886908.1
	Liver basic fatty acid binding protein	LBFABP	-
	Acyl-CoA synthetase long-chain family member 5	ACSL5	KT886909.1
	Solute carrier organic anion transporter family, member 1A2	SLCO1A2	-
Oxidative stress	Metallothionein 4	MT4	-
	Glutathione peroxidase 3	GPX3	-
	Glutathione s-transferase	GSTM3	-
	Heme oxygenase 1	HMOX1	-
	Microsomal glutathione S-transferase 3	MGST3	-
	Transthyretin	TTR	KT886921.1

Thyroid hormone pathway	Insulin-like growth factor 1 (somatomedin C)	IGF1	KT886911.1
	Thyroid hormone responsive (SPOT14 homolog, rat)	THRSP	-
Xenobiotic metabolism	Cytochrome P450 1A4	CYP1A4	-
	Aminolevulinate, delta-, synthase 1	ALAS1	KT886906.1
	Cytochrome P450 A 37	CYP3A7	KT886910.1
	UDP glucuronosyltransferase 1 family, polypeptide A1	UGT1A1	KT886918.1
	Sulfotransferase family 1E, estrogen-preferring, member 1	SULT1E1	KT886920.1
	Fibrinogen alpha chain	FGA	-
	Aldehyde dehydrogenase 1 family, member A1	ALDH1A1	-
	Methionine adenosyltransferase I, alpha	MAT1A	-
Control	Eukaryotic translation elongation factor 1 alpha 1	EEF1A1	KT886916.1
	Ribosomal protein L4	RPL4	KT886917.1
	Glyceraldehyde-3-phosphate dehydrogenase	GAPDH	-
	No Template Control	NTC	-

"- "GenBank number is unavalaible

Table S5.4. List of Genes on the Chicken AestroChip Array

Pathway	Description	Symbol	RefSeq
Estrogen responsive genes	Vitellogenin-1	VTG1	NM_001004408
	Cathepsin D-like	CTSD	NM_205177
	Apovitellenin-1	APOV1	NM_205483
	ELOVL fatty acid elongase 2	ELVOL2	NM_001197308
	Cholesterol 7-alpha-monooxygenase	CYP7A1	NM_001001753
	Vitellogenin-2	VTG2	NM_001031276
	Orosomucoid 1	ORM1	NM_204541
	Carnitine O-palmitoyltransferase 1	CPT1A	NM_001012898
	Avidin	AVD	NM_205320
	Vascular cell adhesion molecule 1, transcript variant X2	VCAM1	XM_004936551

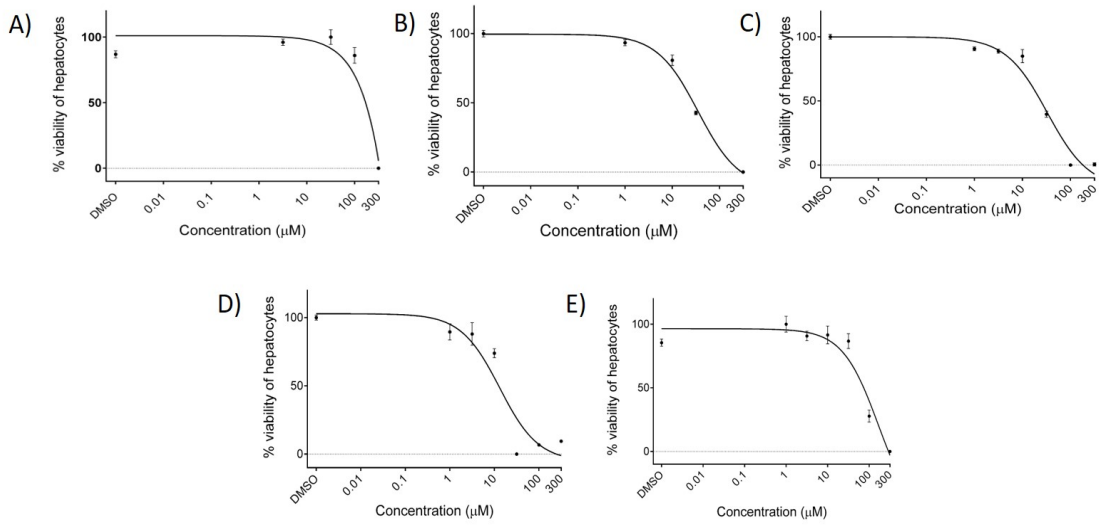

Figure S5.1. Cell viability (%) of CEH exposed to various concentrations of A) BPF, B) TGSH, C) DD-70, D) BPAF and E) BPSIP.

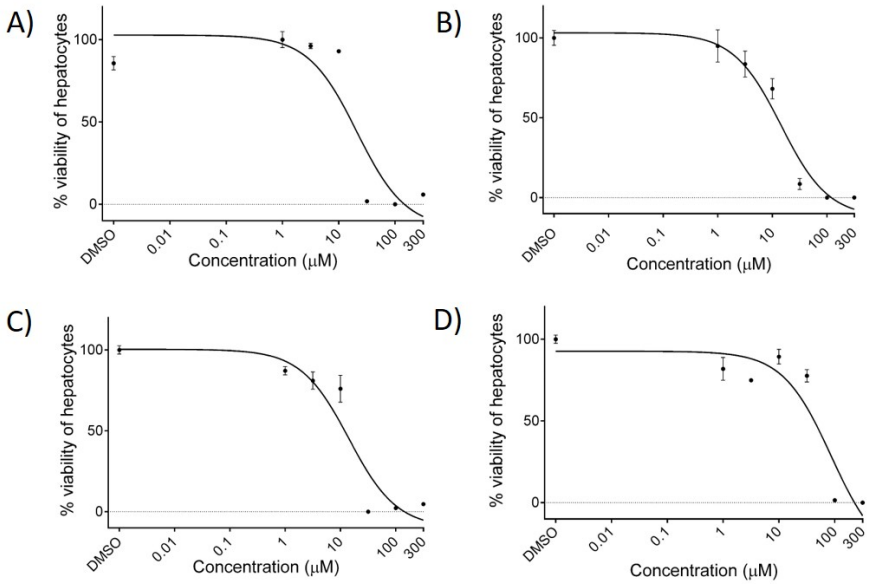

Figure S5.2. Cell viability (%) of DCEH exposed to various concentrations of A) TGSH, B) DD-70, C) BPAF, and D) BPSIP.

Table S5.5. Mean log2 fold changes of all genes on the chicken ToxChip array, unadjusted p-values and false discovery rate (FDR) adjusted p-values.

	Log2 Fold Change						
Genes	BPF	TGSH	DD-70	BPAF	BPSIP	BPA	E2
ACSL5	0.20	1.03	0.34	0.09	0.11	-0.64	-0.92
ALAS1	0.22	1.28	0.46	0.28	0.11	-0.21	0.72
ALDH1A1	0.57	0.23	0.57	-0.25	-0.08	0.05	-0.11
AOC1	-1.18	-2.21	-2.47	-2.74	0.00	0.52	0.19
APOB	-1.05	-1.11	-0.68	-0.32	-0.04	0.14	0.95
BATF3	0.05	0.63	-0.27	0.32	0.41	0.33	0.34
CA3B	-0.46	0.08	0.31	0.35	-0.32	-0.96	-0.95
CYP1A4	1.57	3.94	1.53	1.21	2.36	0.08	0.92
CYP3A7	-0.64	-0.90	0.10	0.56	-0.43	-0.02	0.35
CYP7B1	-0.41	-1.41	-1.03	-0.95	0.06	0.75	1.24
CYPAB	0.80	-0.19	0.34	0.62	0.74	-1.51	-0.87
FGA	-0.26	0.37	-0.63	-0.17	1.09	0.78	0.46
FGF19	-0.97	1.79	-1.09	-0.38	-0.31	-1.26	-0.34
FOXA1	-1.41	-1.35	-1.45	-1.38	0.30	0.23	0.44
G6PC	0.76	0.45	0.23	0.00	-0.12	-0.59	-1.12
GADD45	-0.92	-0.81	-1.63	-1.09	-0.07	0.36	0.56
HMOX1	-1.10	-0.73	-0.85	-0.31	-0.07	0.41	1.23
IGF1	-0.63	-2.13	-0.22	-1.14	-0.94	0.67	-0.31
IL16	0.11	-0.02	0.60	0.03	-0.17	-0.73	-1.22
IL1B	-0.19	-0.90	-0.37	-0.29	0.61	-0.24	-0.57
LBFABP	0.91	0.94	0.96	0.17	0.52	-0.39	-0.93
LEAP2	0.73	1.74	0.44	0.58	0.39	-0.65	-0.28
LSS	-0.89	-1.65	-1.91	-2.17	-0.11	0.09	-0.10
MAT1A	-0.13	-0.25	-0.01	-0.09	0.56	0.05	0.66
MGMT	0.23	0.12	0.10	-0.03	0.27	0.20	0.56
MGST3	0.54	0.64	0.49	0.17	0.24	-0.66	-1.05
MSH2	-0.63	-0.09	-0.55	-0.41	0.12	-0.12	0.02
MT4	0.10	-0.33	0.21	-0.70	0.25	-0.90	-0.43
NAT2	0.09	1.05	0.36	0.03	-0.46	-0.04	-0.17
NOS2	-0.01	0.23	0.51	-0.21	0.07	-0.05	-0.14
PDK4	0.63	2.06	0.82	0.30	1.15	0.36	0.42
POLB	-0.66	-0.70	-0.94	-0.87	-0.09	-0.26	-0.08
POLK	-0.50	-0.24	-0.47	-0.60	0.11	-0.08	-0.88
SCD	-1.27	-1.89	-1.39	-1.15	-0.15	-0.09	-1.59
SLCO1A5	0.24	0.46	0.60	0.36	0.18	-0.11	-0.07
SULT1B1	0.00	-0.21	-0.32	0.13	0.34	0.39	0.73

SULT1E1	0.62	0.64	0.32	-0.06	0.04	-0.56	-0.64
THRSP	-0.24	-2.65	-0.17	0.01	-0.84	-0.40	-1.11
TP63	-0.63	-0.22	-0.76	-0.87	-0.43	-0.68	-0.36
TTR	-0.09	-0.81	0.01	-0.13	-0.20	0.72	0.18
TXN	0.39	1.72	0.25	-0.15	-0.17	-0.53	0.55
UGT1A9	-1.18	-1.65	0.14	-0.77	-0.23	0.31	0.34
EEF1A1	0.21	0.16	0.03	0.16	0.40	-0.13	-0.03
RPL4	0.5	0.8	0.3	0.7	0.3	-0.4	-0.3

Unadjusted p-values

Genes	BPF	TGSH	DD-70	BPAF	BPSIP	BPA	E2
ACSL5	0.26	**0.00**	**0.01**	0.42	0.31	0.47	0.32
ALAS1	0.28	**0.00**	0.07	0.25	0.62	0.29	**0.01**
ALDH1A1	**0.00**	0.11	**0.01**	0.17	0.65	0.96	0.90
AOC1	**0.03**	**0.00**	**0.01**	**0.01**	1.00	0.21	0.61
APOB	**0.01**	**0.01**	**0.01**	0.16	0.86	0.60	**0.01**
BATF3	0.80	**0.02**	0.30	0.23	0.13	0.15	0.14
CA3B	0.14	0.77	0.42	0.35	0.40	0.22	0.22
CYP1A4	**0.01**	**0.00**	**0.00**	**0.00**	**0.00**	0.93	0.36
CYP3A7	**0.00**	**0.00**	0.56	**0.01**	**0.03**	0.92	0.09
CYP7B1	0.12	**0.00**	**0.01**	**0.02**	0.84	0.08	**0.01**
CYPAB	0.20	0.74	0.67	0.44	0.36	0.12	0.33
FGA	0.28	0.14	**0.03**	0.50	**0.00**	**0.01**	**0.04**
FGF19	**0.03**	**0.00**	**0.00**	0.14	0.21	**0.04**	0.51
FOXA1	**0.00**	**0.00**	**0.00**	**0.00**	0.30	0.35	0.10
G6PC	**0.01**	0.09	0.46	0.99	0.71	0.08	**0.01**
GADD45	**0.01**	**0.01**	**0.00**	**0.00**	0.75	0.09	**0.02**
HMOX1	**0.01**	0.06	**0.00**	0.10	0.67	0.22	**0.01**
IGF1	**0.03**	**0.00**	0.41	**0.00**	**0.01**	**0.03**	0.23
IL16	0.76	0.95	0.12	0.93	0.63	0.13	**0.03**
IL1B	0.36	**0.00**	0.54	0.64	0.33	0.55	0.19
LBFABP	**0.00**	**0.00**	**0.00**	0.37	**0.02**	**0.04**	**0.00**
LEAP2	**0.01**	**0.00**	**0.03**	**0.01**	0.05	**0.02**	0.20
LSS	**0.02**	**0.00**	**0.00**	**0.00**	0.82	0.78	0.76
MAT1A	0.37	0.11	0.93	0.53	**0.00**	0.87	0.05
MGMT	**0.03**	0.17	0.42	0.81	0.06	0.34	**0.02**
MGST3	**0.00**	**0.00**	**0.05**	0.44	0.29	0.45	0.25
MSH2	0.12	0.81	0.10	0.20	0.70	0.52	0.91
MT4	0.36	**0.02**	0.53	0.06	0.47	**0.03**	0.25
NAT2	0.78	**0.02**	0.25	0.92	0.16	0.75	0.21
NOS2	0.97	0.47	**0.05**	0.35	0.76	0.82	0.58
PDK4	0.09	**0.00**	**0.02**	0.29	**0.00**	0.23	0.16
POLB	0.06	**0.05**	**0.00**	**0.00**	0.67	0.48	0.82

POLK	0.11	0.40	0.09	**0.04**	0.66	0.93	0.38
SCD	**0.00**	**0.00**	**0.00**	**0.01**	0.65	0.92	0.14
SLCO1A5	0.22	**0.04**	**0.01**	0.08	0.34	0.44	0.60
SULT1B1	1.00	0.20	**0.02**	0.25	**0.01**	**0.02**	**0.00**
SULT1E1	**0.00**	**0.00**	**0.04**	0.67	0.78	0.56	0.51
THRSP	0.53	**0.00**	0.47	0.97	**0.01**	0.20	**0.01**
TP63	0.13	0.57	**0.01**	**0.00**	0.07	0.23	0.51
TTR	0.62	**0.00**	0.95	0.39	0.18	**0.01**	0.38
TXN	0.07	**0.00**	0.41	0.61	**0.56**	**0.03**	**0.02**
UGT1A9	0.10	**0.04**	0.66	**0.03**	0.47	0.38	0.33
EEF1A1	0.49	0.59	0.95	0.74	0.42	0.24	0.75
RPL4	**0.019**	**0.003**	0.191	**0.003**	0.128	**0.003**	**0.012**

False discovery rate (FDR) adjusted p-value

Genes	BPF	TGSH	DD-70	BPAF	BPSIP	BPA	E2
ACSL5	0.42	**0.01**	**0.04**	0.58	0.49	0.63	0.49
ALAS1	0.45	**0.01**	0.18	0.41	0.75	0.46	**0.04**
ALDH1A1	**0.02**	0.24	**0.04**	0.32	0.77	0.97	0.96
AOC1	0.08	**0.02**	**0.04**	**0.03**	1.00	0.37	0.74
APOB	**0.04**	**0.03**	**0.04**	0.31	0.92	0.73	**0.04**
BATF3	0.88	0.07	0.48	0.40	0.27	0.30	0.28
CA3B	0.27	0.85	0.58	0.53	0.56	0.38	0.39
CYP1A4	**0.04**	**0.00**	**0.01**	**0.02**	**0.00**	0.96	0.53
CYP3A7	**0.02**	**0.01**	0.70	**0.04**	0.09	0.96	0.21
CYP7B1	0.25	**0.01**	**0.04**	0.06	0.90	0.19	**0.05**
CYPAB	0.37	0.84	0.77	0.60	0.53	0.25	0.51
FGA	0.45	0.28	0.09	0.66	**0.02**	**0.03**	0.11
FGF19	0.10	**0.02**	**0.02**	0.28	0.38	0.11	0.66
FOXA1	**0.02**	**0.02**	**0.01**	**0.01**	0.48	0.53	0.22
G6PC	0.05	0.21	0.62	1.00	0.81	0.18	**0.03**
GADD45	**0.03**	**0.05**	**0.00**	**0.01**	0.85	0.20	0.06
HMOX1	**0.05**	0.14	**0.01**	0.23	0.78	0.39	**0.03**
IGF1	0.09	**0.00**	0.58	**0.02**	**0.03**	0.09	0.40
IL16	0.85	0.97	0.26	0.96	0.76	0.27	0.08
IL1B	0.53	**0.02**	0.69	0.76	0.51	0.69	0.35
LBFABP	**0.01**	**0.01**	**0.01**	0.54	0.06	0.11	**0.01**
LEAP2	**0.04**	**0.01**	0.10	**0.04**	0.14	0.06	0.37
LSS	0.06	**0.01**	**0.02**	**0.02**	0.88	0.86	0.85
MAT1A	0.54	0.24	0.96	0.67	**0.02**	0.93	0.13
MGMT	0.08	0.32	0.58	0.88	0.14	0.51	0.08
MGST3	**0.02**	**0.01**	0.13	0.60	0.46	0.61	0.41
MSH2	0.25	0.88	0.22	0.37	0.81	0.66	0.96
MT4	0.53	0.06	0.68	0.16	0.63	0.10	0.41

NAT2	0.86	0.06	0.42	0.96	0.30	0.85	0.38
NOS2	0.98	0.63	0.12	0.53	0.85	0.88	0.71
PDK4	0.21	**0.01**	0.06	0.47	**0.02**	0.39	0.32
POLB	0.14	0.12	**0.01**	**0.02**	0.77	0.63	0.88
POLK	0.25	0.57	0.21	0.12	0.77	0.96	0.54
SCD	**0.02**	**0.01**	**0.02**	**0.03**	0.77	0.96	0.27
SLCO1A5	0.39	0.10	**0.04**	0.19	0.52	0.60	0.73
SULT1B1	1.00	0.37	0.06	0.41	0.05	0.07	**0.01**
SULT1E1	**0.01**	**0.01**	0.10	0.77	0.86	0.70	0.66
THRSP	0.68	**0.01**	0.63	0.98	**0.03**	0.37	**0.03**
TP63	0.27	0.70	**0.03**	**0.02**	0.16	0.40	0.66
TTR	0.75	**0.02**	0.97	0.55	0.34	**0.04**	0.54
TXN	0.18	**0.00**	0.58	0.73	0.70	0.08	0.07
UGT1A9	0.22	0.10	0.77	0.10	0.63	0.54	0.51
EEF1A1	0.64	0.73	0.97	0.84	0.58	0.40	0.85
RPL4	0.063	**0.021**	0.356	**0.020**	0.267	**0.020**	**0.046**

Table S5.6. Mean log2 fold changes of all genes on the chicken AestroChip array, unadjusted p-values and FDR adjusted p-values

Log2 Fold Change							
Genes	BPF	TGSH	DD-70	BPAF	BPSIP	BPA	E2
APO	5.8	1.1	0.4	0.0	1.4	2.2	9.8
CATH	0.4	0.4	-1.2	1.1	1.3	0.7	1.8
CYP7A	1.1	2.6	-1.3	-0.2	2.1	1.4	2.8
ELV	0.0	-0.4	1.1	1.0	2.0	0.3	1.0
VTG	0.6	0.7	-2.1	-1.1	-1.5	-0.3	-0.2
AVD	2.8	1.2	0.0	-1.1	-2.4	0.4	-2.7
CPT	1.0	0.7	1.2	-1.8	4.1	1.0	3.2
ORMI	1.6	1.6	1.5	-0.1	1.5	0.3	1.6
VCAM	-0.6	-0.6	1.6	0.9	4.5	-0.5	3.4
VTG2	1.6	0.9	1.8	-2.9	1.5	-2.8	9.3
Unadjusted p-value							
Genes	BPF	TGSH	DD-70	BPAF	BPSIP	BPA	E2
APO	**0.000**	**0.036**	0.637	1.000	0.161	**0.017**	**0.000**
CATH	0.484	0.436	**0.020**	**0.036**	**0.016**	0.261	**0.018**
CYP7A	0.149	**0.008**	0.136	0.790	**0.035**	0.266	0.054
ELV	0.930	0.376	0.132	0.179	**0.018**	0.189	**0.002**
VTG	0.256	0.165	0.139	0.397	0.265	0.420	0.580
AVD	**0.000**	**0.004**	0.925	**0.039**	**0.001**	0.401	**0.002**
CPT	0.187	0.318	**0.039**	**0.004**	**0.000**	**0.035**	**0.000**
ORMI	**0.042**	**0.044**	**0.014**	0.844	**0.016**	0.589	**0.032**
VCAM	0.404	0.347	0.152	0.388	**0.003**	0.706	**0.050**
VTG2	**0.042**	0.190	**0.037**	**0.005**	0.081	**0.004**	**0.000**
False discovery rate (FDR) adjusted p-value							
Genes	BPF	TGSH	DD-70	BPAF	BPSIP	BPA	E2
APO	**0.000**	0.091	0.697	1.000	0.268	0.060	**0.000**
CATH	0.555	0.509	0.064	0.091	0.060	0.365	0.060
CYP7A	0.260	**0.037**	0.249	0.838	0.091	0.365	0.108
ELV	0.943	0.487	0.249	0.283	0.060	0.283	**0.016**
VTG	0.365	0.269	0.249	0.488	0.365	0.498	0.654
AVD	**0.000**	**0.022**	0.943	0.091	**0.010**	0.488	**0.016**
CPT	0.283	0.428	0.091	**0.022**	**0.000**	0.091	**0.000**
ORMI	0.092	0.093	0.060	0.882	0.060	0.654	0.091
VCAM	0.488	0.458	0.260	0.488	**0.021**	0.760	0.103
VTG2	0.092	0.283	0.091	**0.025**	0.158	**0.022**	**0.000**

Table S5.7. Mean log2 fold changes of all genes on the double-crested cormorant ToxChip array, unadjusted p-values and FDR adjusted p-values.

	Mean log2 Fold Change				
Gene	TGSH	DD-70	BPAF	BPSIP	E2
ACSL5	0.1	1.0	0.2	0.1	0.8
ALAS1	-0.9	0.4	0.4	0.4	0.7
ALDH1A1	0.9	-0.7	0.0	-0.8	2.1
AOC1	-0.3	-0.3	1.6	-0.1	0.0
APOB	0.3	0.1	0.3	-0.1	0.9
BATF3	0.0	0.9	0.1	-0.9	-0.4
CDKN1A	0.1	-0.3	1.0	-0.9	-0.3
CYP1A4	0.4	0.3	2.4	1.5	0.8
CYP3A7	2.0	0.5	1.0	1.5	1.4
CYP7B1	-0.5	0.0	0.3	-0.4	-0.1
EEF1A1	-0.4	0.2	-0.1	-0.4	-0.6
FGA	0.4	0.2	0.1	-0.5	0.2
FGF19	0.0	0.7	0.7	1.9	-0.4
FOXA1	-0.2	-0.2	0.7	0.0	0.0
FRZB	-0.4	-0.3	-0.1	-0.9	0.1
G6PC	-0.3	-1.6	1.0	-0.9	1.2
GAPDH	-0.3	0.1	-0.3	-0.2	-0.3
GPX3	0.7	-1.1	1.0	-0.2	1.2
GSTM3	0.2	0.3	0.4	-0.2	0.3
HK1	-0.5	-0.6	-0.2	-0.6	-0.3
HMGCR	-0.1	0.1	-0.1	0.3	-0.1
HMOX1	0.3	-0.2	0.0	1.0	0.6
IL16	-0.9	-0.2	0.0	0.0	-0.2
LBFABP	0.1	0.3	-0.5	-1.3	-0.3
LEAP2	0.1	0.0	0.5	-0.6	-0.7
LIPC	-0.8	-0.1	-0.3	-1.9	-1.1
LSS	-0.1	0.5	0.8	0.6	0.3
M2B	0.1	-0.1	0.0	-0.7	-0.2
MAT1A	0.2	0.0	0.8	0.4	0.8
MDM2	0.3	0.3	0.0	-0.3	0.2
MGMT	-0.1	0.2	0.5	-0.4	-0.2
MGST3	0.2	0.2	-0.1	-0.5	-0.1
MSH2	0.1	-0.1	0.0	-0.4	0.0
MT4	-0.4	0.0	-0.7	2.6	-0.3

NCOA3	0.0	-0.2	0.0	-0.8	0.5
NOS2	-0.7	-0.8	0.1	-1.1	-0.2
PDK4	-1.0	-0.2	1.0	0.1	0.6
POLB	-0.1	-0.1	0.0	-1.1	0.1
POLK	0.3	-0.4	0.5	-1.0	0.5
RGN	-0.8	0.4	0.1	-0.2	0.0
RPL4	0.1	-0.1	-0.1	0.3	1.0
SLCO1A2	0.1	0.2	1.1	-0.3	0.2
SULT1E1	0.4	0.0	0.5	0.5	0.4
THRSP	-0.2	-1.4	0.5	-0.9	-0.1
TTR	0.2	-0.3	-0.5	-1.1	0.2
UGT1A1	0.8	0.2	0.7	0.3	0.6

Unadjusted p-value

Gene	TGSH	DD-70	BPAF	BPSIP	E2
ACSL5	0.834	**0.004**	0.774	0.835	0.268
ALAS1	0.440	0.082	0.076	0.103	0.515
ALDH1A1	0.062	**0.007**	0.928	**0.005**	**0.002**
AOC1	0.494	0.641	0.201	0.895	0.950
APOB	0.440	0.851	0.498	0.707	**0.046**
BATF3	0.916	**0.011**	0.812	**0.009**	0.387
CDKN1A	0.903	0.694	0.120	0.293	0.554
CYP1A4	0.254	0.457	0.143	**0.010**	0.064
CYP3A7	0.074	0.078	**0.002**	**0.001**	0.171
CYP7B1	0.377	0.988	0.138	0.457	0.860
EEF1A1	0.362	0.370	0.638	0.070	0.195
FGA	0.066	0.271	0.679	**0.021**	0.348
FGF19	0.880	**0.001**	0.057	**0.000**	0.246
FOXA1	0.568	0.549	**0.020**	0.859	0.974
FRZB	0.557	0.194	0.747	**0.002**	0.891
G6PC	0.766	0.163	0.512	0.410	0.282
GAPDH	0.377	0.766	0.698	0.597	0.484
GPX3	0.280	**0.023**	0.167	0.595	0.085
GSTM3	0.356	0.163	0.367	0.384	0.188
HK1	**0.019**	**0.005**	0.529	**0.006**	0.095
HMGCR	0.833	0.512	0.648	0.202	0.776
HMOX1	0.365	0.586	0.477	**0.010**	**0.050**
IL16	**0.041**	0.294	0.973	0.826	0.552
LBFABP	0.822	0.086	0.223	**0.000**	0.224
LEAP2	0.886	0.801	0.058	**0.012**	0.235
LIPC	0.377	0.778	0.720	**0.000**	0.248
LSS	0.672	0.174	**0.036**	0.103	0.355
M2B	0.243	0.607	0.957	**0.036**	0.115

MAT1A	0.712	0.857	**0.011**	0.160	0.109
MDM2	0.192	0.338	0.933	0.275	0.371
MGMT	0.720	0.611	0.289	0.306	0.417
MGST3	0.641	0.232	0.665	**0.023**	0.795
MSH2	0.716	0.535	0.842	0.083	0.927
MT4	0.131	0.698	**0.003**	**0.000**	0.233
NCOA3	0.956	0.542	0.910	0.062	0.117
NOS2	0.250	0.090	0.897	**0.030**	0.685
PDK4	0.306	0.267	**0.006**	0.673	0.511
POLB	0.807	0.704	0.829	**0.010**	0.908
POLK	0.572	0.068	0.308	**0.002**	0.410
RGN	0.069	0.082	0.169	0.354	0.897
RPL4	0.678	0.876	0.613	0.395	**0.004**
SLCO1A2	0.617	0.354	0.140	0.239	0.475
SULT1E1	0.482	0.903	0.226	**0.035**	0.383
THRSP	0.667	**0.005**	0.285	**0.038**	0.859
TTR	0.488	0.111	**0.011**	**0.000**	0.338
UGT1A1	**0.011**	0.517	0.088	0.362	**0.035**

False discovery rate (FDR) adjusted p-value

Gene	TGSH	DD-70	BPAF	BPSIP	E2
ACSL5	0.946	0.072	0.927	0.946	0.611
ALAS1	0.738	0.330	0.323	0.366	0.788
ALDH1A1	0.305	0.081	0.957	0.072	**0.048**
AOC1	0.783	0.867	0.534	0.951	0.970
APOB	0.738	0.947	0.784	0.886	0.250
BATF3	0.953	0.093	0.946	0.093	0.679
CDKN1A	0.951	0.886	0.396	0.621	0.811
CYP1A4	0.590	0.757	0.445	0.093	0.308
CYP3A7	0.323	0.325	**0.048**	**0.038**	0.493
CYP7B1	0.678	0.988	0.441	0.757	0.947
EEF1A1	0.678	0.678	0.867	0.308	0.528
FGA	0.308	0.611	0.882	0.148	0.678
FGF19	0.951	**0.038**	0.296	**0.000**	0.586
FOXA1	0.822	0.811	0.148	0.947	0.978
FRZB	0.811	0.528	0.914	**0.048**	0.951
G6PC	0.927	0.487	0.788	0.704	0.618
GAPDH	0.678	0.927	0.886	0.842	0.778
GPX3	0.618	0.158	0.493	0.842	0.331
GSTM3	0.678	0.487	0.678	0.679	0.527
HK1	0.143	0.072	0.800	0.072	0.347
HMGCR	0.946	0.788	0.872	0.534	0.927
HMOX1	0.678	0.837	0.778	0.093	0.266

IL16	0.232	0.621	0.978	0.946	0.811
LBFABP	0.946	0.331	0.578	**0.007**	0.578
LEAP2	0.951	0.945	0.298	0.097	0.581
LIPC	0.678	0.927	0.886	**0.007**	0.586
LSS	0.882	0.495	0.212	0.366	0.678
M2B	0.586	0.849	0.970	0.212	0.387
MAT1A	0.886	0.947	0.093	0.487	0.381
MDM2	0.528	0.678	0.958	0.614	0.678
MGMT	0.886	0.849	0.621	0.633	0.711
MGST3	0.867	0.581	0.882	0.158	0.943
MSH2	0.886	0.804	0.947	0.330	0.957
MT4	0.423	0.886	0.059	**0.000**	0.581
NCOA3	0.970	0.810	0.951	0.305	0.390
NOS2	0.586	0.334	0.951	0.198	0.885
PDK4	0.633	0.611	0.076	0.882	0.788
POLB	0.946	0.886	0.946	0.093	0.951
POLK	0.822	0.308	0.633	**0.048**	0.704
RGN	0.308	0.330	0.493	0.678	0.951
RPL4	0.882	0.951	0.849	0.688	0.072
SLCO1A2	0.850	0.678	0.441	0.585	0.778
SULT1E1	0.778	0.951	0.578	0.212	0.679
THRSP	0.882	0.072	0.618	0.220	0.947
TTR	0.779	0.381	0.093	**0.016**	0.678
UGT1A1	0.093	0.788	0.331	0.678	0.212

A4. Chapter 6: Toxicity Screening of Bisphenol A Replacement Compounds: Cytotoxicity and mRNA Expression in LMH 3D Spheroids

Table S6.1. List of Pathways and Genes on the Chicken ToxChip Array (catalogue # CLAG22572; Qiagen).

Pathway	Description	Symbol	RefSeq
Bile acids/cholesterol regulation	Cytochrome P450, family 7, subfamily B, polypeptide 1	CYP7B1	XM_418276
	Fibroblast growth factor 19	FGF19	NM_204674
	Forkhead box A1	FOXA1	XM_004941922
	Apolipoprotein B (including Ag(x) antigen)	APOB	NM_001044633
	Lanosterol synthase (2,3-oxidosqualene-lanosterol cyclase)	LSS	NM_001006514
Cell cycle	Cdk inhibitor CIP1 (p21)	CDKN1A	NM_204396
	Tumor protein p63	TP63	NM_204351
	Amine oxidase, copper containing 1	AOC1	XM_015281151
DNA repair	Growth arrest and DNA-damage-inducible, alpha	GADD45A	NM_001044678
	O-6-methylguanine-DNA methyltransferase	MGMT	XM_421823
	MutS homolog 2, colon cancer, nonpolyposis type 1 (E. coli)	MSH2	XM_426110
	Polymerase (DNA directed), beta	POLB	XM_004947614
	Polymerase (DNA directed) kappa	POLK	NM_204183
Glucose metabolism	Pyruvate dehydrogenase kinase, isozyme 4	PDK4	NM_001199909
	Glucose-6-phosphatase-like	G6pc	XM_003642817
Immune response	Basic leucine zipper transcription factor, ATF-like 3	BATF3	XM_419428
	Interleukin 16 (lymphocyte chemoattractant factor)	IL16	NM_204352
	Liver expressed antimicrobial peptide 2	LEAP2	NM_001001606
	Interleukin 1, beta	IL1B	NM_204524
	Nitric oxide synthase 2, inducible	NOS2	NM_204961
Lipid homeostasis	Acyl-CoA synthetase long-chain family member 5	ACSL5	NM_001031237
	Solute carrier organic anion transporter family, member 1A2	SLCO1A2	XM_416421
	Stearoyl-CoA desaturase (delta-9-desaturase)	SCD	NM_204890
	Liver basic fatty acid binding protein	LBFABP	NM_204634
Oxidative stress	Thioredoxin	TXN	NM_205453
	Carbonic anhydrase III-like (LOC420209)	CA3B	NM_001277410.1
	Metallothionein 4	MT4	NM_205275

	Heme oxygenase 1	HMOX1	NM_205344
	Microsomal glutathione S-transferase 3	MGST3	NM_001277533
Thyroid hormone pathway	Crystallin, alpha B	CRYAB	NM_205176
	Transthyretin	TTR	NM_205335
	Thyroid hormone responsive (SPOT14 homolog, rat)	THRSP	NM_213577
Xenobiotic metabolism	Insulin-like growth factor 1 (somatomedin C)	IGF1	NM_001004384
	Cytochrome P450 A 37	CYP3A7	NM_001001751
	Cytochrome P450 1A4	CYP1A4	NM_205147
	UDP glucuronosyltransferase 1 family, polypeptide A9	UGT1A9	XM_001234353
	Sulfotransferase family, cytosolic, 1B, member 1	SULT1B1	NM_204545
	Sulfotransferase family 1E, estrogen-preferring, member 1	SULT1E1	XM_420616
	Aminolevulinate, delta-, synthase 1	ALAS1	NM_001018012
	Fibrinogen alpha chain	FGA	NM_001271911
	Methionine adenosyltransferase I, alpha	MAT1A	NM_001199519
	N-acetyltransferase 2 (arylamine N-acetyltransferase)	NAT2	XM_001232799
	Aldehyde dehydrogenase 1 family, member A1	ALDH1A1	NM_204577
Control	Eukaryotic translation elongation factor 1 alpha 1	EEF1A1	NM_204157
	Ribosomal protein L4	RPL4	NM_001007479
	Chicken Genomic DNA Contamination	GGDC	SA_00517
	Reverse Transcription Control	RTC	SA_00104
	Positive PCR Control	PPC	SA_00103

Table S6.2. List of Genes on the Chicken AestroChip Array

Pathway	Description	Symbol	RefSeq
Estrogen responsive genes	Vitellogenin-1	VTG1	NM_001004408
	Cathepsin D-like	CTSD	NM_205177
	Apovitellenin-1	APOV1	NM_205483
	ELOVL fatty acid elongase 2	ELVOL2	NM_001197308
	Cholesterol 7-alpha-monooxygenase	CYP7A1	NM_001001753
	Vitellogenin-2	VTG2	NM_001031276
	Orosomucoid 1	ORM1	NM_204541
	Carnitine O-palmitoyltransferase 1	CPT1A	NM_001012898
	Avidin	AVD	NM_205320
	Vascular cell adhesion molecule 1, transcript variant X2	VCAM1	XM_004936551

Table S6.3. List of genes on the Chicken ComboChip array.

Pathway	Description	Symbol	RefSeq
Bile acid and lipid regulation	Fibroblast growth factor 19	FGF19	NM_204674
	Forkhead box A1	FOXA1	XM_004941922
	Lanosterol synthase (2,3-oxidosqualene-lanosterol cyclase)	LSS	NM_001006514
	Stearoyl-CoA desaturase (delta-9-desaturase)	SCD	NM_204890
DNA repair	Polymerase (DNA directed), beta	POLB	XM_004947614
Estrogen responsive genes	Apovitellenin-1	APOV1	NM_205483
	Cathepsin D-like	CTSD	NM_205177
	Cholesterol 7-alpha-monooxygenase	CYP7A1	NM_001001753
	Vitellogenin-2	VTG2	NM_001031276
Xenobiotic metabolism	Cytochrome P450 1A4	CYP1A4	NM_205147
Control	Eukaryotic translation elongation factor 1 alpha 1	EEF1A1	NM_204157
	Ribosomal protein L4	RPL4	NM_001007479

Table S6.4. Mean log2 fold changes of all genes on the chicken AestroChip array and FDR adjusted p-values

	Log 2 fold change						
Genes	**BPF**	**TGSH**	**DD70**	**BPAF**	**BPSIP**	**BPA**	**E2**
APO	**5.76**	0.06	-0.29	**6.36**	**3.21**	**2.29**	**6.98**
AVD	**2.82**	1.71	0.73	1.87	**2.30**	**2.55**	1.21
CPT1A	**3.65**	**3.79**	**3.24**	**4.07**	**3.59**	**3.45**	**2.35**
CTSD	**3.82**	**3.48**	**3.72**	**3.73**	**4.25**	**2.96**	**3.08**
CYP7A	**2.94**	**1.55**	**2.89**	**3.22**	0.90	**1.82**	**1.71**
EEF1A1	-0.26	-0.58	-0.17	0.70	0.17	**1.41**	0.26
ELVL	**2.61**	**2.50**	**1.96**	-0.18	**2.62**	**2.31**	**1.32**
ORM1	**2.49**	**1.51**	0.89	2.54	**2.46**	**2.03**	**1.39**
VCAM	1.28	-0.20	-0.88	0.91	0.28	-0.43	-0.33
VTG2	**4.18**	0.74	**2.56**	**4.41**	**3.74**	**3.76**	**6.68**
	FDR adjusted p-value						
Genes	**BPF**	**TGSH**	**DD70**	**BPAF**	**BPSIP**	**BPA**	**E2**
APO	1.8E-07	9.1E-01	6.8E-01	8.6E-08	7.6E-05	1.5E-03	3.3E-08
AVD	1.6E-02	1.3E-01	5.3E-01	9.6E-02	4.3E-02	2.6E-02	2.8E-01
CPT1A	2.6E-07	1.8E-07	7.7E-07	9.8E-08	2.8E-07	4.4E-07	2.6E-05
CTSD	2.2E-06	5.4E-06	2.7E-06	2.7E-06	7.1E-07	3.3E-05	2.3E-05
CYP7A	1.6E-04	2.0E-02	1.8E-04	7.0E-05	1.6E-01	7.8E-03	1.2E-02
EEF1A1	5.3E-01	1.5E-01	6.9E-01	8.7E-02	6.9E-01	1.6E-03	5.3E-01
ELVL	1.6E-04	2.1E-04	1.7E-03	7.6E-01	1.6E-04	4.5E-04	2.3E-02
ORM1	1.4E-03	3.3E-02	2.0E-01	1.2E-03	1.5E-03	6.2E-03	4.7E-02
VCAM	2.6E-01	8.5E-01	4.5E-01	4.3E-01	7.9E-01	7.1E-01	7.7E-01
VTG2	1.2E-06	2.0E-01	2.0E-04	7.1E-07	3.8E-06	3.8E-06	2.2E-08

Table S6.5. Mean log2 fold changes of all genes on the chicken ToxChip array and false discovery rate (FDR) adjusted p-values.

	Log2 fold change						
Genes	**BPF**	**TGSH**	**DD70**	**BPAF**	**BPSIP**	**BPA**	**E2**
ACSL5	-0.63	-1.85	-0.03	-0.08	-0.28	0.08	-1.03
ALAS1	0.09	0.52	0.31	0.61	1.21	-0.09	0.65
ALDH1A1	-1.70	-1.69	-0.50	0.03	-0.45	0.12	1.31
AOC1	0.14	-0.92	-1.22	-0.90	-1.78	-0.17	0.58
APOB	0.42	1.48	-0.88	0.65	1.00	-0.06	0.55
BATF3	0.31	0.72	0.37	0.46	0.30	0.06	0.36
CA3B	0.22	-0.20	-0.30	0.73	0.21	-1.29	0.90
CDKN1A	0.26	0.25	-0.29	1.03	-0.81	0.06	0.43
CYP1A4	**2.57**	**2.13**	**2.20**	**1.95**	**2.62**	0.99	0.24
CYP3A7	0.05	-0.15	0.67	0.70	0.22	0.47	1.12
CYPAB	1.80	1.10	1.35	1.37	1.57	0.93	0.82
EEF1A1	0.01	-0.06	0.19	0.05	0.07	0.21	0.00
FGA	0.00	-0.33	0.02	0.34	0.45	-0.18	0.17
FOXA1	-0.38	-1.84	**-2.15**	1.60	-0.79	-0.24	0.24
G6PC	0.25	-0.39	-0.25	-0.15	0.19	-0.81	-0.02
GADD45	0.92	1.10	1.35	1.37	0.05	0.56	**1.96**
HMOX1	0.64	-0.01	**1.80**	0.77	0.85	0.10	0.24
IL16	0.23	0.04	-0.92	-0.20	0.24	0.40	-0.11
IL1B	0.27	-0.07	-0.25	-0.64	-0.58	-0.37	0.16
LEAP2	1.01	1.55	0.38	1.18	1.51	0.83	0.80
LBFABP	0.83	-0.31	0.84	0.77	0.04	0.11	**-1.25**
LSS	0.23	-1.75	**-2.09**	-0.97	-0.68	-0.19	0.17
MAT1A	1.44	0.43	1.33	1.26	1.14	0.78	0.73
MGMT	0.22	-1.03	0.25	-0.18	0.80	-0.12	-0.99
MGST3	-1.85	-1.22	-0.54	-0.42	0.11	-0.02	-0.93
MSH2	0.39	-0.07	-1.07	0.82	0.68	-0.15	-0.29
MT4	0.20	0.97	0.60	1.55	**2.80**	0.94	1.59
NAT2	0.11	0.47	-0.50	1.41	-0.21	0.46	1.14
NOS2	0.35	0.57	-0.01	-0.56	-0.19	0.77	0.94
PDK4	1.56	-1.69	0.78	1.95	**2.22**	1.11	0.64
POLB	1.61	1.24	1.67	1.41	-0.32	0.71	1.64
POLK	**-2.47**	**-2.26**	-0.78	-0.40	0.04	-0.14	-0.34
SCD	0.54	1.60	2.20	1.39	1.72	2.06	1.15
SLCO1A5	-1.11	-0.22	1.47	1.21	1.20	0.13	-1.21
SULT1B1	0.52	0.14	0.19	0.03	0.02	0.34	0.76
SULT1E1	-1.09	**-2.11**	-0.40	-0.56	-0.58	-0.07	0.60

THRSP	0.35	-0.52	-0.02	0.04	1.28	0.15	0.11
TP63	-1.22	-0.30	-1.01	-0.42	-1.65	-0.32	0.23
TTR	0.03	-1.89	0.70	1.66	1.80	-0.10	-0.07
TXN	0.19	0.58	-0.20	0.23	-0.56	-0.03	1.35
UGT1A9	-0.23	-1.22	-0.64	-0.32	-0.50	-0.73	0.41

FDR adjusted p-value

Genes	**BPF**	**TGSH**	**DD70**	**BPAF**	**BPSIP**	**BPA**	**E2**
ACSL5	0.59	0.05	0.99	0.99	0.91	0.99	0.28
ALAS1	0.96	0.47	0.75	0.35	0.06	0.96	0.31
ALDH1A1	0.23	0.23	0.87	0.99	0.90	0.99	0.37
AOC1	0.99	0.71	0.54	0.71	0.30	0.99	0.88
APOB	0.69	0.05	0.24	0.42	0.18	0.99	0.53
BATF3	0.80	0.31	0.72	0.61	0.81	0.99	0.72
CA3B	0.94	0.94	0.91	0.59	0.94	0.24	0.46
CDKN1A	0.91	0.93	0.91	0.30	0.47	0.99	0.80
CYP1A4	0.02	0.05	0.04	0.05	0.02	0.29	0.91
CYP3A7	0.99	0.97	0.71	0.69	0.94	0.86	0.38
CYPAB	0.17	0.44	0.30	0.30	0.23	0.55	0.63
EEF1A1	1.00	0.99	0.93	0.99	0.99	0.91	1.00
FGA	1.00	0.71	0.99	0.71	0.54	0.91	0.91
FOXA1	0.87	0.08	0.05	0.13	0.52	0.93	0.93
G6PC	0.90	0.75	0.90	0.94	0.93	0.31	0.99
GADD45	0.34	0.25	0.16	0.15	0.99	0.66	0.05
HMOX1	0.35	0.99	0.02	0.26	0.21	0.96	0.87
IL16	0.91	0.99	0.27	0.93	0.91	0.75	0.97
IL1B	0.86	0.99	0.87	0.40	0.48	0.72	0.93
LEAP2	0.20	0.05	0.75	0.14	0.06	0.30	0.31
LBFABP	0.14	0.70	0.14	0.17	0.99	0.94	0.05
LSS	0.93	0.08	0.05	0.34	0.57	0.94	0.94
MAT1A	0.15	0.80	0.18	0.20	0.25	0.48	0.53
MGMT	0.94	0.46	0.94	0.96	0.61	0.99	0.48
MGST3	0.20	0.43	0.86	0.91	0.99	0.99	0.61
MSH2	0.94	0.99	0.71	0.82	0.88	0.99	0.96
MT4	0.96	0.55	0.80	0.26	0.05	0.57	0.25
NAT2	0.99	0.90	0.88	0.35	0.96	0.90	0.51
NOS2	0.93	0.86	1.00	0.86	0.97	0.72	0.63
PDK4	0.13	0.10	0.52	0.06	0.05	0.28	0.63
POLB	0.10	0.20	0.09	0.15	0.90	0.54	0.09
POLK	0.04	0.05	0.53	0.86	0.99	0.96	0.90
SCD	0.81	0.20	0.08	0.27	0.17	0.10	0.38
SLCO1A5	0.20	0.92	0.09	0.17	0.17	0.96	0.17
SULT1B1	0.53	0.94	0.91	0.99	0.99	0.73	0.27
SULT1E1	0.27	0.05	0.82	0.69	0.66	0.99	0.63

THRSP	0.88	0.72	0.99	0.99	0.20	0.96	0.99
TP63	0.28	0.91	0.38	0.86	0.14	0.91	0.94
TTR	0.99	0.06	0.57	0.10	0.08	0.99	0.99
TXN	0.94	0.72	0.94	0.94	0.72	0.99	0.22
UGT1A9	0.94	0.29	0.70	0.91	0.80	0.61	0.87

Table S6.6. Mean log2 fold changes of all genes on the chicken AestroToxChip array and FDR adjusted p-values

						Log2 fold change						
Chemical	Dose	**APO**	**CTSD**	**CYP1A4**	**CYP7A1**	**EEF1A1**	**FGF19**	**FOXA1**	**LSS**	**POLB**	**SCD**	**VTG2**
DD-70	0.01	0.26	0.87	1.58	0.57	-0.05	0.89	0.44	1.51	1.51	0.36	0.71
DD-70	0.1	0.19	1.25	0.55	-0.70	0.61	0.29	1.32	0.81	1.56	1.35	-0.35
DD-70	1	-0.28	1.56	**2.27**	**2.98**	0.33	**4.90**	**3.43**	1.24	**2.51**	**3.21**	0.33
BPAF	0.01	**4.20**	1.04	1.26	0.67	0.66	1.87	1.01	0.74	1.53	0.65	1.06
BPAF	0.1	**4.36**	**1.64**	0.33	0.94	0.45	0.04	1.54	1.00	1.38	1.18	0.34
BPAF	1	**5.18**	**2.16**	**2.05**	**2.41**	0.72	0.58	1.20	1.31	**2.35**	**2.74**	1.70
						FDR adjusted p-value						
Chemical	Dose	**APO**	**CTSD**	**CYP1A4**	**CYP7A1**	**EEF1A1**	**FGF19**	**FOXA1**	**LSS**	**POLB**	**SCD**	**VTG2**
DD-70	0.01	0.72	0.32	0.06	0.69	0.96	0.31	0.70	0.19	0.08	0.70	0.48
DD-70	0.1	0.79	0.18	0.48	0.61	0.60	0.71	0.24	0.48	0.08	0.17	0.70
DD-70	1	0.72	0.10	0.01	0.05	0.72	0.00	0.01	0.27	0.01	0.01	0.71
BPAF	0.01	0.00	0.15	0.10	0.23	0.54	0.21	0.31	0.53	0.08	0.27	0.24
BPAF	0.1	0.00	0.04	0.68	0.10	0.69	0.97	0.15	0.39	0.10	0.08	0.70
BPAF	1	0.00	0.01	0.02	0.00	0.51	0.70	0.24	0.25	0.02	0.00	0.08

A5. Chapter 7: Effects of DD-70 and BPAF on mRNA Expression and Developmental Toxicity in Chicken Embryos

Table S7.1. List of Pathways and Genes on the Chicken ToxChip Array (Qiagen catalogue # CLAG22572).

Pathway	Description	Symbol	RefSeq
Bile acids/cholesterol regulation	Cytochrome P450, family 7, subfamily B, polypeptide 1	CYP7B1	XM_418276
	Fibroblast growth factor 19	FGF19	NM_204674
	Forkhead box A1	FOXA1	XM_004941922
	Apolipoprotein B (including Ag(x) antigen)	APOB	NM_001044633
	Lanosterol synthase (2,3-oxidosqualene-lanosterol cyclase)	LSS	NM_001006514
Cell cycle	Cdk inhibitor CIP1 (p21)	CDKN1A	NM_204396
	Tumor protein p63	TP63	NM_204351
	Amine oxidase, copper containing 1	AOC1	XM_015281151
DNA repair	Growth arrest and DNA-damage-inducible, alpha	GADD45A	NM_001044678
	O-6-methylguanine-DNA methyltransferase	MGMT	XM_421823
	MutS homolog 2, colon cancer, nonpolyposis type 1 (E. coli)	MSH2	XM_426110
	Polymerase (DNA directed), beta	POLB	XM_004947614
	Polymerase (DNA directed) kappa	POLK	NM_204183
Glucose metabolism	Pyruvate dehydrogenase kinase, isozyme 4	PDK4	NM_001199909
	Glucose-6-phosphatase-like	G6pc	XM_003642817
Immune response	Basic leucine zipper transcription factor, ATF-like 3	BATF3	XM_419428
	Interleukin 16 (lymphocyte chemoattractant factor)	IL16	NM_204352
	Liver expressed antimicrobial peptide 2	LEAP2	NM_001001606
	Interleukin 1, beta	IL1B	NM_204524
	Nitric oxide synthase 2, inducible	NOS2	NM_204961
Lipid homeostasis	Acyl-CoA synthetase long-chain family member 5	ACSL5	NM_001031237
	Solute carrier organic anion transporter family, member 1A2	SLCO1A2	XM_416421
	Stearoyl-CoA desaturase (delta-9-desaturase)	SCD	NM_204890
	Liver basic fatty acid binding protein	LBFABP	NM_204634

Oxidative stress	Thioredoxin	TXN	NM_205453
	Carbonic anhydrase III-like (LOC420209)	CA3B	NM_001277410.1
	Metallothionein 4	MT4	NM_205275
	Heme oxygenase 1	HMOX1	NM_205344
	Microsomal glutathione S-transferase 3	MGST3	NM_001277533
Thyroid hormone pathway	Crystallin, alpha B	CRYAB	NM_205176
	Transthyretin	TTR	NM_205335
	Thyroid hormone responsive (SPOT14 homolog, rat)	THRSP	NM_213577
Xenobiotic metabolism	Insulin-like growth factor 1 (somatomedin C)	IGF1	NM_001004384
	Cytochrome P450 A 37	CYP3A7	NM_001001751
	Cytochrome P450 1A4	CYP1A4	NM_205147
	UDP glucuronosyltransferase 1 family, polypeptide A9	UGT1A9	XM_001234353
	Sulfotransferase family, cytosolic, 1B, member 1	SULT1B1	NM_204545
	Sulfotransferase family 1E, estrogen-preferring, member 1	SULT1E1	XM_420616
	Aminolevulinate, delta-, synthase 1	ALAS1	NM_001018012
	Fibrinogen alpha chain	FGA	NM_001271911
	Methionine adenosyltransferase I, alpha	MAT1A	NM_001199519
	N-acetyltransferase 2 (arylamine N-acetyltransferase)	NAT2	XM_001232799
	Aldehyde dehydrogenase 1 family, member A1	ALDH1A1	NM_204577
Control	Eukaryotic translation elongation factor 1 alpha 1	EEF1A1	NM_204157
	Ribosomal protein L4	RPL4	NM_001007479
	Chicken Genomic DNA Contamination	GGDC	SA_00517
	Reverse Transcription Control	RTC	SA_00104
	Positive PCR Control	PPC	SA_00103

Table S7.2. List of Genes on the Chicken AestroToxChip Array

Pathway	Description	Symbol	RefSeq
Estrogen responsive genes	Vitellogenin-1	VTG1	NM_001004408
	Cathepsin D-like	CTSD	NM_205177
	Apovitellenin-1	APOV1	NM_205483
	ELOVL fatty acid elongase 2	ELVOL2	NM_001197308
	Cholesterol 7-alpha-monooxygenase	CYP7A1	NM_001001753
	Vitellogenin-2	VTG2	NM_001031276
	Orosomucoid 1	ORM1	NM_204541
	Carnitine O-palmitoyltransferase 1	CPT1A	NM_001012898
	Avidin	AVD	NM_205320
	Vascular cell adhesion molecule 1, transcript variant X2	VCAM1	XM_004936551

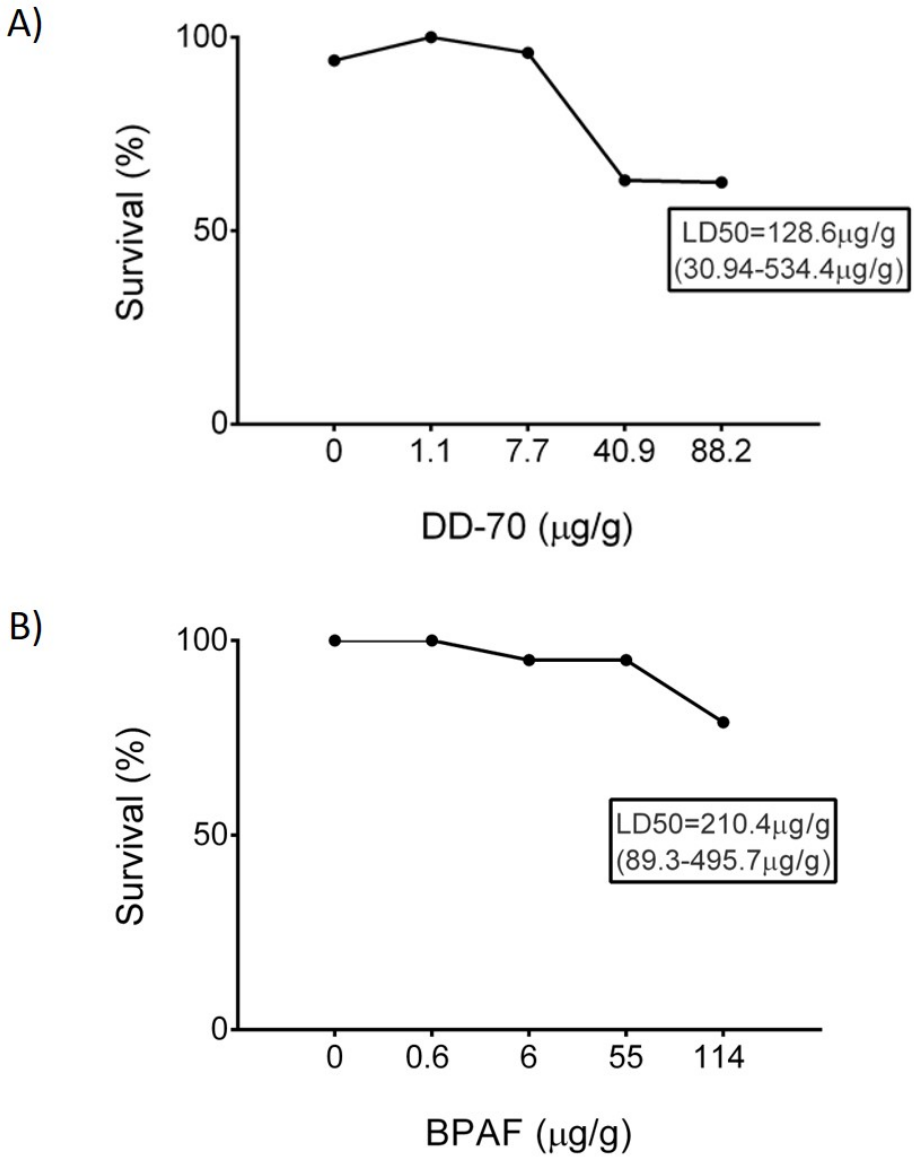

Figure 7.1 Lethal median 50 (LD50) values and confidence intervals of (A) DD-70 and (B) BPAF in mid-incubation chicken embryos.

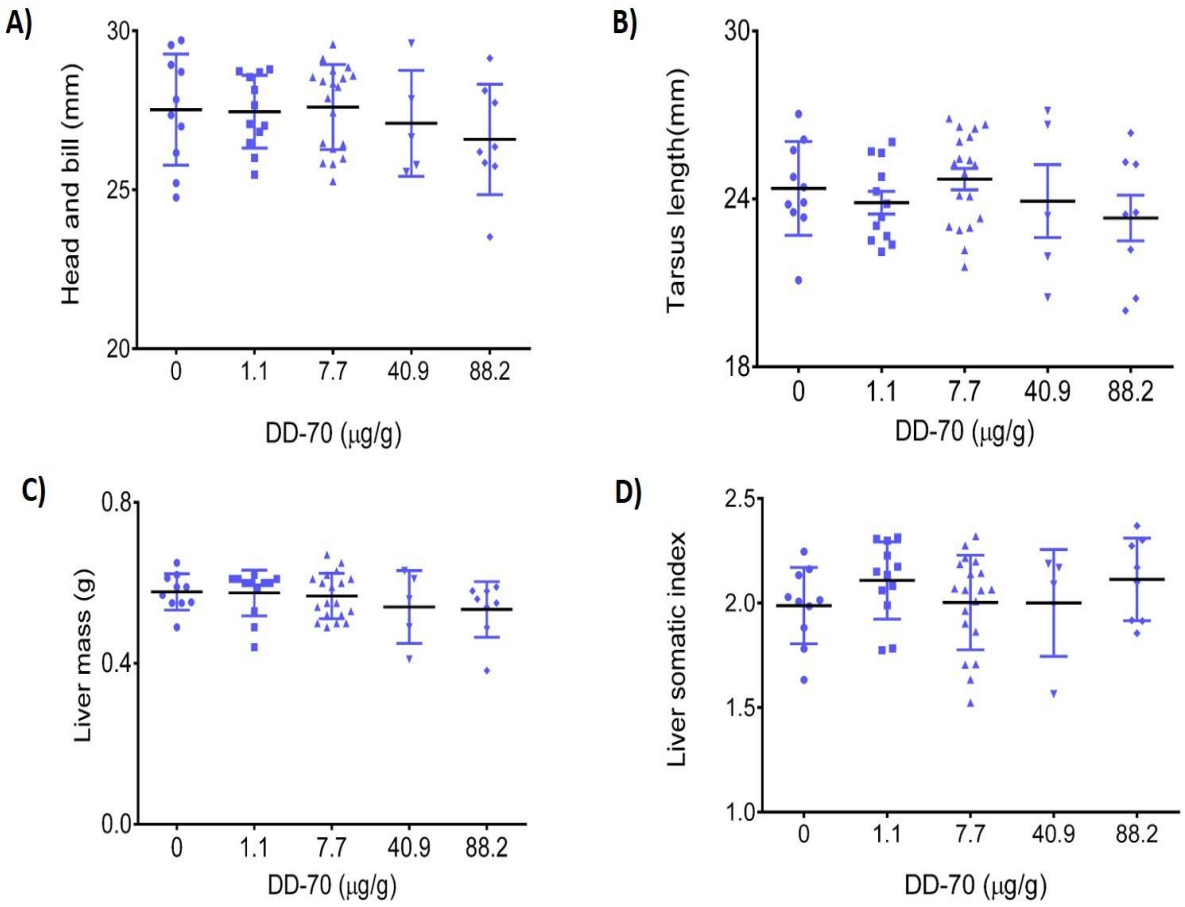

Figure S1. Morphometric effects of in ovo 1,7-bis (4-Hydroxyphenylthio)-3,5-dioxaheptane(DD-70) exposure on (A) head and bill length, (B) tarsus length, (C) liver mass, and (D) liver somatic index. Endpoints were determined for all embryos that pipped (n= 4-13/dose group). Error bars represent the standard deviation, and significant changes are indicated relative to the dimethyl sulfoxide (DMSO) control(*$p < 0.05$; one way ANOVA).

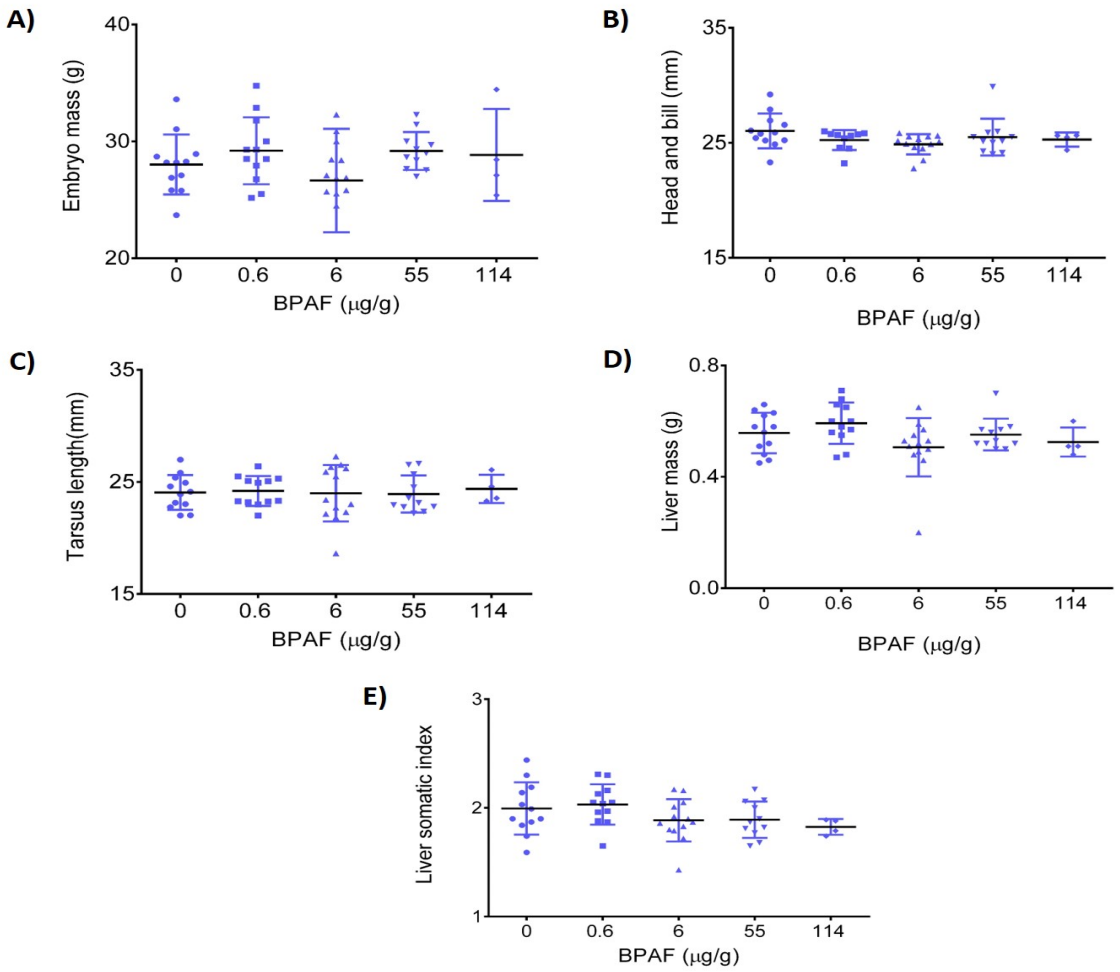

Figure S2. Morphometric effects of in ovo Bisphenol AF (BPAF) exposure on (A) embryo mass, (B) head and bill length, (C) tarsus length, (D) liver mass, and (E) liver somatic index. Endpoints were determined for all embryos that pipped (n= 4-13/dose group). Error bars represent the standard deviation, and significant changes are indicated relative to the dimethyl sulfoxide (DMSO) control (*$p < 0.05$; one way ANOVA).

Table 7. 3. Mean log2 fold change, standard deviation and Bonferroni adjusted p-values of genes on the ToxChip and AestroChip array following expsosure to DD-70 and BPAF.

		DD-70_M	DD-70_T	BPAF_M	BPAF_T
		100		114	
		Log2 fold change			
ToxChip	ACSL5	-0.04	0.27	0.97	-0.04
	ALAS1	0.15	0.38	0.68	0.21
	ALDH1A1	-1.93	-0.57	0.44	-0.64
	AOC1	-3.01	1.00	1.05	0.27
	APOB	-0.08	-0.54	0.94	0.28
	BATF3	0.27	-0.08	0.42	-1.70
	CDKN1A	0.93	-0.31	-0.32	0.48
	CRYAB	-0.53	0.63	-1.76	0.44
	CYP1A4	1.06	0.85	0.60	-0.10
	CYP3A7	2.40	1.98	2.50	1.83
	CYP7B1	0.30	0.31	1.50	0.35
	FGA	-0.32	0.17	0.41	0.02
	FGF19	6.81	3.53	2.51	NA
	FOXA1	-0.02	-0.05	0.80	0.14
	G6PC	-0.37	-0.17	0.70	0.91
	GADD45A	0.29	-0.09	-0.24	0.11
	HMOX1	0.80	-0.40	-0.20	0.26
	IGF1	-0.04	-0.41	-2.02	-0.71
	IL16	0.55	-0.27	-0.18	-0.16
	IL1B	0.45	-0.77	0.08	0.25
	LBFABP	0.73	-0.48	0.24	-2.08
	LEAP2	-0.68	-0.12	0.87	-1.21
	LSS	1.15	-0.14	0.49	0.41
	MAT1A	-0.09	-0.50	0.50	-0.35
	MGMT	-0.17	0.13	0.84	0.08
	MGST3	-0.81	0.51	-0.24	-0.39
	MSH2	1.49	0.46	1.28	-0.40
	MT4	-0.07	0.62	1.40	-2.06
	NOS2	-0.03	-0.06	0.28	0.07
	PDK4	0.96	-0.33	1.26	0.41
	POLB	0.08	0.70	0.02	-1.14
	POLK	0.48	0.16	-0.44	-0.24

	RPL4	0.53	-0.02	0.38	-0.22
	SCD	1.02	-0.5315	-0.68416667	1.28
	SLCO1A2	2.37	-0.06	1.11	-2.86
	SULT1B1	0.99	-0.14	0.76	0.26
	SULT1E1	-0.03	-0.21	-0.03	-0.19
	TP63	0.94	-0.88	-0.87	-0.55
	TTR	-0.72	-0.51	0.22	-0.47
	TXN	0.91	0.43	-0.53	-0.19
	UGT1A9	-0.37	-0.34	NA	-1.75
AestroChip	APOV1	-4.04	NA	2.68	-1.26
	CATH	0.97	-0.21	0.43	-0.88
	CYP7A1	0.38	-0.45	0.68	-1.10
	ELV	-1.89	1.09	0.17	-0.80
	VTG	-1.47	0.35	0.34	-0.94
	AVD	0.85	1.54	0.23	0.06
	CPT1A	-0.12	1.30	0.75	1.62
	ORM1	1.31	1.05	-1.20	0.35
	VCAM1	0.05	0.67	0.85	0.45
	VTG2	-4.14	NA	NA	NA
ToxChip			Standard deviation		
	ACSL5	0.52	0.32	0.58	0.51
	ALAS1	0.41	0.71	1.26	0.44
	ALDH1A1	2.43	1.17	1.57	0.55
	AOC1	2.87	2.21	1.13	0.82
	APOB	0.45	0.69	0.34	0.08
	BATF3	0.50	0.74	1.01	0.30
	CDKN1A	0.70	0.97	0.82	0.48
	CRYAB	2.12	0.90	0.56	1.15
	CYP1A4	0.45	0.98	0.94	0.99
	CYP3A7	1.53	1.73	0.99	2.22
	CYP7B1	0.89	0.64	1.03	0.34
	FGA	0.43	0.36	0.60	0.14
	FGF19	0.93	0.63	1.78	NA
	FOXA1	0.64	0.22	0.93	0.24
	G6PC	0.82	0.34	1.25	0.27
	GADD45A	0.60	0.55	0.33	0.60
	HMOX1	0.61	0.36	0.77	0.51
	IGF1	1.45	0.85	0.72	1.15
	IL16	0.83	1.01	0.59	0.20

	IL1B	0.80	1.13	0.54	0.85
	LBFABP	0.60	0.91	0.94	1.81
	LEAP2	0.28	0.72	0.83	0.64
	LSS	0.85	0.68	1.43	0.20
	MAT1A	0.28	0.58	0.52	0.83
	MGMT	0.40	0.35	0.58	0.26
	MGST3	0.83	0.38	0.45	0.36
	MSH2	3.03	0.68	2.72	0.27
	MT4	2.46	1.41	0.62	1.16
	NOS2	0.28	0.51	0.56	0.10
	PDK4	0.81	1.15	0.66	0.62
	POLB	0.14	0.75	0.35	0.50
	POLK	0.47	0.39	0.35	0.22
	RPL4	0.50	0.15	0.64	0.15
	SCD	0.54	0.87	0.70	0.13
	SLCO1A2	2.52	1.50	0.59	0.60
	SULT1B1	0.48	0.29	0.67	0.09
	SULT1E1	0.64	0.25	0.85	0.10
	TP63	0.98	0.26	1.11	0.48
	TTR	0.45	0.70	0.56	0.54
	TXN	0.73	0.23	0.65	0.50
AestroChip	UGT1A9	0.18	0.64	NA	0.54
	APOV1	0.61	NA	1.83	1.22
	CATH	0.26	0.46	0.33	0.57
	CYP	1.77	1.88	2.28	0.88
	ELV	0.28	1.43	0.85	1.71
	VTG	1.42	1.09	0.54	1.37
	AVD	1.21	0.89	0.52	1.18
	CPT1A	0.54	0.49	0.29	0.60
	ORM1	0.67	0.87	0.63	0.28
	VCAM1	0.82	0.77	0.57	0.15
	VTG2	3.87	NA	NA	NA
	Bonferroni adj p value (by gene)				
ToxChip	ACSL5	1.000	0.968	0.376	1.000
	ALAS1	1.000	1.000	1.000	1.000
	ALDH1A1	1.000	1.000	1.000	0.888
	AOC1	0.680	1.000	1.000	1.000
	APOB	1.000	0.588	0.460	0.948
	BATF3	1.000	1.000	1.000	0.144

	CDKN1A	0.724	1.000	1.000	1.000
	CRYAB	1.000	1.000	0.536	1.000
	CYP1A4	0.272	1.000	1.000	1.000
	CYP3A7	0.236	0.620	**0.036**	1.000
	CYP7B1	1.000	1.000	0.680	1.000
	FGA	1.000	1.000	1.000	1.000
	FGF19	**0.003**	**0.009**	0.309	NA
	FOXA1	1.000	1.000	1.000	1.000
	G6PC	1.000	1.000	1.000	0.160
	GADD45A	1.000	1.000	1.000	1.000
	HMOX1	0.464	0.532	1.000	1.000
	IGF1	1.000	1.000	0.244	1.000
	IL16	1.000	1.000	1.000	1.000
	IL1B	1.000	0.728	1.000	1.000
	LBFABP	0.796	1.000	1.000	0.312
	LEAP2	0.324	1.000	0.832	0.244
	LSS	0.352	1.000	1.000	1.000
	MAT1A	1.000	0.756	1.000	1.000
	MGMT	1.000	1.000	0.584	1.000
	MGST3	0.772	0.444	1.000	1.000
	MSH2	1.000	1.000	1.000	1.000
	MT4	1.000	1.000	0.772	0.124
	NOS2	1.000	1.000	1.000	1.000
	PDK4	0.772	1.000	0.180	1.000
	POLB	1.000	0.348	1.000	0.132
	POLK	0.992	1.000	0.456	1.000
	RPL4	0.636	1.000	1.000	1.000
	SCD	0.876	1	0.66	0.104
	SLCO1A2	1.000	1.000	0.356	0.108
	SULT1B1	0.244	1.000	0.548	1.000
	SULT1E1	1.000	1.000	1.000	1.000
	TP63	0.784	0.024	1.000	1.000
	TTR	0.232	0.688	1.000	0.544
	TXN	0.424	0.844	1.000	1.000
	UGT1A9	1.000	1.000	NA	0.438
AestroChip	APOV1	**0.012**	NA	0.195	0.642
	CATH	0.396	1.000	1.000	1.000
	CYP	1.000	1.000	1.000	1.000
	ELV	0.080	1.000	1.000	1.000

VTG	0.448	1.000	1.000	1.000
AVD	0.856	**0.048**	1.000	1.000
CPT1A	1.000	**0.028**	0.036	0.240
ORM1	0.472	0.552	1.000	1.000
VCAM1	1.000	0.512	0.540	0.132
VTG2	0.079	NA	NA	NA